



UNIVERSITY OF
BIRMINGHAM

NEUTROPHIL EXTRACELLULAR TRAPS IN PERIODONTITIS

by

Lisa Joanne Palmer

A thesis submitted to
The University of Birmingham
for the degree of
DOCTOR OF PHILOSOPHY

Department of Periodontology
School of Dentistry
College of Medicine and Dentistry
The University of Birmingham
March 2010

UNIVERSITY OF
BIRMINGHAM

University of Birmingham Research Archive

e-theses repository

This unpublished thesis/dissertation is copyright of the author and/or third parties. The intellectual property rights of the author or third parties in respect of this work are as defined by The Copyright Designs and Patents Act 1988 or as modified by any successor legislation.

Any use made of information contained in this thesis/dissertation must be in accordance with that legislation and must be properly acknowledged. Further distribution or reproduction in any format is prohibited without the permission of the copyright holder.

Abstract

This thesis has investigated the role of neutrophil extracellular traps (NETs) in the pathogenesis of periodontitis. A fluorometric assay was developed for the *in vitro* quantification of NET release and used to assess relative levels in chronic periodontitis patients, indicating elevated release under several stimulatory conditions compared with controls. Studies also demonstrated that challenge with periodontitis-associated bacteria evoked differential NET release. In addition, an extensive panel of periodontal pathogens was screened for two potential virulence traits that may confer a survival advantage when challenged with NETs. Deoxyribonuclease (DNase) secretion, capable of degrading NETs, and resistance to killing by histone, a core structural and antimicrobial protein within NETs, were both shown to be relatively common characteristics possessed by pathogens associated with severe disease. Additionally, an *in vivo* study demonstrated DNase activity in plaque and GCF during the development of experimental gingivitis. Further studies examined the association between neutrophil reactive oxygen species production and NET release implicating a regulatory role for myeloperoxidase generated hypochlorous acid in NET production. In conclusion, the results contained within this thesis indicate a putative role for NETs in the pathogenesis of periodontitis and highlight a high prevalence of potential counter-NET mechanisms in certain periodontal organisms.

Acknowledgements

I would like to thank Dr Helen Wright, Dr Paul Cooper and Professor Iain Chapple for their endless support, guidance and patience. Thanks also go to all my fellow tea drinkers in the postgraduate office who have made this time a pleasure, particularly my desk-neighbours Jen and Erum. Most importantly I would like to thank all those willing to role up their sleeve in the name of science, without their blood this thesis would not have been possible. Equally vital are the nurses of the Periodontology Unit whose venepuncture skills meant my volunteers kept coming back for more.

In addition I would like to thank Iru at Aston University for her time spared in providing me with HL60 cells on more than one occasion, and also Rachel Sammons for allowing me use of her microbiology lab.

I would also like to acknowledge the University of Birmingham, School of Dentistry for their financial support.

Table of Contents:

List of figures

List of tables

Abbreviations

CHAPTER 1 INTRODUCTION.....	1
1.1 Periodontal diseases.....	2
1.1.1 The prevalence of periodontitis	4
1.1.2 Risk factors for periodontitis	5
1.1.3 The progression of periodontitis.....	5
1.2 The role of bacteria in periodontal disease	6
1.3 The role of the host in periodontal disease	9
1.4 Neutrophils and disease	12
1.4.1 Neutrophil activation	13
1.4.2 Neutrophil killing mechanisms - Non-oxidative and oxidative.....	14
1.4.3 Extracellular neutrophil killing mechanisms	17
1.4.4 Microbial mechanisms for evading killing by neutrophils.....	18
1.5 Neutrophil extracellular traps (NETs)	19
1.5.1 Dependence on ROS.....	22
1.5.2 The function of NETs	26
1.5.2.1 Aiding other immune processes	28
1.5.2.2 Extracellular antimicrobial activity	30
1.5.2.3 NETs in non-infectious diseases	32
1.5.3 Stimuli for NET production.....	37
1.5.4 Non-neutrophil derived extracellular traps.....	40
1.6 HL60 cells as a model for neutrophils	41
1.7 Microbial mechanisms for the evasion of NETs	44
1.7.1 Inhibition of antimicrobial peptides (AMPs).....	44
1.7.2 Charge modifications of the bacterial surface	45
1.7.3 Expression of bacterial capsules.....	47
1.7.4 Bacterial DNases	48
1.8 The role of NETs in the pathogenesis of periodontal disease	52
1.9 Summary and aims.....	56
CHAPTER 2 MATERIALS AND METHODS	58
2.1 NET production <i>in vitro</i>	59
2.1.1 Isolation of neutrophils.....	59
2.1.1.1 Percoll density gradient	59
2.1.1.2 Lysis buffer.....	60
2.1.1.3 Phosphate buffered saline (PBS)	60
2.1.1.4 Method for isolation of neutrophils	60
2.1.2 Culture and differentiation of HL60 cells.....	61
2.1.3 NET staining.....	62

2.1.3.1 Paraformaldehyde (PFA) 8%	62
2.1.3.2 NET staining.....	62
2.1.3.3 Image capture and processing	63
2.1.4 Fluorometric analysis of NET release	64
2.1.5 Micrococcal nuclease (MNase) assay of NET release	64
2.1.6 SEM of NETs	65
2.1.7 Enhanced chemiluminescence assay for ROS.....	65
2.1.7.1 GPBSS (glucose supplemented PBS).....	66
2.1.7.2 Blocking buffer (PBS BSA)	66
2.1.7.3 Luminol and isoluminol.....	66
2.1.7.4 Lucigenin	66
2.1.7.5 Method for enhanced chemiluminescent assay for ROS.....	66
2.1.8 Stimuli used to induce NETs	67
2.1.8.1 Preparation of bacterial stimuli	68
2.1.8.2 Opsonisation of <i>S. aureus</i>	69
2.1.9 Modulators of neutrophil function used in NET assays	69
2.2 Comparison of NET production between periodontal patients and healthy individuals	71
2.2.1 Selection of volunteers	71
2.2.2 Assay of peripheral blood neutrophils.....	71
2.3 HL60 cell characterisation	72
2.3.1 Gene expression analysis by RT-PCR in HL60 cells and primary neutrophils	72
2.3.1.1 mRNA extraction.....	75
2.3.1.2 Reverse transcription	76
2.3.1.3 PCR amplification of selected transcripts	76
2.3.1.4 Gel electrophoresis and image capture	77
2.3.2 Staining of HL60 cells	78
2.3.2.1 Haematoxylin and Eosin staining	78
2.3.2.2 Immunocytochemical staining.....	78
2.4 Culture of bacteria	79
2.4.1 Storage of bacteria	81
2.4.2 Culture conditions	81
2.4.3 Blood agar	81
2.4.3.1 Enriched blood agar.....	82
2.4.3.2 Hemin (100x concentration).....	82
2.4.3.3 N-acetylmuramic acid (NAM; 100x concentrated solution).....	82
2.4.3.4 Vitamin K (100x concentrated solution)	82
2.4.3.5 Preparation of enriched blood agar.....	83
2.4.4 Planktonic growth of bacteria.....	83
2.4.4.1 Tryptone soya broth.....	83
2.4.4.2 Enriched tryptone soya broth.....	84
2.5 Identification of bacteria.....	84
2.5.1 Gram stain	84
2.5.1.1 Crystal violet solution.....	85
2.5.1.2 Carbol fuchsin	85
2.5.1.3 Method for Gram stain	85
2.5.2 Catalase test	86

2.5.3 PCR identification	86
2.5.3.1 PCR primers	86
2.5.3.2 Bacterial PCR	92
2.6 Antimicrobial susceptibility testing using histone proteins	92
2.6.1 Microtitre plate analysis for antimicrobial susceptibility testing	93
2.6.2 Determination of bacterial growth by spectrophotometry.....	93
2.6.3 Determination of bacterial growth by colony count.....	95
2.6.4 Determination of bacterial growth by fluorescence	95
2.7 Deoxyribonuclease (DNase) activity assays.....	95
2.7.1 Plate flooding method.....	95
2.7.1.1 Preparation of DNase test plates.....	96
2.7.1.2 Toluidine blue O (TBO) 0.05%.....	96
2.7.1.3 Inoculation of DNase test plates.....	96
2.7.1.4 Plate flooding method.....	97
2.7.1.5 Image analysis	97
2.7.2 Agarose gel method.....	98
2.7.2.1 Preparation of test samples.....	98
2.7.2.2 Reaction mixture for agarose gel method of DNase assay.....	99
2.8 Detection of DNase in plaque and GCF samples	100
2.8.1 Clinical study period.....	100
2.8.2 Clinical measures of gingival inflammation.....	101
2.8.3 Plaque sampling.....	101
2.8.4 GCF sampling.....	101
2.8.4.1 PBS-BSA	102
2.8.4.2 GCF sampling.....	102
2.8.5 Assay of samples for DNase activity.....	102
2.9 Statistical analysis.....	102
 CHAPTER 3 RESULTS	
Assay of NET release.....	103
3.1 Fluorometric quantification of NET release	106
3.1.1 Sensitivity of fluorometric detection of DNA	106
3.1.2 Determination of optimal concentrations of cells.....	107
3.1.3 Correlation analysis of real-time fluorometric assay and visualisation of NET formation.....	110
3.1.4 Quantification of NET production following MNase digestion.....	112
3.1.5 Comparison of quantitative NET production data obtained by end-point fluorescence and MNase assay	115
3.2 Determination of optimal concentration of serum for NET release	118
3.2.1 Effect of foetal calf serum (FCS) on NET release.....	118
3.2.2 Effect of BSA concentrations on NET release	121
3.2.3 Effect of BSA and FCS on NET release using fluorometric quantification.....	124
3.3 Determination of optimal concentration of stimuli	128
3.3.1 Dose-response analysis following PMA stimulation	128
3.3.2 Dose-response analysis following stimulation with opsonised <i>S. aureus</i>	130
Discussion	132

CHAPTER 4 RESULTS

Modulation of NET release	138
4.1 ROS inhibitor, diphenyleneiodonium (DPI)	139
4.1.1 Effect of DPI on cell viability	141
4.2 Phagocytosis inhibitor, cytochalasin B (cytoB)	144
4.3 Effect of combination of ROS and phagocytosis inhibitors on NET release	147
4.4 Superoxide dismutase (SOD)	152
4.5 Antioxidant/radical scavenger, curcumin	154
4.6 Myeloperoxidase inhibitor, sodium azide	156
Discussion	160

CHAPTER 5 RESULTS

HL60 cells as a model system for NET release	167
5.1 Differentiation of HL60 cells by DMSO	168
5.2 PCR characterisation of dHL60 cells	170
5.3 Cytological analysis of dHL60 cells	177
5.4 NET production in dHL60 cells	179
5.4.1 Visualisation of NETs in dHL60 cells.....	180
5.4.2 Fluorometric quantification of NET release from dHL60 cells	181
5.4.3 MNase assay of dHL60 cell NET production	183
5.5 ROS production by dHL60 cells	185
Discussion	188

CHAPTER 6 RESULTS

Comparison between NET release in periodontitis patients and healthy controls and the NET responses to periodontal pathogens	191
6.1 Comparison between NET release in periodontitis patients and self-reported healthy controls	193
6.1.1 Selection of test subjects.....	193
6.1.2 ROS production	194
6.1.3 NET release	198
6.1.4 NADPH oxidase-dependant NET release.....	200
6.1.5 Comparison between ROS production and NADPH oxidase-dependant NET release	202
6.2 NET production by stimulation with periodontal pathogens and comparison with ROS production	204
6.2.1 SEM of periodontal pathogens interacting with NETs.....	204
6.2.2 MNase assay of periodontal pathogen stimulated-NET release	208
6.2.3 ROS production in response to periodontal pathogens	209
6.2.4 Correlation analysis between NET release and ROS generation in response to periodontal pathogens.....	211
Discussion	213

CHAPTER 7 RESULTS

Characterisation of periodontal pathogens and their susceptibility to killing by histone	218
7.1 Characterisation of periodontal pathogens	219
7.1.1 PCR identification of bacteria	219

7.1.2 Gram stain and cell morphology analysis.....	226
7.1.3 Haemolysis and colony morphology	230
7.1.4 Catalase testing	231
7.1.5 Summary of identification	232
7.2 Susceptibility of periodontal pathogens to killing by histones	234
7.2.1 Spectrophotometric analysis.....	234
7.2.2 Plating method (colony count)	236
7.2.3 Fluorometric quantification of bacterial growth.....	238
Discussion	243
CHAPTER 8 RESULTS	
DNase expression by periodontal pathogens and in dental plaque.....	247
8.1 DNase expression by periodontal pathogens.....	248
8.1.1 DNase test plate assay	248
8.1.1.1 Duration of incubation of test plates.....	249
8.1.1.2 Plate-based assay of periodontal pathogens	250
8.1.2 ‘Gel-based assay’ of DNase activity in bacterial broth culture	252
8.1.2.1 Optimum duration of ‘gel-based assay’	252
8.1.2.2 DNase standards	253
8.1.2.3 Stability of DNase	256
8.1.2.4 Gel-based assay of periodontal pathogen DNase activity	257
8.1.3 Summary of DNase expression by periodontal pathogens by both methods.....	261
8.2 <i>In vivo</i> DNase activity in gingival inflammation	263
8.2.1 Clinical measure of inflammation	263
8.2.2 DNase activity within biological samples	265
Discussion	267
CHAPTER 9 CONCLUDING REMARKS	271
9.1 Mechanism of NET release	272
9.2 Microbial interactions with NETs.....	274
9.3 NETs in periodontitis	277
References.....	281
APPENDIX	299

List of Figures

Figure		Page
1	The periodontium in health and disease	3
2	Clinical presentation of periodontitis	4
3	Proportion of teeth affected by different levels of loss of attachment	5
4	Diagrammatic representation of microbial complexes	8
5	Transmission electron micrograph of a neutrophil	12
6	Blood smear stained with the Romanowsky stain	12
7	Electron micrograph of a neutrophil phagocytosing a bacterium	13
8	Schematic of the generation of reactive oxygen species	15
9	Immunostaining of IL-8 stimulated NETs	19
10	SEM of NETs showing smooth and globular domains	20
11	Immunofluorescent staining of PMA-stimulated NETs	21
12	Immunostaining of neutrophils stimulated with TNF α	25
13	Immunostaining of pneumococci trapped in NETs	27
14	SEM of NET capturing the yeast <i>C. albicans</i>	27
15	SEM of parasite <i>L. amazonensis</i> captured in NET	27
16	Serum inhibits NET formation	38
17	NETs trapping <i>S. pneumoniae</i>	48
18	Toluidine blue staining of NETs in purulent crevicular exudate	54
19	TEM of pocket epithelium	54
20	Immunofluorescent staining of gingival tissue sections	55
21	Variation in NET production between donors	56
22	DNase test plate flooded with TBO	97
23	Binarised image of Figure 22	98
24	Fluorometric detection of SYTOX [®] stained calf thymus DNA	107
25	Fluorescent time course analysis using a range of cell concentrations	109
26	Time course fluorescence and visualisation of PMA stimulated NET production	111
27	MNase assay of NET release from PMA stimulated cells	113
28	Microscopic images of cells used for assay in Figure 27	114
29	MNase assay of NET release from <i>F. nucleatum</i> stimulated cells	115
30	End-point fluorescence and MNase values of various cell concentrations	116
31	Validity of inferring one assay value from the other based on equation of trend line	117
32	SYTOX [®] stained NETs produced in FCS supplemented media	120
33	Effect of FCS supplementation on MNase detection of NETs	121
34	SYTOX [®] stained neutrophils in BSA supplemented RPMI	123

Figure		Page
35	Effect of BSA and FCS on real-time fluorescence	125
36	Effect of BSA plate blocking and/or FCS supplementation of media	127
37	Effect of PMA concentrations on NET release.	129
38	Dose response of opsonised <i>S. aureus</i> on NET release	131
39	Effect of DPI on ROS production	140
40	Effect of DPI on MNase assay of NET production	141
41	Time course analysis of the effect of DPI on cell viability	142
42	Effect of DPI on cell viability detected by SYTOX [®] fluorescence and MNase assay	144
43	Analysis of cytochalasin B on peak ROS production	146
44	Analysis of cytochalasin B on NET production	147
45	Effect of DPI and/or cytochalasin B on real-time fluorescence	149
46	Effect of DPI and/or cytochalasin B on MNase assay	151
47	Effect of SOD on peak ROS production	153
48	Effect of SOD on MNase assay of NET production	154
49	Effect of curcumin on peak ROS production	155
50	Effect of curcumin on NET release	156
51	Effect of sodium azide on peak ROS production	158
52	Effect of sodium azide on NET production	159
53	Peak ROS production in dHL60 cells	170
54	RT-PCR analysis HL60 cells compared to primary neutrophils	173
55	Densitometric profiles of transcript levels in HL60 cells	175
56	Haematoxylin and eosin staining of HL60 cells	178
57	Immunocytochemical staining of HL60 cells	179
58	SYTOX [®] stained DNA in dHL60 cells	181
59	Real time fluorescence of dHL60 cells with and without DPI	183
60	MNase assay of dHL60 cells with and without DPI	184
61	Peak ROS production by dHL60 cells	186
62	Time course of ROS production by dHL60 cells	187
63	Luminol detected ROS production by patient-control pairs	195
64	Isoluminol detected ROS production by patient-control pairs	196
65	Lucigenin detected ROS production by patient-control pairs	197
66	NET release from peripheral neutrophils of patient-control pairs	199
67	NADPH oxidase-dependant NET release from patient-control pairs	201
68	Comparison between luminol-dependant ROS and NADPH oxidase-dependant NET release	203
69	SEM of neutrophils stimulated with periodontal pathogens	206
70	MNase assay of neutrophils in response to periodontal pathogens	208
71	ROS production in response to periodontal pathogens	210
72	Correlation between MNase assay and ROS detection	212

Figure		Page
73	PCR amplification of species specific genes in bacterial mixes	222
74	Gram stains of bacterial cultures	227
75	Haemolysis by periodontal pathogens	231
76	Spectrophotometric analysis of bacteria with pen-strep	235
77	Spectrophotometric analysis of histone	236
78	Colony count analysis of bacteria exposed to pen-strep	237
79	Percentage growth of periodontal pathogens with mixed histone measured by plating out method	238
80	Standard curve of SYTOX [®] detection of <i>F. nucleatum</i> subsp. <i>polymorphum</i>	239
81	Fluorometric quantification of the antimicrobial activity against periodontal pathogens	241
82	Time-course analysis of DNase test agar plates	250
83	Zone ratio of DNA hydrolysis on DNase test agar plates	251
84	Time-course analysis of DNA degradation	253
85	DNA degradation by bovine pancreatic DNase standards in PBS or culture media	255
86	Degradation of bovine pancreatic DNase at 37°C	257
87	Gel based assay of membrane bound DNase activity in periodontal pathogens	259
88	Gel based assay of secreted DNase activity in periodontal pathogens	260
89	Clinical measures of inflammation during the 21 day experimental model of gingivitis	264
90	Gel based assay of DNase activity in biological samples	266
91	Schematic of relationship that may exist between NET production and DNase production	279
	Appendix	
92	Gene alignments for design of primers	300
93	Effect of low PMA concentrations on NET release	304
94	Time course analysis of the effect of DPI on cell viability	305
95	Effect of DPI on cell viability detected by SYTOX [®] fluorescence	306
96	Kinetics of PMA stimulated ROS production	306
97	Primer specificity for <i>A. naeslundii</i> and <i>A. viscosus</i>	307

List of Tables

Table		Page
1	Publications reporting extracellular traps	36
2	Stimuli used to induce NETs	68
3	Modulators of NET release	70
4	Primers and conditions used for gene expression analysis in HL60 cells	73
5	Antibodies and dilutions used for immunocytochemical staining	79
6	Oral microorganisms used in this study	80
7	Primers and PCR conditions used for bacterial identification	88
8	OD values of bacteria	94
9	Ages of volunteers	193
10	Bacterial mixes used for PCR analysis	220
11	Catalase production by periodontal bacteria	232
12	Summary of bacterial identification tests	233
13	Summary of detected bacterial DNase expression	262

Abbreviations

AFU	arbitrary fluorescent units
AMP	antimicrobial peptide
ANCA	antineutrophil cytoplasm autoantibody
ATCC	American type culture collection
BSA	bovine serum albumin
bp	base pairs
CAL	clinical attachment loss
cDNA	complementary DNA
CDT	cytolethal distending toxin
CEJ	cemento-enamel junction
CGD	chronic granulomatous disease
cytoB	cytochalasin B
dHL60	differentiated HL60
DMSO	dimethylsulphoxide
DNase	deoxyribonuclease
DPI	diphenylene iodonium
FCS	foetal calf serum
FeLV	feline leukemia virus
fMLP	N-formyl-methionyl-leucyl-phenylalanine
GAS	group A streptococci
GCF	gingival crevicular fluid
GM-CSF	granulocyte-macrophage colony stimulating factor
GO	glucose oxidase
HET	heterophil extracellular trap
HK	high molecular weight kininogen
HNK	hemin, NAM, vitamin K
IL	interleukin
IFN	interferon
Ig	immunoglobulin
Ipa	invasion plasmid antigen
ISG	interferon stimulated genes
kV	kilovolt
LOA	loss of attachment
LPS	lipopolysaccharide
M	molar
MCET	mast cell extracellular trap
MMP	matrix metalloproteinase
MNase	micrococcal nuclease
MOI	multiplicity of infection
MPO	myeloperoxidase
mRNA	messenger ribonucleic acid
NADPH	nicotinamide adenine dinucleotide phosphate
NAM	N-acetylmuramic acid
NET	neutrophil extracellular trap

OD _{600nm}	optical density at 600 nanometres
PAD4	peptidylarginine deiminase 4
PBS	phosphate buffered saline
PCR	polymerase chain reaction
PDL	periodontal ligament
PFA	paraformaldehyde
PKC	protein kinase C
PMA	phorbol 12-myristate 13-acetate
PMNL	polymorphonuclear leukocyte
PR3	proteinase 3
PS	phosphatidylserine
PTX3	pentraxin 3
RANKL	receptor activator of NFκB ligand
rcf	relative centrifugal force
RLU	relative light units
RNase	ribonuclease
ROS	reactive oxygen species
rRNA	ribosomal RNA
RT-PCR	reverse transcriptase polymerase chain reaction
SD	standard deviation
SEM	scanning electron microscopy
SLE	systemic lupus erythamatosi
SOD	superoxide dismutase
STBM	syncytiotrophoblast microparticles
SVV	small vessel vasculitis
TBO	toluidine blue O
TIMP	tissue inhibitors of matrix metalloproteinases
TEM	transmission electron microscopy
TLR	toll-like receptor
TNF	tumour necrosis factor

CHAPTER 1 INTRODUCTION

1.1 Periodontal diseases

Periodontitis is an inflammatory lesion mediated by host-bacterial interactions which results in a non-resolving inflammation that leads to local connective tissue attachment loss from the tooth surface, loss of alveolar bone and ultimately tooth loss (Gaffen *et al.* 2008). Indeed, periodontal disease is the leading cause of tooth loss in the western world (Papapanou 1999). Over 1200 bacterial phlotypes have been identified within the subgingival biofilm (Paster *et al.* 2009) and they have been classified by cluster analysis into complexes associated with varying degrees of health and disease (Socransky *et al.* 1998). Outward signs of infection occur in periodontitis with the destruction of the supporting structures arising through dysregulated inflammatory processes. Indeed, the bacteria themselves are estimated to account only for 20% of disease prevalence (Grossi *et al.* 1994), the remainder of host tissue damage being attributed to the host response.

Pathogenic bacteria within the dental plaque biofilm which colonise the gingival crevice initiate an inflammatory response, the initial signal being through a microbial-epithelial interaction (Dale 2002; Milward *et al.* 2007). When the inflammation is restricted to the gingiva the condition is known as gingivitis (Figure 2a). The disease becomes periodontitis when the inflammatory lesion progresses to include the supporting periodontal tissues i.e. the periodontal ligament (PDL), alveolar bone and root cementum. It is the host-bacterial cellular and molecular interactions that ultimately results in the destruction of the periodontal tissues (Page *et al.* 1997). Tissue destruction begins within the gingival connective tissues and leads to apical migration of the junctional epithelium, resulting in gingival recession, the formation of periodontal pockets, and the exposure of the cementum or root dentine (Figure 1). The

cemento-enamel junction provides a point of reference against which to measure the extent of periodontal destruction, the so called ‘clinical attachment level’.

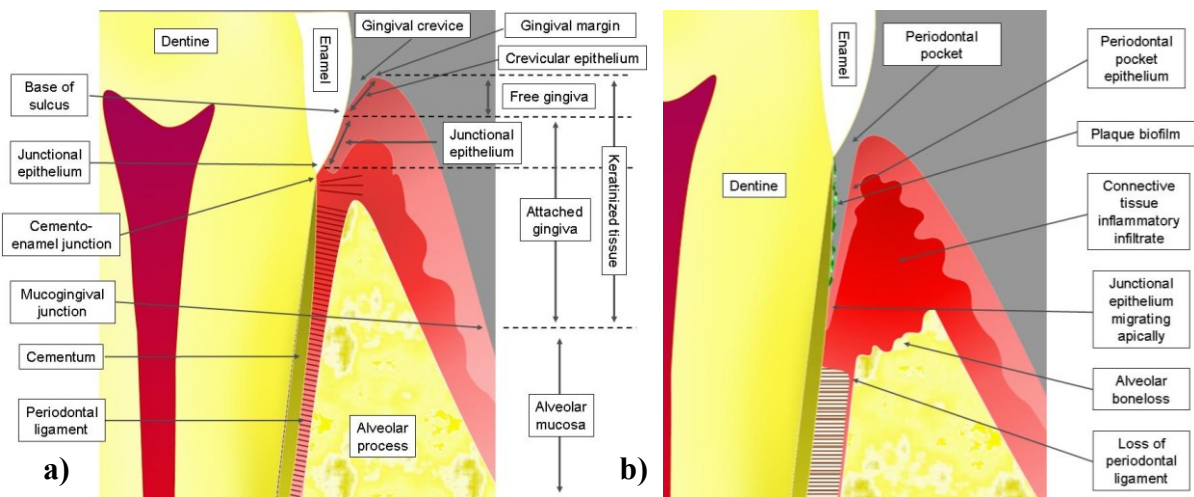


Figure 1. The periodontium in a) health and b) disease. Courtesy of M.R. Milward.

Attachment loss continues when the PDL is progressively damaged and since the PDL anchors the tooth to the alveolar bone, bone loss follows resulting from host-mediated enzyme and oxygen radical release. In addition to the direct bone destruction by immune cells, the osteoclast-osteoblast balance can become modified, favouring osteoclastic bone resorption. This can result from increased osteoclastogenesis which is primarily stimulated by receptor activator of NF κ B ligand (RANKL) expressed on the surface of osteoblasts and from activated T lymphocytes. In addition, cytokine expression such as high interleukin-1 can promote osteoclastogenesis (Assuma *et al.* 1998). Alternatively, bone formation can be down regulated via tumour necrosis factor α (TNF α) expression from macrophages and T lymphocytes (Baker 2000). As bone resorption progresses the tooth becomes mobile within its socket and is eventually lost unless treatment is initiated. Destruction of the alveolar bone itself is detectable radiographically (Figure 2b).



Figure 2. Clinical presentation of periodontitis
a) bleeding on probing, gingival inflammation and gingival recession, **b)** x-ray showing bone resorption. Courtesy of Prof I. Chapple.

Clinically, the severity of periodontitis can be defined by the formation of pockets measurable by probing. A normal probing pocket depth is approximately 0.5-3.0 mm (Chapple *et al.* 2002). Alternatively, clinical attachment loss (CAL) can be measured from the level of the cemento-enamel junction (CEJ) to the base of the clinical pocket. This has the advantage of using a fixed reference point (the CEJ), thus eliminating false results caused by gingival recession and gingival inflammation or swelling. CAL measures are the most reliable for determining cumulative tissue loss.

1.1.1 The prevalence of periodontitis

Epidemiological studies have shown that chronic gingivitis is found in the majority of the population (Morris *et al.* 2001). Indeed, the mouth is inhabited by a multitude of commensal microorganisms whose accumulation reportedly initiate gingivitis (Loe *et al.* 1965). The most recent assessment of the prevalence of periodontal disease in the UK population was provided by the 1998 Adult Dental Health Survey (Morris *et al.* 2001). This was the fourth decennial survey to assess oral health in UK adults and involved the examination 3817 individuals. Data demonstrated that 72% of the population surveyed had evidence of visible plaque on their teeth and 43% of the population had developed CAL on at least one tooth, which in this survey was defined as a loss of attachment (LOA) of 3.5 mm or more. When analysing each

tooth individually only 10% of those examined showed attachment loss of greater than 3.5mm. Figure 3 shows the distribution of attachment loss in those individuals with severe attachment loss of 5.5mm and greater.

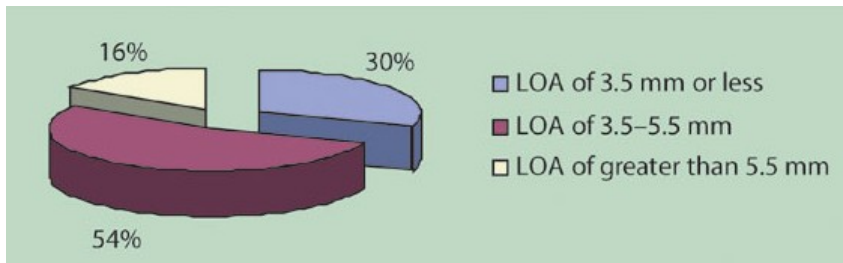


Figure 3. Proportion of teeth affected by different levels of loss of attachment (LOA; measured from CEJ) in people with some LOA in excess of 5.5 mm (Morris *et al.* 2001)

1.1.2 Risk factors for periodontitis

Putative risk factors for periodontitis include genetic predisposition (Michalowicz *et al.* 1991), smoking (Baharin *et al.* 2006), diabetes mellitus (Mealey *et al.* 2006), poor oral hygiene, post menopausal hormonal changes (Baltacioglu *et al.* 2006) and the more recently demonstrated low plasma micro-nutrient levels (Chapple *et al.* 2007c). Some may be ‘risk indicators’ i.e. share common risk factors so present together, rather than be true risk factors in which the risk factor itself increases the chance of developing periodontal disease and its removal will trigger disease resolution (Beck *et al.* 1995).

1.1.3 The progression of periodontitis

Periodontitis is always preceded by gingivitis (Kinane *et al.* 2005). Gingivitis may be seen at almost any age and does not always progress to periodontitis with approximately 10% of the population appearing to be resistant to periodontitis (Loe *et al.* 1986). The early lesion of chronic marginal gingivitis develops after 4 days of plaque accumulation and is histologically

detectable after 7 days (Page *et al.* 1976). Periodontitis patients may have had gingivitis for several years before the disease progressed to periodontitis (Page *et al.* 1976). The transition may be triggered by impairment of host defences, introduction of a new pathogen into the biofilm, or activation of a destructive immune-inflammatory process in susceptible patients (Samaranayake 2002).

Periodontitis, like most inflammatory diseases, shows discontinuous progression meaning it is subject to episodes of disease progression interspersed with periods of quiescence. This hypothesis was first described as the random burst theory (Socransky *et al.* 1984). Chronic periodontitis, unlike other forms of periodontitis such as juvenile periodontitis, is not seen before early adolescence in patients who are otherwise systemically healthy, but is believed to develop from adolescence (Clerehugh *et al.* 1990; Clerehugh *et al.* 1995) and increases in prevalence with increasing age, to 85% of patients over 65 years of age (Morris *et al.* 2001).

1.2 The role of bacteria in periodontal disease

The sub-gingival flora is complex so a single causative pathogen for periodontal disease cannot be identified (Socransky *et al.* 1984). The theory that a limited number of specific species of bacteria trigger periodontal inflammation is known as the 'specific plaque hypothesis' (Loesche 1976; Slots 1999). In support of this theory are the findings that in 'necrotising ulcerative gingivitis' the prime causative pathogens are *Fusobacteria* sp. and spirochaetes, and in aggressive periodontitis *Aggregatibacter actinomycetemcomitans* appears to be closely involved (Slots 1999). The opposing hypothesis, known as the 'non-specific plaque hypothesis' (Theilade 1986) proposes that a combination of non-specific bacteria are

responsible and will be pathogenic when a threshold volume of plaque is reached. It has been reported that the diversity of bacterial species within periodontal pockets is substantial and varies between different samples from different patients and also within the same patient. The non-specific plaque theory implies that **any** plaque will cause periodontal disease. Current thinking however supports the ‘environmental’ or ‘ecological’ plaque hypothesis (Haffajee *et al.* 1991; Marsh *et al.* 2009). In this case, Marsh argues that a change in the microbial environment can initiate a shift in the balance of bacteria within the plaque biofilm which may confer pathogenicity. However, if the change in the microbial environment results in reduced growth of certain commensals, for example *S. sanguis*, pathogenic bacteria may not necessarily benefit because they rely upon mutual support to survive. This theory has potential therapeutic implications i.e. that periodontal disease could be prevented by improved oral hygiene measures which aim to create a shift in biofilm composition from a pathogenic to a health-associated microflora. The plaque stimulates an inflammatory response within the host tissues, part of which creates an increase in the flow of gingival crevicular fluid (GCF). This provides an abundance of host molecules some of which can be metabolised by the Gram negative anaerobic bacteria normally present in the plaque biofilm. The relative number of Gram negative anaerobic species increases in the microbial plaque, suppressing the growth of other species found in a healthy flora. The bacteria then express virulence factors to avoid or combat the host defence strategy and establish an infection. As periodontal disease progresses and the gingival crevice deepens to become a periodontal pocket, the micro-environmental conditions become more anaerobic, further aiding the growth of obligate anaerobic bacteria. Whilst numerous studies have investigated the composition of plaque, Socransky *et al.* (1998) employed cluster analysis on large numbers of plaque samples from

healthy and diseased sites and defined 5 bacterial complexes ranked by the strength of the groups relationship with clinical measures of periodontitis (Figure 4).

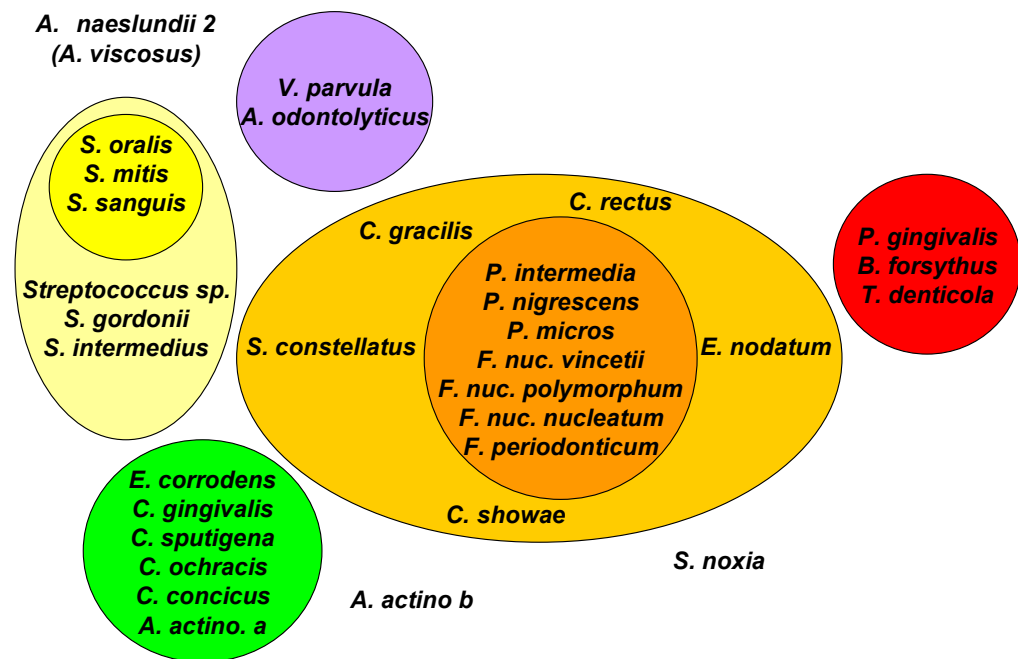


Figure 4. Diagrammatic representation of the relationship of species within microbial complexes and between microbial complexes. Coloured groups represent bacteria found together in pathogenic plaque and their relationship to the clinical parameters of periodontitis, the red complex showing the highest association with disease. (Socransky *et al.* 1998)

The normal subgingival flora consists of mainly facultative (both aerobic or anaerobic capabilities) anaerobic Gram positive bacteria, and only 5% spirochaetes and motile rods. Generally speaking, as periodontal disease progresses the proportion of anaerobic, Gram negative, spirochaetes and other motile bacteria increases. In chronic periodontitis approximately 75% of cells are Gram negative of which 90% are strict anaerobes (Samaranayake 2002). This shift in microbial composition is represented by a change from mainly purple complex bacteria through to a large proportion of red complex bacteria in sites of active disease.

1.3 The role of the host in periodontal disease

The destruction of the periodontal tissues that constitutes ‘inflammatory periodontitis’ results from the interaction between the host and the pathogenic bacteria. An inflammatory response is mounted within the host tissues at the site of infection primarily consisting of an innate immune response and ultimately resulting in the activation of the acquired immune response and a subsequent increase in antibodies in the GCF against bacteria found in the gingival crevice or periodontal pocket (Tew *et al.* 1985). These responses initially have a protective function and aid the phagocytosis of pathogens and prevent their spread. Indeed, the importance of neutrophils for the maintenance of periodontal health can be observed in patients with cyclic neutropenia in which periodontal inflammation and destruction are associated with decreased peripheral neutrophil numbers (Matarasso *et al.* 2009). However, the host inflammatory response can also lead to a damaging ‘hypersensitivity reaction’. The innate immune system is the first line of defence and consists of cells such as monocytes which then differentiate into phagocytic macrophages and antigen presenting dendritic cells (Alberts *et al.* 2002), and also neutrophils which are thought to be the main cause of damage to host tissues. This occurs through the release of reactive oxygen species (ROS) and degradative proteolytic agents such as matrix metalloproteinases (MMPs) and serine proteases especially neutrophil elastase. In addition, ROS produced by neutrophils can inactivate protease inhibitors such as alpha-1 antitrypsin, a serine proteinase inhibitor (serpin) produced to protect the host tissue from the same fate as the microorganism at the hands of serine proteinases (Henson *et al.* 1987). Indeed, it has been shown *in vivo* that GCF levels of free neutrophil elastase, i.e. not bound by serpins, is increased in periodontitis sites compared to gingivitis sites (Figueredo *et al.* 2005). Neutrophils are recruited to the periodontal tissues from the blood stream in a process requiring margination, tethering and rolling, adhesion and

finally transmigration. This occurs in response to bacterial products themselves such as LPS and formyl peptides or by cytokines secreted by other host cells in response to the bacterial challenge. For example monocytes secrete IL-1 which up-regulates endothelial expression of adhesion molecules such as ICAM-1 thereby facilitating adhesion of neutrophils via $\beta 2$ integrin. Complement C5a and leukotriene B4 then facilitate the endothelial transmigration (diapedesis) by increasing vascular permeability, and cytokines such as IL-8 with a high specificity for neutrophils create a chemotactic gradient across the endothelium to direct the neutrophils to the site of inflammation. Although these cytokines are essential for homeostasis of the healthy periodontium, in diseased tissue cytokine expression is increased. In chronic periodontitis it has been shown that patients have elevated plasma levels of interferon- α (IFN- α) compared to healthy controls (Wright *et al.* 2008). Elevated levels of IFN- α affect neutrophil function, potentially by priming, as microarray analysis of messenger RNA (mRNA) derived from hyperactive peripheral blood neutrophils in periodontitis patients demonstrated a panel of interferon stimulated genes (ISGs) to be up-regulated relative to those from healthy control individuals. This up-regulation of ISGs was reduced to the levels of healthy controls by successful periodontal treatment indicating that the increased plasma IFN- α levels were associated with the active state of periodontal disease. The up-regulation of ISGs could be reproduced in peripheral neutrophils of healthy controls by priming with IFN- α , which resulted in enhanced neutrophil ROS production (Wright *et al.* 2008). ROS production has previously been found to be both hyperactive (i.e. in resting cells) and hyper-reactive (i.e. in stimulated cells) in the peripheral neutrophils of patients compared to controls (Matthews *et al.* 2007a; Matthews *et al.* 2007b). The hyper-reactive neutrophil phenotype was also demonstrated *in vivo* by Figueredo *et al.* (2005). The ratio of lactoferrin (released normally from neutrophils) to elastase (released only upon activation) was used to assess the

activity of neutrophils *in vivo* in the gingival crevice independently of neutrophil number. It was found that the ratio of elastase:lactoferrin and therefore neutrophil activity was increased in GCF samples from periodontal patients compared to those with chronic gingivitis. This was true not only when deep inflamed pockets were sampled from the patients with periodontitis, but also when shallow pockets were sampled with a similar level of inflammation to the pockets of patients with gingivitis. It was also found that lactoferrin levels, used as a surrogate marker of total neutrophil number, were in fact higher in gingivitis patients than in periodontitis patients. This suggests that although gingival inflammation is associated with increased neutrophil recruitment compared to healthy sites, it is the **activity** of those neutrophils that determines whether the inflammation is mild or severe. To date, peripheral neutrophils from periodontitis patients have been found to be hyper-reactive with regards to ROS generation primarily in response to Fc γ receptor stimulation (i.e. with opsonised *S. aureus*), and unstimulated neutrophils have also been shown to express higher levels of active elastase and IL-1 β (an inducer of bone resorption) (Figueredo *et al.* 2000) and produce higher levels of ROS (Matthews *et al.* 2007a) than peripheral neutrophils from healthy individuals.

1.4 Neutrophils and disease

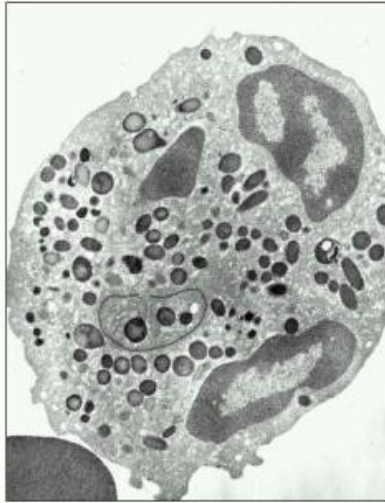


Figure 5. Transmission electron micrograph (TEM) of a neutrophil. The single nucleus is multilobed, however in this view connections are out of plane (Nichols *et al.* 1971) (Alberts *et al.* 2002)

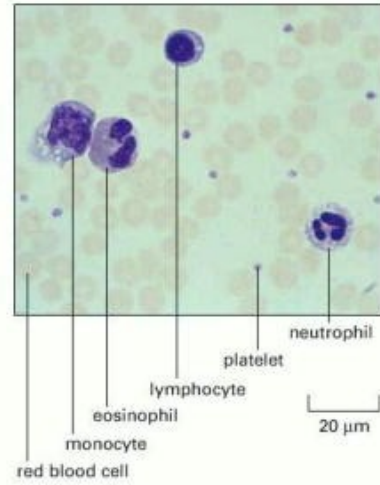


Figure 6. Light micrograph of a blood smear stained with the Romanowsky stain. A neutrophil with multilobed nucleus is visible along with other immune cells (Alberts *et al.* 2002).

Neutrophils are also known as polymorphonuclear leukocytes (PMNL) due to their multilobed nucleus (Figures 5 and 6). Their function is to phagocytose and kill microorganisms, particularly bacteria. For this purpose they contain abundant granules containing hydrolytic enzymes, proteolytic enzymes and other antimicrobial peptides (AMPs) such as defensins, to degrade the internalised microorganism (Borregaard *et al.* 1997).

Neutrophils, are fundamental cells of the innate immune system. The innate immune system mounts an immediate and low specificity defence against invading microorganisms regardless of whether the pathogen has been encountered previously. The adaptive immune system acts later in the infection with a response highly specific to the pathogen (Alberts *et al.* 2002).

1.4.1 Neutrophil activation

Neutrophils originate from the bone marrow and differentiate from granulocyte/macrophage progenitor cells prior to entering the blood circulatory system. Here, their half life is approximately 6.7 hours, and up to 1-2 days when they have infiltrated tissues (Squier *et al.* 1995). The neutrophil targets the pathogen for phagocytosis via a variety of cell-surface receptors, such as, pattern recognition receptors e.g. toll-like receptors (TLRs), Fc γ receptors for the Fc region of antibodies, and receptors for C3b, an opsonising molecule of the complement system (Garcia-Garcia 2005). Binding of the pathogen to any of these receptors triggers the neutrophil to engulf the microorganism (Figure 7) and internalise it within a vacuole called a phagosome. The contents of the neutrophil granules (lysosomes) are then released as it fuses with the phagosome to create a phagolysosome (Tapper 1996).

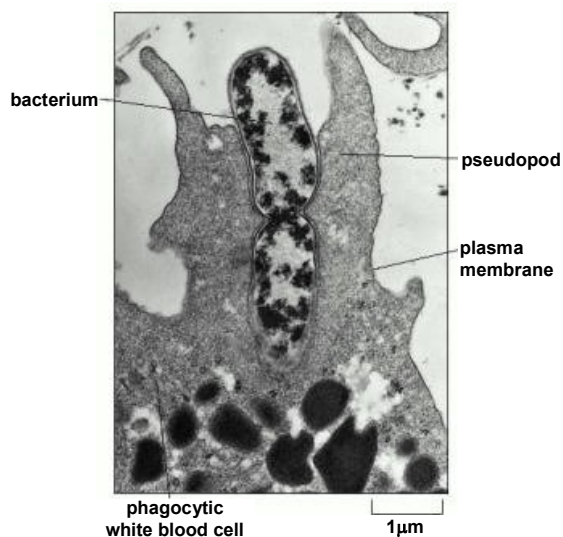


Figure 7. Electron micrograph of a neutrophil phagocytosing a bacterium that is currently undergoing division. (Williams and Fudenberg, *Phagocytic Mechanisms in Health and Disease*. New York: Intercontinental Book Corporation, 1971; (Alberts *et al.* 2002)

1.4.2 Neutrophil killing mechanisms - Non-oxidative and oxidative

The non-oxidative killing mechanisms of neutrophils involve the release of proteases and AMPs contained within neutrophil granules. There are three types of neutrophil granule released in the following order (Faurischou *et al.* 2003),

- specific (secondary)
- gelatinase (tertiary)
- azurophilic (primary)

The specific and gelatinase granules contain lysozyme, lactoferrin, gelatinase and metalloproteases. Their granule membranes also contain 95% of the cells cytochrome b_{558} which makes up the NADPH oxidase (nicotinamide adenine dinucleotide phosphate-oxidase) enzyme. The azurophilic granules are so called because they stain with the dye azure A, and are the only granules that contain myeloperoxidase (MPO) required to enzymatically convert H_2O_2 (a secondary product of NADPH oxidase, Figure 8) to hypochlorous acid (HOCl). They also contain neutrophil elastase, and AMPs such as defensins. Defensins are small positively charged peptides which make up 15% of a neutrophils protein content (Borregaard *et al.* 1997). The mechanism of their anti-microbial activity is uncertain but the defensin may insert into the microbial membrane to disrupt its integrity (Lichtenstein 1991), as well as that of the bacteria's DNA (Gera *et al.* 1991).

The oxidative killing mechanism employed by neutrophils is via the non-mitochondrial generation of ROS through a process known as the respiratory burst. Assembly of the NADPH oxidase responsible for ROS generation requires phosphorylation of the four cytosolic subunits (p47-phox, p40-phox, p67-phox and Rac) to enable combination with cytochrome b_{558} (comprised of gp91phox and p22phox) (Figure 8). Once the NADPH

oxidase is assembled in the vacuole membrane, it reduces oxygen to superoxide anions ($O_2^{\cdot-}$) which form H_2O_2 , either spontaneously or via superoxide dismutase (SOD), and ultimately with the help of MPO, form hypochlorous acid. HOCl chlorinates bacterial targets such as, the origin of replication site for DNA synthesis and membrane proteins, to bring about bacterial death.

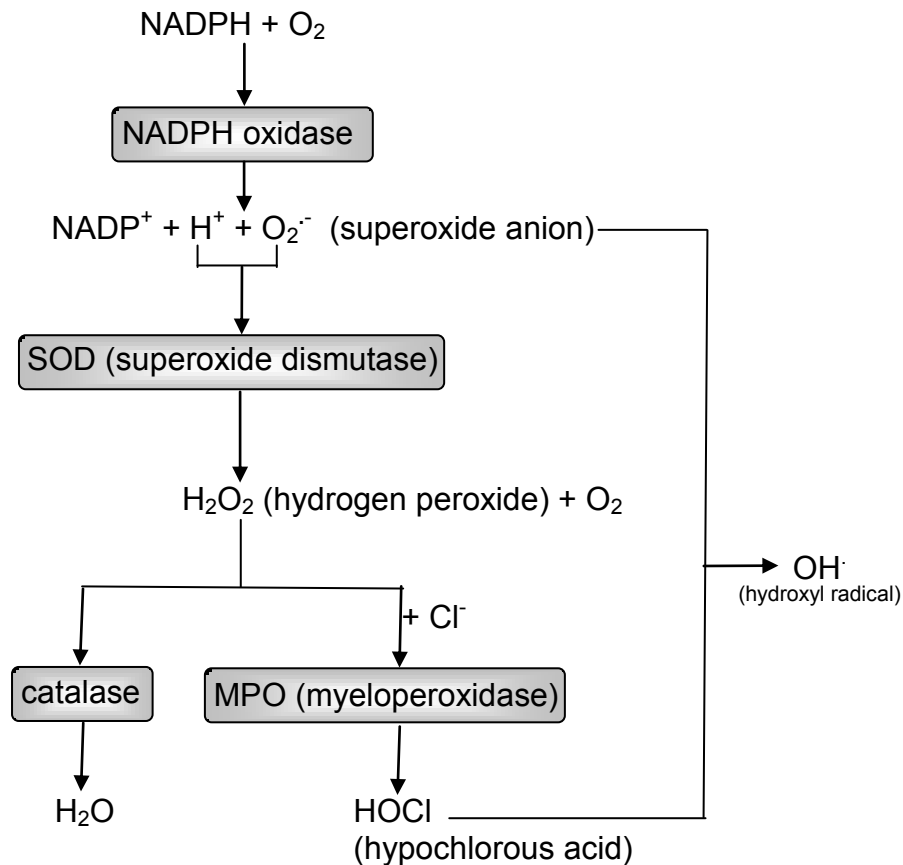


Figure 8. Schematic of the generation of reactive oxygen species (Robinson 2008)

ROS also have an indirect bactericidal action as they can activate granule proteases. Potassium ions (K^+) enter the phagosome via Ca^{2+} channels to compensate for the charge difference created by the transfer, across the vacuole membrane, of electrons when $O_2^{\cdot-}$ is released into the vacuole via NADPH oxidase (Ahluwalia *et al.* 2004). The high K^+ concentration within the vacuole activates latent proteases released from the anionic sulphated proteoglycan granule matrix (Ahluwalia *et al.* 2004). The importance of ROS to the function

of neutrophils is demonstrated in chronic granulomatosis disease (CGD). This is a disorder in which genetic defects results in dysfunctional NADPH oxidase, and thus a failure to generate ROS. Individuals with this disorder are susceptible to frequent and life-threatening bacterial and fungal infections (Dinauer 2005).

ROS can also act extracellularly to cause damage to the surrounding tissues. One particular cell type that ROS acts upon are osteoclasts, with ROS activation culminating in increased bone resorption. Evidence shows ROS are capable of both increasing osteoclast numbers (Garrett *et al.* 1990) and activating osteoclasts (Bax *et al.* 1992). In addition, ROS can damage various components of the connective tissues as they have been found to degrade proteoglycans of alveolar bone and the periodontium (Moseley *et al.* 1997). This yields glycosaminoglycans which can be further degraded, although the sulphated glycosaminoglycans are more resistant to ROS degradation than the unsulphated forms. Type I collagen has also been shown to be susceptible to degradation by ROS *in vitro* (Nguyen *et al.* 2005). ROS can act directly to cause fragmentation and polymerisation or indirectly by modifying the collagen and making it more susceptible to proteolysis. In tissues such as in blood vessels, high levels of extracellular superoxide dismutase enzyme is normally present which protects the type I collagen from the damaging effects of ROS (Petersen *et al.* 2004). Aside from the obvious destructive effect that collagen degradation will have on the connective tissues, it has also been found *in vitro* to increase neutrophil adhesion and chemotaxis (Monboisse *et al.* 2000). This process occurs when the collagen is in a glycated state, a modification facilitated by the oxidative processes of ROS. ROS can also disrupt the protective function of tissue inhibitors of matrix metalloproteinases (TIMPs) either by directly modifying the molecules or indirectly by preventing TIMP expression (Hadjigogos 2003).

Neutrophil apoptosis is vital to the resolution of bacterial infection. The size and duration of the neutrophil response must be appropriate to fight the infection but must also be confined within the neutrophil membrane in order to limit collateral host tissue damage. It is important that neutrophils undergo apoptosis and not necrosis, which would result in their toxic contents being uncontrollably released externally and subsequently causing substantial damage to the surrounding tissues. It is thought that the phagocytic event may alter gene expression to trigger apoptosis (Kobayashi *et al.* 2003). A further theory is that the respiratory burst acts as an apoptosis trigger so the neutrophil undergoes apoptosis shortly following phagocytosis (Watson *et al.* 1996).

1.4.3 Extracellular neutrophil killing mechanisms

Neutrophil anti-microbial granules can be released into the extracellular space via degranulation with the aim of degrading microorganisms within the extracellular environment. This may be a more rapid method of killing, however it is also less discriminate and is associated with a higher risk of damage to the host tissues. Tissue damage is primarily caused by serine proteinases such as elastase and cathepsin G (Forsyth *et al.* 1994). Endogenous soluble inhibitors of serine proteinases (serpins), such as alpha-1 antitrypsin and alpha1-antichymotrypsin, may constrain the range of action of these enzymes (Forsyth *et al.* 1994). Recently, neutrophils have been seen to release webs of DNA which physically trap and immobilise microorganisms, preventing their spread within tissues. In addition, this process may also act to localise neutrophils AMPs, limiting the extent of damage caused to otherwise healthy tissue or conversely may serve to concentrate damaging proteases within

the locality and increase local tissue damage. These webs are known as neutrophil extracellular traps (NETs; (Brinkmann *et al.* 2004) and are discussed below (1.5).

1.4.4 Microbial mechanisms for evading killing by neutrophils

Neutrophils are a primary line of defence against infection enabling time for an adaptive immune response to be mounted. Without them, as in conditions of neutropenia such as those induced by chemotherapy, an individual is left immuno-compromised. However, infections can become established even when the innate immune system is functioning correctly. This is because the more virulent bacteria possess strategies for, amongst other things, evading host defences. The strategies for evading neutrophil killing include,

- i) Launching a general survival response such as in group A streptococci (GAS) (Voyich *et al.* 2003).
- ii) Avoiding contact by secretion of chemotaxis inhibitory protein (*S. aureus*; de Haas *et al.* 2004).
- ii) Preventing phagocytosis by secretion of actin polymerisation inhibitors (*Yersinia enterocolitica*) (Grosdent *et al.* 2002).
- iv) Release of exotoxins e.g. leukotoxin from *A. actinomycetemcomitans* (Baehni *et al.* 1979).
- v) Surviving intracellularly e.g. *P. gingivalis* within oral epithelial cells (Lamont *et al.* 1995).
- vi) Inducing cell death such as GAS which produce streptolysin O (Sierig *et al.* 2003).
- vii) Avoiding killing by NETs such as deoxyribonuclease (DNase) expression by *Streptococcus pyogenes* (Buchanan *et al.* 2006).

1.5 Neutrophil extracellular traps (NETs)

Neutrophil extracellular traps are strand-like webs of decondensed chromatin, which also contain granule proteins (Brinkmann *et al.* 2004). The granule proteins present are derived from all three types of neutrophil granule. Azurophilic granule proteins such as neutrophil elastase (Figure 9 A), cathepsin G and MPO; specific granule proteins e.g. lactoferrin; and tertiary granule proteins e.g. gelatinase. In addition, LL37, a cleaved form of the granule protein cathelicidin has been identified in NETs (*in vitro* and *in vivo*) (Kessenbrock *et al.* 2009), as has the innate immune receptor pentraxin 3 (PTX3) found to originate from specific granules (Jaillon *et al.* 2007). The DNA component of NETs has been shown to be more vital to NET structure than the protein component. When treated with DNase NETs are degraded, but when treated with proteases, NETs remains intact (Brinkmann *et al.* 2004). The exception to this is the parasite *L. amazonensis* which was still killed although at a reduced level, by NETs after digestion with DNase (Guimaraes-Costa *et al.* 2009). This finding however, appears to be exclusive to the killing of parasites.

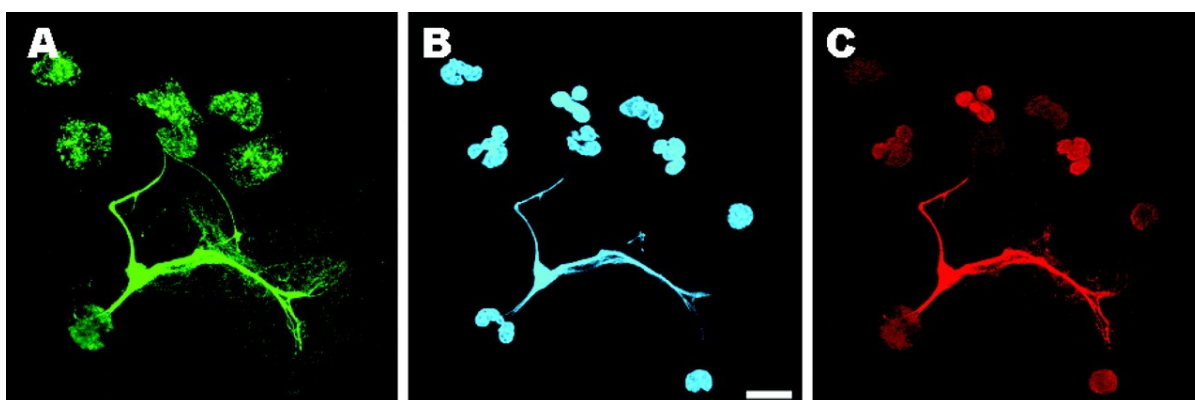


Figure 9. Immunostaining of neutrophils stimulated with IL-8 to produce NETs. A neutrophil elastase, **B** DNA, **C** histone (H2A-H2B)-DNA complex. (Brinkmann *et al.* 2004)

The structure of NETs can be observed by high resolution scanning electron microscopy (SEM) and this approach demonstrates that they consist of relatively smooth regions of 15-17 nm diameter with globular domains of approximately 25-50 nm diameter (Brinkmann *et al.* 2004; Figure 10). Ermert *et al.* (2009) claimed to have observed that murine and human NETs differ in their structure, observing that the globular domains of murine NETs were tightly packed and covered the entire surface. However, the cells used were bone marrow derived mature neutrophils, not peripheral neutrophils as employed in human studies.

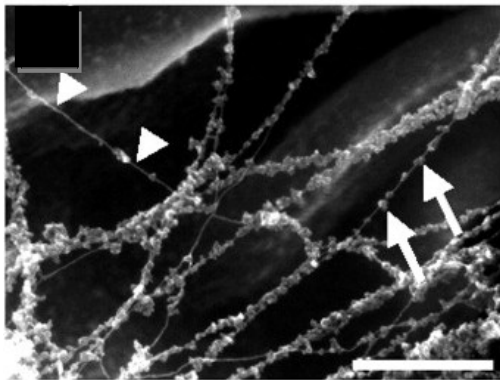


Figure 10. High resolution SEM of NETs showing smooth (arrow heads) and globular (arrows) domains. Bar represents 500 μ m (Brinkmann *et al.* 2004).

Research indicates that NETs are formed by controlled extrusion, rather than random spilling of granule and nuclear contents during necrosis or apoptosis, but NET release does precede apoptosis. Preliminary evidence for this is that NETs form in as little as 10 minutes after cellular activation, a process more rapid than apoptosis (Brinkmann *et al.* 2004). Furthermore, NET production was not accompanied by the release of the cytoplasmic marker lactate dehydrogenase and vital dyes did not enter the cell for at least 2 hours post stimulation, indicating that necrosis is not involved as the cell membrane remained intact (Brinkmann *et al.* 2004). Other findings contrary to apoptotic or necrotic theories of NET release are that IL-8 and lipopolysaccharide (LPS), which prolong the life of neutrophils (Sabroe *et al.* 2003), also induce NET formation. Furthermore, cells have been observed to retain motility during

NET release, and DNA intercalating dyes. which prevent the formation of NETs, do not affect the induction of apoptosis (Brinkmann 2004). In 2007 Fuchs *et al.* used live cell imaging to follow the production of NETs whilst simultaneously monitoring cell viability. They observed that upon stimulation with phorbol 12-myristate 13-acetate (PMA) neutrophils flattened (Figure 11b) and their nuclei lost their characteristic lobular morphology, and filled the majority of the intracellular cytoplasmic space. During this time the chromatin began to decondense so the distinction between euchromatin and heterochromatin was lost. The space between the inner and outer nuclear membrane increased to eventually form distinct vesicles. Neutrophil granule membranes were lost which allowed the release of granule proteins, specifically neutrophil elastase, which then co-localised with chromatin (Figure 11c). A single report by Vitkov *et al.* (2009) contradicts this data by claiming that *in vivo* neutrophil activation lacked this co-localisation step previously observed *in vitro*.

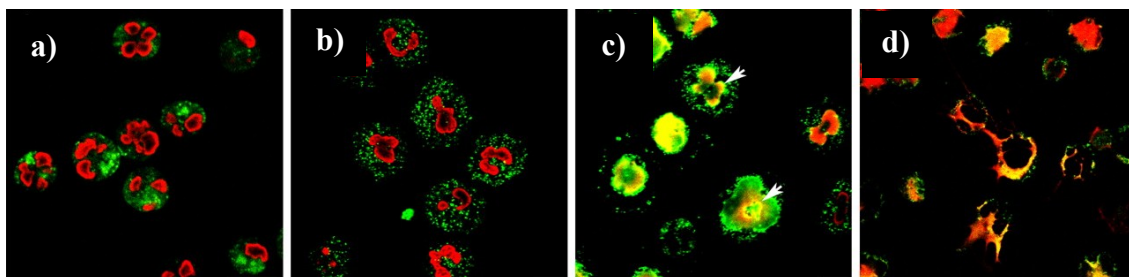


Figure 11. Neutrophils stimulated with PMA and immunofluorescently stained for neutrophil elastase (green), chromatin (red). (a) 0 minutes stimulation – naïve cells have lobulated nucleus (b) 60 minutes - cells have flattened and neutrophil elastase granules are individually visible (c) 120 minutes - granules disintegrated so neutrophil elastase and chromatin are colocalised (yellow) (d) 180 minutes – NETs start to form (Fuchs *et al.* 2007).

After mixing of the nuclear and granule contents, cells began to lose the vital dye calcein blue, indicating loss of membrane integrity and subsequent loss of cytoplasm. At the same time, NETs are first visualised and the cells became Annexin V-positive by binding to phosphatidylserine (PS) on the inner leaflet of the cell membrane. As the cells became

Annexin V-positive and lost vital dye simultaneously, this indicates a rupture of the neutrophil cell membrane. Notably, if the cells had been apoptotic they would have become Annexin V-positive prior to calcein release. Fuchs *et al.* (2007) concluded that NETs were formed during a novel cell death programme that was proven distinct from apoptosis and necrosis. The differences from necrosis were observed visually in that the stimuli used to induce necrosis (secreted pore-forming toxins from *S. aureus*) did not result in extracellular DNA release and, although similar in the loss of nuclear lobules and loss of differentiation between eu- and hetero-chromatin, the nuclear and granule membranes remained intact only during necrosis. It has previously been shown that PMA can exert a cytotoxic effect on neutrophils that is distinct from apoptosis and dependant on ROS (Takei *et al.* 1996) so recent advances in the understanding of NETs may provide an explanation (1.5.1).

1.5.1 Dependence on ROS

A further conclusion from the work of Fuchs *et al.* (2007) was that NET production is dependant on ROS production via the NADPH oxidase. It is known that the neutrophils from patients with CGD are unable to generate ROS due to a deficiency in the NADPH oxidase enzyme responsible for its production. Notably, neutrophils from these patients were also found to be incapable of producing NETs. However, the ability to produce NETs could be induced in the neutrophils of CGD patients by the addition of glucose oxidase (GO), as this enzyme can substitute for the dysfunctional NADPH oxidase to generate hydrogen peroxide. GO was also used with neutrophils from healthy subjects and was shown to significantly increase NET production and restore NET production following application of the NADPH oxidase inhibitor, diphenylene iodonium (DPI). In further investigations catalase was used to

remove H₂O₂ from the system and a reduction in NETs was observed. Conversely the introduction of 3-amino-1,2,4-triazole (AT) to inhibit endogenous catalase activity caused an increase in NET production. This work demonstrated that NET production was not just dependant on ROS production but specifically H₂O₂, which has since been used directly as a stimulus to induce NET release (Neeli *et al.* 2009). The use of DPI has also since been used by multiple research groups as a negative control for NET release (von Kockritz-Blickwede *et al.* 2008; Yousefi *et al.* 2008; Behrendt *et al.* 2010). Significantly, a study utilising neutrophils derived from patients with x-linked gp91^{phox}-deficient CGD was able to demonstrate that using gene therapy, replacement of the absent gp91^{phox} subunit could restore the capacity for NET production (Bianchi *et al.* 2009). After 6 weeks the percentage of neutrophils expressing gp91^{phox} had reached 26-29% and the yeast infections patients had been suffering from, caused by *Aspergillus nidulans* conidia, were resolved. This correlated with the ability of patient neutrophils to produce NETs when challenged with *A. nidulans* and PMA which were subsequently effective in inhibiting growth of conidia and its hyphae. This effect was abrogated when micrococcal nuclease (MNase) was introduced indicating that the fungicidal activity was due to NET-DNA release and not due to another killing mechanism such as phagocytosis. In studies utilising murine NETs, a gp91 knockout mouse (gp91^{-/-}) was used as a model of CGD (Ermert *et al.* 2009). Upon stimulation with 100nM PMA the bone marrow derived mature neutrophils from these mice were incapable of producing ROS or NETs, although the cells exhibited a flattened appearance, as observed in the early stages of NET production. In fact, PMA stimulation promoted cell survival over the 16 hour observation period in this knock-out strain.

Although these data demonstrate that the generation of ROS is involved in the process culminating in NET release, the precise signalling mechanisms linking the two processes are unclear. For example in the case of bovine mastitis it was found that although the proteins in the milk inhibited the respiratory burst in neutrophils (Mehrzhad *et al.* 2001), NET production could still occur (Lippolis *et al.* 2006). These data indicate that there is either i) an alternative pathway not requiring ROS capable of regulating NET production, or, ii) that the step of the ROS generation pathway that is inhibited by milk proteins is downstream of the point at which the ROS pathway and NET pathway cease to be common. Moreover, research by Yost *et al.* (2009) analysing the immune function in human neonates found that although their neutrophils were capable of ROS production, they were unable to form NETs. They concluded that although ROS was required, it was not alone sufficient for NET production indicating a dis-connect in the subsequent downstream signalling events.

Later studies by Wang *et al.* (2009) and Neeli *et al.* (2008) have shown NET release to be dependant upon histone citrullination by PAD4 (peptidylarginine deiminase 4). This enzyme, present in neutrophils and other cell types, converts arginine and methylarginine residues on histones to citrulline, enabling decondensation of the chromatin and subsequent extrusion in the form of NETs. This process was shown to be essential for NET release in calcium ionophore (CI) stimulated neutrophil-like HL60 cells, as pre-treatment with CI-amidine, a PAD4 inhibitor, eradicated all NET production (Wang *et al.* 2009). NETs released from human neutrophils in response to TNF α were also shown to be composed of highly decondensed chromatin containing citrullinated histones (Figure 12).

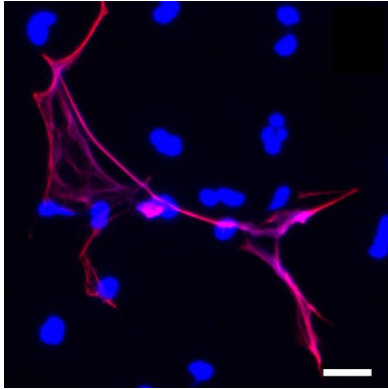


Figure 12. Immunostaining of neutrophils stimulated with TNF α . DNA (blue), citrullinated histone H4 (pink). Bar represents 20 μ m. (Wang *et al.* 2009)

Recent investigations have examined the role of actin and microtubules in NET release (Neeli *et al.* 2009). Pre-treatment with the tubulin polymerisation inhibitor nocodazole resulted in a reduction in LPS stimulated NET release from 30% to 5%. Pre-treatment with the actin polymerisation inhibitor cytochalasin D did not inhibit the disintegration and mixing of the nuclear and granule compartments but only 9% of cells extruded NETs. Notably some of the remaining cells swelled to twice their normal diameter, indicating that actin may be necessary for NET extrusion. As integrins are receptors responsible for transmitting extracellular signals to the cytoskeleton, the Mac-1 integrin was also inhibited using a monoclonal antibody. Data indicated that this inhibition resulted in a significant decrease in NET production and a 51% reduction in histone citrullination (Neeli *et al.* 2009).

Viral infection may also be capable of modifying the NET response in neutrophils. Feline leukemia virus (FeLV) is naturally occurring in cats and can cause modulation of immune cells including neutrophil responses and give rise to opportunistic infections. Work by Wardini *et al.* (2010) found that neutrophils from symptomatic FeLV infected cats had a higher unstimulated level of NET production compared to asymptomatic infected or uninfected cats. However, these neutrophils were unable to increase NET production in

response to protozoal or PMA stimulation, suggesting an exacerbated NET response in FeLV infected neutrophils.

1.5.2 The function of NETs

NET formation has so far been observed in humans (Brinkmann *et al.* 2004; Gupta *et al.* 2005; Jaillon *et al.* 2007), mice (Beiter *et al.* 2006; Buchanan *et al.* 2006; Wartha *et al.* 2007), rabbits (Brinkmann *et al.* 2004), horses (Alghamdi *et al.* 2005), cows (Lippolis *et al.* 2006); (Behrendt *et al.* 2010), fish (Palic *et al.* 2007), chickens (Chuammitri *et al.* 2009), chinchillas (Hong *et al.* 2009; Reid *et al.* 2009) and cats (Wardini *et al.* 2010). NETs function to immobilise microorganisms (Gram negative, Gram positive bacteria, yeast and parasites, see Figures 13, 14 and 15), to augment the bactericidal action of neutrophils, and to prevent the spread of infection. Even the intracellular bacterium *Mycobacterium tuberculosis* has been shown to be trapped in NETs although not killed (Ramos-Kichik *et al.* 2009). NET formation is also reportedly induced by parasites, including *Leishmania amazonensis* and enhanced by the addition of PMA (Guimaraes-Costa *et al.* 2009). In this study NET killing of *L. amazonensis* was largely attributed to the histone component of the NET complex as in this case DNase treatment of the NETs did not inhibit killing of the parasite. NET formation induced in bovine neutrophils by live *Eimeria bovis* sporozoites was increased compared to PMA-induced NETs, however, dead and homogenised *E. bovis* sporozoites were less efficient at inducing NETs than the live form or PMA (Behrendt *et al.* 2010). These NETs were thought to act primarily by immobilising the sporozoites as subsequent *in vitro* incubation with host epithelial cells resulted in a reduction in infection rate from 43.9% to 15.5%.

DNase treatment allowed a similar infection rate of host epithelial cells as if the parasites had not previously been exposed to NETs.

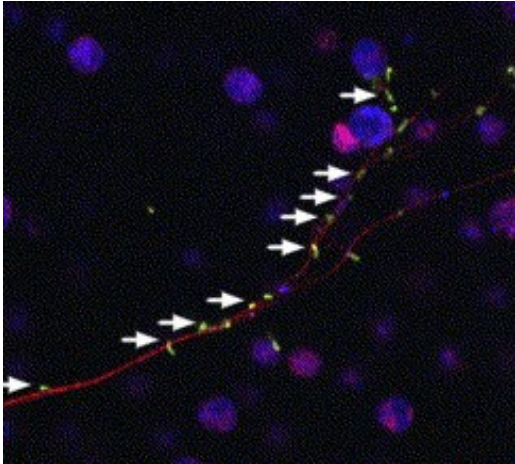


Figure 13. Immunostaining of pneumococci (FITC-labelled, green) trapped in NETs (neutrophil elastase stained red) produced by neutrophils (DNA stained blue) (Beiter *et al.* 2006).

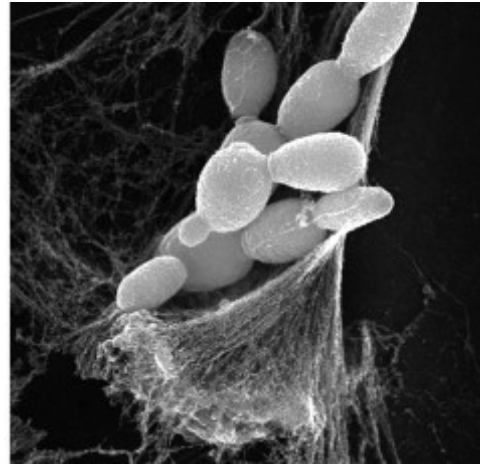


Figure 14. SEM of NET capturing the yeast *C. albicans* (Volker Brinkmann) (Urban *et al.* 2006a).

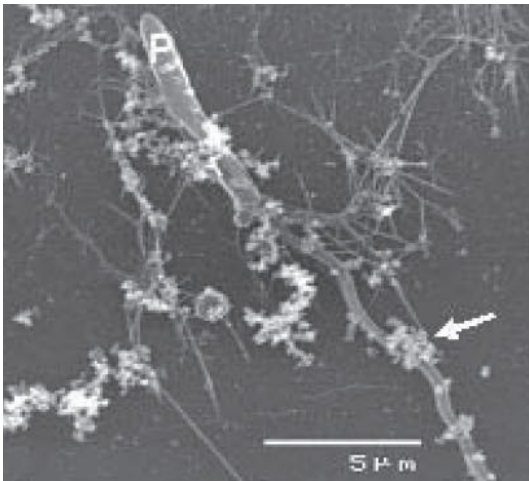


Figure 15. SEM of parasite *L. amazonensis* (P) captured in NET (Guimaraes-Costa *et al.* 2009) arrow indicates neutrophil granules.

1.5.2.1 Aiding other immune processes

The primary function of neutrophils is phagocytosis, for which they are highly specialised with their characteristic lobulated nuclei which enables flexible movement. Although a parasite is physically too large to be phagocytosed, and the primary cells responsible for combating parasitic infection are eosinophils, it appears that neutrophils can also aid the attack and destruction of a parasitic infection by NET release, a strategy also displayed by eosinophils themselves (Yousefi *et al.* 2008).

There is evidence that the AMPs associated with NETs cause local tissue damage (Clark *et al.* 2007). However, NETs may function to limit the diffusion of the degradative agents released from neutrophils to the site of infection, thus limiting the extent of tissue damage to otherwise healthy tissue. Research by Lippolis *et al.* (2006) on bovine mastitis, in which phagocytosis and the respiratory burst are hindered by milk fat and proteins, has suggested that NETs can be formed as an **alternative** to phagocytosis. Although these two antimicrobial mechanisms were inhibited, the neutrophils were still able to produce NETs even following 6 hours incubation with milk. Fuchs *et al.* (2007) also demonstrated that in the absence of PMA and therefore NETs, *S. aureus* was killed exclusively by phagocytosis (DNase independent killing). However, as the cells were pre-incubated with PMA for increasing amounts of time the capacity for phagocytosis was almost completely lost by 3 hours and the killing of *S. aureus* by NETs (DNase sensitive killing) increased. This also suggests that phagocytosis is the preferred method of bacterial killing by neutrophils but that NETs can take over as a secondary killing approach. However, the mechanisms that decide which killing processes are employed by a neutrophil are as yet unclear. In another study regarding the pathogenesis of bovine mastitis by Grinberg *et al.* (2008) β -hydroxybutyrate was found to inhibit neutrophil

responses to the mammary pathogenic *E. coli* strain P4. β -hydroxybutyrate, a ketoacid, is known to be elevated in the blood and milk of cows with ketosis, a state also seen in diabetics, and associated with immune impairment and susceptibility to infection. Purified β -hydroxybutyrate caused not only a reduction in phagocytosis of *E. coli* (90% down to 20%) but also a reduction in the number of cells releasing NETs (29% down to 3.5%), whilst intracellular killing was unaffected. There is a possibility that this effect is linked to ROS release as β -hydroxybutyrate has previously been found to inhibit ROS production by neutrophils (Hoeben *et al.* 1997).

It has been suggested by Oehmcke *et al.* (2009) that the DNA strands of NETs may provide a base for the adherence and subsequent activation of the human contact system. This is a humoral innate immune response consisting of 3 serine proteases and 1 high molecular weight kininogen (HK) which, as the name suggests, needs to contact a surface for activation. This activation results in the release of AMPs, release of the pro-inflammatory mediator bradykinin and coagulation factors. It was demonstrated that when plasma was incubated with NET-stimulated neutrophils, one of the serine proteases (Factor XII) and HK were able to bind to NETs and subsequently activate the contact system measured by the activity of another of the serine proteases (plasma kallikrein). This activation of the contact system was abrogated by the addition of DNase and absent in unstimulated neutrophils. It is suggested that in this way NETs may act to further amplify the innate immune response *in vivo*.

1.5.2.2 Extracellular antimicrobial activity

Even if not completely killed, pathogens can also be disarmed within NETs. Using *Shigella flexneri* (Gram negative bacteria) the virulence factor IpaB (invasion plasmid antigen) has been shown to be degraded by neutrophil elastase extracellularly within NETs (Brinkmann *et al.* 2004) as opposed to intracellularly post-phagocytosis. Neutrophil elastase (a neutrophil granule protein associated with NETs) is a major protein required for the disarming of the Ipa virulence factors, which enable bacteria to escape from the phagosome (Weinrauch *et al.* 2002). This is the first example of a neutrophil enzyme specifically targeting bacterial virulence factors, in this case acting on Ipa, at a 1000-fold lower concentration than that needed to degrade other bacterial proteins (Weinrauch *et al.* 2002). The amount of α -toxin, a virulence factor of *Staphylococcus aureus* (Gram positive), was also reduced in NETs compared to free bacteria, due to the action of another neutrophil protease (Brinkmann *et al.* 2004). This is evidence that NETs may act as an adjuvant to degranulation, to facilitate the **extracellular** degradation of bacterial virulence factors by a range of neutrophil antimicrobial agents, prior to neutrophil engulfment of the microorganism.

Histones H2A and H2B are major components of NETs (Figure 9C) contributing approximately 69% of the protein content of NETs (Urban *et al.* 2009) and exert an antibacterial effect presumed to be due to the highly basic residues disrupting the plasma membranes of pathogens. Investigations into the antimicrobial properties of histones has a history dating back to 1942 (Miller *et al.*) although the most commonly cited research is by Hirsch *et al.* (1958) who concluded that histones, rather than just inhibiting bacterial growth as previously thought, did indeed have a bactericidal effect similar to protamines. To date the majority of research on histone bioactivity has focussed upon their role in fish immunity. The

isolation of potent AMPs from fish mucosa and gut lumen identified a range of histones and histone fragments as having potent activity. The majority of antimicrobial histones have been identified as the linker histone H1, and its related peptides. However, an AMP, Buforin I (isolated from the stomach of an Asian toad), was identified as the first 39 amino acids of histone H2A (Park *et al.* 1996), and Parasin I, an antimicrobial found in catfish was determined to represent the first 19 amino acids of histone H2A (Park *et al.* 1998b). In addition, Hipposin, an antimicrobial found in the Atlantic halibut was identified as the first 50 residues of H2A (Birkemo *et al.* 2003). Histone H2B related anti-microbial peptides have been found in trout and bass (Noga *et al.* 2001) and shrimp hemocytes (Patat *et al.* 2004). Bacteria particularly susceptible to histones are *Escherichia* sp., *Salmonella* sp., *Pseudomonas* sp., *Micrococcus pyogenes* and *Shigella* sp. (Hirsch 1958). H2A alone (a subunit of the histone complex) was found to destroy *Shigella flexneri*, *Salmonella typhimurium* and *Staphylococcus aureus* at concentrations lower than required for other antimicrobial agents (Brinkmann *et al.* 2004). However, the bactericidal effect of the histone is antagonised by acid polysaccharides, including nucleic acids and bacterial lipopolysaccharides (Hirsch 1958). Whilst this is not consistent with the antimicrobial action for the histones within NETs, it is however hypothesised that as well as providing a scaffold for the folding and structure of NETs, histones may still contribute to the NETs antibacterial effects along with its other AMPs such as neutrophil elastase. It has previously been shown that NETs are destroyed by treatment with DNase allowing the pathogen to escape killing, however, treatment of NETs with protease did not hinder their function (Brinkmann *et al.* 2004). If the AMPs coating the NET were removed this would create a greater necessity for histones to contribute as the antibacterial agents to maintain NET function. It has been shown that in intact NETs formed in response to *L. amazonensis*, histones play an active part in NET-mediated parasitic killing

as demonstrated by the addition of an anti-histone antibody to neutralise the histones, which resulted in a 42% increase in parasite survival (Guimaraes-Costa *et al.* 2009). This was confirmed by the treatment of *L. amazonensis* with purified histone H2A (20µg/ml) which caused 62% of promastigotes cell death. However, in this case the neutrophil elastase inhibitor, methoxysuccinyl-Ala-Ala-Pro-Val chloromethyl ketone, had no effect on the killing efficacy of the NETs implying neutrophil elastase was not active in this process. It is possible that the AMPs found in NETs are microbial specific, with specific AMPs being important for killing specific pathogens.

1.5.2.3 NETs in non-infectious diseases

NETs have also been found to play a role in non-infectious disease such as pre-eclampsia (Gupta *et al.* 2005). Pre-eclampsia is characterised by hypertension in pregnancy due to an immune reaction triggered by the placenta. It is also thought that circulating peptides released from the placenta such as syncytiotrophoblast microparticles (STBM) may contribute to triggering the generalised maternal immune response. Gupta *et al.* subsequently found that a significant number of NETs were present within the intervillous space of pre-eclamptic placentae and that NET release was stimulated by, and subsequently trapped STBM. This is particularly notable as STBM are significantly smaller (<200nm) than the bacteria (>2µm) that NETs have previously been reported to trap.

Small vessel vasculitis (SVV) is an example of an auto-inflammatory condition in which NETs have been found to contribute. Anti-neutrophil cytoplasm autoantibodies (ANCA) are antibodies directed against neutrophil granule proteins such as proteinase-3 (PR3) and MPO,

and are known to be implicated in the pathogenesis of SVV. It was shown by Kessenbrock *et al.* (2009) that ANCAs could stimulate NET release *in vitro* from 23% of TNF α primed neutrophils. In addition to ANCAs purified from patient blood, a mouse monoclonal antibody against proteinase-3 was able to elicit NET release from ~17% of TNF α primed neutrophils. These data also support the link between NET and ROS generation, as binding of ANCA to PR3 and MPO on the neutrophil surface has already been found to activate the respiratory burst (Falk *et al.* 1990). Analysis of NETs both *in vitro* and *in vivo* (kidney biopsies) found them to contain the autoantigens MPO and PR3 and that they were still available for autoantibody (ANCA) binding. The implication for this is that the NETs could act to ‘mop up’ ANCAs by binding them within extracellular traps, or conversely, that the exposure of the autoantigens could stimulate further production of ANCAs. Prior to the discovery of NETs it had been found that circulating levels of nucleosomes were raised in a range of autoimmune disorders including ANCA-associated vasculitis and also systemic lupus erythematosus (Holdenrieder *et al.* 2006). In the light of NETs being associated with SVV, antibodies were used to detect serum levels of DNA-MPO complexes i.e. presumed NET fragments. This confirmed a significant increase in circulating DNA-MPO fragments compared to the sera of healthy individuals or SVV patients who were in remission.

The level of circulating free DNA has potential use as a therapeutic marker of neutrophil activity and levels have been used for this purpose in septic arthritis (Lögters *et al.* 2009). Double stranded DNA was quantified in samples of joint synovial fluid using a fluorescent dye, and the likelihood of this DNA originating from NETs rather than general cell death was confirmed using an MPO specific antibody. Results demonstrated a significant increase in the levels found in samples from those with septic arthritis compared to non-septic inflammation.

A pilot study involving 37 trauma patients also evaluated the levels of circulating free DNA in plasma over 10 days and found a correlation with the likelihood of the patients developing sepsis, multiple organ failure and death (Margraf *et al.* 2008).

Apoptosis is a strictly controlled and regulated response which aims to ensure that no cell contents are released into the extracellular space. NETosis on the other hand actually aims to release cell contents although this too must be highly regulated and only specific cell contents are released. Molecules normally found intracellularly can have diverse functions on neighbouring cells extracellularly. For example, it has been shown that in the case of TNF α /ANCA-stimulated NETs and PMA-stimulated NETs, that the antimicrobial peptide LL37 is present. This peptide is known to convert self-DNA to an active form capable of stimulating plasmacytoid dendritic cells to release IFN- α (Lande *et al.* 2007), the effects of which were seen locally at the site of NET accumulation *in vivo* in kidney biopsies, and, in addition were shown to significantly increase serum levels of IFN- α in SVV patients (Kessenbrock *et al.* 2009). Another example of the potentially more widespread consequences of NET release is that extracellular double stranded DNA can stimulate the maturation of antigen presenting cells such as bone marrow dendritic cells by up-regulating expression of major histocompatibility complex class II (MHC II), CD40 and CD54 (Ishii *et al.* 2001). This suggests that the release of NETs may have an effect on the adaptive immune response.

Recently it has been hypothesised (Lee *et al.* 2004) that excessive NET production is counter-productive and can contribute to pathological conditions. Evidence for this is provided by examining DNase treatments used in mucolytic therapy for cystic fibrosis. Cystic fibrosis is

characterised by excess mucous containing DNA and elastase in the airways, this milieu therefore exhibits a similar composition to NETs. In a clinical trial examining the daily administration of aerosolised recombinant human DNase, a reduction in symptoms was observed (Fuchs *et al.* 1994). It is thought that the webs formed by NETs impair the ciliary clearance of mucous from the airways, and treatment with DNase reduced the viscosity of the mucous enabling its removal.

The full range of species, tissues, pathologies and physiologies in which extracellular traps have been reported to date is presented in Table 1 below.

Table 1. Publications reporting extracellular traps, in chronological order.

Location/Pathology/Physiology	Species	Reference
Experimental dysentery (<i>Shigella</i>) Spontaneous human appendicitis	rabbit, human	(Brinkmann <i>et al.</i> 2004)
Pre-eclampsia	human	(Gupta <i>et al.</i> 2005)
Insemination (reproductive tract)	equine (<i>in vitro</i>)	(Alghamdi <i>et al.</i> 2005)
Necrotising fasciitis (group A streptococci)	murine	(Buchanan <i>et al.</i> 2006)
Mastitis	bovine	(Lippolis <i>et al.</i> 2006)
Blood sepsis	human (<i>in vitro</i>)	(Clark <i>et al.</i> 2007)
Kidney	zebra fish	(Palic <i>et al.</i> 2007)
Malaria (<i>Plasmodium falciparum</i>)	human	(Baker <i>et al.</i> 2008)
Tuberculosis (<i>Mycobacterium tuberculosis</i>)	human	(Ramos-Kichik <i>et al.</i> 2009)
Septic arthritis (synovial fluid)	human (<i>in vivo</i>)	(Lögters <i>et al.</i> 2009)
Leishmania (parasite: <i>Leishmania amazonensis</i>)	human (<i>in vivo</i> and <i>in vitro</i>)	(Guimaraes-Costa <i>et al.</i> 2009)
Small vessel vasculitis	human (<i>in vivo</i> kidney and <i>in vitro</i>)	(Kessenbrock <i>et al.</i> 2009)
Periodontitis	human (<i>in vivo</i>)	(Vitkov <i>et al.</i> 2009)
Aspergillosis (fungi: <i>Aspergillus nidulans</i> conidia)	human (<i>in vitro</i>)	(Bianchi <i>et al.</i> 2009)
Otitis media (<i>Streptococci pneumoniae</i>)	chinchilla (<i>in vivo</i>)	(Reid <i>et al.</i> 2009)
Otitis media (<i>Haemophilus influenza</i>)	chinchilla (<i>in vivo</i>)	(Hong <i>et al.</i> 2009)
Feline leukaemia virus (<i>L. amazonensis</i>)	feline (<i>in vitro</i>)	(Wardini <i>et al.</i> 2010)
<i>Eimeria bovis</i> parasitosis (<i>E. bovis</i> sporozoites)	bovine (<i>in vitro</i>)	(Behrendt <i>et al.</i> 2010)
Non-neutrophil extracellular traps,		
Mast cells (MCETs; <i>Streptococcus pyogenes</i>)	human (<i>in vitro</i>), murine (<i>in vivo</i>)	(von Kockritz-Blickwede <i>et al.</i> 2008)
Eosinophils (murine cecum)	human (<i>in vitro</i>), murine (<i>in vivo</i>)	(Yousefi <i>et al.</i> 2008)
Heterophils (HETs)	chicken (<i>in vitro</i>)	(Chuammitri <i>et al.</i> 2009)

1.5.3 Stimuli for NET production

The point at which NETs are released from neutrophils is critical because by their very nature, being 'traps', they will impede other functions of the neutrophil e.g. migration to the pathogen, recruitment of other white blood cells and to a certain extent phagocytosis. The individual neutrophil also dies at the point of NET release so will not be capable of further functions itself. Currently recognised stimuli for NET release are cytokines (Brinkmann *et al.* 2004), bacteria (Fuchs *et al.* 2007), bacterial endotoxins (Brinkmann *et al.* 2004), parasites (Guimaraes-Costa *et al.* 2009) and yeast (Urban *et al.* 2006b). It has been reported that approximately one third of PMA-activated neutrophils isolated from human venous blood make NETs *in vitro* (Fuchs *et al.* 2007). Brinkmann *et al.* (2004) exposed neutrophils to the cytokine IL-8 for 30-60 minutes, as well as PMA and LPS. IL-8 is produced by macrophages, endothelial and epithelial cells to induce neutrophil chemotaxis, whilst LPS is a component of the outer membrane of Gram negative bacteria and acts at TLR4. PMA is known to be a potent activator of neutrophils and its receptor is the intracellular calcium dependant signal transduction enzyme, protein kinase C (PKC). It has been noted that whole bacteria induce NETs more efficiently than IL-8 or LPS alone, suggesting that activation of multiple receptors is required for optimal NET stimulation (Fuchs *et al.* 2007). Guimaraes-Costa *et al.* (2009) found that the parasite *L. amazonensis* was capable of stimulating NET release but pre-treatment of the neutrophils with PMA resulted in a 53% increase in promastigote killing. The purified promastigote membrane component lipophosphoglycan (LPG) was also able to elicit NET release but to a lesser extent than the whole organism. In addition, dead sporozoites of the bovine parasite *Eimeria bovis* were able to elicit NET release upon direct contact with neutrophils but the cellular reaction was significantly stronger with live sporozoites (Behrendt *et al.* 2010). Yeast such as *Candida albicans* (Urban *et al.* 2006b)

and *Aspergillus nidulans* (Bianchi *et al.* 2009) are known to induce NETs although in the case of *A. nidulans* this effect was shown to be greatly increased by the addition of PMA. It has also been shown that in mouse bone marrow-derived neutrophils challenged with *C. albicans*, the hyphal form is more effective at inducing NET release than the yeast form (Ermert *et al.* 2009). In some cases cytokine priming has been necessary before NET release is elicited. Yousefi *et al.* (2009) primed mature peripheral neutrophils with granulocyte-macrophage colony stimulating factor (GM-CSF) for 20 minutes, before stimulation with LPS or complement C5a which then caused dramatic NET release within 15 minutes in ~80% of the cell population. In studies by Fuchs *et al.* (2007), although it was acknowledged that microorganisms themselves were capable of stimulating NET release, PMA and glucose oxidase (GO) were also used to pre-activate the neutrophils before stimulation by *S. aureus*. Glucose oxidase is an exogenous enzyme which promotes H₂O₂ synthesis within the cells in addition to the endogenous NADPH oxidase. Notably, high concentrations of serum in the culture medium was shown to inhibit NET formation, although the mechanism of this inhibition is currently unknown (Figure 16).

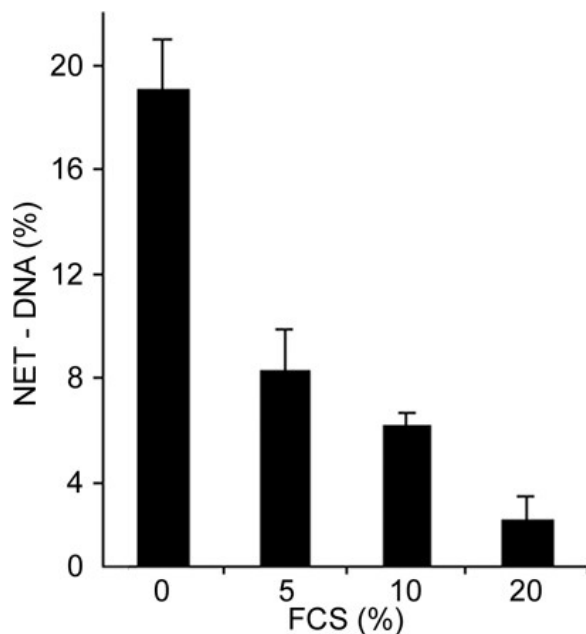


Figure 16. Serum inhibits NET formation. Neutrophils were activated with 10 nM PMA for 240 minutes in the presence of indicated concentration of foetal calf serum (FCS), and NET-DNA was quantified. The inhibitory effect increased in a dose-dependent manner. At 20% FCS, NET formation is almost completely suppressed. The data shown is a representative triplicate experiment and is presented as a mean value \pm the SD. (Fuchs *et al.* 2007)

Unpublished data from our own laboratory have shown that opsonised Gram positive bacteria (*S. aureus* coated in immunoglobulin G) stimulate NET release acting via the Fcγ receptor (H.J. Wright, personal communication). Similarly, others have found that IgG coated beads were capable of inducing NETs, although IgG free in solution was not (Fuchs *et al.* 2007). Clark *et al.* (2007) investigating the role of NETs in severe blood sepsis, found that platelets act as mediators to stimulate NET release when they detect the bacterial component, LPS, in the circulation. LPS binding of TLR4 on platelets subsequently binds adherent neutrophils inducing NET release within the capillaries. In a similar way, host fibrinogen has been found to form a complex with the M1 protein from the surface of *S. pyogenes* and stimulate NET release even though neither component alone was capable of inducing NETs (Oehmcke *et al.* 2009).

It has been suggested that priming may have a significant effect on the nature of the response from the neutrophils (Yousefi *et al.* 2009). GM-CSF priming for 20 minutes and subsequent short-term stimulation with LPS or complement C5a for only 15 minutes resulted in extracellular release of mitochondrial DNA only and the cells remained viable. This is in contrast to all previous reports of NETs which consist of nuclear DNA and subsequent cell death. It is unclear as to whether observation for longer than 15 minutes would have resulted in the cells undergoing nuclear DNA extrusion as a more advanced stage of NET release. Characteristics in common with the more universally described process of NET release are that it was dependent on ROS, that granule proteins were present within the NETs, and cytoplasmic and membrane markers were absent. In contrast, histones were also absent but nuclear proteins were present. This description of NET release appears to be highly specific to the stimuli used as although both GM-CSF + C5a and GM-CSF + LPS induced NETs in

the same way, ethidium bromide detection of cell viability found GM-CSF + C5a extended the life of neutrophils whilst GM-CSF + LPS had no effect.

The change in gene expression during neutrophil maturation was investigated by Martinelli *et al.* (2004). Of 12,599 genes examined, 1049 were found to be differentially expressed in immature versus mature neutrophils. Mature neutrophils were found to have a higher expression of genes which transduce signals of type I and type II interferons as well as higher expression of genes for apoptosis and inflammatory responses. As IFN- γ is known to be able to enhance the anti-fungal activity of neutrophils, studies investigated whether this may be due to NET formation (Martinelli *et al.* 2004). It was found that the altered IFN sensitivity of mature neutrophils was indeed important for the formation of NETs. IFN- α or IFN- γ appeared to prime neutrophils and when followed by stimulation with C5a, NETs were produced. This occurred in mature but not immature bone marrow derived neutrophils, i.e. those receptive to IFN signals.

1.5.4 Non-neutrophil derived extracellular traps

Neutrophils are not the only immune cell capable of extracellular trap formation. Mast cells have also been shown to be capable of this phenomenon to ensnare *S. pyogenes* (von Kockritz-Blickwede *et al.* 2008). A primary function of mast cells is to mediate allergic reactions and they are found in tissues exposed to the external environment such as the mucosa of the respiratory tract. Whilst they are capable of phagocytosis they do not perform this at a significant level physiologically. The extracellular traps formed by mast cells (termed MCETs) were shown to be similar to NETs in their composition, dependence on ROS

production and required stimuli. A similar NET release process has also been reported in eosinophils whose primary function is to combat parasites (Yousefi *et al.* 2008). DNA extruded into the extracellular space also occurred in a process independent from cell death and dependant on ROS generation similar that of NETs. Unlike NETs, eosinophil derived extracellular traps were found to consist of mitochondrial DNA rather than nuclear chromatin and required priming by IL-5 or IFN- γ prior to stimulation with LPS.

1.6 HL60 cells as a model for neutrophils

Owing to the invasive nature of obtaining primary neutrophils for scientific study and in consideration of the multitude of influencing factors the cells may be exposed to in the peripheral bloodstream before experimentation, the human promyelocytic cell line, HL60, has been used, since its discovery in 1977 (Collins *et al.*), as a model for neutrophil growth and differentiation. These cells were originally isolated from a 36 year old female patient with acute promyelocytic leukemia and can be stimulated to differentiate to a monocytic cell using vitamin D (Miyaura *et al.* 1981), a macrophage-like cell using PMA (Rovera *et al.* 1979), or a granulocytic cell with retinoic acid (Breitman *et al.* 1980) or dimethylsulphoxide (DMSO) (Gallagher *et al.* 1979). DMSO differentiated HL60 cells (dHL60) have been described as neutrophil-like with regards to various morphological, biochemical and functional characteristics. Characterisation in 1979 by the group who originally isolated them found the cells to test positive for surface Fc receptors by the erythrocyte-antibody test when using bovine erythrocytes and positive for complement receptors when using sheep erythrocytes (Gallagher *et al.* 1979). They also found the cells to be capable of phagocytosing *Candida albicans*. Subsequently dHL60 were shown to be capable of phagocytosing Ig-

opsonised paraffin droplets containing albumin, complement-opsonised paraffin droplets containing LPS and latex beads (Newburger *et al.* 1979). dHL60 cells were found to generate superoxide in response to PMA and opsonised zymosan at early stages during their differentiation, which occurred prior to morphological changes being observed. Notably, the superoxide response took longer and never reached the levels achieved in primary neutrophils (Newburger *et al.* 1979). With respect to the components of the NADPH oxidase responsible for the respiratory burst, Roberts *et al.* (1982) described an increase in cytochrome *b* expression during differentiation and Teufelhofer *et al.* (2003) also observed an upregulation of mRNA encoding the NADPH oxidase subunits gp91phox, p47phox and p67phox. Although along with a low level expression of NADPH oxidase subunits in undifferentiated cells Teufelhofer *et al.* also claimed to observe PMA-induced superoxide production in undifferentiated cells. Immunoblot analysis for NADPH oxidase subunits by Levy *et al.* (1990) did find a low level of expression of p47, p22 and gp91 in undifferentiated HL60 cells but found the cytosolic component p67 to be absent and concluded that undifferentiated HL60 cells did not generate significant superoxide in response to PMA (100ng/ml). Newburger *et al.* (1979) examined the granule content of dHL60 and found that as cells differentiated, levels of peroxidase (found in primary granules), β -glucuronidase (also found in primary granules) and lysozyme (found in tertiary granules) increased, as did the quantities released by degranulation in response to opsonised zymosan. Finally, the same researchers demonstrated that dHL60s were capable of bacterial killing when challenged with opsonised *S. aureus*. However, dHL60 cells appear to be devoid of secondary granules (Harris *et al.* 1985) and in comparison to primary neutrophils have been reported to contain only half the amount of MPO from primary granules (Stendahl *et al.* 1986). dHL60s have been shown by Shuto *et al.* (2007) to i) express IL-8 receptors, ii) exhibit chemotaxis in response to N-

formyl-methionyl-leucyl-phenylalanine (fMLP), iii) produce cytokines IL-1 β and IL-8 in response to TLR2 and TLR4 stimulation by bacterial peptidoglycan / lipoteic acid or LPS respectively, iv) produce low levels of cytokines in response to TLR1/2 stimulation by Pam3Cys, TLR3 stimulation by poly(I-C) and TLR9 stimulation by bacterial DNA and v) to show surface expression of MD-2 (myeloid differential protein-2) and CD14 (components of the TLR4 complex).

Notable differences between dHL60 cells and primary neutrophils are that they do not contain lactoferrin indicating they do not possess secondary granules (Newburger *et al.* 1979). dHL60s also lack the capacity for ROS production in response to the calcium ionophore ionomycin but retain the ability to degranulate to a similar level observed in primary neutrophils (Dahlgren 1989). Ionomycin was however, able to prime dHL60s for enhanced ROS release upon subsequent stimulation with fMLP or PMA, an effect also seen in primary neutrophils. It is agreed that the level of ROS produced in dHL60s is significantly reduced compared to primary neutrophils, however it is unclear whether this is due to i) a low level of expression of the components required for activity, ii) the components being dysfunctional or iii) only a certain percentage of the cell population is responsive to the differentiation stimuli and therefore become mature cells. Indeed one study reported that only 65% of cells from a day 5 differentiated culture were capable of PMA-induced ROS production (Dahlgren 1989).

Wang *et al.* (2009) have subsequently analysed the role of PAD4 histone hypercitrullination in stimulated HL60s NET release, which is known to be involved in NET release from primary neutrophils. Notably, as HL60s were differentiated with DMSO the expression of PAD4 increased. Subsequent treatment with calcium ionophore resulted in ~36% of cells

showing the citrullinated form of histone H3 and this was accompanied by >8% of cells releasing NETs. Using IL-8 and bacterial stimulation (*S. flexneri*) 9.8% of differentiated cells showed citrullinated H3 and 3.2% released NETs after 3 hours. Spontaneous histone citrullination was observed in undifferentiated HL60 cells but this was not a characteristic of the cell population as a whole and no NET release was seen under these conditions.

1.7 Microbial mechanisms for the evasion of NETs

Certain bacteria have been demonstrated to exhibit resistance to NET capture and/or NET mediated killing. Mechanisms described include the production of extracellular DNases to degrade NETs (Buchanan *et al.* 2006), cationic modification of surface proteins to repel like-charged AMPs (Kristian *et al.* 2005), and the expression of a capsule to evade NET capture (Wartha *et al.* 2007).

1.7.1 Inhibition of antimicrobial peptides (AMPs)

Certain bacteria have been reported to be trapped by NETs but not killed. An example of this is the M1 serotype GAS. The M1 surface protein is already recognised as a virulence factor but a novel action has recently been described indicating that it can inhibit the action of cathelicidin LL37 within NETs and also MCETs (Lauth *et al.* 2009). Although it is the M1 protein that is largely responsible for inducing neutrophils to release NETs when exposed to GAS (as demonstrated by M1 knockouts and re-transfection of the M1 gene), once trapped it is the M1 protein (and specifically the N-terminal hypervariable region of the M1 protein) which allows bacterial survival within the NET.

1.7.2 Charge modifications of the bacterial surface

In specific cases, modifications of molecules comprising the bacterial cell surface serve to alter its charge. Usually the surfaces of bacteria are anionic and exhibit a net negative charge due to a high density of charged phosphate groups. In Gram positive bacteria these are found on teichoic acids of the cell wall, and in Gram negative bacteria they are found on LPS, the major component of the outer membrane. AMPs are cationic, i.e. positively charged, so they are electrostatically attracted to their site of action, namely the bacteria. Modifications which provide the bacterial surface with a positive charge subsequently mean harmful cationic AMPs are repelled. This phenomenon may not be specific to NETs although one of the functions of NETs is to concentrate AMPs around the bacteria. Therefore repulsion of these peptides becomes all the more vital for bacterial survival in this situation. Reported examples in which bacteria are able to make modifications to their surface charge in response to the environmental conditions include the addition of L-lysine to phosphatidylglycerol within the cell membrane via the *mprF* gene loci in *Staphylococcus aureus* (Peschel *et al.* 2001; Kristian *et al.* 2003). Another example is the modulation of cell wall teichoic acids by D-alanylation which is catalysed and regulated by 5 genes carried by the *dlt* operon found in certain Gram positive bacteria. This latter mechanism is a two-step process requiring a D-alanine-D-alanyl carrier protein ligase and a D-alanyl carrier protein (Linzer *et al.* 1973).

Bacterial teichoic acids are either anchored to glycolipids in the cell membrane (lipoteic acids), or attached to peptidoglycan in the cell wall. Studies of *dlt* mutants have found that the *dlt* operon is important for resistance to AMPs in *Bacillus subtilis* (Bensaci *et al.* 2007), *Staphylococcus aureus* (Peschel *et al.* 1999), *Listeria monocytogenes* (Abachin *et al.* 2002), *Streptococcus agalactiae* (group B streptococci, (Poyart *et al.* 2003) and the virulent M1

serotype GAS (Kristian *et al.* 2005). In the case of GAS, D-alanylation also promotes epithelial cell invasion and resistance to neutrophil killing (Kristian *et al.* 2005). With regards to oral pathogens, the *dlt* operon was found to be important in *Streptococcus mutans* for the accumulation of intracellular polysaccharide (IPS) (Spatafora *et al.* 1999) and acid tolerance (Boyd *et al.* 2000), and also in *Streptococcus gordonii* for intrageneric coaggregation (Clemans *et al.* 1999). In *Salmonella enterica* surface charge is altered by the transcriptional activation of two *pmr* genes, facilitating the addition of aminoarabinose to lipid A of LPS (Gunn *et al.* 2000). This modification is also made in *Proteus mirabilis* but in this case requiring an acetyltransferase (McCoy *et al.* 2001). Lipid A is also modified with phosphoethanolamine in addition to, or in place of, aminoarabinose in *S. enterica* (Zhou *et al.* 2001). *Haemophilus influenzae*, a common cause of otitis media, is able to escape killing by PMA-induced NETs but mutants in lipooligosaccharide (LOS or LPS) surface glycolipids were found to be more susceptible (Hong *et al.* 2009). Mutants with defects in the core region or lipid A region, truncated oligosaccharide region and asialylated forms were found to be more susceptible to killing by not only phagocytosis but also NETs.

Modifications of surface charge can work in conjunction to confer virulence to specific bacteria. For example *Staphylococcus aureus* has the *mprF* gene for the addition of L-lysine into the cell membrane and also the *dlt* operon for the D-alanylation of teichoic acids in the cell wall. This enables AMPs to be repelled by the cell wall, however if they cross this barrier they are then repelled at the cell membrane. Another example of a bacterium with dual mechanisms for charge modification is *Bacillus subtilis* which has the *pssA* operon for the synthesis of phosphatidylethanolamine which acts at the level of the cell membrane, whilst its

dlt operon for D-alanylation of teichoic acids provides further resistance at the cell wall (Cao *et al.* 2004).

1.7.3 Expression of bacterial capsules

A bacterial capsule is a layer of polysaccharide that conceals the antigenic molecules on the surface from being recognised and targeted for phagocytosis by neutrophils and macrophages. In light of the relatively recent discovery of NETs as an antibacterial mechanism employed by neutrophils, it is thought that the capsule expressed in virulent strains of bacteria also functions to enable NET evasion. In *Streptococcus pneumoniae* significantly fewer of the encapsulated serotypes were captured in NETs than their corresponding non-encapsulated serotypes (Figure 17) (Wartha *et al.* 2007). Interestingly, in this same study, bacteria expressing capsules which exhibited no net charge were equally proficient at evading NET capture compared to those with anionic capsules, making electrostatic repulsion an unlikely reason for this phenomenon. The majority of the invasive forms of pneumococci which are responsible for causing pneumonia express a capsule, with over 90 serotypes being described. *Streptococcus mutans*, a key coloniser of the oral cavity, secretes a specialised polysaccharide capsule that provides an adherent, nutritious and protected environment which enables biofilm colonisation. The polymerisation of glucose to dextran by *S. mutans* allows adherence to the tooth enamel and enables dental plaque formation. The bacteria can also depolymerise the dextran to recover and utilise the glucose as an energy source. It is this process that yields lactic acid responsible for the decalcification of the tooth enamel observed in caries (Hamada *et al.* 1980). In addition to concealing antigens, the bacterial capsule may express molecules that mimic those of the host and are therefore recognised as ‘self’ by immune cells and

subsequently therefore do not evoke an immune response. This process has been described by Carlin *et al.* (2009) using a highly encapsulated group B *Streptococci* which express a sialoglycan as part of the bacterial capsule. The sialic acid of this molecule is recognised as ‘self’ by human neutrophil Siglec-9 which has an inhibitory cytoplasmic domain resulting in down regulation of the oxidative burst and NET formation and ultimately enabling bacterial survival. This was demonstrated by competitive inhibition of the sialic acid binding site of Siglec-9 using an antibody which allowed more ROS and NET production than in the presence of an antibody which did not block the binding site. These data indicate that not only does this capsule component avoid recognition and evoking of an immune response by the host, it actively down-regulates the immune response. A secondary action of bacterial sialoglycan engagement of Siglec-9 was the upregulation of mRNA expression of the anti-inflammatory cytokine IL-10 (Carlin *et al.* 2009).

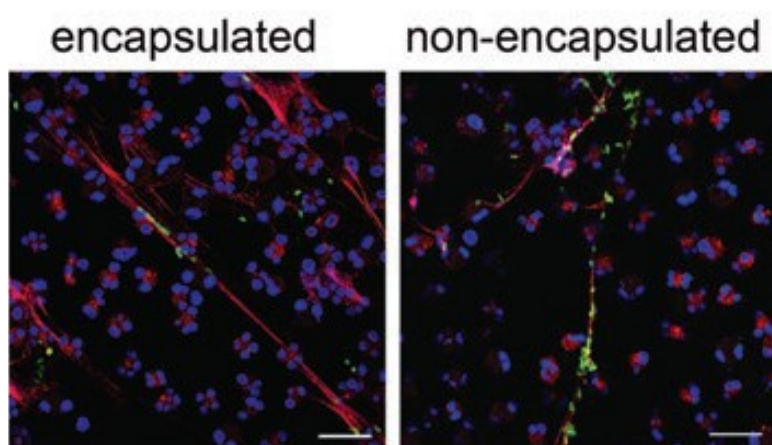


Figure 17. NETs trapping *S. pneumoniae*. NETs stained for DNA (Draq5, blue) and neutrophil elastase (AlexaFluor488 labelled antibody, red). Encapsulated *S. pneumoniae* (FITC, green) are able to exist free of NETs. Non-encapsulated pneumococci are mainly associated with NETs. (Wartha *et al.* 2007)

1.7.4 Bacterial DNases

DNases are virulence factors produced by certain bacteria to evade NETs (Beiter *et al.* 2006; Buchanan *et al.* 2006). The enzyme degrades the principal component of NETs, DNA,

enabling the microorganism to evade this form of capture and killing and thereby facilitate its spread throughout the tissue. It has been known for decades that many bacteria, particularly Gram negative bacteria, produce extracellular DNases although until recently their role and benefit to the bacteria had been a mystery. In 1974 Porschen and Sonntag examined the production of DNase in anaerobic bacteria, and found that DNase activity was extremely common in Gram negative bacteria and present in all strains of *Fusobacterium* tested (Porschen *et al.* 1974). DNase production was found to be less common in Gram positive bacteria although certain bacteria, e.g. *Clostridium perfringens*, did show significant nuclease activity. This is of particular relevance as it is thought that the pathogens predominantly responsible for periodontitis are Gram negative anaerobic bacteria. In 1967 Cuatrecasas *et al.* found that *Staphylococcus aureus* was able to produce an extracellular nuclease which cleaves the 5'-phosphyl ester bond in nucleic acids to produce mono- and di- 3'-phosphonucleotides (Cuatrecasas *et al.* 1967). This nuclease was capable of cleaving RNA but had a higher affinity for DNA and this bacterial property is now used in diagnostic laboratories for the identification of *S. aureus* infections. One function of DNases may be that they create a wider range of available nucleotides conferring a growth advantage (Fox *et al.* 1968). However, in the light of recent advances in the characterisation of NETs, investigations have been undertaken into the potential of *streptococcal* group A DNases in particular, to degrade NETs and subsequently enhance their virulence. There is now evidence which indicates that extracellular DNases are of particular importance to GAS because all strains produce at least one type and the majority produce several distinct DNases (Wannamaker 1958; Miyakawa *et al.* 1985). Significantly, gene expression of prophage encoded DNase can be up regulated by exposure to hydrogen peroxide (Banks *et al.* 2003).

Buchanan *et al.* (2006) examined the DNase Sda1 expressed by the M1 serotype GAS strain. An Sda1 mutant which exhibited decreased DNase activity had increased susceptibility to neutrophil killing *in vitro*, and an *in vivo* mouse model of necrotising fasciitis subsequently demonstrated that the Sda1 mutant was also significantly less virulent than the wild type strain. The addition of G-actin to inhibit the DNase also reduced virulence of the bacteria in the mouse model. Significantly, exudates of abscesses from the infected mice showed higher levels of NETs remaining in the Sda1 mutant than in infections due to the wild type strain. Walker *et al.* (2007) also studying GAS found that expression of Sda1 paradoxically provided a selection pressure for a shift in the bacterial population to a highly invasive phenotype. Natural selection meant those bacteria expressing Sda1 were able of escaping NETs and increased in number. In the MIT1 GAS serotype the Sda1 phenotype was only observed when accompanied by a mutation in the *covRS* regulator, causing suppressed SpeB expression. SpeB is a cysteine protease which degrades plasmin, however in its absence, plasmin is able to accumulate on the bacterial surface enabling the bacteria to invade from the local tissue into the blood causing a systemic infection (Cole *et al.* 2006). ‘End A’, another DNase found expressed on the surface of *Streptococcus pneumoniae*, which is the primary cause of community-acquired pneumonia, was examined in strain TIGR4 (serotype 4) (Beiter *et al.* 2006). The EndA mutant strain was able to infect the upper respiratory tract in mice but failed to disseminate into the lung and bloodstream indicating that although neutrophils are unable to kill *S. pneumoniae*, NETs are able to limit dissemination.

Sumby *et al.* (2005) recently hypothesised that the multiple forms of DNases produced by GAS may preserve their ability to degrade DNA if the host produces antibodies to inhibit one form of the enzyme. In addition, multiple forms of DNase may enable activity under a range

of conditions e.g. pH and cationic requirement. Multiple DNase genes may also enable expression at various stages of infection and may aid the dissemination of phages on which many virulence factors, including DNases, are found.

Another group of endonuclease producing bacteria are Gram negative bacteria which secrete the bacterial toxin cytolethal distending toxin (CDT). This group of bacteria include the pathogenic strains of *E. coli* (Johnson *et al.* 1988b), *Aggregatibacter actinomycetemcomitans* (Sugai *et al.* 1998) and *Campylobacter* (Johnson *et al.* 1988a). CDT works by creating a nick in the DNA of host cells which is recognised by the cell causing cell cycle arrest at G2/M and eventually cell death (Elwell *et al.* 2000; Lara-Tejero *et al.* 2002). The name, cytolethal distending toxin, refers to its cytotoxic nature and morphological changes seen in cells as the toxin targets the nucleus causing it to swell (Johnson *et al.* 1988b). The active subunit of the toxin, CdtB, is a molecule similar to DNase I. Investigations into the DNase activity of CDT have found it to be generally very low. This may be due to either the purification process, a lack of appropriate co-factors, or simply because this nuclease acts locally only requiring the ability to make a single nick in a cell's DNA to be toxic and, therefore, may only require relatively low activity.

Aside from their role in infectious diseases, DNases are expressed by non-bacterial cells, as investigated by Alghamdi *et al.* (2005) who demonstrated their role in fertilisation. The process of insemination evokes the recruitment of neutrophils to the reproductive tract to remove excess spermatozoa and bacterial contaminants. It is thought that if the neutrophil response is too early or is exaggerated then the production of NETs may entangle the spermatozoa and reduce fertility. However, the inclusion of seminal plasma with the

spermatozoa appeared to greatly increase the chance of successful fertilisation in equine artificial insemination. This is thought to be due to a 'fertility associated antigen' found in seminal plasma which shares sequence homology with DNase I, which is thought to be able to digest NETs and free trapped spermatozoa.

Another area of study regarding eukaryotic DNase I activity includes that of systemic lupus erythematosus (SLE). SLE is an autoimmune disorder in which antibodies are produced against the patients own DNA causing multiple organ inflammation including pleuritis, arthritis, rash, myocytis, vasculitis and kidney inflammation. The pathogenesis of this disorder is unclear but recent research suggests that it may be caused by disturbed clearance of nuclear DNA after cell death (Napirei *et al.* 2000). This may be the result of faulty or reduced levels of DNase, and a reduced level of DNase I in the urine of patients with SLE supports this hypothesis. Knock-out mice for the DNase I gene have also been shown to develop symptoms of SLE (Napirei *et al.* 2000). Replacement therapy involving administration of recombinant DNase I in a different mouse model of SLE delayed disease progression and prolonged their lifespan (Macanovic *et al.* 1996).

1.8 The role of NETs in the pathogenesis of periodontal disease

Evidence suggests that the nature of the inflammatory response and a patient's innate susceptibility determines the destructive nature and progression of periodontal disease. As neutrophils are the major immune cell type involved in the periodontal inflammatory response, it is therefore reasonable to speculate that perturbations in their function may determine a patient's periodontal state.

To extrapolate this premise to NETs, it is reasonable to hypothesise that the prevalence or effectiveness of NETs in diseased periodontal tissue may be reduced. This could be the result of i) hypo-active NET production, or ii) periodontal bacteria rendering the NETs ineffective by either complete degradation via DNase activity or evasion of trapping by capsule expression or membrane charge modification. The result of this ineffective NET function, would be that bacteria could more freely infiltrate the periodontal tissues, evoking a more widespread inflammatory response culminating in neutrophil mediated tissue destruction e.g. ROS and protease damage. As NETs are thought to function to maintain a high local concentration of AMPs, DNase digestion of NETs may result in liberation of NET-associated AMPs, resulting in more widespread tissue destruction.

Conversely it is conceivable that periodontal disease may associate with an excessive production of NETs, consistent with the theory that patients exhibits a 'hyperreactive phenotype' (Matthews *et al.* 2007a). Patient neutrophils could therefore exhibit constitutive hyperactivity and a raised baseline level of NET production, or they could be hyper-reactive resulting in excessive NET production in response to periodontal bacteria and local pro-inflammatory mediators. In either scenario the implication is that both the neutrophils and their associated degradative enzymes are concentrated within the abundant NETs for an extended duration. Supporting evidence for this hypothesis is derived from data demonstrating that NET release is dependant upon ROS production (Fuchs *et al.* 2007), which is also shown to be increased in periodontal disease (Matthews *et al.* 2007a). In addition, increased neutrophil ROS production has been associated with elevated type-I IFN levels in periodontal disease (Wright *et al.* 2008) and these molecules are also able to prime for NET release (Martinelli *et al.* 2004). It is also interesting to speculate that an abundance of NETs

within a tissue could trigger a localised autoimmune-like response resulting in elevated neutrophil recruitment and tissue destruction (Mayadas *et al.* 2009). This hyperactive NET hypothesis in periodontitis is also supported by Vitkov *et al.* (2009) who visualised NETs in purulent exudates from the gingiva of chronic periodontitis patients. These data are comparable to those previously presented by Buchanan *et al.* (2006) in the examination of abscess exudates from GAS infections of mice, and in human mixed bacterial infection *in vivo* (appendicitis; Brinkmann *et al.* 2004). Vitkov *et al.* also observed that all 22 of the samples collected showed significantly high levels of NETs and that in 7 samples trapped bacteria were associated with the NETs (Figure 18). Notably, transmission electron microscopic (TEM) analysis of pocket epithelium biopsies from chronic periodontitis patients also showed the presence of NETs (Figure 19). Additionally, preliminary work relating to this project has indicated that the structures comprising NETs are present within the gingival tissues at sites of inflammation but less easily seen in healthy gingival tissue when visualised by immunofluorescent staining (Figure 20).

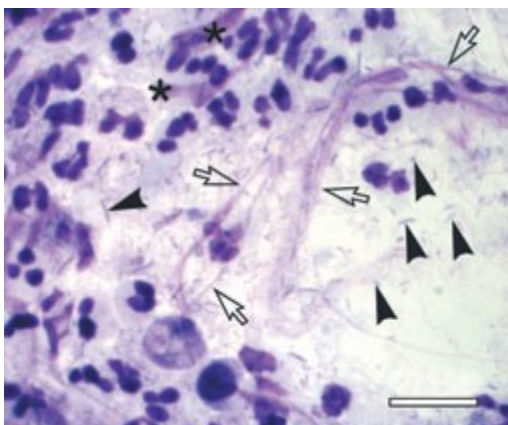


Figure 18. Toluidine blue staining of bacteria (black arrows) associated with NETs (white arrows) from purulent crevicular exudate (Vitkov *et al.* 2009) scale bar represents 20 μ m.

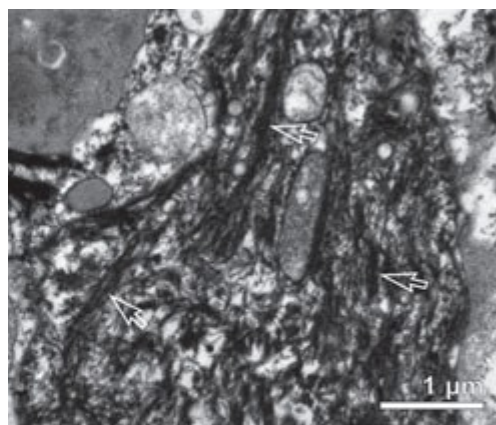


Figure 19. TEM of pocket epithelium (Vitkov *et al.* 2009) Arrows indicate NET fibres.

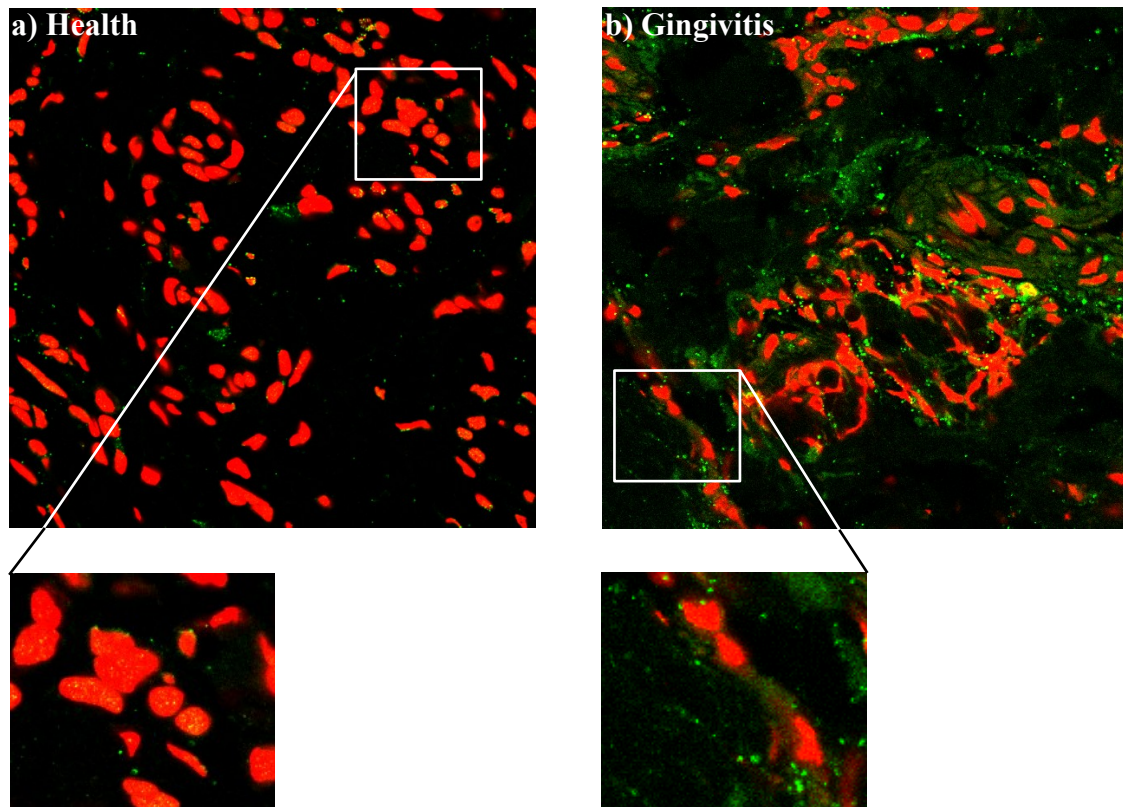


Figure 20. Immunofluorescent staining of gingival tissue sections. a) Healthy gingival tissue, and b) gingivitis derived tissue. MPO (green) and DNA (red). Courtesy of Dr S. Yousefi, University of Berne, Switzerland.

Unifying the two hypotheses (hyper- and hypo-active NET production) is the possibility that the degradation and evasion of NETs by virulent periodontal pathogens may cause neutrophils to respond by up-regulating the release of NETs, resulting not in the trapping of bacteria but instead the immobilisation and localisation of neutrophils responsible for periodontal tissue destruction.

Therefore the factors determining whether one individual develops inflammatory periodontitis whilst another does not, may be determined by i) the type of bacteria inhabiting the gingival crevice, ii) whether these bacteria possess virulence factors for NET evasion, and iii) the individual's innate ability for NET production. In support of biological variation with regard to NET production, data provided by Fuchs *et al.* (2007) demonstrate a significant range in

levels of NET production between neutrophils obtained from several healthy individuals (Figure 21).

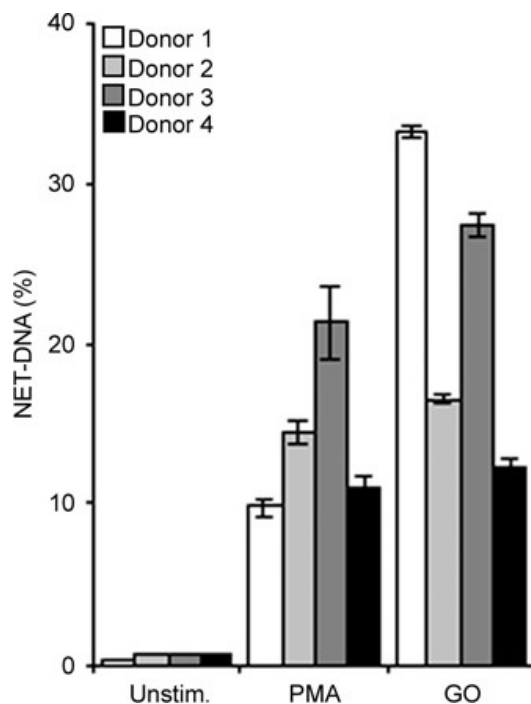


Figure 21. Variation in NET production between donors. Cells were unstimulated, stimulated with 10nM PMA or 100 mU/ml glucose oxidase for 180mins. Extracellular DNA was quantified by micrococcal nuclease digestion and expressed as a percentage of total DNA. Experiments repeated in triplicate to give mean value \pm SD (Fuchs *et al.* 2007).

1.9 Summary and aims

Since the first report in 2004 that neutrophils can extrude their own DNA to form extracellular traps against microorganism survival and dissemination, their role has been examined in a multitude of infectious and non-infectious pathologies as well as physiologies (Table 1). As a disorder mediated by the balance between the innate immune system (namely neutrophils) and the plaque bacteria, periodontitis is a likely disease in which NETs may play a significant role. A variety of *in vitro* and *in vivo* studies have indicated that there is a hyper-active and hyper-reactive neutrophil phenotype with regards to generation of ROS in the active state of periodontitis (Matthews *et al.* 2007a; Matthews *et al.* 2007b). As NET release has been found to depend in part on ROS generation, specifically hydrogen peroxide (Fuchs *et al.* 2007), one

aim of this work was to elucidate whether a hyper-active or hyper-reactive neutrophil phenotype existed with regard to NET generation.

The process of NET release has by no means been fully characterised and their function can only be implied. However, examining the mechanisms bacteria possess which can confer virulence when challenged with NETs can provide further clues to the function of NETs. Although reports of NETs are mixed and often contradictory, characteristics which are common to all reports to date are that they comprise DNA and antimicrobial granule proteins. Thus an obvious candidate for a bacterial virulence factor is expression of DNase. DNase expression has been reported sporadically through the years and found to be a feature of Gram negative anaerobes (Porschen *et al.* 1974) which is of particular relevance to periodontal disease as it is characterised by a high proportion of Gram negative anaerobic bacteria within the subgingival biofilm. In recent years with regards to NETs, *S. pneumoniae* (Beiter *et al.* 2006) and group A streptococci (Buchanan *et al.* 2006) have been found to express DNase which is associated with increased virulence. However, there are no reports of the frequency of DNase expression amongst periodontal pathogens. The other universal component of NETs are the granule peptides suggesting that an antimicrobial property is key to the action of NETs. However, bacteria, particularly the pathogenic varieties responsible for periodontal disease possess an arsenal of strategies to resist antimicrobial attack (Kristian *et al.* 2005; Lauth *et al.* 2009). Therefore it has been suggested that histones, as a component of the chromatin core of NETs, exert a primitive antimicrobial effect. As such, an aim of this work was to examine the susceptibility of periodontal pathogens to the antimicrobial action of histones.

CHAPTER 2 MATERIALS AND METHODS

2.1 NET production *in vitro*

Utilising the fact that DNA is a major structural component of NETs (Brinkmann *et al.* 2004), the fluorescent DNA stain, SYTOX[®] green, was used to both visualise NET release from peripheral neutrophils and HL60 cells, and also for fluorometric quantification of NET release. In addition, scanning electron microscopy (SEM) was used to examine the interaction of periodontal pathogens with extruded NETs.

2.1.1 Isolation of neutrophils

The following section details the isolation of peripheral neutrophils from whole blood using a discontinuous Percoll density gradient for the study of *in vitro* NET release. A Percoll density gradient was used, rather than a dextran/ficoll method (Weinrauch *et al.* 2002), since the latter can pre-activate neutrophils (Rebecchi *et al.* 2000).

2.1.1.1 Percoll density gradient

8ml of 1.098 Percoll was carefully layered underneath 8ml 1.079 Percoll in a 25ml centrifuge tube. The Percoll composition is documented in the table below.

Density	1.079	1.098
Percoll	19.708 ml	24.823 ml
Water	11.792 ml	6.677 ml
NaCl	3.5 ml	3.5 ml

Materials were obtained as Percoll 1.13g/ml (17-0891-01 GE Healthcare); distilled sterile water (Versol); NaCl 1.5M in distilled sterile water (S9625 Sigma). Percoll densities were stored at 4°C.

2.1.1.2 Lysis buffer

1 litre of lysis buffer was made by adding 8.3g NH₄Cl (A9434 Sigma), 1g KHCO₃ (P9144 Sigma), 0.04g Na₂ EDTA 2H₂O (E5134 Sigma) and 2.5g bovine serum albumin (BSA; A4530 Sigma) to 1 litre of water (Versol) and stored at 4°C until use.

2.1.1.3 Phosphate buffered saline (PBS)

1 litre of PBS was made by combining 7.75g NaCl (S9625 Sigma), 0.2g KH₂PO₄ (P5379 Sigma) and 1.5g K₂HPO₄ (P8281 Sigma) with 1 litre distilled water. This solution was autoclaved and stored at 4°C.

2.1.1.4 Method for isolation of neutrophils

12ml venous blood was collected in two 7ml lithium heparin Vacutainers (Greiner, Bio-One) and layered onto a Percoll density gradient (2.1.1.1) in a 30ml centrifuge tube (63.9922.254PP Sarstedt), then centrifuged (IEC Centra CL3R) for 8 minutes at 150 relative centrifugal force (rcf), and 10 minutes at 1200 rcf. The plasma, lymphocyte and monocyte layers were carefully removed and discarded by manual aspiration using a glass Pasteur pipette. The neutrophil layer was located at the top of the red blood cell layer and transferred, again using

a glass Pasteur pipette, to a 50ml centrifuge tube containing 30ml lysis buffer (2.1.1.2). The tube was gently inverted to mix, and incubated at room temperature for 5-10 minutes until red blood cells had lysed. This was then centrifuged for 6 minutes at 500 rcf to pellet the neutrophils. The supernatant was discarded and the pellet re-suspended in a further 2ml lysis buffer and incubated for 5 minutes at room temperature prior to re-centrifugation (6 minutes at 500 rcf). The supernatant was removed, the pellet washed in 2ml PBS, and centrifuged once more for 6 minutes at 500 rcf before re-suspension in 2ml PBS. Cells were counted using a haemocytometer (Naubauer, Reichart) and viability checked by trypan blue exclusion (1:1 mix of cells with trypan blue; T8154 Sigma) and visualisation by light microscope (Leitz Laborlux s).

Neutrophils were resuspended at 1×10^6 cells/ml in glucose supplemented PBS for assay of ROS generation (2.1.7) or RPMI for assay of NET release (2.1.3-2.1.6) and used immediately.

2.1.2 Culture and differentiation of HL60 cells

To develop a readily available source of neutrophil-like cells for the study of NET release, and potentially eliminate inter-personal and temporal variation observed using primary neutrophils, the promyelocytic cell line, HL60, was cultured for comparison to primary neutrophils with regards to NET release.

HL60 cells were a kind gift from the laboratory of Professor Helen Griffiths at Aston University, originally obtained from the European Collection of Cell Cultures (ECACC 98070106). Cells were seeded at a concentration of 2×10^5 cells/ml in RPMI 1640 (L0500

Biosera) supplemented with 300mg/L L-glutamine, 10% foetal calf serum (FCS; S1810 Biosera) and 1% penicillin-streptomycin (P4333 Sigma). Cells were incubated at 37°C in 5% CO₂ for 2 days or until confluent and then stimulated to differentiate into neutrophil-like cells by the addition of 1.25% DMSO (Sigma D2438 sterile filtered) and incubated for 3 days. Subsequently cells were washed twice by centrifuging for 5 minutes at 150 rcf, removing the supernatant and re-suspending the pellet in sterile PBS before a cell count was performed using a haemocytometer and cell viability assessed by trypan blue exclusion. Cells were resuspended at 1x10⁶/ml for use in subsequent experiments.

2.1.3 NET staining

For qualitative assessment of NET release from isolated peripheral neutrophils, cells were seeded onto glass slides and fluorescently stained for visualisation for extruded NETs as detailed below.

2.1.3.1 Paraformaldehyde (PFA) 8%

1.6g PFA (P-6148 Sigma) was dissolved in 20ml PBS by gentle mixing and heating to 60°C. The solution was allowed to cool before passing through filter paper and stored at 4°C.

2.1.3.2 NET staining

Multiwell slides (10.5mm diameter; PH068 C.A. Hendley, Essex) were sterilised overnight at 140°C in an oven (OP30, LTE Scientific Ltd.) and coated in 0.01% poly-L-lysine (P4707

Sigma) diluted in water. Slides were then placed in a humid container lined with damp filter paper. 1×10^5 neutrophils in 100 μ l of RPMI (L0500 Biosera) plus 10% heat inactivated FCS were placed on each well of the slide and allowed to settle for 30 minutes at 37°C. Neutrophils were stimulated with 12.5 μ l of designated stimulus (Table 2) diluted to the appropriate concentration in sterile PBS and left to incubate for up to 3 hours at 37°C. The medium was then removed and cells fixed with 100 μ l (per well) of 4% PFA (2.1.3.1) for 20 minutes at room temperature. PFA was removed and the cells were stained with 100 μ l 1.25 μ M SYTOX[®] green in PBS (S7020 Invitrogen) for 10 minutes and from this point slides were kept covered in aluminium foil to exclude light. Cells were rinsed in 100 μ l PBS before the slides were mounted using aqueous mounting agent (G0918 VWR) and a coverslip

2.1.3.3 Image capture and processing

Cells were visualised using an epi-fluorescent microscope (Nikon Eclipse TE300) with fluorescent filter excitation 472nm and emission 520nm (BrightLine[®] GFP-3035B, Semrock). Images were captured using a digital camera (Nikon Coolpix 990). To demonstrate the extent of fluorescent staining, a light microscope image of the same field was also captured and the fluorescent and light microscope images overlaid using ImageJ (1.38d). Both images were opened and the 'channel merge' function used to assign each image to a separate channel (red, green or blue) and generate a composite image.

2.1.4 Fluorometric analysis of NET release

The release of extracellular NET-DNA was quantified fluorometrically using a fluorescent DNA dye (SYTOX[®] green). Assays were performed in black 96-well microplates (3915 Corning). Added to each well were 1×10^5 cells in 100 μ l media (RPMI L0500 Biosera plus 10% FCS), 25 μ l 10 μ M SYTOX[®] green in PBS (S7020 Invitrogen) and 50 μ l PBS, the volume of which could be replaced with modulating agents as necessary (2.1.9). The fluorescence from each well was recorded at 37°C in arbitrary fluorescent units (AFU) using a fluorometer (Twinkle LB970, Berthold Technologies) with an excitation wavelength of 485nm and an emission wavelength of 525nm. After 30 minutes settling time, 25 μ l of each stimulus was added and the plate was read for up to 3 hours.

2.1.5 Micrococcal nuclease (MNase) assay of NET release

To separate extruded NET-DNA from cellular debris, MNase was used to digest and liberate the DNA into the supernatant for subsequent fluorometric quantification. NETs were produced in black 96-well plates as previously described (2.1.4). 3 hours post stimulation, MNase (LS004797 Worthington Biochemical Corporation) 1 unit/ml was added to each well, and allowed to digest at room temperature for 20 minutes prior to centrifugation at 1800rcf for 10 minutes to pellet the cells. 150 μ l of the supernatant containing the liberated extracellular DNA was then read in the fluorometer for 10 minutes to quantify the DNA.

2.1.6 SEM of NETs

Neutrophils were seeded onto baked and poly-L-lysine coated 13mm glass coverslips and stimulated as previously described (2.1.3.2). After 3 hours samples were fixed in 4% PFA for 20 minutes, rinsed in PBS for at least 20 minutes and dehydrated through graded solutions of ethanol (459844 Sigma) diluted in distilled water (20%, 30%, 40%, 50%, 60%, 70%, 90%, 95%, 95%, 100%, 100% for at least 10minutes each). Samples were then critical point dried (Bio-Rad E3000). Samples were initially placed in to the critical point drier chamber immersed in 100% ethanol. The ethanol was then replaced with carbon dioxide (CO₂; from gas cylinder) by rinsing through the chamber approximately 5 times. The chamber was then gently heated to 32°C, the critical point of carbon dioxide, in order to evaporate all the liquid CO₂. The dried sample was then mounted onto 25mm aluminium stubs (G3024 Agar Scientific) using silver in isobutyl methyl ketone (G3648 Agar Scientific) and coated in gold for 90 seconds (Denton Vacuum Desk II). Samples were analysed using a JOEL JSM-840 scanning electron microscope at an accelerating voltage 10 kilovolts (kV).

2.1.7 Enhanced chemiluminescence assay for ROS

Given that NADPH oxidase activation is necessary for NET formation (Fuchs *et al.* 2007), generation of ROS was analysed alongside NET production to assess the responsiveness of the cells to the various stimuli.

2.1.7.1 GPBSS (glucose supplemented PBS)

GPBSS comprised 1.8g glucose, 0.15g CaCl₂ (10070 BDH) and 1.5ml MgCl₂ (1M; 22093 BDH) which were added to 1 litre PBS and stored at 4°C.

2.1.7.2 Blocking buffer (PBS BSA)

10g BSA (A4503 Sigma) was dissolved in 1 litre PBS to give 1% BSA in PBS. The solution was aliquoted into working volumes and stored at -20°C until use.

2.1.7.3 Luminol and isoluminol

A 30mM stock solution was made by dissolving 0.5g luminol (A8511 Sigma) or isoluminol (A8264 Sigma) in 94.05ml 1mM NaOH and stored at 4°C. The working solution was made by diluting 1ml stock luminol or isoluminol with 9ml PBS and the pH adjusted to 7.3.

2.1.7.4 Lucigenin

A 1mg/ml stock solution of lucigenin (B49203 Sigma) in PBS was prepared and stored at 4°C. The working solution was made by diluting 1:3 in PBS.

2.1.7.5 Method for enhanced chemiluminescent assay for ROS

Neutrophils and HL60 cells were prepared as previously described (2.1.1 and 2.1.2) and 100µl (1x10⁵ cells) in GPBSS were added to white 96-well plates (Microlite; 7567 Thermo

Scientific) that had been coated with blocking buffer (2.1.7.2) overnight at 4°C. To detect total radical generation 30µl luminol (2.1.7.3) was added. To detect extracellular radical generation, 60µl isoluminol (2.1.7.3) in addition to 1.5 units horseradish peroxidase (in PBS; P8415 Sigma) were added. To specifically detect superoxide generation, 30µl lucigenin (2.1.7.4) was added. The total volume of each well was made up to 175µl using PBS and the light output was recorded for 1 second per well in relative light units (RLU) using a Berthold microplate luminometer (LB96v Bethold Technologies U.K. Ltd.) at 37°C. The plate was read for 30 minutes before 25µl of stimuli were added to give a total volume of 200µl per well and read for a further 120 minutes.

2.1.8 Stimuli used to induce NETs

The stimuli listed in Table 2 were used for *in vitro* stimulation of peripheral neutrophils and HL60 cells for the assay of NET and ROS production. PMA is an established stimulus for NETs which bypasses cell surface receptors and directly activates intracellular PKC. fMLP is a chemotactic peptide which acts via surface fMLP receptors and is reported to primarily induce degranulation. A variety of Gram negative and Gram positive periodontal bacteria were also used (Table 6) and can act via a multitude of antigen-receptor interactions. One of the major cell wall components of Gram negative bacteria, such as *F. nucleatum*, is LPS which activates TLR4/2 in conjunction with CD14, MD-2 and LPS binding protein. In Gram positive bacteria the major constituent of the cell wall is lipoteic acid which acts via TLR2. *S. aureus* is a Gram positive bacteria and was opsonised with IgG to enable stimulation of cellular Fcγ-receptors. The calcium ionophore, A23187, was used for the stimulation of HL60 cells to increase intracellular free calcium levels.

Table 2. Stimuli used to induce NETs

Stimuli	Acronym	Supplier/Cat N^o
Phorbol 12-myristate 13-acetate stock concentration 1.62M in DMSO working concentration 405nM in PBS final concentration 50nM	PMA	Sigma P8139
N Formyl Met-Leu-Phe stock concentration 1mM in 99% ethanol working concentration 8000nM in PBS final concentration 1000nM	fMLP	Sigma F3506
Various bacteria working concentration 6x10 ⁸ /ml in PBS final concentration MOI ¹ 1:150		Grown in house (Section 2.1.8.1)
Calcium ionophore A23187 Stock concentration 5mM in DMSO Working concentration 32μM in PBS Final concentration 4μM	CI (Ionomycin)	Sigma C7522

¹MOI multiplicity of infection i.e. number of bacteria per neutrophil.

2.1.8.1 Preparation of bacterial stimuli

For use as stimuli of neutrophils or HL60 cells, bacteria were grown in broth cultures as described later (2.4.4), rinsed twice by centrifugation at 1087 rcf for 40 minutes and re-suspended in sterile PBS, before being stored at -20°C. Bacterial numbers were estimated by spectrophotometry (2.6.2) and diluted to 6x10⁸ per ml in sterile PBS for use in experiments and stored at 4°C.

2.1.8.2 Opsonisation of *S. aureus*

Staphylococcus aureus (ATCC 9144) was cultured on agar without blood as described later (2.4.3) and used to inoculate tryptone soya broth as described later (2.4.4) with the exception of aerobic culture at 30°C (Gallenkamp Plus II Incubator). After overnight growth bacteria were pelleted by centrifugation at 3800 rcf for 5 minutes, the supernatant removed and the pellet re-suspended in sterile PBS. This was repeated 3 times. After the third centrifugation step the bacterial pellet was re-suspended in 3% formaldehyde (P6148 Sigma) in PBS and incubated at room temperature for 1 hour to fix. The bacteria were again washed 3 times by centrifugation and re-suspension in sterile PBS. Bacterial concentration was estimated by spectrophotometry (2.6.2) and diluted in additional sterile PBS to give a suspension of 1×10^9 bacteria per ml. The bacteria were heat treated by incubation at 80°C for 20 minutes prior to the addition of 33µl Vigam liquid (5mg/ml IgG; Bio Products Laboratory) per ml of bacteria and incubated overnight at room temperature with constant agitation to allow opsonisation. Finally, bacteria were again rinsed twice in sterile PBS by centrifugation and re-suspension, and stored at -80°C. Bacterial numbers were again estimated by spectrophotometry to allow resuspension in PBS to give 6×10^8 /ml prior to use.

2.1.9 Modulators of neutrophil function used in NET assays

The agents listed in Table 3 were used to assess their effect on NET release based on their modulation of neutrophil functions, especially ROS generation which reportedly affects NET release. DPI directly inhibits the NADPH oxidase enzyme, sodium azide primarily inhibits the azurophilic granule protein myeloperoxidase responsible for the conversion of hydrogen peroxide to hypochlorous acid and SOD is an endogenous enzyme responsible for the

conversion of superoxide to hydrogen peroxide. In addition, curcumin was used as it is an antioxidant with widespread anti-inflammatory properties, and also cytochalasin B which is an actin polymerisation inhibitor and as such prevents bacterial phagocytosis. In each case the background fluorescence due to the addition of the agents and/or stimuli was controlled for by simultaneously processing wells containing all reagents but no cells, and this value was subtracted from that of the test wells.

Table 3. Modulators of NET release

Modulating agent	Cat N° / Supplier
Diphenyleneiodonium chloride (DPI) stock concentration 0.6mM in PBS working concentration 0.2mM final concentration 50µM	D2926 Sigma
Superoxide dismutase (SOD) stock concentrations 4750U/ml in PBS mixed working concentration 1267U/ml final concentration 95U/ml	S5395 Sigma (Cu/Zn-SOD) S5639 Sigma (Mn-SOD)
Curcumin stock concentration 10mM in 99% ethanol working concentration 0.1mM in PBS final concentration 5µM	28260 Fluka
Cytochalasin B (cytoB) stock concentration 14mg/ml in DMSO working concentration 143.3µg/ml final concentration 10µg/ml	C6762 Sigma
Sodium azide stock concentration 2.1M in dH ₂ O working concentration 42mM in PBS final concentration 2mM	S2002 Sigma

15µl of the working concentration of each modulating agent was added to a 200µl well at the start of the experiment, prior to the addition of the cells.

2.2 Comparison of NET production between periodontal patients and healthy individuals

The following section details the use of the previously described NET and ROS assays to compare the responses of peripheral neutrophils of periodontitis patients to healthy controls.

2.2.1 Selection of volunteers

Periodontitis patients were recruited as part of an ongoing clinical trial (ID: NCT00952536), and ethical approval was obtained from the South Birmingham Local Research Ethics Committee (05/Q2707/252). Inclusion criteria were patients with chronic periodontitis suffering from at least 30% bone loss and aged between 30 and 60 years. Exclusion criteria included diabetes, pregnancy, smokers and use of vitamin supplements. A 12ml blood sample was obtained using two 7ml lithium heparin vacutainers (Greiner, Bio-One) at baseline, i.e. prior to treatment. On the same day, blood samples were also taken from age and sex matched periodontally healthy controls who were recruited using the same exclusion criteria.

2.2.2 Assay of peripheral blood neutrophils

Neutrophils were isolated as previously described using a Percoll density gradient (2.1.1). NET production was evaluated as previously described by MNase assay (2.1.5) and ROS production was also assayed as previously described (2.1.7). Cells were stimulated using PMA, *F. nucleatum* subsp. *polymorphum* (ATCC 10953), opsonised *S. aureus* (2.1.8) or were unstimulated (PBS exposure).

2.3 HL60 cell characterisation

2.3.1 Gene expression analysis by RT-PCR in HL60 cells and primary neutrophils

Reverse transcriptase-polymerase chain reaction (RT-PCR) was used to compare the gene expression profile of neutrophil related gene transcripts (primers listed in Table 4) in differentiated HL60 cells and primary neutrophils.

Table 4. Primers and conditions used for gene expression analysis in HL60 cells

Gene (Gene Abbreviation) Primer sequence (5'→3')	Cycle number	Product size	Source	Accession number
Glyceraldehyde-3-phosphate dehydrogenase (GAPDH) F-TCT AGA CGG CAG GTC AGG TCC R-CCA CCC ATG GCA AAT TCC ATG	24	391bp	(McLachlan <i>et al.</i> 2004)	
Haemoxygenase 1 (HMOX1) F-AAC CTC CAA AAG CCC TGA GT R-CAC CCC AAC CCT GCT ATA AA	34	207bp	Designed in-house*	NM_0002133.1
Superoxide dismutase 2 (SOD2) F-TGG AGG CAT CTA GTG GAA AAA R-CCC AGT CTC TCC CCA TTA CA	34	305bp	Designed in-house*	S77127
Toll like receptor 2 (TLR2) F-GAT GCC TAC TGG GTG GAG AA R-CGC AGC TCT CAG ATT TAC CC	34	392bp	Designed in-house*	NM_003264.3
Toll like receptor 4 (TLR4) F-AAC CAT CCT GGT CAT TCT CG R-CGG AAA TTT TCT TCC CGT TT	34	315bp	Designed in-house*	NM_138444-2
Toll like receptor 9 (TLR9) F-CTG CGT CTC CGT GAC AAT TA R-GTC CTG TGC AAA GAT GCT GA	34	443bp	Designed in-house*	AB045180.1
Phox22 (p22) F-GTT TGT TTT GTG CCT GCT GGA GT R-TGG GCG GCT GCT TGA TGG T	30	325bp	(Jones <i>et al.</i> 1996)	

Gene (Gene Abbreviation) Primer sequence (5'→3')	Cycle number	Product size	Source	Accession number
Phox47 (p47) F-ACC CAG CCA GCA CTA TGT GT R-AGT AGC CTG TGS CGT CGT CT	37	767bp	(Jones <i>et al.</i> 1996)	
Phox67 (p67) F-CGA GGG AAC CAG CTG ATA GA R-AGT AGC CTG TGA CGT CGT CT	37	726bp	(Jones <i>et al.</i> 1996)	
Gp91 Phox (gp91) F-GCT GTT CAA TGC TTG TGG CT R-TCT CCT CAT CAT GGT GCA CA	37	403bp	(Jones <i>et al.</i> 1996)	
NFκB2 F-CGT ACC GAC AGA CAA CCT CA R-CCG TAC GCA CTG TCT TCC TT	34	186bp	Designed in-house*	NM_002502.2
Heat shock protein 40 (Hsp40) F-TAC AGG AGC ACT GTG GAA CG R-AGG TCT GAG CAC TGG ACT GG	30	192bp	Designed in-house*	D49547.1
CXCL3/GRO3 F-TAA ATG ACA GGG TGG GGA AC R-GCA TTA TGC CCT ACA AGC AA	44	224bp	Designed in-house*	NM_002090
Colony stimulating factor 1 (CSF1) F-GCA CTA ATT GGG TCC CAG AA R-GAT GCA GGG AGT GGA GAA GA	35	159bp	Designed in-house*	M64592.1

All primers supplied by Invitrogen (UK) except p22, p47, p67 gp91 (AltaBioscience, University of Birmingham, UK). *Designed in-house from the Affymetrix probe target identifier sequences using the Primer3 program (frodo.wi.mit.edu/cgi-bin/primer3/primer3_www.cgi).

2.3.1.1 mRNA extraction

Following differentiation of HL60 cultures using 1.25% DMSO for 3 days (2.1.2), cells were washed twice and re-suspended in sterile PBS at 2.5×10^6 cells per ml. For comparison, primary neutrophils were also isolated as described previously (2.1.1) before also being re-suspended in sterile PBS at 2.5×10^6 cells per ml. 1ml of cells was added to 500 μ l PBS containing either PMA (50nM), *F. nucleatum* (MOI 1:150) or PBS alone and incubated (uncapped) at 37°C for 3 hours. Cells were then pelleted by centrifugation for 5 minutes at 1800 rcf, the supernatant removed and the cell pellet re-suspended by vigorous agitation using a bench top vortex (VortexGenie2, Scientific Industries) in 1ml TRI REAGENT™ (T9424 Sigma). RNA was extracted using a phenol, phenol-chloroform, chloroform extraction technique. 200 μ l chloroform (C2432 Sigma) was added to the 1ml TRI REAGENT, mixed for 15 seconds and left at room temperature for 15 minutes. This was centrifuged at 12000 rcf for 5 minutes to separate the protein, DNA and RNA layers. The clear top layer containing the RNA was transferred by pipette to a separate microfuge tube and 500 μ l isopropanol (I-9516 Sigma) added, mixed thoroughly and kept on ice for 10 minutes. At this stage 1 μ l GlycoBlue (9515 Ambion) was added to enable visualisation of the RNA pellet following centrifugation at 12000 rcf for 5 minutes. The supernatant was removed and the pellet washed by re-suspension in 1ml ethanol (E7023 Sigma) by vortexing. The RNA was again pelleted by centrifugation at 7500 rcf for 5 minutes, the supernatant was carefully removed and the pellet allowed to air dry for 10 minutes. The RNA was subsequently re-suspended in ribonuclease (RNase) free water and stored at -80°C until further processing.

2.3.1.2 Reverse transcription

RNA was reverse transcribed to complementary DNA (cDNA) using an Omniscript RT Kit (205111 Qiagen). 2µg RNA (estimated by absorbance at 260nm) in 12µl water was combined with 2µl Oligo (dT) primer (10µM; AM5730G Ambion) and heated at 80°C for 10 minutes then cooled on ice for 5 minutes. The reagents supplied in the Omniscript RT Kit were added to each reaction and consisted of 2µl buffer RT, 2µl dNTP Mix, 1µl Omniscript Reverse Transcriptase plus 1µl RNasin[®] RNase inhibitor (10units/µl; N211B Promega). The mix was incubated at 37°C for 60 minutes then 95°C for 5 minutes. The reverse transcribed cDNA was washed with RNase free water and concentrated by centrifugation at 7267 rcf through Microcon[®] centrifugal filters (30,000 MWCO; 42410 Millipore) until only approximately 50µl remained in the filter. This was collected into a sterile microfuge tube by inverting the filter and centrifuging at 1162 rcf for 3 minutes.

For analysis of primary neutrophils, the cDNA from 4 different healthy individuals (2 male and 2 female) was pooled, and for analysis of HL60 cells the cDNA from 2 different flasks of cells cultured in successive passages was pooled. cDNA samples were stored at -20°C until use.

2.3.1.3 PCR amplification of selected transcripts

Amplification of genes characteristic of neutrophil functions (Table 4) was performed by mixing 1.25µl cDNA with 12.5µl REDTaq ReadyMix PCR mix (R2523 Sigma), 10.25µl molecular biology grade water and 0.5µl each of the forward and reverse primers (12.5µM). Amplification was performed in a GeneAmp[®] PCR System 2700 (Applied Biosystems). The

temperature profile consisted of an initial denaturing step at 94°C for 5 minutes, followed by a specified number of cycles (Table 4) of a denaturation step of 94°C for 20 seconds, a primer annealing step of 61°C for 20 seconds, and an extension step at 72°C for 20 seconds. Finally an extension step of 72°C for 10 minutes was employed.

2.3.1.4 Gel electrophoresis and image capture

A 1.5% agarose gel was made by dissolving 1.5g agarose (AGR-500 Web Scientific) per 100ml TAE buffer (129237 Qiagen) by gentle heating (Microwave, Sanyo) prior to addition of ethidium bromide (E7637 Sigma) to a final concentration of 0.5µg/ml. The gel was poured and allowed to set at room temperature before a 6µl PCR sample was loaded per well and electrophoresed in TAE buffer at 80 volts for up to 1 hour. The gel was visualised under ultraviolet transillumination (EtBr/UV filter) using G:BOX (SynGene) and an image was captured using GeneSnap software (SynGene).

For relative expression level analysis the band intensity of the amplified products were normalised to the band intensity of the housekeeping gene GAPDH using GeneTools software (SynGene). Briefly images were opened in GeneTools in the ‘manual band quantification’ mode and the ‘spot: rectangle’ tool was used to isolate individual bands. The ‘assign quantity’ tool was used to assign the brightest or control band a value of 100% by setting the ‘calibrated quantity’ at 100. All other band intensities were subsequently displayed as a percentage relative to this reference band (100%).

2.3.2 Staining of HL60 cells

To compare the cell morphology of undifferentiated and differentiated HL60 cells to primary neutrophils, cells were washed in PBS, re-suspended at 1×10^6 cells/ml in PBS and placed onto poly lysine treated multiwell slides (2.1.3) for 30 minutes. The cells were then fixed using dry acetone (20065 VWR) for 15 minutes prior to air drying for 10 minutes and storage at -80°C until staining.

2.3.2.1 Haematoxylin and Eosin staining

For Haematoxylin and Eosin staining slides were treated with Gill's III Haematoxylin (Surgipath Europe Ltd.) for 2 minutes 30 seconds, rinsed in water, 0.3% acetic acid (Merck Ltd.) for 1 minute, 0.3% HCl (Merck Ltd.) in 70% ethanol (459844 Sigma) for 1 minute, rinsed in tap water, followed by Scotts Tap Water Substitute (Surgipath Europe Ltd.) for 1 minute, rinsed in tap water, Eosin (Surgipath Europe Ltd.) for 30 seconds, rinsed in tap water, 100% ethanol (459844 Sigma), xylene (Genta Medical) for 1 minute x3 and finally mounted using XAM neutral medium (361194Y BDH).

2.3.2.2 Immunocytochemical staining

For immunocytochemical staining of neutrophil elastase and myeloperoxidase, endogenous peroxidase activity was first blocked using 0.3% H_2O_2 (H-1009 Sigma) in methanol (20847 VWR) for 10 minutes then rinsed in PBS. Primary antibody diluted in 1% BSA in PBS (Table 5) was applied for 2 hours, the cells were then rinsed twice in PBS before the secondary antibody (Table 5) diluted in 10% human serum, was applied for 2 hours. Cells

were again washed twice in PBS and a concentrated label (peroxidase-conjugated streptavidin; HK320-UK BioGenex) was diluted 1:50 in 10% human plasma, and applied for 1 hour. Cells were washed twice in PBS and 0.05% diaminobenzidine in PBS supplemented with 1.25µl/ml H₂O₂ (30%; H-1009 Sigma) was applied for 5 minutes. The slides were washed well in water before being dehydrated through 70%, 80%, 90% and 100% ethanol for 5 minutes each, and kept in xylene until being mounted in XAM.

Table 5. Antibodies and dilutions used for immunocytochemical staining.

Primary antibody	Polyclonal Sheep Anti-Human Neutrophil Elastase (The Binding Site, PC052)	Polyclonal Rabbit Anti-Human MPO (Dako, A0398)
Dilution	11.75µg/ml	11µg/ml
Secondary antibody	Donkey Anti-Sheep/Goat Ig (biotin conjugate) 1:1600 (AB360 The Binding Site)	MultiLink [®] (biotinylated anti-immunoglobulins)1:50 (HK268-UK BioGenex)

2.4 Culture of bacteria

A panel of 34 anaerobic periodontal bacteria (Table 6) obtained from the Forsyth Institute, Boston and originally purchased from the American Type Culture Collection (ATCC) were cultured i) for use as stimuli of neutrophils and HL60 cells in the assay of NET and ROS generation (2.1), ii) for bacterial DNase activity characterisation (2.7) and iii) for antimicrobial susceptibility testing using histones (2.6).

Table 6. Oral microorganisms used in this study

ATCC number	Bacterial strain
10556	<i>Streptococcus sanguis</i>
10558	<i>Streptococcus gordonii</i>
10790	<i>Veillonella parvula</i>
10953	<i>Fusobacterium nucleatum</i> subsp. <i>polymorphum</i>
11827/8	<i>Propionibacterium acnes</i>
12102	<i>Actinomyces israelii</i>
12104	<i>Actinomyces naeslundii</i> <i>genospecies 1</i>
14201	<i>Leptotrichia buccalis</i>
17929	<i>Actinomyces odontolyticus I</i>
19696	<i>Neisseria mucosa</i>
25175	<i>Streptococcus mutans</i>
25586	<i>Fusobacterium nucleatum</i> subsp. <i>nucleatum</i>
25611	<i>Prevotella intermedia</i>
25845	<i>Prevotella melaninogenica</i>
27335	<i>Streptococcus intermedius</i>
27823	<i>Streptococcus constellatus</i>
27824	<i>Gemella morbillorum</i>
29523	<i>Aggregatibacter actinomycetemcomitans</i> serotype a
33236	<i>Campylobacter gracilis</i>
33238	<i>Campylobacter rectus</i>
33270	<i>Peptostreptococcus micros</i>
33277	<i>Porphyromonas gingivalis</i>
33397	<i>Streptococcus anginosus</i>
33612	<i>Capnocytophaga sputigena</i>
33563	<i>Prevotella nigescens</i>
33624	<i>Capnocytophaga gingivalis</i>
35037	<i>Streptococcus oralis</i>
35308	<i>Prevotella denticola</i>
43037	<i>Tannerella forsythensis</i>
43146	<i>Actinomyces viscosus</i> (<i>naeslundii</i> <i>genospecies 2</i>)
43718	<i>Aggregatibacter actinomycetemcomitans</i> serotype b
49456	<i>Streptococcus mitis</i>
51146	<i>Campylobacter showae</i>

2.4.1 Storage of bacteria

All bacteria were stored at -80°C in 2ml cryovials containing 1.5ml tryptone soya broth (2.4.4.1) supplemented with 10% v/v DMSO. Initial inoculae were established by defrosting the frozen microorganism aliquots at room temperature prior to pouring on to agar plates (2.4.3) for 1 week anaerobic incubation with plates facing upwards. Subsequently cultures were grown and assayed on agar plates or planktonically in liquid culture.

2.4.2 Culture conditions

All oral microorganisms were grown in an anaerobic chamber (Don Whitley Scientific, Modular Atmosphere Controlled System, CAL-3200, Shipley, UK) to provide an environment of carbon dioxide 9.97%, hydrogen 9.92% with nitrogen balance at 37°C. Re-plating of all oral organisms was required every 7 days and were used in subsequent assays on day +5 or +6.

2.4.3 Blood agar

All oral microorganisms were cultured on blood agar plates. These comprised tryptone soya agar (CM0131 Oxoid) prepared according to the manufactures instructions at 40g in 1 litre distilled water. After autoclaving at 121°C for 15 minutes the agar was cooled to 50°C in a water bath, before 5% defibrinated horse blood (SR0050B Oxoid) was aseptically added. Agar was poured into triple vented Petri dishes (101VR20 Sterilin) and left inverted for 24 hours to allow ventilation of excess moisture, prior to storage at 4°C. Before use, dishes were allowed to equilibrate at room temperature for 1 hour.

2.4.3.1 Enriched blood agar

The growth of *P. gingivalis* and *T. forsythensis* required blood agar enriched with the components described below - hemin (2.4.3.2), NAM (2.4.3.3) and vitamin K (2.4.3.4) - and termed HNK agar.

2.4.3.2 Hemin (100x concentration)

50mg hemin (H-5533 Sigma) and potassium phosphate 1.74g (P-5504 Sigma) were added to 100ml of distilled water. This solution was boiled until the hemin had dissolved. After cooling to room temperature, the solution was stored at 4°C covered in aluminium foil.

2.4.3.3 N-acetylmuramic acid (NAM; 100x concentrated solution)

100mg of NAM (A3007 Sigma) was dissolved in 10ml of distilled water and filter sterilised (0.2µm, BC591 Appleton Woods) prior to storage at -20°C.

2.4.3.4 Vitamin K (100x concentrated solution)

5mg menadione (M-5625 Sigma) was dissolved in 1ml of 95% ethanol (Sigma). 99ml distilled water was added and the resultant solution filter sterilised (430944 Corning) prior to storage at -20°C.

2.4.3.5 Preparation of enriched blood agar

For the preparation of 10 HNK agar plates the following were added to 250ml distilled water: 5.0g tryptone soya agar (CM0131 Oxoid), 6.5g brain heart infusion (CM225 Oxoid), 2.5g yeast extract (Y-1001 Sigma) and 2.5ml hemin (2.4.3.2). This solution was sterilised by autoclaving at 121°C for 15 minutes. The agar was cooled to 50°C and 300µl NAM (2.4.3.3), 2.5ml vitamin K (2.4.3.4) and 12.5ml defibrinated horse blood (SR0050B Oxoid) was subsequently added before pouring into 90mm triple vented Petri dishes and allowed to set at room temperature.

2.4.4 Planktonic growth of bacteria

All liquid media were allowed to equilibrate at room temperature for 1 hour before use. Sterile broth was inoculated by transfer of bacterial growth from agar plate cultures using a flame sterilised loop. Cultures were then incubated anaerobically with gentle agitation (Vibrax VXR basic, IKA) until turbidity was observed.

2.4.4.1 Tryptone soya broth

Tryptone soya broth (CM0129 Oxoid) was prepared according to the manufacturers instructions. 10ml of the tryptone soya broth was aliquotted into borosilicate glass culture tubes (FB59537 Fisher Scientific) with vented plastic caps (TB51373 Fisher Scientific) and autoclaved at 121°C for 15 minutes prior to storage at 4°C.

2.4.4.2 Enriched tryptone soya broth

An enriched tryptone soya broth was required for the growth of *T. forsythensis* and *P. gingivalis*. 1mg/ml glucose powder and 0.01ml per ml hemin were added to the standard tryptone soya broth prior to autoclaving, in addition to either 10µg/ml NAM or 0.3µg/ml vitamin K for *T. forsythensis* and *P. gingivalis* respectively after autoclaving.

2.5 Identification of bacteria

The identification of bacteria was verified by streak plating out to single colonies to observe colony morphology. Bacteria were also Gram stained to observe microscopic cell morphology and tested for catalase activity primarily to distinguish streptococci and staphylococci. The reference system used for identification was Bergey's Manual of Determinative Bacteriology (Holt 1994). Bacterial identity was also validated using PCR amplification of species specific genes which predominantly included analysis of the 16s ribosomal RNA. This analysis was possible for 29 of the 34 test bacteria used in these studies.

2.5.1 Gram stain

Gram staining distinguishes between Gram positive bacteria which have peptidoglycan outer layer and are stained purple by crystal violet, and Gram negative bacteria which have an outer lipid membrane which is removed by acetone along with the purple staining and are therefore counter-stained pink with carbol fuchsin.

2.5.1.1 Crystal violet solution

10g of crystal violet (C0775 Sigma) was dissolved in 100ml 95% ethanol. 20ml of this was mixed with 80ml of 1% ammonium oxalate (A8545 Sigma) in distilled water and allowed to stand for several weeks prior to use.

2.5.1.2 Carbol fuchsin

Strong carbol fuchsin (351874U BDH) was diluted 1:9 in distilled water.

2.5.1.3 Method for Gram stain

A drop of sterile 85% saline was placed on a microscope slide. A sterile loop was used to transfer bacterial colonies and emulsified in the saline. The suspension of bacteria was dried by passing the slide several times through a flame to fix the bacteria. The bacteria were then covered with crystal violet for 30 seconds, rinsed under tap water, Lugols iodine (L6146 Sigma) was applied for 15 seconds, rinsed, flooded with acetone and washed immediately, then treated with carbol fuchsin for 15 seconds and rinsed. The slide was blotted dry and viewed under oil immersion microscope (Leitz Dialux 22). Images were captured using a digital camera (Nikon Coolpix 990). 'Blank' photographs taken at the same magnification and focus of an empty field were also obtained to perform background subtraction using ImageJ software. Both images were subsequently opened in the ImageJ software and the 'morphology': 'calculator plus' plugin used to 'divide' the image by the background image. The resultant image was subsequently saved.

2.5.2 Catalase test

A small glass capillary tube was used to contact a bacterial colony on an agar plate and the other end dipped into 3% hydrogen peroxide (H-1009 Sigma). The tube was inverted and the hydrogen peroxide was allowed to run down the capillary tube until it came into contact with the bacteria. A positive result was indicated by the production of bubbles observed visually, as oxygen was liberated from the hydrogen peroxide as it was converted by catalase.

2.5.3 PCR identification

Genes specific to each bacterial species were amplified by PCR

2.5.3.1 PCR primers

Where possible, primer sequences were taken from the existing literature. Where no primers existed, bacterial gene sequences were obtained from NCBI Entrez nucleotide database (<http://www.ncbi.nlm.nih.gov/sites/entrez?db=nucleotide&itool=toolbar>) and primers were designed in-house. A search for genes with similar sequences was performed using nucleotide BLAST (basic local alignment search tool) with microbial genomes (http://www.ncbi.nlm.nih.gov/sutils/genom_table.cgi) and genes with a >90% homology with the desired gene as well as those from related bacterial species were aligned using ClustalW2 (Larkin *et al.* 2007) (<http://www.ebi.ac.uk/Tools/clustalw2/index.html>). Regions of sequence unique to the gene of interest were identified to give primers of approximately 20 base pairs (bp) in length which could be used to amplify DNA products of approximately 300-650bp

(Table 7). For gene sequence alignments which were used for species specific primer design, see Appendix (Figure 92).

Table 7. Primers and PCR conditions used for bacteria identification

Bacterial species (gene) Primer sequence (5'-3')	Cycles	Annealing conditions	Source	Accession number
<i>S. sanguis</i> (glucosyltransferaseP) GGA TAG TGG CTC AGG GCA GCC AGT T GAA CAG TTG CTG GAC TTG CTT GTC	30	70°C 1min	(Hoshino <i>et al.</i> 2004)	
<i>V. parvula</i> (16S rRNA) TGA AAG GTG GCC TCT ATT TAT CAA TCC TTC TAA CTG TTC GCA AG	35	60°C 20sec	(Rôças <i>et al.</i> 2006)	
<i>F. nucleatum</i> (16S rRNA) CTA AAT ACG TGC CAG CAG CC CGA CCC CCA ACA CCT AGT AA	33	55°C 20sec	(Kulekci <i>et al.</i> 2001)	
<i>L. buccalis</i> (16s rRNA) TGC CAG CAC GCA TGT GCC CGG CA ACG GAC ACT CTT CAT GCC C	30	50°C 20sec	Designed in-house	X90831
<i>A. odontolyticus</i> (16s rRNA) GCT CAT GGT CAA GCC GC ATC TCT GCA GTG CCG CC	30	50°C 20sec	Designed in-house	AJ234054
<i>N. mucosa</i> (penicillin binding protein A) GGT TTT GTC TTT GGA TCA AC ATG GTG TTA AAA CGA TCA GC	35	50°C 20sec	Designed in-house	X59635
<i>S. mutans</i> (glucosyltransferaseD) GGC ACC ACA ACA TTG GAA GCT CAG TT GGA ATG GCC GCT AAG TCA ACA GGA T	30	70°C 1min	(Hoshino <i>et al.</i> 2004)	

Bacterial species (gene) Primer sequence (5'-3')	Cycles	Annealing Conditions	Source	Accession number
<i>P. intermedia</i> (16S rRNA) TTT GTT GGG GAG TAA AGC GGG TCA ACA TCT CTG TAT CCT GCG T	36	55°C 1min	(Ashimoto <i>et al.</i> 1996)	
<i>S. intermedius</i> (intermedilysin) CTC ACC CTC AAT CAT GAT GGT GC CGA CTC ACT ATA GGG AGA TCA GCA TGG	36	55°C 1min	(Goto <i>et al.</i> 2002)	
<i>S. constellatus</i> (hyaluronate lyase) TGG TGG GAC TAC GAG ATT GG CTC TCT CTT GAG ATT GTT GC	30	58°C 15sec	(Takao <i>et al.</i> 2004)	
<i>A. actinomycetemcomitans</i> a (mannosyltransferase) GCA ATG ATG TAT TGT CTT CTT TTG GA CTT CAG TTG AAT GGG GAT TGA CTA AAA C	40	55°C 5sec	(Suzuki <i>et al.</i> 2001)	
<i>C. gracilis</i> (16S rRNA) AAC GGA ATT TAA GAG AGC TT CTT TCC CGA TTT ATC TTA TG	26	53°C 45sec	(Siqueira Júnior <i>et al.</i> 2003)	
<i>C. rectus</i> and <i>C. showae</i> (16S rRNA) TTT CGG AGC GTA AAC TCC TTT TC TTT CTG CAA GCA GAC ACT CTT	36	60°C 1min	(Slots <i>et al.</i> 1995)	
<i>P. micros</i> (16S rRNA) TCG AAC GTG ATT TTT GTG GA TCC AGA GTT CCC ACC TCT	28	55°C 1min	(Riggio <i>et al.</i> 2001)	

Bacterial species (gene) Primer sequence (5'-3')	Cycles	Annealing conditions	Source	Accession number
<i>P. gingivalis</i> (fimbrial protein) ATA ATG GAC AAC AGC AGG AA TCT TGC CAA CCA GTT CCA TTG C	40	55°C 30sec	(Watanabe <i>et al.</i> 1993)	
<i>S. anginosus</i> (16S rRNA) GCG TAG GTA ACC TGC CTA TTA GA CGC AGG TCC ATC TAC TAG C	30	58°C 15sec	(Takao <i>et al.</i> 2004)	
<i>C. sputigenia</i> (16s rRNA) AGA GTT TGA TCC TGG CTC AG GAT GCC GCT CCT ATA TAC CAT TAG G	35	55°C 20sec	(Hayashi <i>et al.</i> 2001)	
<i>P. nigrescens</i> (16S rRNA) ATG AAA CAA AGG TTT TCC GGT AAG CCC ACG TCT CTG TGG GCT GCG A	36	55°C 1min	(Ashimoto <i>et al.</i> 1996)	
<i>C. gingivalis</i> (16s rRNA) AGA GTT TGA TCC TGG CTC AG GGA CGC ATG CCC ATC TTT CAC CAC CGC	30	65°C 20sec	(Hayashi <i>et al.</i> 2001)	
<i>S. oralis</i> (glucosyltransferaseR) TCC CGG TCA GCA AAC TCC AGC C GCA ACC TTT GGA TTT GCA AC	30	66°C 1min	(Hoshino <i>et al.</i> 2004)	
<i>T. forsythensis</i> (16S rRNA) GCG TAT GTA ACC TGC CCG CA TGC TTC AGT GTC AGT TAT ACC T	36	60°C 1min	(Slots <i>et al.</i> 1995)	

Bacterial species (gene) Primer sequence (5'-3')	Cycles	Annealing conditions	Source	Accession number
<i>A. viscosus</i> (unknown protein) ATG TGG GTC TGA CCT GCT GC CAA AGT CGA TCA CGC TCC G	40	55°C 20sec	(Suzuki <i>et al.</i> 2004)	
<i>A. actinomycetemcomitans</i> b (deoxyglucose reductase) CGG AAA TGG AAT GCT TGC CTG AGG AAG CCT AGC AAT	40	55°C 5sec	(Suzuki <i>et al.</i> 2001)	
<i>P. acnes</i> (16s rRNA) GGG TTG TAA ACC GCT TTC GCC T GGC ACA CCC ATC TCT GAG CAC	30	54°C 20sec	(Sfanos <i>et al.</i> 2008)	
<i>A. israelii</i> (16s rRNA) AGA GTT TGA TCC TGG CTC AG CCA AAA CAC CAC AAA AGT GA	30	58°C 20sec	(Conrads <i>et al.</i> 1997)	
<i>A. naeslundii</i> (fimbrial protein) GTC CAC GTC TAC CCC AAG AAC CAG GAA GAT GAC GCC GTT GGC	36	60°C 20sec	(Tran <i>et al.</i> 1996)	
<i>P. melaninogenica</i> (haemolysin) CGT CAT GAA GGA GAT TGG ATA GAA CCG TCA ACG CTC	35	54°C 20sec	(Yoshida <i>et al.</i> 2005)	
<i>P. denticola</i> (16s rRNA) TTC TTC GAT GAC GGC ATC AGA TT GTC AGA CGT TGG GCG CCT ACA	35	55°C 20sec	Designed in-house	L16467

2.5.3.2 Bacterial PCR

1x10⁶ bacteria suspended in 1µl molecular biology grade water were mixed with 12.5µl REDTaq ReadyMix PCR reaction mix (R2523 Sigma), 10.5µl molecular biology grade water and 0.5µl each of the forward and reverse primers (25µM). Amplification was performed in a GeneAmp[®] PCR System 2700 (Applied Biosystems). The temperature profile consisted of an initial denaturing step at 94°C for 5 minutes which also served to lyse the bacteria. This was followed by a specified number of cycles (Table 7) of a denaturation step of 94°C for 20 seconds, a primer annealing step (Table 7), and an extension step at 72°C for 20 seconds. Finally an extension step of 72°C for 10 minutes was performed.

PCR products were analysed by 1.5% agarose gel electrophoresis and images captured as previously described (2.3.2.4).

2.6 Antimicrobial susceptibility testing using histone proteins

A major structural component of NETs is chromatin (i.e. DNA in complex with histones), and purified histone H2A has been reported to exert an antimicrobial effect (Brinkmann *et al.* 2004). Therefore the antimicrobial capacity of mixed histone to inhibit the growth of periodontal pathogens was assayed by the methods detailed below.

2.6.1 Microtitre plate analysis for antimicrobial susceptibility testing

10ml tryptone soya broth (2.4.4.1) was inoculated with bacteria and incubated anaerobically overnight with agitation. The culture was homogenised by mixing and 1ml of the culture read in a spectrophotometer (2.6.2). All cultures were then adjusted to 2×10^5 bacteria/ml by addition of sterile tryptone soya broth using values listed in Table 8. In a clear sterile 96-well plate (3360 Corning) 100 μ l bacteria were added to 80 μ l sterile tryptone soya broth and 20 μ l mixed histone (H9250 Sigma) in PBS 1mg/ml, 20 μ l penicillin-streptomycin as a positive control (100units penicillin/100 μ g streptomycin per ml diluted in PBS) or 20 μ l PBS as a negative control. The plate was incubated anaerobically overnight at 37°C with gentle agitation (Vibrax VXR basic, IKA).

2.6.2 Determination of bacterial growth by spectrophotometry

Cell growth was estimated using a spectrophotometer (Jenway 6300) by measuring optical density at 600nm (OD_{600nm}). Non-inoculated samples of media were used to correct for media changes in absorbance at OD_{600nm} not due to bacterial growth. The OD_{600nm} values used to estimate bacterial growth were calculated by the Forsyth Institute, Boston and are listed in Table 8. For spectrophotometric readings of bacterial growth in microtitre plates after overnight anaerobic incubation (2.6.1), an automated plate reader (ELx800, Bio-Tek Instruments Inc.) was used to record absorbance at 590 or 630 nm.

Table 8. OD values of bacteria

ATCC number	Bacterial strain	Bacteria per ml if OD₆₀₀=1
10556	<i>S. sanguis</i>	1.69 x 10 ⁹
10558	<i>S. gordonii</i>	1.69 x 10 ⁹
10790	<i>V. parvula</i>	6.80 x 10 ⁹
10953	<i>F. nucleatum</i> subsp. <i>polymorphum</i>	1.62 x 10 ⁹
11827/8	<i>P. acnes</i>	1.69 x 10 ⁹
12102	<i>A. israelii</i>	8.30 x 10 ⁸
12104	<i>A. naeslundii</i> I	8.30 x 10 ⁸
14201	<i>L. buccalis</i>	8.30 x 10 ⁸
17929	<i>A. odontolyticus</i> I	8.30 x 10 ⁸
19696	<i>N. mucosa</i>	1.69 x 10 ⁹
25175	<i>S. mutans</i>	1.69 x 10 ⁹
25586	<i>F. nucleatum</i> subsp. <i>nucleatum</i>	1.62 x 10 ⁹
25611	<i>P. intermedia</i>	1.69 x 10 ⁹
25845	<i>P. melaninogenica</i>	1.69 x 10 ⁹
27335	<i>S. intermedius</i>	1.69 x 10 ⁹
27823	<i>S. constellatus</i>	1.69 x 10 ⁹
27824	<i>G. morbillorum</i>	1.69 x 10 ⁹
29523	<i>A. actinomycetemcomitans</i> a	6.80 x 10 ⁹
33236	<i>C. gracilis</i>	6.80 x 10 ⁹
33238	<i>C. rectus</i>	6.80 x 10 ⁹
33270	<i>P. micros</i>	1.69 x 10 ⁹
33277	<i>P. gingivalis</i>	1.69 x 10 ⁹
33397	<i>S. anginosus</i>	1.69 x 10 ⁹
33612	<i>C. sputigena</i>	1.62 x 10 ⁹
33624	<i>C. gingivalis</i>	1.62 x 10 ⁹
33563	<i>P. nigescens</i>	1.69 x 10 ⁹
35037	<i>S. oralis</i>	1.69 x 10 ⁹
43037	<i>T. forsythensis</i>	8.30 x 10 ⁸
43146	<i>A. viscosus</i>	8.30 x 10 ⁸
43718	<i>A. actinomycetemcomitans</i> b	6.80 x 10 ⁹
49456	<i>S. mitis</i>	1.69 x 10 ⁹
51146	<i>C. showae</i>	6.80 x 10 ⁹

2.6.3 Determination of bacterial growth by colony count

After overnight incubation in a microtitre plate (2.6.1) a sample from each well was diluted 1 in 30,000 and 1 in 3,000,000 in sterile PBS and 50µl of each spread on a tryptone soya agar plate (without horse blood; 2.4.3). These plates were incubated anaerobically for 2 days and colony counts performed.

2.6.4 Determination of bacterial growth by fluorescence

The microtitre plate was frozen at -20°C until fluorometric assay of bacterial growth was performed. The plate was then defrosted and a 25µl sample from each well was mixed with 150µl water and 25µl SYTOX[®] green (10µM) in a black 96 well microplate (3915 Corning). DNA fluorescence was then measured in the fluorometer at excitation 485nm and emission 525nm for 10 minutes at 37°C.

2.7 Deoxyribonuclease (DNase) activity assays

Two methods were used to assess the DNase activity of the panel of oral microorganisms. This data may indicate their ability to degrade and evade NETs.

2.7.1 Plate flooding method

DNase test agar plates are used routinely by the NHS for identification of pathogenic staphylococci. The method involves growing bacteria on solid agar enriched with DNA, the

hydrolysis of which is detected by staining with a metachromatic dye (toluidine blue O), indicating DNase expression and activity.

2.7.1.1 Preparation of DNase test plates

DNase test agar (70136 Sigma) was prepared according to the manufacturers instructions and preparation of solid culture media described previously (2.4.3). An enriched DNase test agar was also prepared for the testing of *P. gingivalis* and *T. forsythensis* by the addition of previously prepared hemin, N-acetylmuramic acid and vitamin K (2.4.3.1).

2.7.1.2 Toluidine blue O (TBO) 0.05%

0.3g solid TBO (Hopkin and Willams, Essex, UK) was dissolved in 500ml distilled water and stored at room temperature.

2.7.1.3 Innoculation of DNase test plates

A sterile loop was used to take an inoculum from 4-7 day culture plates and touched once onto the test plate. One test plate was used for 3 spot inoculae. Plates were subsequently incubated under anaerobic conditions for 5 days.

2.7.1.4 Plate flooding method

Plates were flooded with 0.05% TBO (2.7.1.2) for 3 minutes prior to rinsing under tap water and observed after a further 10 minute incubation at room temperature.

2.7.1.5 Image analysis

A positive result was indicated by a zone of purple staining around DNase producing colonies (Figure 22). The absence of any zone was used to indicate a negative result.

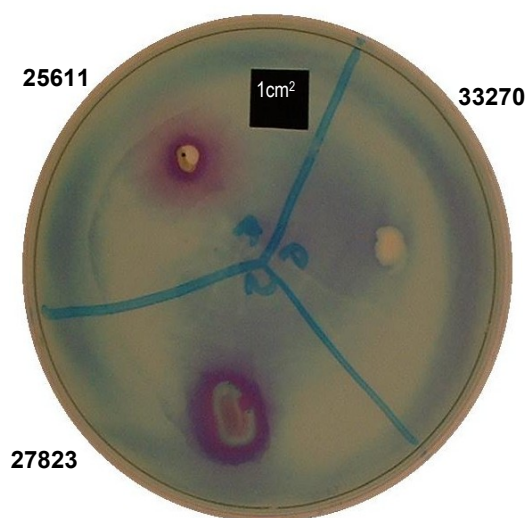


Figure 22. DNase test plate flooded with TBO. Bacteria identified by ATCC number. 25611 and 27823 are examples of DNase positive bacteria and 33270 was regarded as being DNase negative.

For relative quantification analysis, digital photographs of plates were captured (Fujifilm FinePix 2800z) under white light illumination (Light box, Hancocks). ImageJ (1.38d) software analysis was then used to quantify the area of DNase positive zones. Images were binarised using the 'binary' process function (Figure 23). The area around a single bacterial colony and its zone of hydrolysis was determined using the 'selection' tool, and the remainder of the image was cleared using the 'clear outside' function. The number of black pixels, representing the zone of DNA hydrolysis, was quantified using the 'analyze particles' function. The 'selection' tool was again used to select only the area of bacterial growth

(shown in white; Figure 23). The white pixels were then converted to black using the ‘invert’ function to allow quantification of the pixels (analyze particles function). The 1cm black square was also selected and pixels quantified in the same way to enable conversion of number of pixels to area in millimetres. DNase activity was expressed as the area of hydrolysis per area of bacteria growth (mm^2 per mm^2).

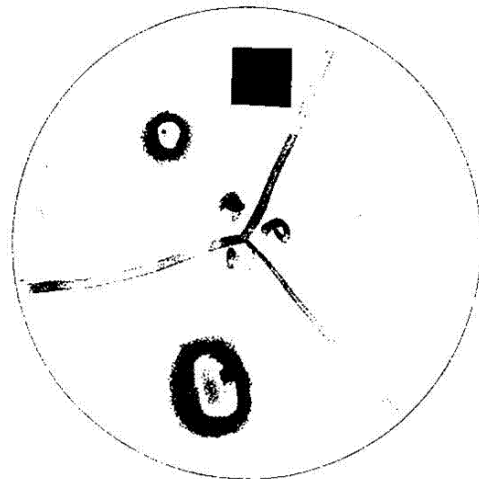


Figure 23. Binarised image of Figure 22 using ImageJ software.

2.7.2 Agarose gel method

To allow more robust quantification than DNase test plate assay, and to utilise bacteria grown in the planktonic rather than solid state an agarose gel method for DNase detection was developed.

2.7.2.1 Preparation of test samples

Day +5 or +6 broth cultures of bacteria were briefly vortexed for homogenisation. Cultures were then transferred to DNase free centrifuge tubes (91015 TTP) and bacteria were pelleted by centrifugation at 1087 rcf for 40 minutes at 4°C. 500 μ l of the supernatant was filter

sterilised (BC591 Appleton Woods) and retained for further analysis. The remaining supernatant was removed and the bacterial pellet re-suspended in 1ml of sterile PBS. This was again centrifuged at 1087 rcf for 40 minutes, and the pellet was re-suspended in 1ml PBS for storage, along with the sterile filtered supernatant at -20°C.

2.7.2.2 Reaction mixture for agarose gel method of DNase assay

Pellet samples were adjusted by the addition of molecular biology grade water (443847D VWR) to give a suspension of 1×10^9 bacteria per ml. 10µl of test sample, 10µl DNase I reaction buffer (BO303S New England Biolabs), 10µl molecular biology grade water (443847D VWR) and 20µl calf thymus DNA 1µg/µl (89370 Sigma) were incubated at 37°C for 2 hours.

The positive control samples included consisted of 0.5-250 Kunitz/L bovine pancreatic DNase (D4263 Sigma) diluted with molecular biology grade water. A negative control reaction was performed using 10µl of a non-inoculated bacterial culture media. Kunitz are a measure of enzymatic activity specifically of DNase developed since M. Kunitz first described a spectrophotometric method for measuring the degradation of DNA by the newly identified bovine pancreatic DNase in 1950 (Kunitz 1950).

'Unit definition: One Kunitz unit will produce a change in A_{260} of 0.001 per minute per ml at pH 5.0 at 25 °C using DNA, Type I or III, as the substrate. This enzyme assay reaction is performed in 83 mM acetate buffer, pH 5.0, at 25°C, containing 4.2mM Mg^{2+} , in a 3 ml reaction.' **Sigma.**

The reaction was stopped by the addition of 8.25µl of 0.5M ethylamineditetraacetic acid (EDTA; E-7889 Sigma) which functioned to chelate the divalent cations (Mg^{2+} and Ca^{2+} contained within the DNase I reaction buffer) reported to be essential for the activity of DNase (Pan *et al.* 1999). A sample was mixed with 10x loading buffer (Bioline) before electrophoresis on a 0.8% agarose gel and image capture as previously described (2.3.1.4).

2.8 Detection of DNase in plaque and GCF samples

The *in vivo* presence of DNase in an experimental 21-day model of gingivitis was examined by assay of plaque and GCF samples.

2.8.1 Clinical study period

A 21 day model of experimental gingivitis involving ten undergraduate dental students was undertaken by the Periodontal Department of the School of Dentistry as described by Chapple *et al* (1996). Ethical approval for this study was obtained from the South Birmingham Local Research Ethics Committee (LREC 2004/074). 10 volunteers with no periodontal disease (past or present), unremarkable medical histories, who were not undergoing orthodontic or prosthetic appliance therapy, or taking medication that may have affected results were enrolled and informed consent obtained. A split mouth model was employed whereby a soft vinyl mouth guard was constructed to cover maxillary left 4-6 teeth which was to be worn during tooth brushing for the 3 week study period to shield from mechanical or chemical cleaning. The maxillary right 4-6 teeth were used as control teeth undergoing normal oral hygiene. Volunteers were asked to refrain from chewing gum during the study period which

consisted of an initial assessment at baseline followed by 3 weeks using the tooth shield to facilitate plaque accumulation at test teeth with assessment at days 7, 14 and 21.

2.8.2 Clinical measures of gingival inflammation

To document the progression of gingival inflammation 3 clinical parameters were measured – gingival index scores 0-3, plaque index measured by the modified Quigley-Hein index, and GCF volume measured by Periotron 8000TM (Oraflow, USA). Gingival and plaque scores were recorded by Mr Mike Milward and GCF volume by Professor Iain Chapple.

2.8.3 Plaque sampling

Plaque samples were taken from test and control teeth in each subject by methods modified from Kalfas *et al* (1990) and Lingström *et al* (1993) and performed by Professor Iain Chapple. A sterile size 30 finger spreader (25mm, Claudius Ash) was used to remove plaque from the palatal aspect of the tooth and the sample suspended in 100µl PBS. Samples were vigorously vortexed (VortexGenie2, Scientific Industries) to homogenise the plaque sample and they were stored at -20°C until assay. Different sites were sampled on each of the 4 test days so that the sample represented undisturbed plaque accumulation from day 0.

2.8.4 GCF sampling

GCF was collected by Professor Iain Chapple using a modified version of the methods reported by Chapple *et al* (2007a).

2.8.4.1 PBS-BSA

50mg BSA (A4530 Sigma) was added to 1litre sterile PBS and stored at 4°C.

2.8.4.2 GCF sampling

A periopaper™ strip was inserted into the mesio-buccal gingival crevice of each of the 3 test teeth and 3 control teeth for 30 seconds. These were read on a pre-calibrated Periotron 8000™ (Chapple *et al.* 1999) for calculation of GCF volume before the 3 strips were pooled into 300µl PBS-BSA and stored in liquid nitrogen.

2.8.5 Assay of samples for DNase activity

DNase assay was performed as previously described gel based assay (2.7.2). 10µl plaque or 30µl GCF sample was used in the assay.

2.9 Statistical analysis

Microsoft Office Excel or GraphPad InStat (Graphpad Inc.) were used for all statistical analysis. For parametric and normally distributed data paired student T test was used. For non-parametric data (e.g. clinical indices) and non-normally distributed data Wilcoxon matched pairs test was used. For correlation analysis of normally distributed data Pearson test was used. $P \leq 0.05$ was considered significant in all cases.

CHAPTER 3 RESULTS

Assay of NET release

Vitkov *et al.* (2009) have previously described the presence of NETs on the gingival pocket surface and in purulent crevicular exudate (Figures 18 and 19). Immunofluorescence analysis of tissue sections obtained in our laboratory has also shown for the first time the presence of NET structures within the gingival tissues with these appearing more abundant in inflamed than healthy tissues (Figure 20; confocal microscopy by Dr S Yousefi, University of Berne, Switzerland). However, as it is known that the neutrophils recruited from the peripheral vasculature to the diseased or infected tissues are the primary source of NETs, it is these cells that are routinely isolated and used to study *ex vivo* NET release in response to stimuli (Gupta *et al.* 2005, Clark *et al.* 2007). Therefore, in the current study peripheral blood neutrophils were isolated from systemically and periodontally healthy individuals and stimulated to mimic exposure to NET inducers that may arise within the periodontal tissues. Stimuli used included the periodontal pathogen *F. nucleatum*, in addition to opsonised *S. aureus* (an Fcγ-receptor ligand), fMLP and PMA. The latter has routinely been reported within the literature as a positive control to stimulate NETs (Gupta *et al.* 2005, Ermert *et al.* 2009). Methods previously described for the assay of NET production vary widely, and different methods for cell isolation, culture, stimulation, fixing and staining, and quantification have all been reported. Therefore, initially for this study, an optimised and standardised NET production technique was developed to enable quantification and comparison between experimental approaches employed in subsequent studies. The NET detection methods described in this chapter are,

- i) **Visualisation** of SYTOX stained NETs on glass slides or in culture dishes.
- ii) **Real-time** fluorometric quantification of SYTOX stained DNA throughout the 3 hour neutrophil incubation period.

iii) **End-point fluorescence** of SYTOX stained DNA at end of neutrophil incubation period only i.e. after 3 hours.

iv) **MNase assay** – fluorometric quantification of extracellular NET-DNA liberated by MNase treatment of neutrophils after 3 hours incubation period.

3.1 Fluorometric quantification of NET release

NETs can be produced by seeding and stimulating neutrophils on glass slides and visualised by staining the NET-DNA with SYTOX[®] green fluorescent dye. However, to enable comparison between experimental conditions it is important to be able to objectively quantify NET release. One reported approach for quantification utilises fluorometric analysis of the light output generated by DNA-bound SYTOX[®] dye and is measured in arbitrary fluorescent units (AFU) (Brinkmann *et al.* 2004; Martinelli *et al.* 2004). To develop this technique for a high throughput approach, the fluorescently labelled (SYTOX[®]) extracellular NET-DNA was assayed in a 96-well format (2.1.4) and fluorescence quantified throughout the 3 hour incubation period.

3.1.1 Sensitivity of fluorometric detection of DNA

Initially the sensitivity range for fluorometric detection of DNA following SYTOX[®] (1.25 μ M) staining was determined using known concentrations of calf thymus DNA (Figure 24). As stimulation of cells is routinely performed over a 3 hour incubation period at 37°C, the fluorescence of the DNA standards was read at 10 minutes (following mixing) to allow the dye to bind and then again at 3 hours. Data demonstrated that there was on average a 38% decrease in fluorescence at 3 hours compared to the readings obtained at 10 minutes.

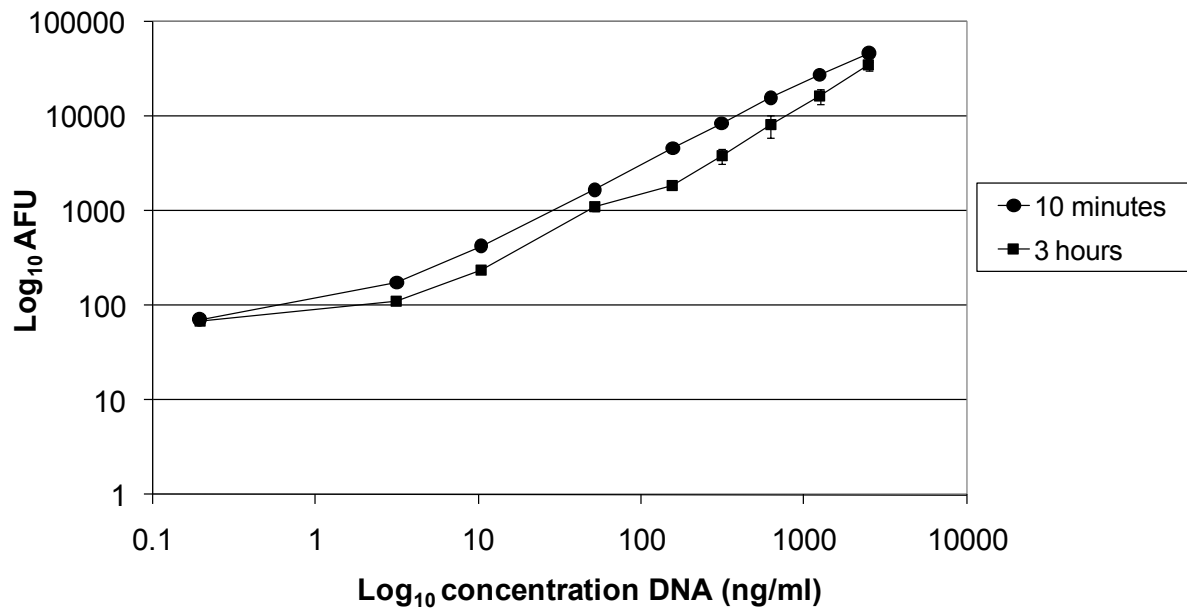


Figure 24. Fluorometric detection of SYTOX[®] stained calf thymus DNA. Readings were obtained after 10 minutes and 3 hours incubation at 37°C. Data represents mean values of experiment performed in triplicate \pm standard deviation (SD). Fluorescence is measured in arbitrary fluorescent units (AFU).

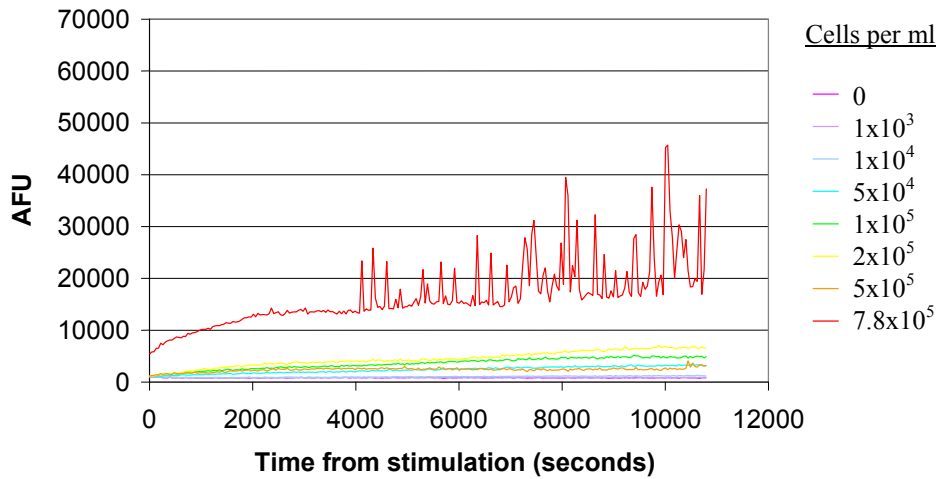
3.1.2 Determination of optimal concentrations of cells

Unlike calf thymus DNA, NET derived nuclear DNA is complexed with histone and non-histone proteins in the form of chromatin which may affect dye binding and subsequent fluorescence. Reportedly neutrophils contain $\sim 620\text{ng}$ DNA per 1×10^5 cells (Fuchs *et al.* 2007) therefore the predicted fluorescence for this number of cells in the assay would locate on the first half of the standard curve (Figure 24). However, as the SYTOX[®] dye can enter and stain the nuclei of dead cells only, and as components of the cell media may influence background fluorescence, the optimal concentration of cells for use in the subsequent monitoring of fluorescence over 3 hours incubation at 37°C was assayed. The aim of this analysis was to determine cellular conditions which would enable consistent readings to be

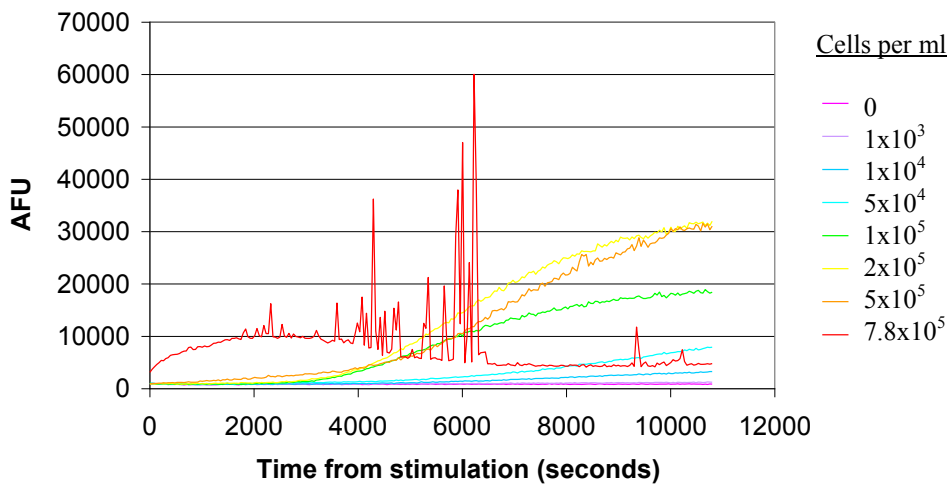
obtained using the fluorometer in future experiments to determine NET production following stimulation (Figure 25).

A range of cell concentrations (1×10^3 to 7.8×10^5 cells/ml) encompassing those previously reported (Martinelli *et al.* 2004; Fuchs *et al.* 2007) were used in the microplate assay and real-time fluorescence measured (Figure 25). The fluorescence intensity of unstimulated cells throughout the incubation period was minimal for all cell concentrations used except the highest (7.8×10^5 cells/ml) which produced elevated and highly variable readings (Figure 25a). All lower concentrations of cells gave consistent fluorescence readings which did not increase notably over the 3 hour incubation period indicating a low level of cell death in unstimulated cells. When stimulated with 50nM PMA (Figure 25b) the lower concentrations of cells used (50000 cells/ml and below) produced a minimal increase in fluorescence over 3 hours and this increase occurred at a later time-point in comparison to the higher concentrations used (1×10^5 - 5×10^5 cells/ml). With PMA stimulation, the highest concentration of cells (7.8×10^5 cells/ml) again gave highly variable readings throughout the test period. The highest concentration which gave highest total fluorescence and provided consistent readings, was 5×10^5 cells/ml. This concentration was used in all subsequent assays for detection of both NET and ROS production.

a) Unstimulated cells



b) PMA stimulated cells



c) PMA stimulated minus unstimulated cells

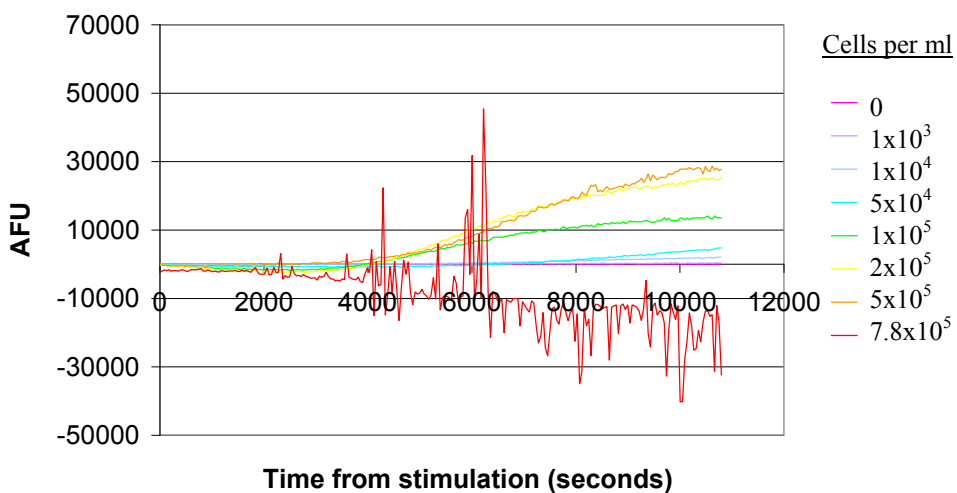


Figure 25. Fluorescent time course analysis using a range of cell concentrations (cells per ml) a) unstimulated cells, b) PMA stimulated cells (50nM), c) PMA stimulated minus unstimulated fluorescence (i.e. values in b-a). Results show mean values of experiment performed in triplicate.

3.1.3 Correlation analysis of real-time fluorometric assay and visualisation of NET formation

Whilst real-time fluorescence analysis of cells identifies extracellular DNA release, and therefore NET release, this technique also detects the nuclei of dead cells. Therefore to determine the likely accuracy of real-time fluorescence analysis for detecting NET production, SYTOX[®] stained and PMA stimulated cells were concomitantly visualised for NET production at various time points to examine correlations with the real-time fluorometry readings (Figure 26).

Prior to stimulation, and for 60 minutes post stimulation, relatively low levels of fluorescence were detected (Figure 26A) which correlated with the visualisation data obtained by SYTOX[®] staining indicating that relatively few dead cells were present and that NET release was minimal (Figure 26B a and d). At 60 to 190 minutes post stimulation, fluorescence levels increased steadily. Microscopic visualisation of stimulated neutrophils over this time period, initially indicated relatively small and distinct stained nuclei, which gradually increased to indistinct nebulous staining prevalent by 190 minutes post-stimulation (Figure 26c). These nebulous stained areas proved to be extracellular DNA which could be disrupted by brief mechanical stimulation (i.e. addition of 50µl PBS to the well) to resemble a more typical strand-like NET morphology (Figure 26B g, h and i) (as described by (Brinkmann *et al.* 2007; Behrendt *et al.* 2010).

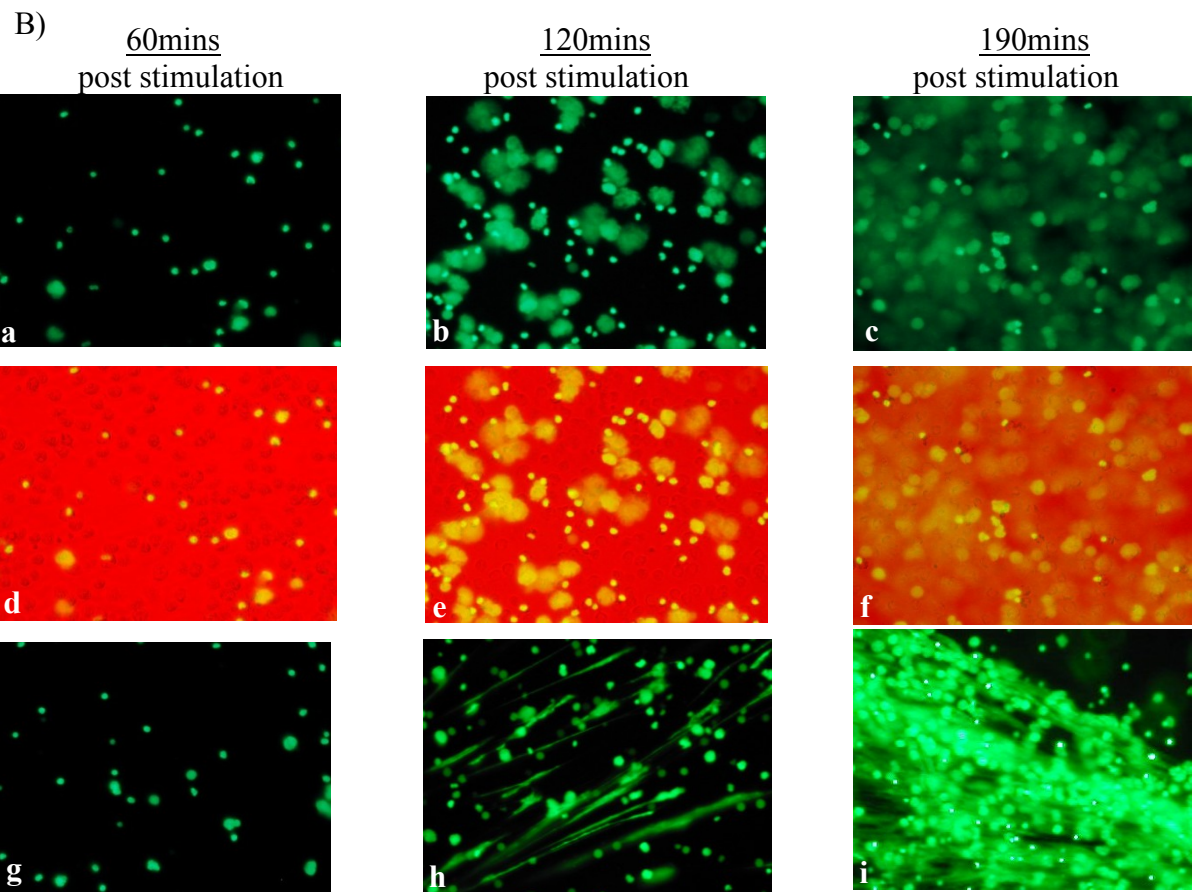
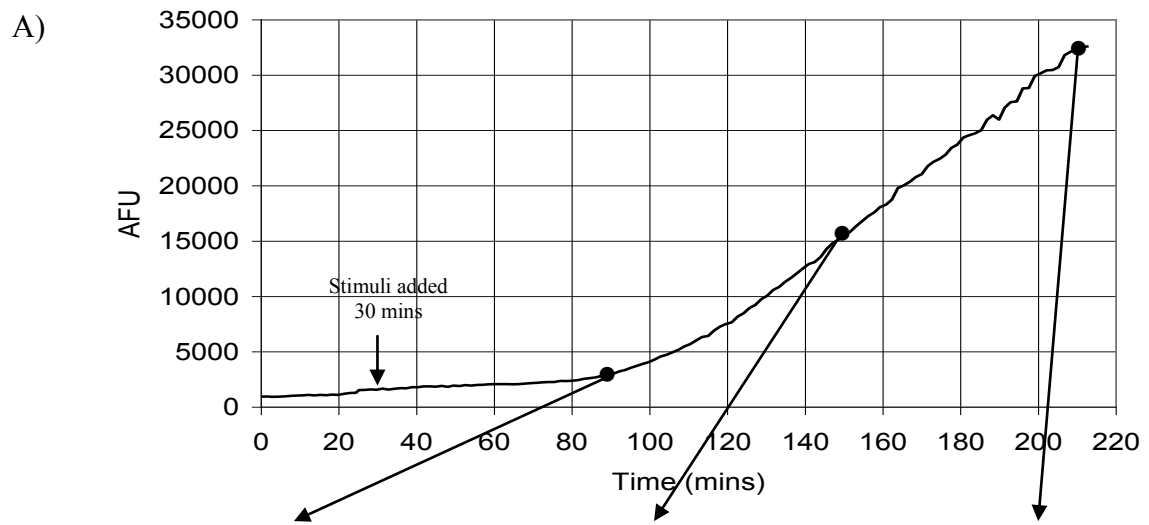


Figure 26. A) Time course analysis of fluorescence and B) visualisation of PMA 50nM stimulated NET production. A) Time course of fluorescence representative of experiment performed in triplicate. B) Visualisation of NETs and neutrophil viability **a-c)** SYTOX[®] stained neutrophils showing nuclei of dead cells and extracellular DNA (green) **d-f)** Merged images derived from light microscope (red) and fluorescence microscope (yellow) to show proportion of dead cells (SYTOX-positive nuclei) and extracellular DNA (images overlaid using ImageJ section 2.1.2.3) **g-i)** NET visualisation after mechanical disruption. Results representative of 3 independent experiments.

3.1.4 Quantification of NET production following MNase digestion

As real-time fluorescence analysis following SYTOX[®] staining detects extracellular DNA, the nuclei of dead/dying cells and the presence of bacterial DNA (Roth *et al.* 1997), a further analytical approach was evaluated which may enable a more specific assay of NET production. Subsequently, micrococcal nuclease (MNase) was used to digest the extracellular NET-DNA, as previously described (Fuchs *et al.* 2007, Ramos-Kichik *et al.* 2009, Wang *et al.* 2009), and following centrifugal pelleting of cells and cellular debris the liberated DNA present in the supernatant was quantified fluorometrically. MNase was added after the incubation time (at 3 hours) and DNA-digestion was allowed to progress for 10 minutes (Fuchs *et al.* 2007) and for comparison, MNase was included for the duration of the incubation (at time 0). It was hypothesised that MNase inclusion throughout the incubation period may enable more complete NET-DNA digestion and would not therefore require the additional digestion step after the incubation period. However, it was recognised that MNase co-incubation may interfere with normal cellular processes.

As PMA is a well characterised inducer of NETs (Gupta *et al.* 2005, Ermert *et al.* 2009) this was initially used to stimulate their release (Figure 27). The addition of MNase at 3 hours and subsequent fluorometric analysis resulted in a significant increase in fluorescence detected from stimulated cells ($P=0.02$), however no significant difference in unstimulated cells was observed ($P=0.18$). Immediately prior to MNase treatment at 3 hours and subsequent fluorometric quantification, the cells were visualised to indicate whether the readings were likely to be representative of NET formation (Figure 28). Observational data indicated an increase in background fluorescence in stimulated wells suggesting the presence of solubilised

NET-DNA fragments. Image merge (Figure 28a and b) showed the number of dead cells (SYTOX-positive nuclei) was not notably affected by the addition of MNase to otherwise unstimulated cells. However, the nuclei of those cells that had taken up the SYTOX[®] dye were observed to have a more segmented appearance than was present in the absence of MNase.

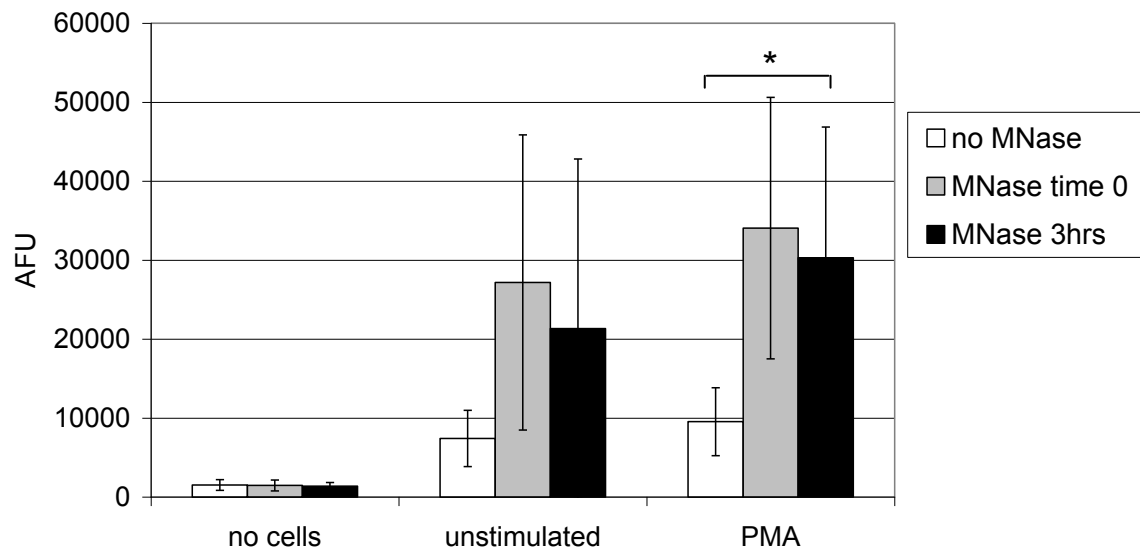


Figure 27. Quantitative analysis of NET release from PMA (50nM) stimulated cells by MNase digestion of NET-DNA. No MNase or MNase (1 unit/ml) was added either initially at time 0 or after 3 hours incubation. Results show mean values of 6 independent experiments \pm SD. * $P < 0.05$ by two-tailed paired T-test.

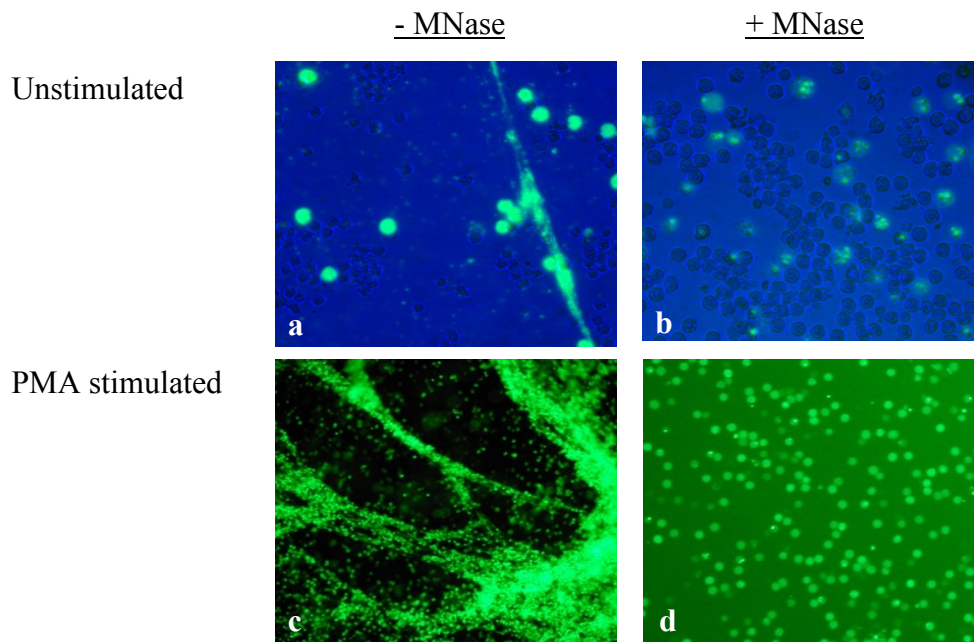


Figure 28. Microscopic images from wells of 24-well plates used for assay in Figure 27. Unstimulated or 50nM PMA stimulated cells with no MNase (-MNase) or MNase added at time 0 (+MNase). **a)** and **b)** light microscope (blue) and fluorescent images (green) merged using ImageJ to show proportion of unstimulated cells that have died and taken up SYTOX[®] stain. **c)** and **d)** SYTOX[®] stained images showing intact NETs in the absence of MNase and solubilised NET-DNA in supernatant in the presence of MNase.

Subsequently the MNase assay procedure for quantitative NET detection was repeated using the periodontal pathogen, *F. nucleatum*. This analysis was performed to determine whether reported bacterial fluorescence interfered with the detection of NET-DNA (Figure 29). The addition of MNase at 3 hours did not result in a significant increase in the amount of DNA detected (with or without stimuli) compared to absence of MNase. However, whilst the difference between unstimulated and bacteria-stimulated cells was not statistically significant ($P=0.1$) in the absence of MNase, upon addition of MNase at time 0 or 3 hours the difference between unstimulated and bacterial-stimulated cells was significant ($P=0.01$ and $P=0.04$ respectively).

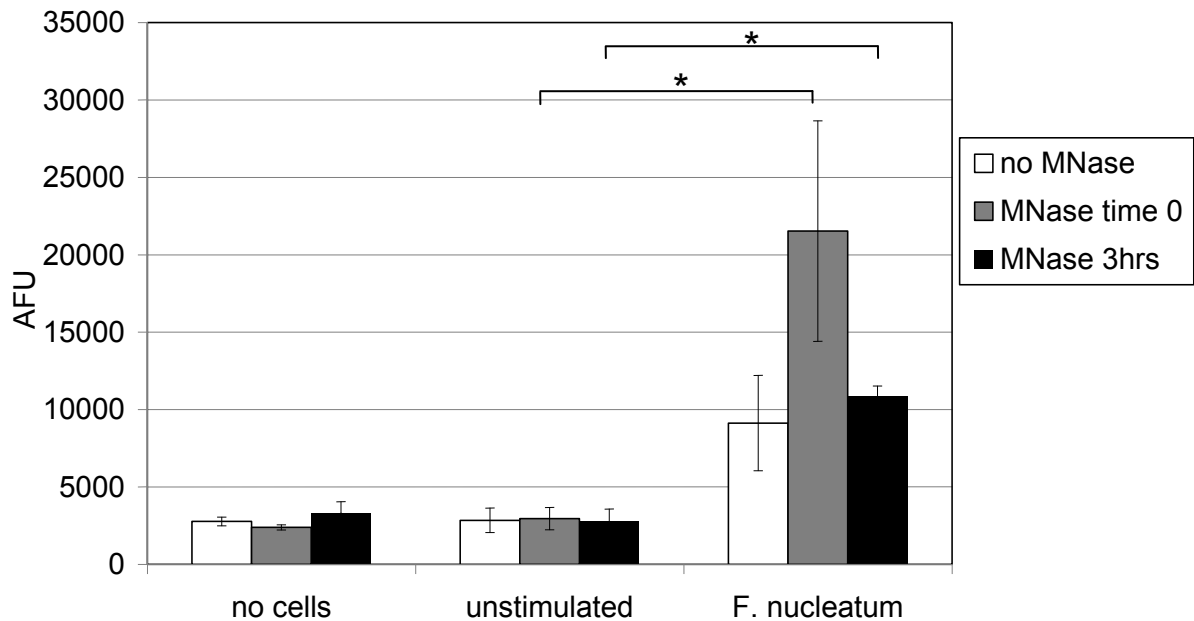
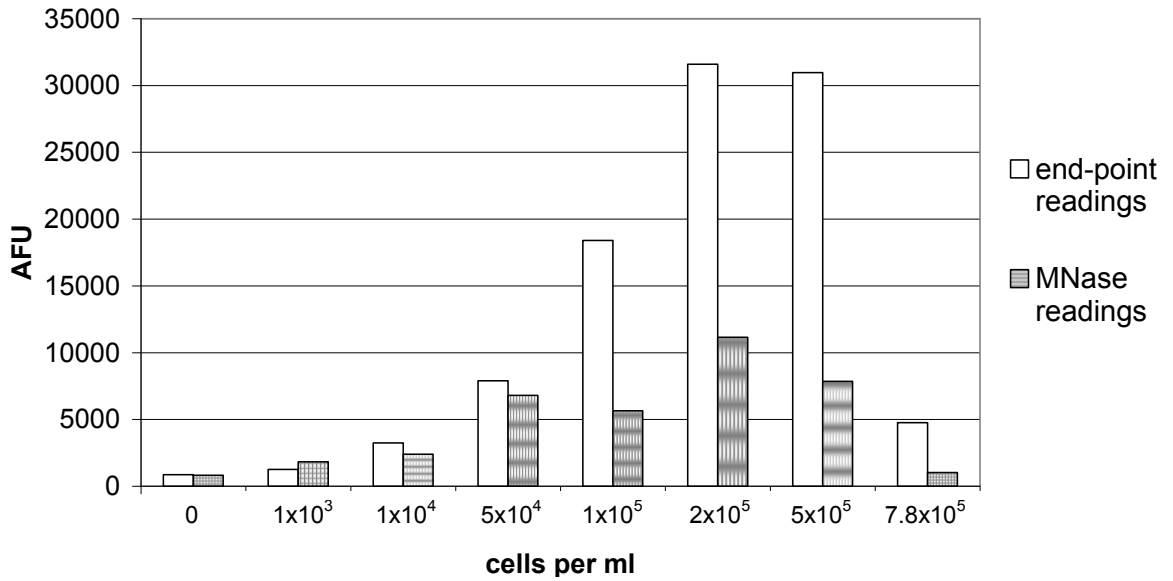


Figure 29. Quantification of NET release from *F. nucleatum* stimulated cells following MNase digestion of NET-DNA. Mean of 3 experiments performed in triplicate \pm SD. (Multiplicity of infection; MOI 150). * $P < 0.05$ by two-tailed paired T-test.

3.1.5 Comparison of quantitative NET production data obtained by end-point fluorescence and MNase assay

Finally the relationship between the real-time fluorescence after 3 hours incubation (termed end-point fluorescence) was compared to the DNA detected in the supernatant after MNase digestion and assay of PMA-stimulated cells (Figure 30). When the DNA from various concentrations of PMA stimulated cells was measured, a similar trend was observed by both assay procedures (Figure 30a). Subsequent statistical analysis confirmed a significant and positive correlation between the readings obtained by the two assay procedures by Pearson correlation ($R^2=0.80$) (Figure 30b).

a) Comparison of end-point and MNase fluorescence at various cell concentrations



b) Correlation of end-point and MNase fluorescence

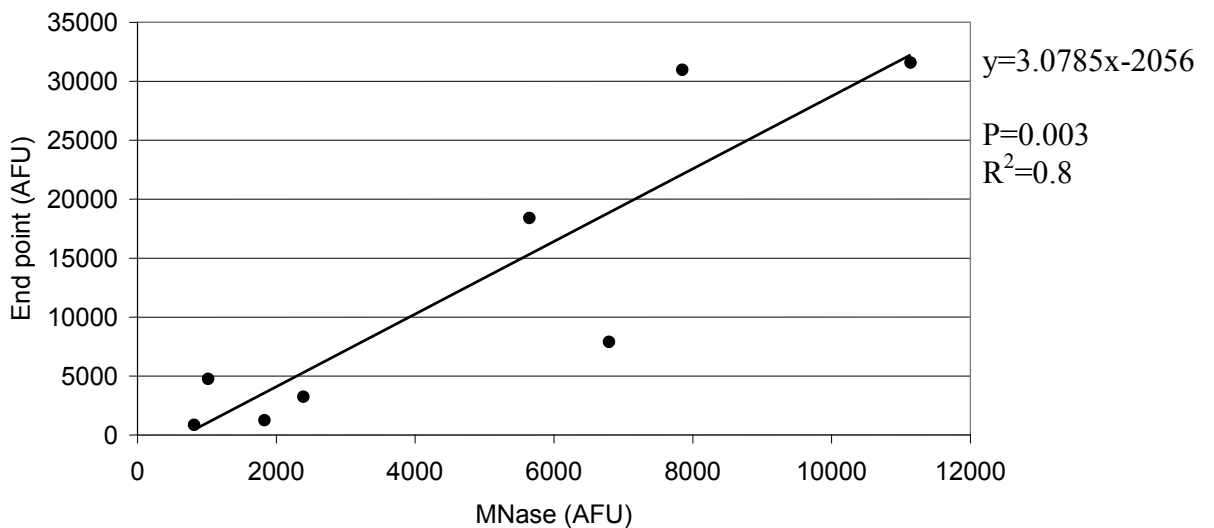
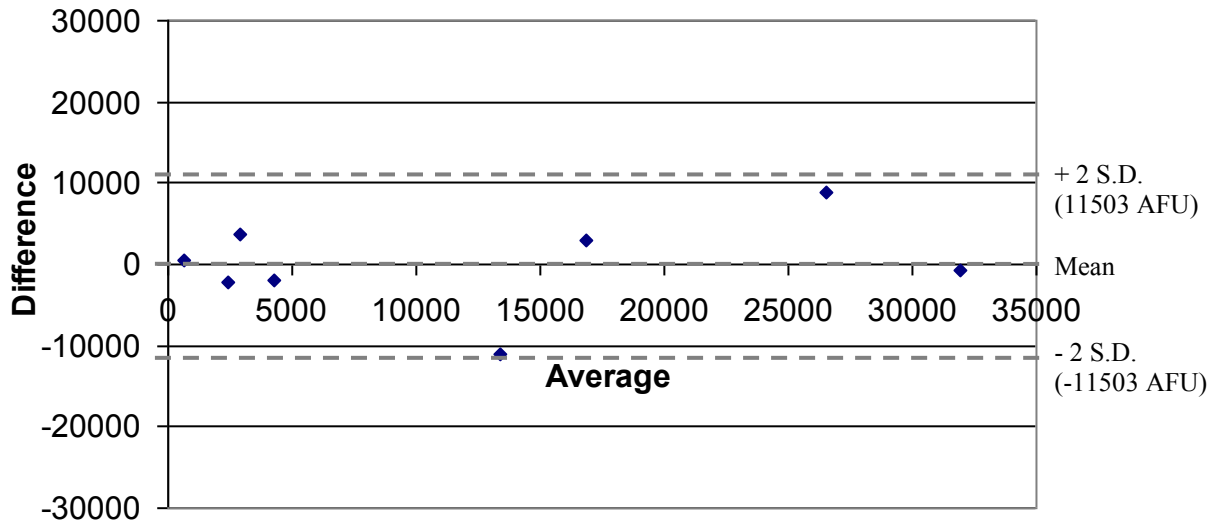


Figure 30. End-point fluorescence (i.e. at 3 hours incubation) and fluorescence values after MNase assay of various cell concentrations (0 to 7.8x10⁵ cells/ml) stimulated with 50nM PMA. a) Comparison between data sets, b) correlation between data sets analysed by Pearson correlation.

To validate whether the equation generated by the trendline (Figure 30b) could be used to accurately estimate the value of the other assay and therefore whether the two assay methods were interchangeable, the actual values and the values predicted by the equation were used to plot the mean of the two values against the difference between the two values (Bland *et al.*

1986) (Figure 31). 100% of the data points were between 2 standard deviations either side of the mean, indicating that although the data set consisted of only 8 points it is likely that either of two methods for the quantification of PMA induced NET release could be used to replace the other method.

a) Real and predicted end-point fluorescence values



b) Real and predicted MNase assay values

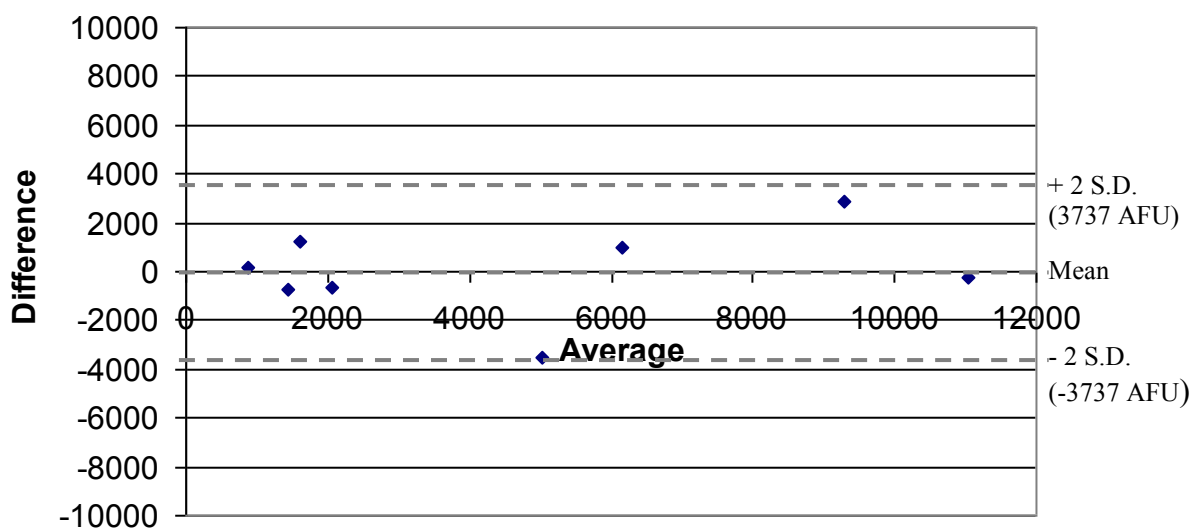


Figure 31. Validity of inferring one assay value from the other based on equation of trend line (Figure 30b) $y=3.0785x-2056$. a) End-point fluorescence values and b) MNase assay values. When the average of the real and predicted values are plotted against the difference between the real and predicted values 100% of the data points lie within +/- 2 S.D. from the mean.

3.2 Determination of optimal concentration of serum for NET release

3.2.1 Effect of foetal calf serum (FCS) on NET release

FCS is commonly used as a supplement in cell culture to provide nutrients for growth, whilst bovine serum albumin (BSA), a purified fraction of FCS, is used to coat assay plates to prevent activation of cells in response to contact with the plastic culture surface (Matthews *et al.* 2007a). With regard to the assay of NETs, it has previously been reported that FCS supplementation of media inhibited NET production (Fuchs *et al.* 2007). Therefore the optimum concentration of FCS necessary to prevent neutrophil activation in the absence of stimulation, yet still enable NET release in the presence of stimulation, was investigated both by visualisation (Figure 32) and using the MNase assay described above (Figure 33). A range of stimuli were used to activate several neutrophil receptor pathways. These included the gram negative periodontal pathogen *F. nucleatum* which reportedly activates TLR4/2 (Remer *et al.* 2003) and opsonised bacteria (*S. aureus*) to stimulate Fc γ -receptors (Huizinga *et al.* 1989). The chemotactic peptide N Formyl Met-Leu-Phe (fMLP) was also used as it has been reported to evoke neutrophil responses such as degranulation and superoxide generation via fMLP receptor binding (Kuan 2005).

Visualisation of SYTOX[®] stained neutrophils on glass slides (Figure 32) demonstrated that as the concentration of FCS increased, the amount of NETs produced decreased in response to all 3 stimuli used. In addition, spontaneous NET production (from unstimulated cells) also appeared to be inhibited dose-dependently by FCS. Notably whilst 10% and 20% FCS

supplementation of media resulted in minimal NET release from unstimulated cells, some NET production in response to stimuli (*F. nucleatum*, opsonised *S. aureus* and fMLP) was observed.

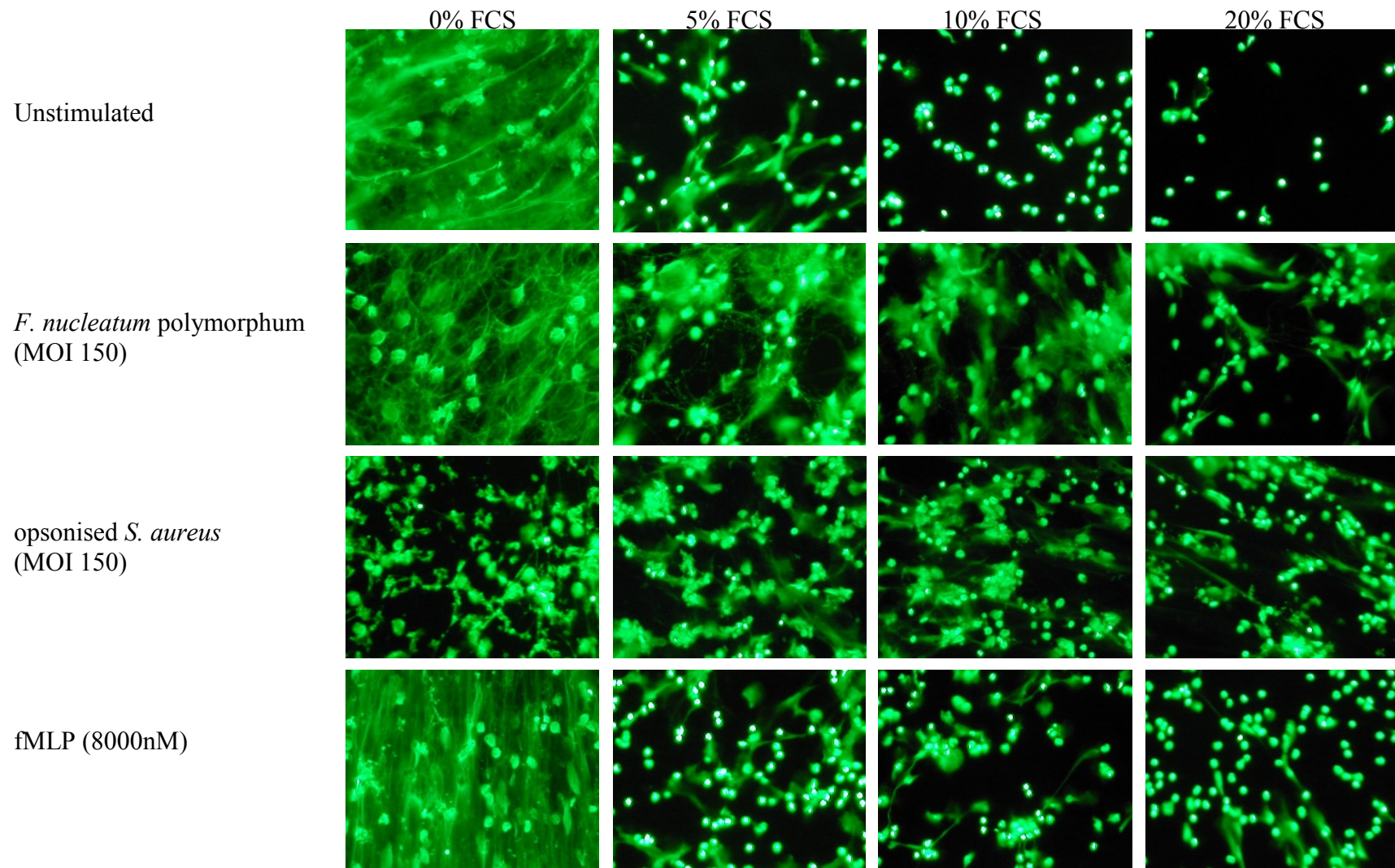


Figure 32. SYTOX[®] stained NETs produced on glass slides in media supplemented with 0-20% heat inactivated (FCS). Cells were stimulated with *F. nucleatum* polymorphum (MOI 1:150), opsonised *S. aureus* (MOI 1:150), fMLP 8000nM or were unstimulated. Cells were incubated for 3 hours prior to fixing and staining. Images shown are representative of two independent experiments.

The inhibition of NET release by increasing concentrations of FCS was also confirmed by the quantitative MNase assay in unstimulated cells, i.e. baseline NET release (Figure 33). The addition of 10% FCS caused a significant decrease in NET-DNA detected compared to the control (absence of FCS; $P=0.008$). A further significant reduction was also observed when the FCS was increased from 10% to 20% ($P=0.001$). Based on this data and that of previous publications which have used FCS supplementation for the assay of NET release (Martinelli *et al.* 2004; Ramos-Kichik *et al.* 2008), 10% FCS was deemed the most appropriate concentration to prevent spontaneous neutrophil activation whilst enabling the detection of responses to stimulation.

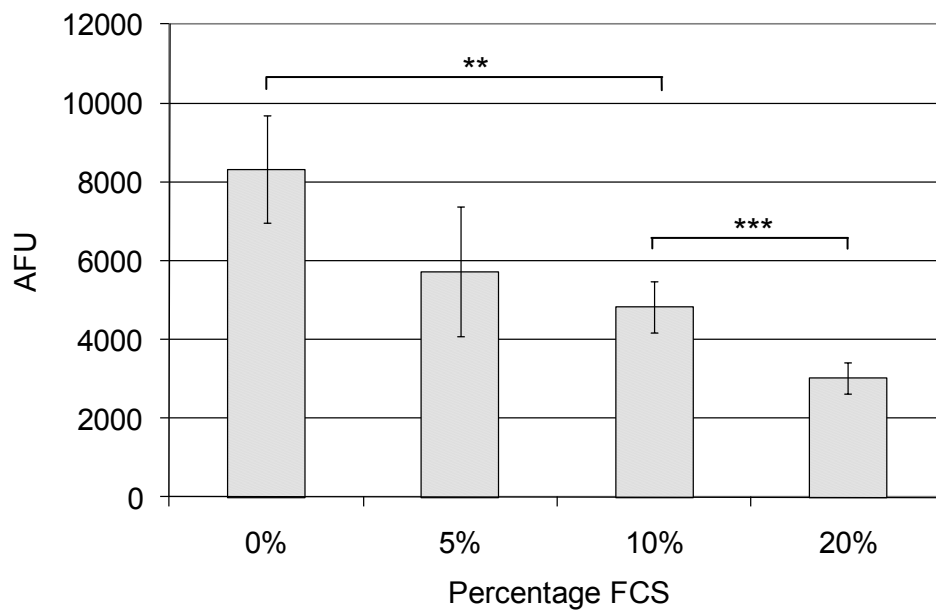


Figure 33. Effect of FCS supplementation of media on MNase detection of NET-DNA from unstimulated cells. Results show mean \pm SD of 5 independent experiments. ** $P \leq 0.01$, *** $P \leq 0.001$ by two tailed paired T-test.

3.2.2 Effect of BSA concentrations on NET release

For the short term assay of cells the nutrients provided by FCS supplementation of media are less important to cell viability. In addition serum proteins can interfere with the

chemiluminescent assay of ROS production (Chapple *et al.* 1997) which is utilised later in this thesis in conjunction with the assay of NETs. Therefore as BSA is commonly used to ‘block’ assay plates for ROS analysis (Steinckwich *et al.* 2007) its potential use in the assay of NETs was analysed. Initially, cells were seeded onto glass slides for staining and visualisation of NET release, however as the glass slides had already been coated in poly-L-lysine to aid the adherence of extruded NETs, the BSA was used to supplement the media at concentrations up to 2% rather than to coat the slide (Figure 34). The range of concentrations used were based upon previous publications describing NET release in the presence of human serum albumin (HSA) at 2% (Fuchs *et al.* 2007, Beiter *et al.* 2006) and BSA at 1% (Alghamdi *et al.* 2005). The effect of BSA on NET release was less clear as extracellular staining was evident, but this was not found as distinct strands characteristic of previously observed NETs. Even in unstimulated cells the nuclei did not stain with a distinct edge and exhibited a hazy and distorted appearance. Evidence of dose-dependant inhibition of NET formation was however apparent (Figure 34).

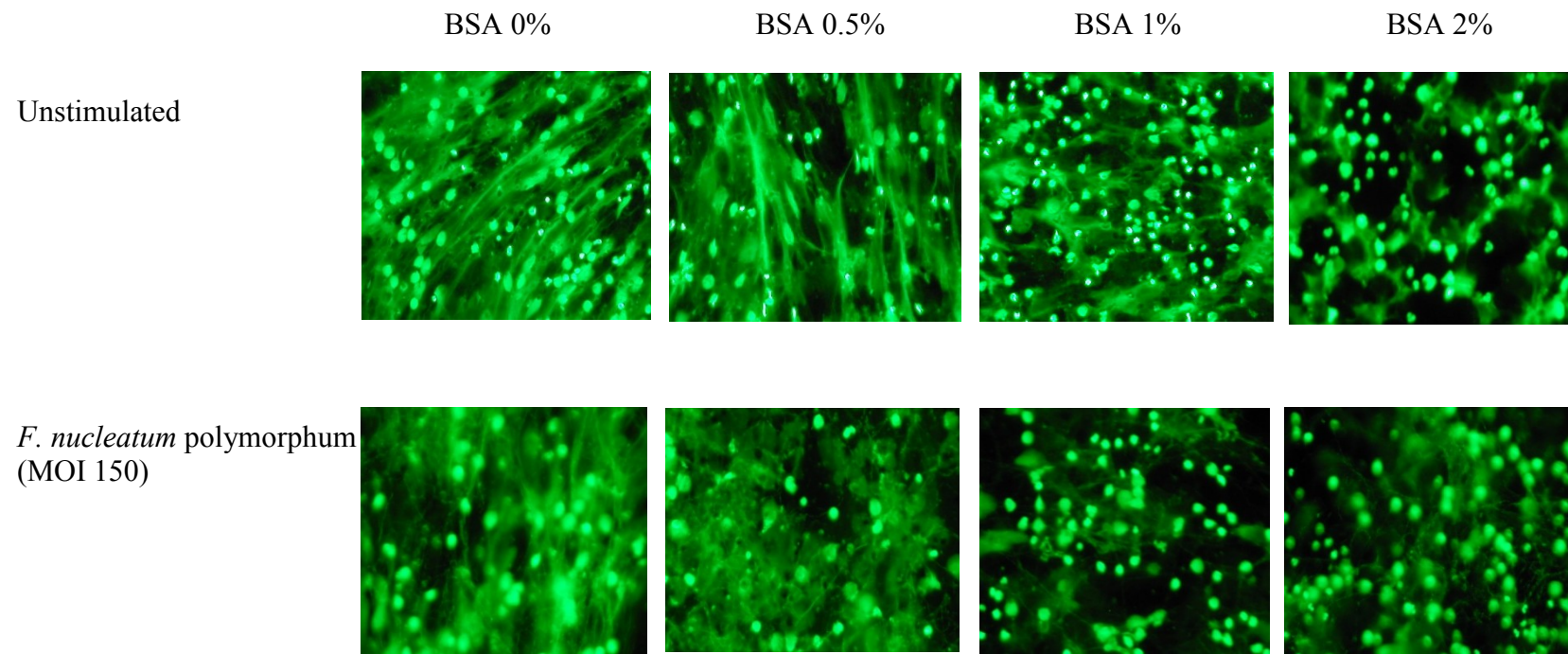


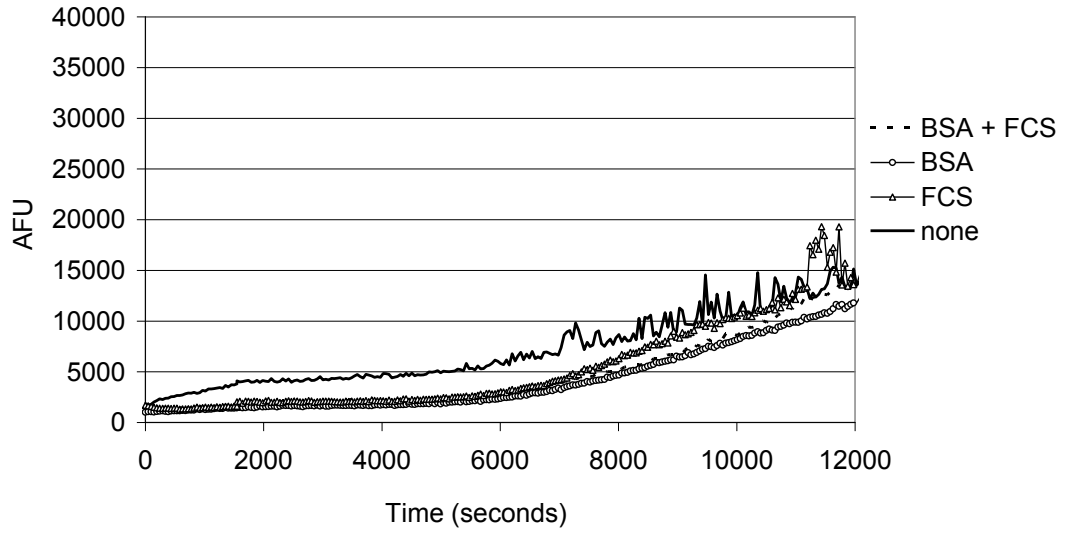
Figure 34. Visualisation of SYTOX[®] stained neutrophils in RPMI supplemented with a range of concentrations of BSA. Cells were stimulated on glass slides for 3 hours using *F. nucleatum polymorphum* MOI 1:150 or were unstimulated.

3.2.3 Effect of BSA and FCS on NET release using fluorometric quantification

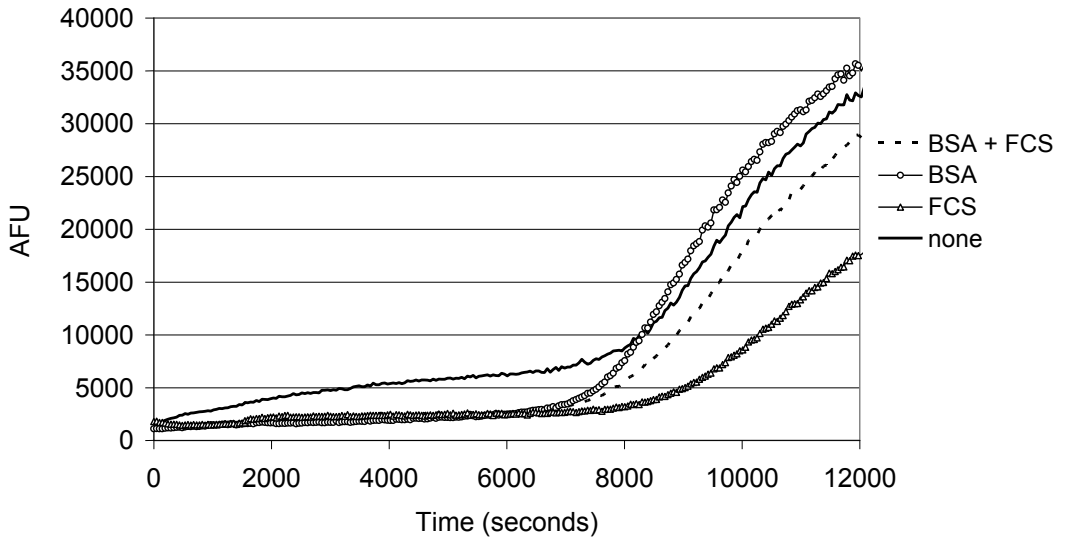
Data indicated that the established MNase assay provided a robust quantification of NET release, and also facilitated a high throughput analysis. Therefore BSA was also used in this assay to pre-treat the wells of the microplate (rather than to supplement the media). This treatment was assessed, alongside and in addition to, 10% FCS supplementation of the media to determine the most effective conditions to prevent spontaneous NET activity, whilst still maintaining cellular responses to stimulation (Figure 35).

Baseline levels of detected fluorescence (i.e. prior to stimulation) and up to 5400 seconds (1.5 hours) after stimulation was higher for cells which had no serum supplementation or BSA 'blocking'. Fluorescence under these conditions also increased less rapidly when stimulated, as demonstrated with PMA (Figure 35b) or opsonised *S. aureus* (Figure 35c) exposure. The absence of BSA or FCS resulted in highly variable readings in the unstimulated cells. With PMA stimulation it is apparent that the addition of BSA, FCS or both allowed the initiation of increased fluorescence from 5400 seconds (1.5 hours) onwards. The largest fluorescence increase was observed in the presence of BSA, the smallest increase was observed with the addition of FCS, whilst a moderate increase was observed in the presence of both BSA and FCS. After 3 hours incubation (Figure 35e) BSA plate-coating resulted in the lowest readings in unstimulated cells although FCS supplementation gave the lowest fluorescent readings following stimulation.

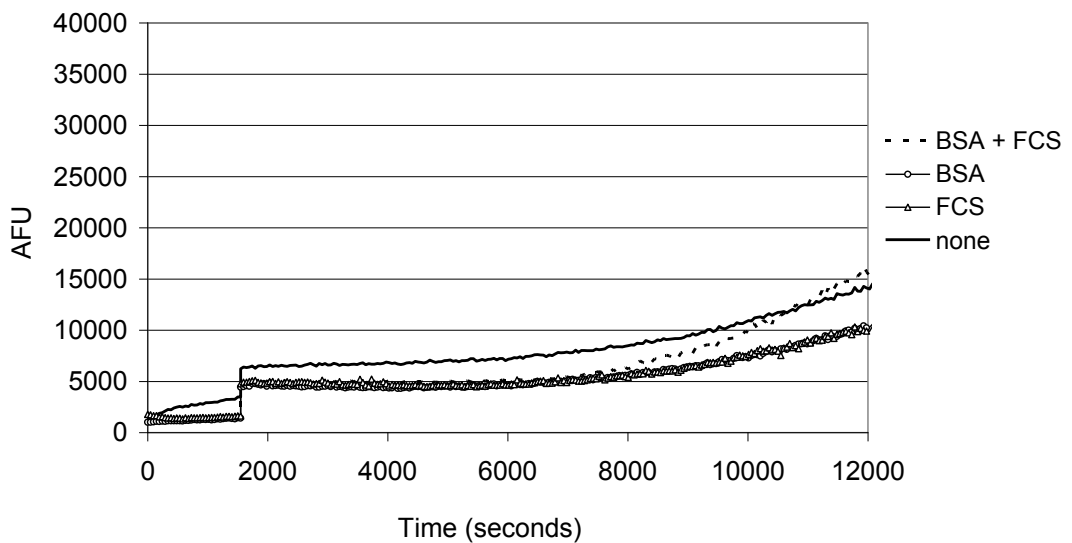
a) Unstimulated cells



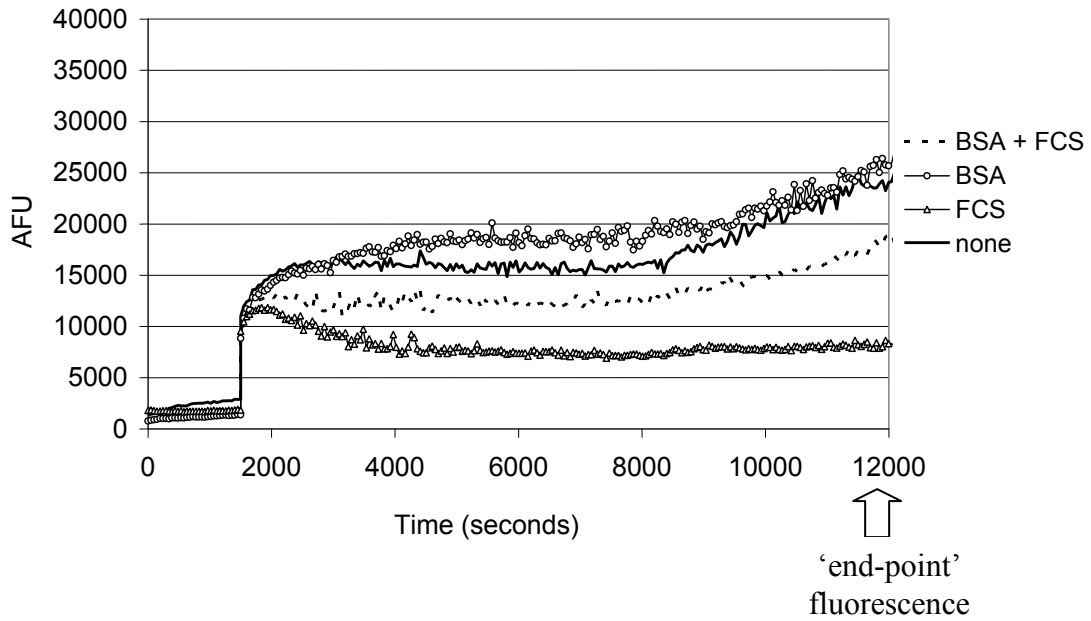
b) PMA stimulated cells



c) opsonised *S. aureus* stimulated cells



d) *F. nucleatum* poly. stimulated cells



e) End-point fluorescence (12000 seconds)

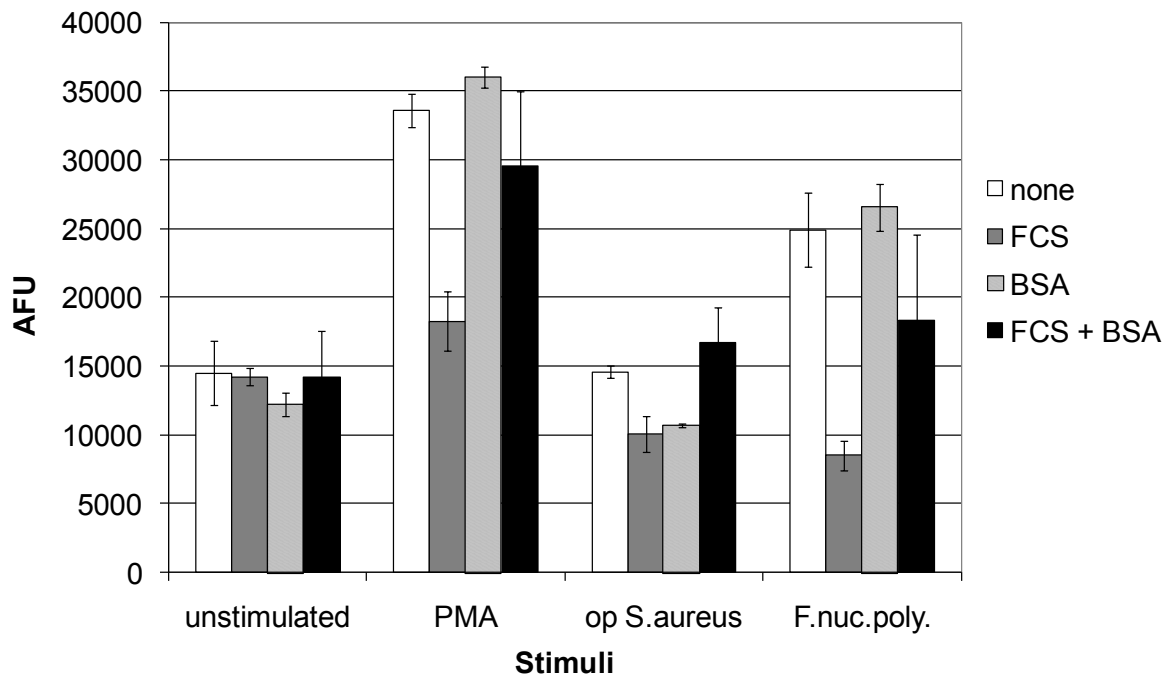


Figure 35. Real-time traces of the effect of BSA and FCS on SYTOX[®] detected fluorescence in response to a) no stimulation b) PMA (50nM) c) opsonised *S. aureus* (MOI 1:150) and d) *F. nucleatum* poly. (MOI 1:150) e) Combined results under all stimuli conditions displaying end-point fluorescence at 3 hours post-stimulation (~12000 seconds). Results show mean of experiment performed in triplicate. Results are representative of 3 independent experiments.

The cells incubated for 3 hours with FCS supplementation and/or BSA plate-blocking (Figure 35) were subsequently treated with MNase and the NET-DNA in the supernatant was fluorometrically quantified (Figure 36). The absence of FCS supplementation and BSA blocking generated the highest fluorescent under all stimulatory conditions except that of PMA stimulation. FCS supplementation, followed by BSA plate blocking, followed by a combination of both caused a sequential decrease in detected fluorescence under all conditions of stimulation except *F. nucleatum*. The MNase assay was the method utilised in the majority of subsequent NET release experiments, therefore as 10% FCS media supplementation in this assay demonstrated a reduction in unstimulated DNA detection and the largest increase in NET-DNA fluorescence in response to PMA (the positive control NET stimulus), this was the preferred treatment for subsequent experiments.

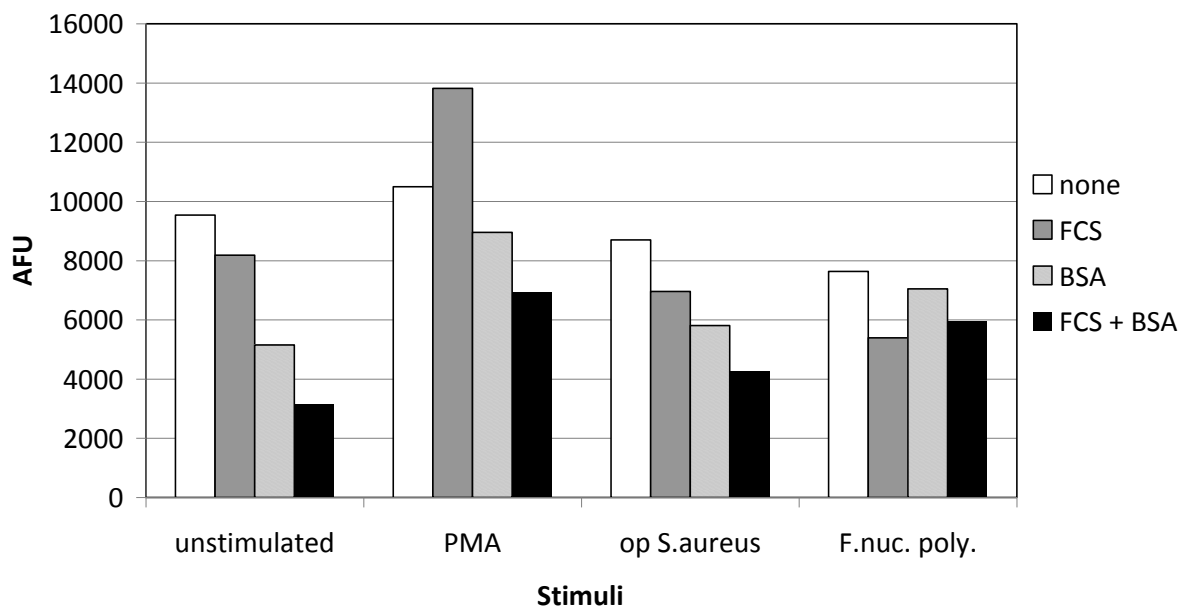


Figure 36. Effect of BSA plate blocking and/or 10% FCS supplementation of media on MNase assay of NET release. A single well of cells used in Figure 35 i.e. unstimulated, PMA 50nM, opsonised *S. aureus* (MOI 1:150) or *F. nucleatum* poly. (MOI 1:150) stimulated were subsequently processed by the MNase assay procedure.

3.3 Determination of optimal concentration of stimuli

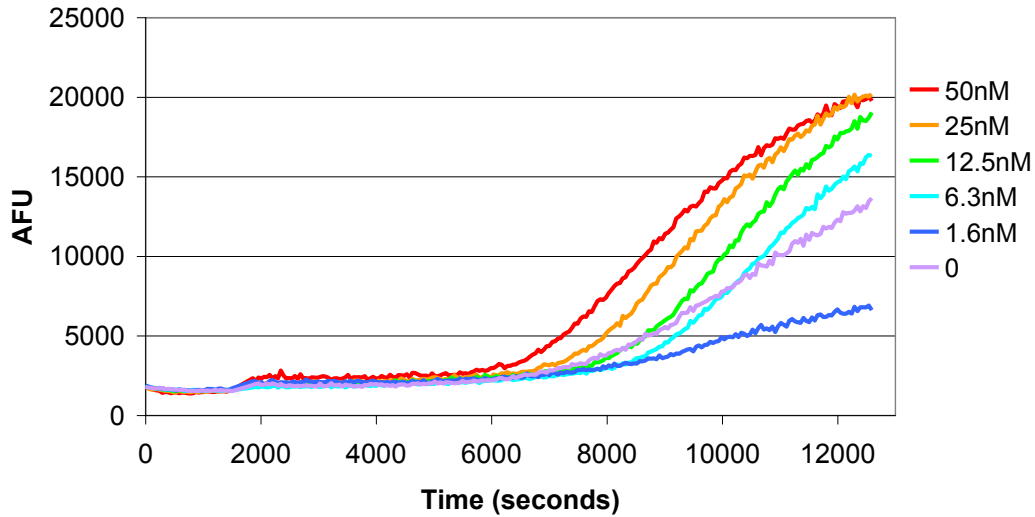
Previously published data has demonstrated that NET release is a part of a cell suicide mechanism (Fuchs *et al.* 2007, Brinkmann and Zychlinsky 2007). Therefore the concentration of stimuli needed to evoke this response in the neutrophils above any other responses, including phagocytosis or degranulation, was determined using PMA exposure (Figure 37) and the Fc γ receptor agonist, opsonised *S. aureus* (Figure 38).

3.3.1 Dose-response analysis following PMA stimulation

Based on previous publications reporting the stimulation of NET release using 25nM PMA (Gupta *et al.* 2005; Beiter *et al.* 2006; Fuchs *et al.* 2007) up to 50nM PMA (Brinkmann *et al.* 2004), a range of 0-50nM were used to stimulate neutrophils in a 96 well microplate. Figure 37a displays the real-time fluorescence trace recorded over a 3 hour stimulatory period. The lowest concentration of PMA, 1.6nM (and lower concentrations; see appendix Figure 93) reduced the fluorescent signal compared to unstimulated cells. Concentrations of 6.3nM PMA and above resulted in a dose-dependant increase in measured fluorescence. Of the two highest concentrations of PMA tested, 50nM PMA initiated an increase in fluorescence marginally earlier than the 25nM PMA concentration, however both reached the same level of fluorescence output by 3 hours post stimulation (Figure 37b). This pattern of response was also confirmed by subsequent MNase assay of the released DNA (Figure 37b). This too demonstrated reduced DNA release at low PMA concentrations followed by an increase and plateau at high PMA concentrations. 50nM PMA resulted in the most rapid increase in fluorescence (Figure 37a) and one of the highest final fluorescent readouts measured by both

the end-point and MNase assays (Figure 37b) and was therefore used for all subsequent experiments.

a) Real-time fluorescence



b) 3 hour fluorescence and MNase assay

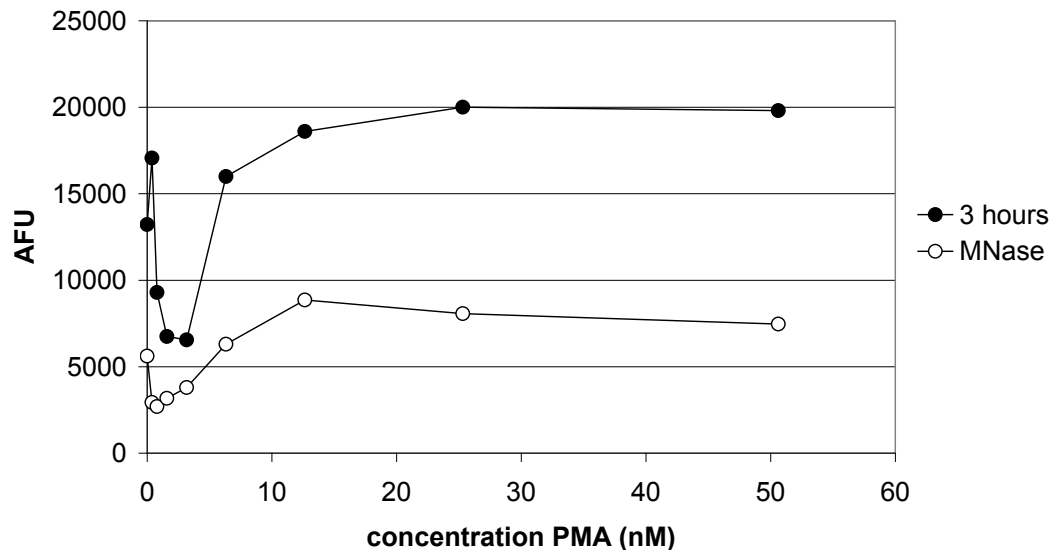
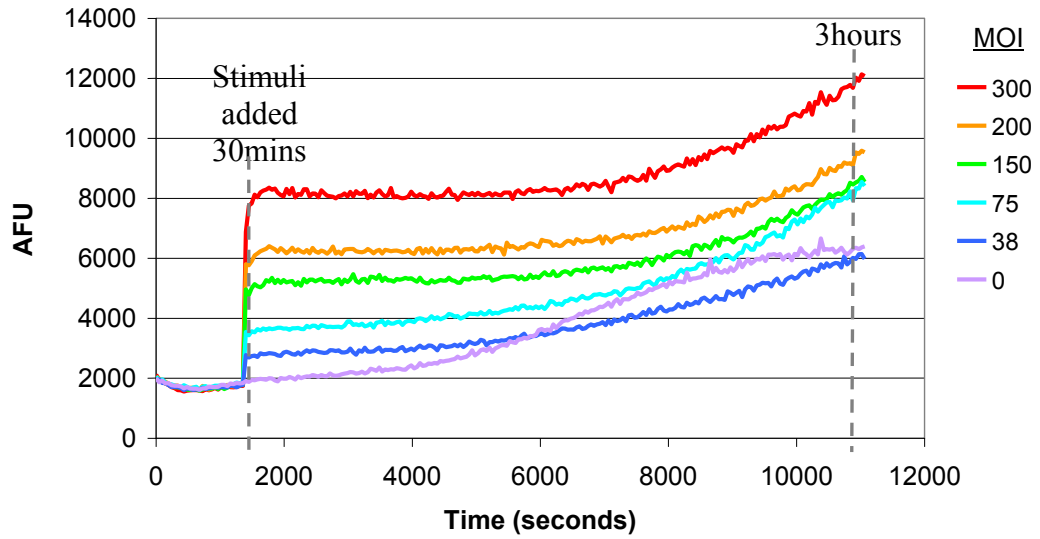


Figure 37. Effect of PMA concentrations (0-50nM) on NET release. Measured by **a)** real-time fluorescence and **b)** 3 hour fluorescence and MNase assay. Results show mean of experiment performed in triplicate.

3.3.2 Dose-response analysis following stimulation with opsonised *S. aureus*

Real-time fluorescence analysis of NET-DNA release from opsonised *S. aureus* stimulated cells is complicated by the use of dead bacteria whose nuclei bind the SYTOX[®] DNA fluorescent stain in a dose dependant manner. Evidence for this is presented in Figure 38a at approximately 1800 seconds (30 minutes) when the bacterial stimulus was added resulting in an immediate and significant increase in detected fluorescence. Although it has been reported that the most potent NET stimulus, PMA, can evoke NET release in as little as 10 minutes (Brinkmann *et al.* 2004) this was not observed here (Figure 37a), therefore it is unlikely to be as dramatic with the bacterial stimulus applied in this study. The increase in fluorescence upon addition of the bacterial stimulus occurred notably more rapidly and was complete within approximately 2 minutes indicating it is likely to result from dead bacteria, with minimal neutrophil contribution. Therefore the fluorescence at 1800 seconds was subtracted from the 3 hours fluorescence readings and data is shown in Figure 38b. The results demonstrate a peak in released DNA at an intermediate multiplicity of infection (MOI), of between 75-150 bacteria per neutrophil. For all experiments bacterial stimuli were therefore used at an MOI of 1:150.

a) Real-time fluorescence



b) MNase assay and 3 hour fluorescence

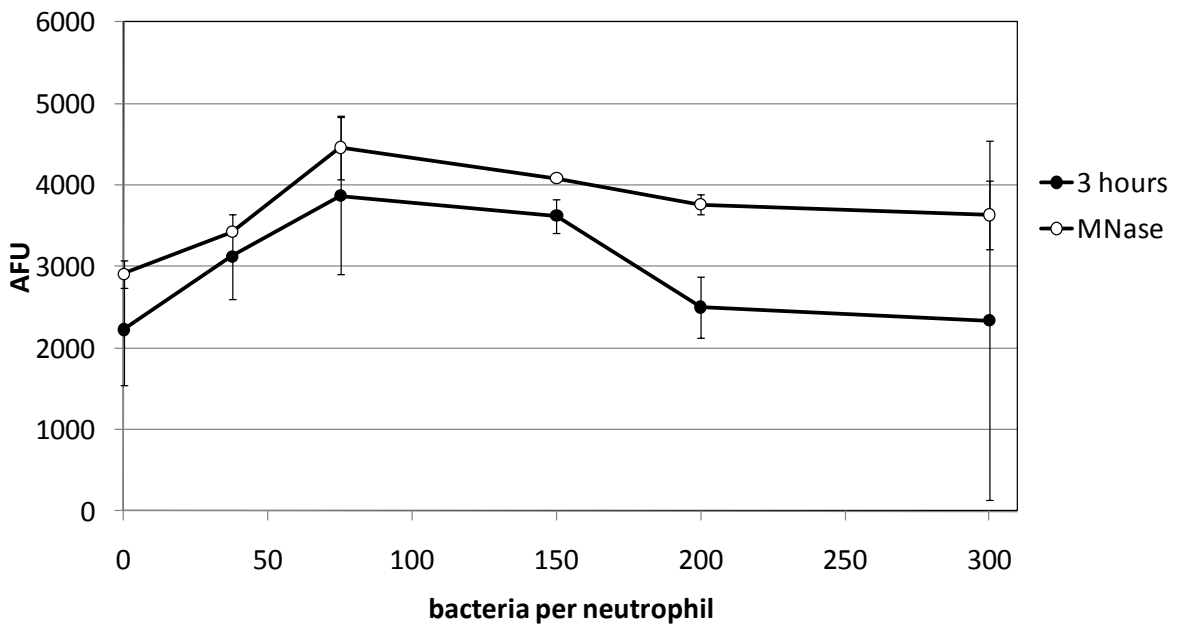


Figure 38. Dose response of opsonised *S. aureus* (MOI 0-300) on NET release determined by a) real-time fluorescence and b) MNase assay and 3 hour real-time fluorescence (minus fluorescence at 30 mins i.e. post stimuli addition). Results show mean fluorescence of experiment performed in triplicate \pm SD.

Discussion

Developing a robust in-house methodology for the assay of NET release proved challenging due to the relatively few reports of this recently described antimicrobial mechanism within the literature and the variability in the reported assay conditions employed.

Quantification techniques

The most basic method for observing NET release is visualisation on glass slides by staining various components of NETs. Previous reports have utilised antibodies to detect the DNA-histone complex and granule protein components (Fuchs *et al.* 2007), however, the major constituent of NETs is the DNA backbone and as such are stained by dyes which fluoresce upon binding to DNA e.g. SYTOX[®] as utilised here and previously (Grinberg *et al.* 2008). Although it has been claimed that DNA intercalating dyes inhibit the formation of NETs (Brinkmann *et al.* 2004), this was not found to be the case in this analysis or in subsequent publications (Ermert *et al.* 2009). Notably, in concordance with previously published descriptions (Behrendt *et al.* 2010) the staining of PMA induced NET-DNA, produced a cloudy and diffuse appearance (Figure 26) prior to mechanical stimulation, which resulted in the appearance of discrete DNA strands resembling those more frequently described (Brinkmann *et al.* 2004; Urban *et al.* 2009). A further observation from these studies, was that the DNA strands aggregated and associated with cells, especially when NETs were abundant (Figure 26Bi) resulting in clustering as previously described (Alghamdi *et al.* 2009). This meant that capturing clear images of NET production was highly dependant upon the field visualised. Previous studies have reported attempts to quantify NET release based on

captured images such as the number of discrete areas of DNA larger in size than a neutrophil (Buchanan *et al.* 2006), or the number of neutrophils forming NETs as a percentage of total cell count (Grinberg *et al.* 2008). These approaches are however highly subjective and unreliable when individual cells cannot be distinguished amongst clusters. Therefore, a quantitative approach using a fluorescence plate reader was employed. This technique meant that time course studies could be performed, allowed a relatively high throughput, and was a technique previously described by Alghamdi *et al.* (2005) and subsequently by Ermert *et al.* (2009). Fluorescence readings were representative of NET release and were comparable to visually obtained results (Figure 26). Initially however, the concentration of cells used required optimisation and notably high cell densities resulted in significant fluctuations in fluorescent output (Figure 25). These fluctuations commenced from approximately 1 hour post-stimulation, a time coinciding with NET release. Therefore it is possible that the abundance of cells were physically shielding the fluorescence emitted from NET-DNA bound SYTOX[®] dye. Similar fluctuations in fluorescent output were often observed with the addition of *F. nucleatum* as a stimulus which also may have been shielding the fluorescent emission.

A complicating factor in the fluorometric measurement of extracellular NET-DNA was the staining of intracellular DNA of dead cells. Therefore, to separate the extracellular DNA and cells that have died by processes other than NETosis, cultures were treated with the MNase enzyme as previously described (Fuchs *et al.* 2007; Ramos-Kichik *et al.* 2009), prior to centrifugation of cell debris. MNase is a DNase secreted by *S. aureus* and acts as an endo- and exo-nuclease to yield 3' mono- or di-nucleotides. It is relatively non-specific in terms of base sequence preference, making it suitable for the digestion of extracellular genomic DNA

and it preferentially cleaves chromatin at the linker region between nucleosomes (Noll 1974). In addition to including the MNase at the end of the incubation period as previously described, it was also included for the duration of the 3 hour incubation period in an attempt to minimise the number of processing steps. Although continuous incubation with MNase produced a more effective liberation of the DNA, when examining the appearance of the unstimulated cells treated continuously with MNase (Figure 28) the nuclei of dead cells (SYTOX[®] positive cells) appeared multilobulated and discrete areas of intracellular DNA staining could be observed. Additionally mammalian DNase has previously been demonstrated to bind actin, preventing polymerisation and promoting depolymerisation (Hitchcock 1980). As MNase may exert other cellular effects, it was therefore deemed more appropriate to add the MNase at the 3 hour time point. It was also interesting to note that the MNase assay gave a similar pattern of results to the real time fluorometer assay of PMA-stimulated NET production (Figure 31) indicating the potential validity of both methods. However, in the majority of subsequent experiments described in this thesis MNase assay was deemed the most appropriate method for the quantification of NET release.

Serum supplementation of media

Of particular importance to NET analysis is the concentration and type of serum proteins present. As previously reported (Fuchs *et al.* 2007) and also demonstrated here (Figures 32 and 33) serum exerts a dose-dependant inhibition of NET release. Whilst the majority of publications reported the use of isolated neutrophils suspended in RPMI, the serum protein supplementation in this media ranged significantly, including 10% FCS (Martinelli *et al.* 2004), 2% human serum albumin (Beiter *et al.* 2006; Fuchs *et al.* 2007) and 2% heat activated autologous plasma (Buchanan *et al.* 2006) and the absence of serum (Alghamdi *et al.* 2005;

Gupta *et al.* 2005). In addition, Fuchs *et al.* (2007) claimed that NET induction was optimal at low serum concentrations ($\leq 2\%$), which was also representative of conditions at sites of inflammation. When assay conditions were optimised for the study reported here, FCS supplementation of media (0-20%), BSA supplementation of media (0-2%) and BSA coating of the assay plate were all analysed. Initially NETs were produced and visualised on glass slides and therefore FCS supplementation of media was the most practical and appropriate, however, in subsequent investigations the assay of NETs was compared to the chemiluminescent assay of ROS and therefore BSA coating of the plate was more appropriate. As it has previously been reported (Fuchs *et al.* 2007) and supported by the variability in the data obtained here (Figure 27 and 29) that NET release exhibits significant inter-individual variation, the optimum concentration of serum may also be subject to inter-individual and temporal variation. In general however, 10% FCS media supplementation proved optimum for the assay of NET release both qualitatively (Figure 32) and quantitatively (Figure 33). Recently it has been reported that the dose-dependant reduction in NET detection by the addition of serum is due to the presence of serum nucleases degrading extruded NETs (von Kockritz-Blickwede *et al.* 2009). Notably it was reported that the serum nuclease activity could be destroyed by heat inactivation at 70°C but not by the standard heat inactivation at 56°C as used in this study. However, when NETs were produced in the presence of MNase (Figure 28), this resulted in an obvious green colouration of the supernatant due to SYTOX[®] green staining of liberated nucleic acid fragments. This effect was absent when NETs were produced in the presence of FCS alone, indicating that this does not represent a significant source of nuclease activity. Whilst the endogenous nuclease activity of the FCS used in these experiments does not appear to have an effect comparable to exogenously added MNase, it is possible that the sensitivity of the NET assay is reduced.

Conversely it has also been reported that serum contains high levels of DNA (Behrendt *et al.* 2010). Experiments to assess the nuclease activity of FCS are therefore warranted and could include incubation of the culture media with purified DNA and subsequent analysis by agarose gel electrophoresis to visualise the extent of degradation. Alternatively it has been indicated by Chapple *et al.* (1997) that FCS possesses antioxidant properties. For this reason FCS cannot be used in the enhanced chemiluminescent assay of neutrophil radical production and BSA coating of the assay plate is used instead. If NET release is dependent on the presence of reactive oxygen species as suggested (Fuchs 2007), it is possible that antioxidant activity within the FCS is responsible for the dose-dependent reduction in NET release.

Stimuli

The reported stimuli capable of evoking the release of NETs include those deriving from host cells (e.g. cytokines, complement and opsonising molecules), those deriving directly from bacteria (e.g. endotoxins), as well as other pathogens such as parasites and yeast. During the 5 years of research into NETs, PMA has emerged as a positive control or ‘gold standard’ for NET release. This molecule is derived from croton oil purified from the leaves of an Asiatic shrub (Busch 1971) and is known for its tumour promoting and also inflammatory properties. In neutrophils it is able to activate protein kinase C (PKC) and as such, takes the place of the physiological activator diacylglycerol (DAG). PMA is lipophilic so is able to directly cross the cell membrane and act rapidly because it has a relatively short signalling pathway, bypassing any cell surface receptor interactions. It is also less readily metabolised than DAG so results in a relatively prolonged activation of PKC (Newton 1995). The ability of PMA to induce a cell death process distinct from apoptosis and necrosis was observed years before NETosis was described (Takei *et al.* 1996). In this early report, PMA induced cytotoxicity

was described as involving loss of lobulation of the nucleus, decondensation of the chromatin, subsequent disintegration of the nuclear membrane with organelles remaining intact, and an increase in cell permeability only occurring at the end of the process. Significantly this form of cell death appeared not to involve DNA degradation (a hallmark of apoptosis) and was also dependant on oxygen radical production and therefore in hindsight was likely to represent one of the first descriptions of NETosis. The relationship between PMA concentration and NET release showed an unusual pattern in that a decrease in NET release was observed at mid-range concentrations of PMA (Figure 37). Published data on the effect of increasing PMA concentrations on the amount of NET release, previously found no correlation (Palic *et al.* 2007) and results here appear to corroborate this finding. Research by Palic *et al.* (2007), utilising fish neutrophils, also tested several stimuli for dose effects on NET production with mixed findings. With LPS stimulation NET release reached a peak in response at 0.5µg/ml and then decreased as LPS concentration was increased further. In addition a yeast β glucan commonly used to stimulate fish neutrophil degranulation was found to significantly increase DNA release at only two unrelated concentrations and displayed no pattern. This indicates that the trigger for NET release is complex or that the sensitivity of the assay is not sufficient to detect subtle variations in release. Similarly the NET response to opsonised *S. aureus* did not display a linear relationship and instead peaked at an intermediate concentration of 75 bacteria per neutrophil (Figure 38).

CHAPTER 4 RESULTS

Modulation of NET release

Having characterised assays for the release of NETs in the previous chapter, these were subsequently utilised to examine the relationship between NET production and other neutrophil bactericidal functions, namely ROS generation which has been reported to be necessary for NET release (Fuchs *et al.* 2007), and also phagocytosis. Various relevant inhibitors, enzymes and antioxidants were employed to modify various stages of the ROS generation pathway as well as the actin polymerisation process required for phagocytosis.

4.1 ROS inhibitor, diphenyleneiodonium (DPI)

DPI is a widely reported inhibitor of NADPH oxidase (O'Donnell *et al.* 1993). To examine the relationship between NADPH oxidase dependant ROS production and NET release, initially an effective concentration for inhibiting ROS production was determined.

Addition of DPI to the enhanced chemiluminescent assay for detection of ROS caused a dose-dependent reduction in luminol (total ROS), isoluminol (extracellular ROS) and lucigenin (primarily superoxide) dependant ROS production in PMA stimulated neutrophils (Figure 39). The magnified view (Figure 39) shows that this trend in reduction continued at the higher concentrations of DPI used. Based on this data, 25 μ M DPI was applied in all subsequent experiments as it resulted in optimal reduction in ROS generated.

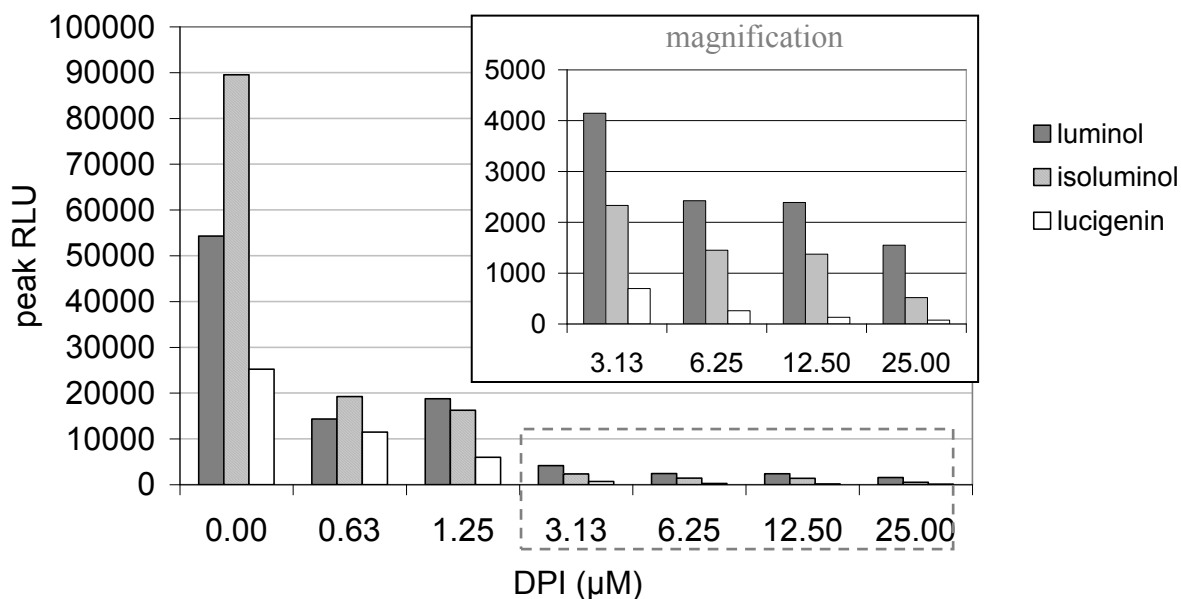


Figure 39. Effect of DPI on ROS production. Peak ROS from PMA (50nM) stimulated cells with DPI (0-25μM). Results representative of two independent experiments. Dashed box indicates range displayed in magnification (inset).

To determine whether DPI inhibition of NADPH oxidase-ROS production also inhibited NET release, 25μM DPI was used in the MNase assay. Data indicated that DPI inclusion resulted in a significant decrease in NET release stimulated by PMA ($P=0.001$), opsonised *S. aureus* ($P=0.01$) and *F. nucleatum* ($P=0.04$) (Figure 40). Exposure of unstimulated neutrophils to DPI had no significant effect on spontaneous NET formation (Figure 40). The fluorescence observed in unstimulated cells may indicate a baseline level of spontaneous NET release that is independent of NADPH oxidase ROS generation as DPI exerted no apparent effect, or may be due to spontaneous cell death and lysis occurring naturally in the neutrophil population over the 3 hour incubation period. There was also a background level of SYTOX[®] fluorescence resulting from the media which was 2000-3000 AFU and therefore a ‘blank’ consisting of all reagents minus cells was assayed and subtracted during all subsequent inhibition studies utilising the MNase assay.

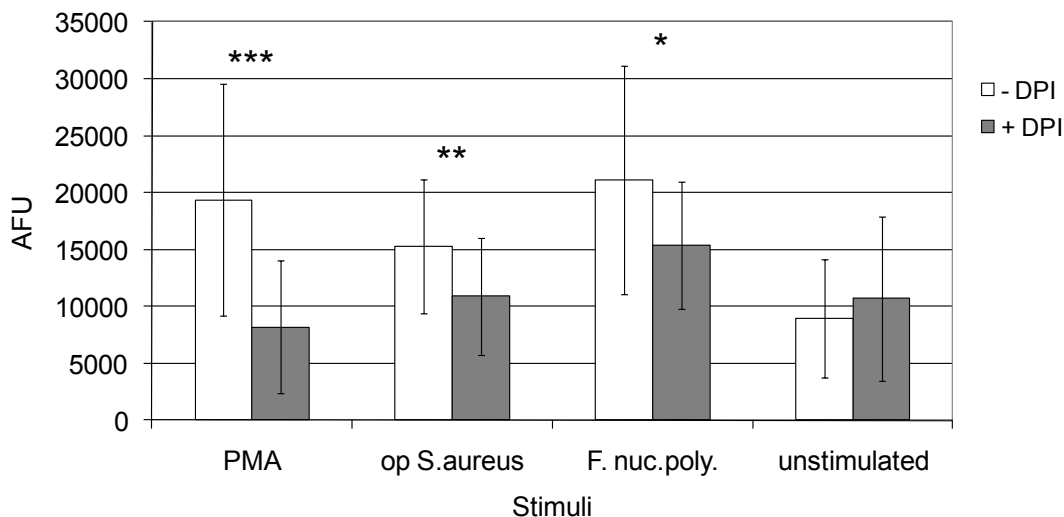


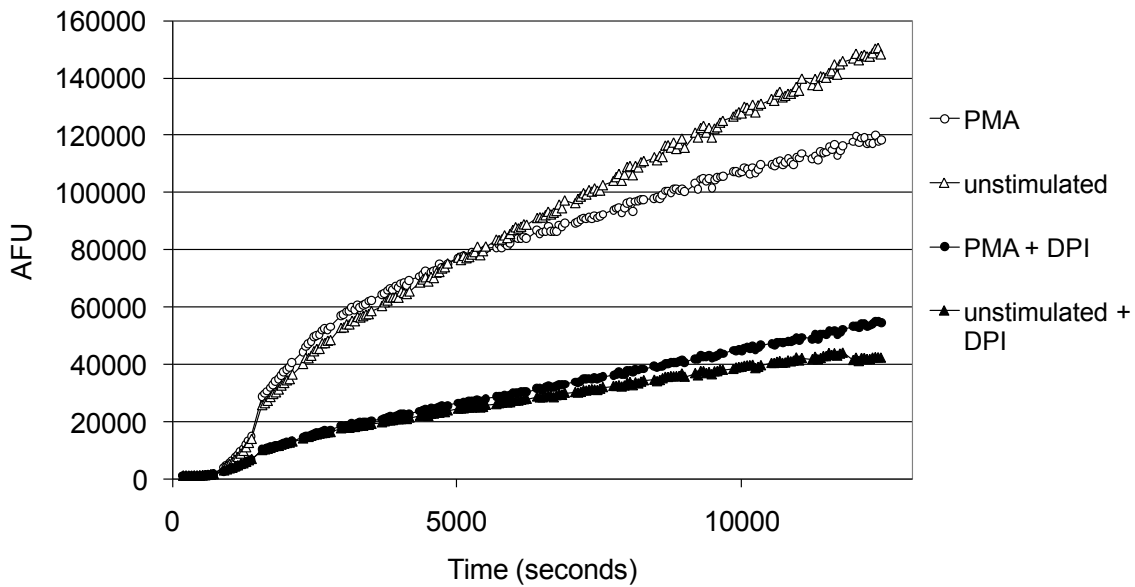
Figure 40. Effect of 25µM DPI on MNase assay of NET production. Sixteen individuals were assayed in triplicate. * $P \leq 0.05$, ** $P \leq 0.01$, *** $P \leq 0.001$ by two-tailed paired T-test.

4.1.1 Effect of DPI on cell viability

Whilst data presented in Figure 40 indicates that DPI inhibition of ROS generation may subsequently regulate NET production, it is possible that modulation of ROS may affect cell viability which may subsequently affect readouts obtained from the fluorescence assay, i.e. SYTOX[®] staining of dead cells. Therefore a fluorescence cell viability assay (MultiTox-Fluor Multiplex Cytotoxicity assay, Promega) was employed which utilised a protease and therefore provided a DNA independent readout of cell death (Figure 41). This approach clearly demonstrated that there were fewer dead cells present in wells exposed to DPI. Dead cell fluorescence in the presence of DPI increased gradually over the time period studied and readouts appeared unaffected by the addition of the stimuli as there was no increase in fluorescence at 1500 seconds when the stimuli were included. In the absence of DPI, detected cell death increased from the point of stimulus addition (with both PMA and blank), however dead cell fluorescence of stimulated cells also increased in comparison to unstimulated cells from 5400 seconds (1.5 hours) onwards. The data obtained using the live cell stain was in

contrast to the dead cell stain data in that fewer live cells were observed in the presence of DPI. However, the differences in live cell-fluorescence with and without DPI were less obvious. A similar pattern was seen with all stimuli used (opsonised *S. aureus* and *F. nucleatum*; see appendix Figure 94).

a) Dead cell stain (protease dependant)



b) Live cell stain (protease dependant)

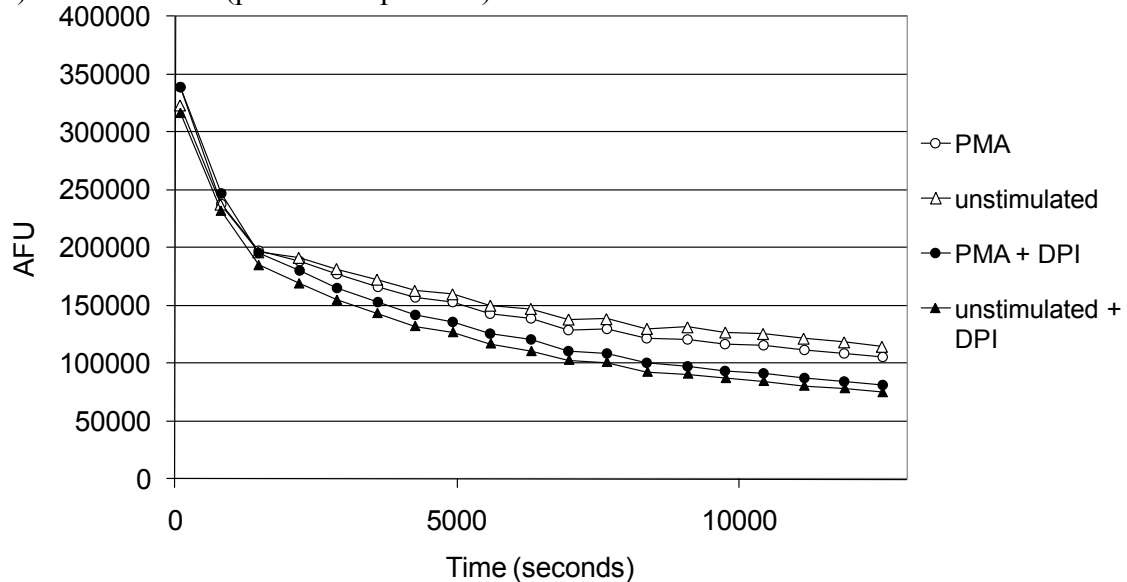
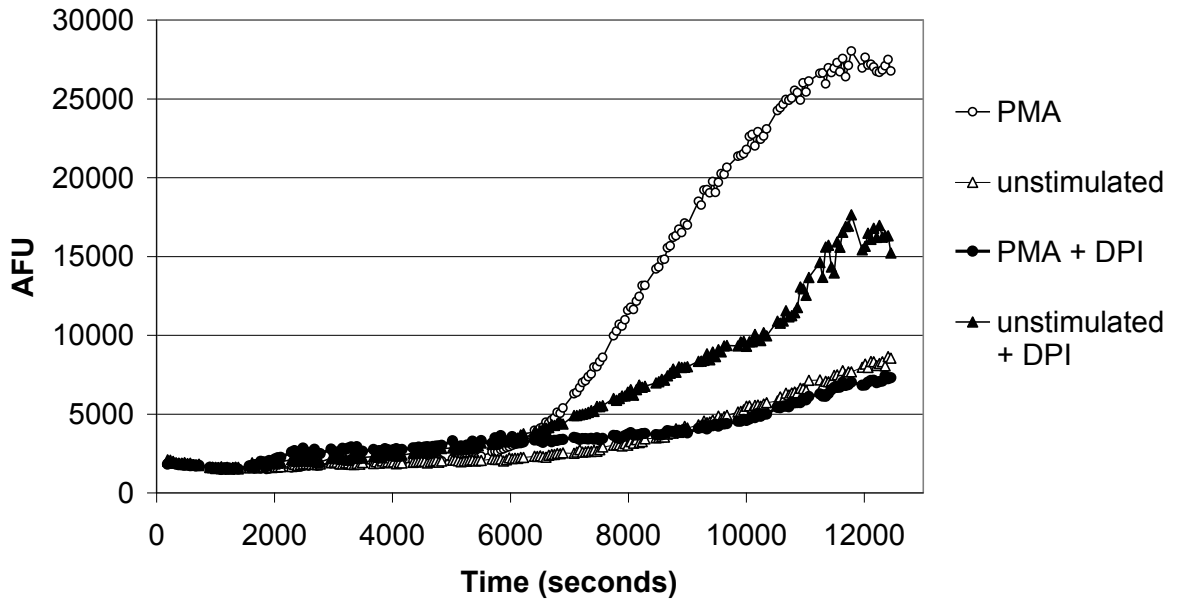


Figure 41. Time course analysis of the effect of DPI (25 μ M) on cell viability using the protease dependant MultiTox-Fluor Multiplex Cytotoxicity assay (Promega). a) Dead cell stain read using filter 485/535nm, b) Live cell stain read at 355/460nm. Cells stimulated with PMA (50nM) or left unstimulated over 3 hour incubation period. Results show mean of experiment performed in triplicate.

As SYTOX[®] green also enters dead cells it was used simultaneously with the cell viability kit (Figure 41) to examine its detection of cell viability (Figure 42a) in addition to its use for detection of extruded NET-DNA. After 3 hours incubation, the cells were processed as previously described for MNase detection of extracellular NET-DNA (Figure 42b).

SYTOX[®] detection of cell death increased from 6000 seconds (~1 hour post stimulation) onwards in PMA stimulated cells which, based on previous data (Figure 26A) coincides with NET release (Figure 42a). This effect was absent in PMA stimulated cells with the addition of DPI which remained at a low level of fluorescence throughout, displaying a similar trace to that of unstimulated cells. Notably, the addition of DPI to unstimulated cells resulted in a moderate increase in fluorescence which occurred concomitantly with the increase in PMA stimulated fluorescence (~1 hour post stimulation). Time course SYTOX[®] fluorescence of bacterially stimulated cells (opsonised *S. aureus* and *F. nucleatum*) resembled that of unstimulated cells exhibiting a low level of fluorescence throughout the incubation period (see appendix Figure 95). MNase assay of the same cells (Figure 42b) confirmed this increased DNA release in unstimulated cells by the addition of DPI (P=0.02). It also confirmed the decreased DNA release by PMA stimulated cells caused following addition of DPI (P=0.02; both by unpaired two-tailed T-test).

a) SYTOX[®] green time course fluorescence.



b) MNase assay

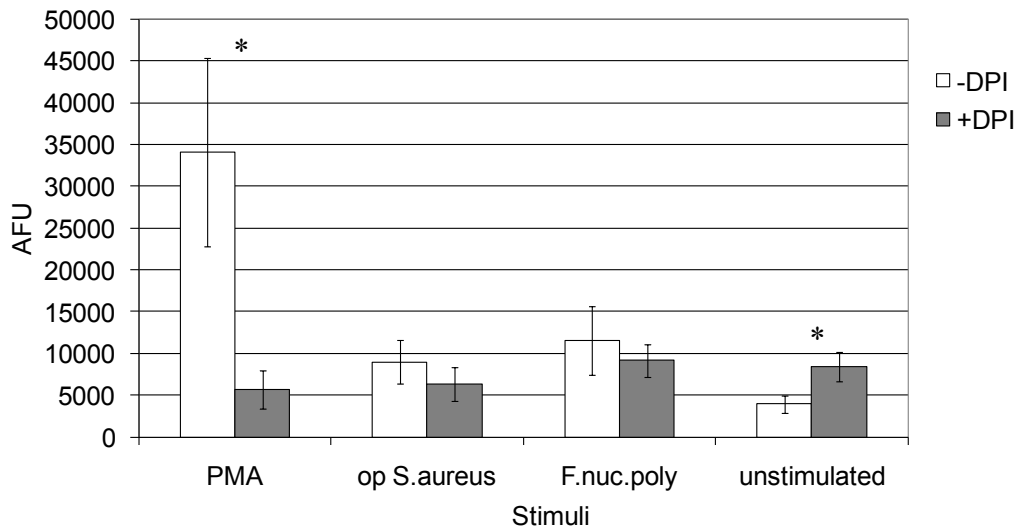


Figure 42. Effect of DPI on a) cell viability detected by SYTOX[®] fluorescence over 3 hours incubation, and b) MNase assay detection of extracellular DNA in supernatant. Results show mean of experiment performed in triplicate \pm SD. * $P \leq 0.05$ by two-tailed paired T-test.

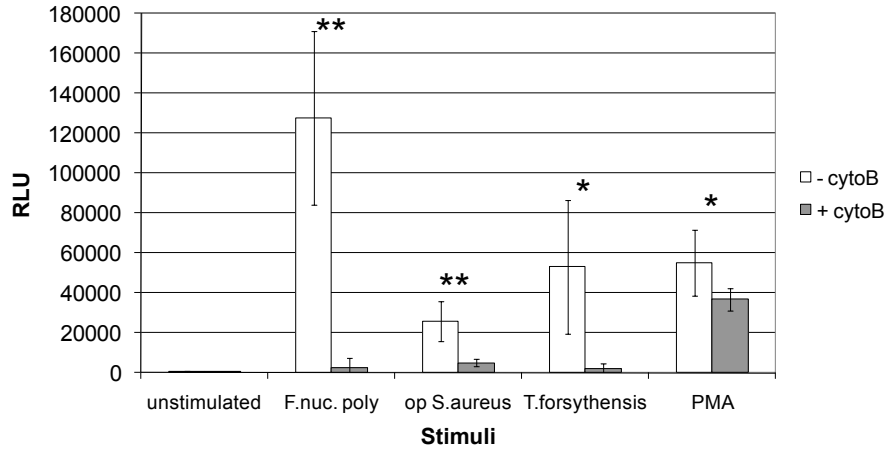
4.2 Phagocytosis inhibitor, cytochalasin B (cytoB)

The primary function of neutrophils is phagocytosis thus bacterial stimulation evokes this response. Whilst not the killing mechanism of interest in this study, it is of interest to

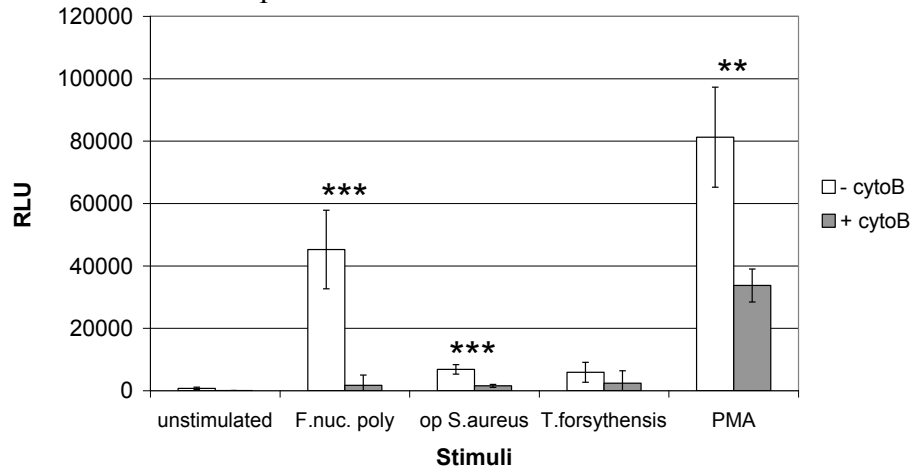
determine whether the process of phagocytosis contributes to detected NET release, therefore neutrophils were treated with the actin polymerisation inhibitor, cytochalasin B. The effect of 10µg/ml cytochalasin B (Grinberg *et al.* 2008) on ROS generation (Figure 43) was also assayed alongside MNase assay of NET production (Figure 44).

As cytochalasin B is a known inhibitor of neutrophil phagocytosis of bacteria, three different bacterial stimuli were used in this experiment including the periodontal pathogen *T. forsythensis*. The addition of cytochalasin B to the assay caused a reduction in the level of luminol-, isoluminol- and lucigenin-dependent ROS produced in response to all stimuli (Figure 43). This difference was significant for all stimuli used except *T. forsythensis* however notably a large variation in the level of ROS detected in the absence of cytochalasin B with *T. forsythensis* stimulation was observed. Compared to the reduction in PMA-stimulated ROS, the reduction in bacteria-stimulated ROS appeared more dramatic and was reduced to similar levels to those detected in unstimulated cells.

a) Luminol detection of peak ROS



b) Isoluminol detection of peak ROS



c) Lucigenin detection of peak ROS

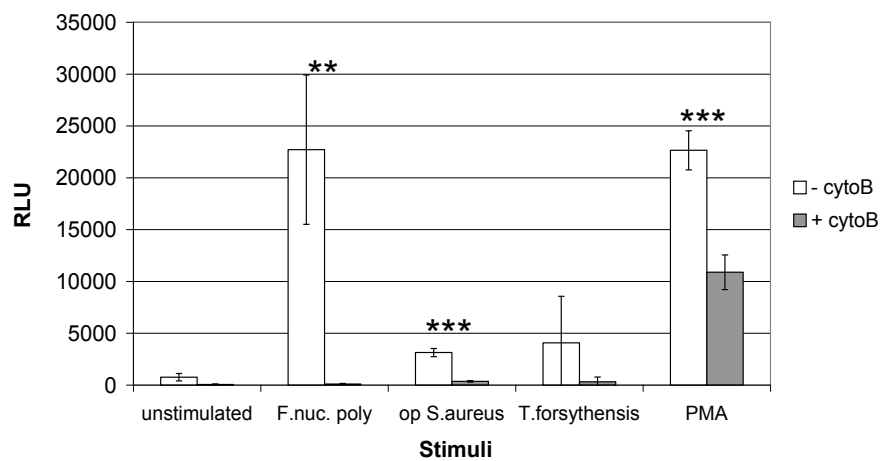


Figure 43. Analysis of cytochalasin B (10µg/ml) on peak ROS production in response to bacterial stimuli (MOI 1:150) or PMA 50nM. Detected by **a)** luminol, **b)** isoluminol and **c)** lucigenin. Results show mean of 3 experiments ± SD. * P≤0.05 **P≤ 0.01 ***P ≤ 0.001 by two-tailed paired T-test.

Notably MNase assay of NET production (Figure 44) demonstrated a reduction in NETs detected in the presence of cytochalasin B in all stimulated and unstimulated cells. This reduction was statistically significant for all stimuli used except *F. nucleatum* and *T. forsythensis*.

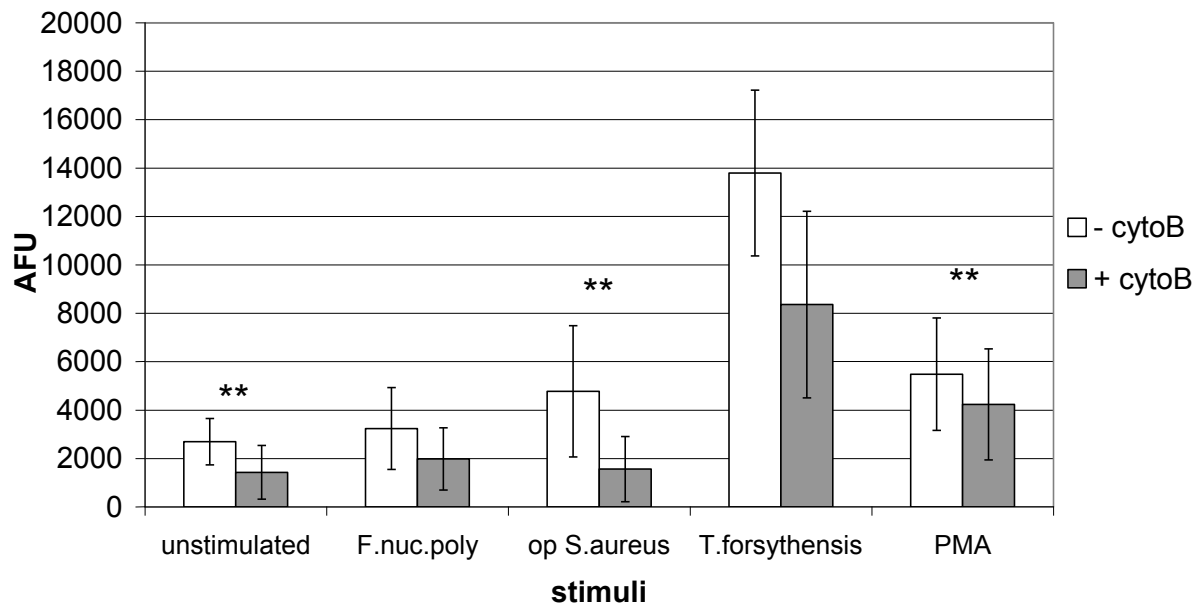


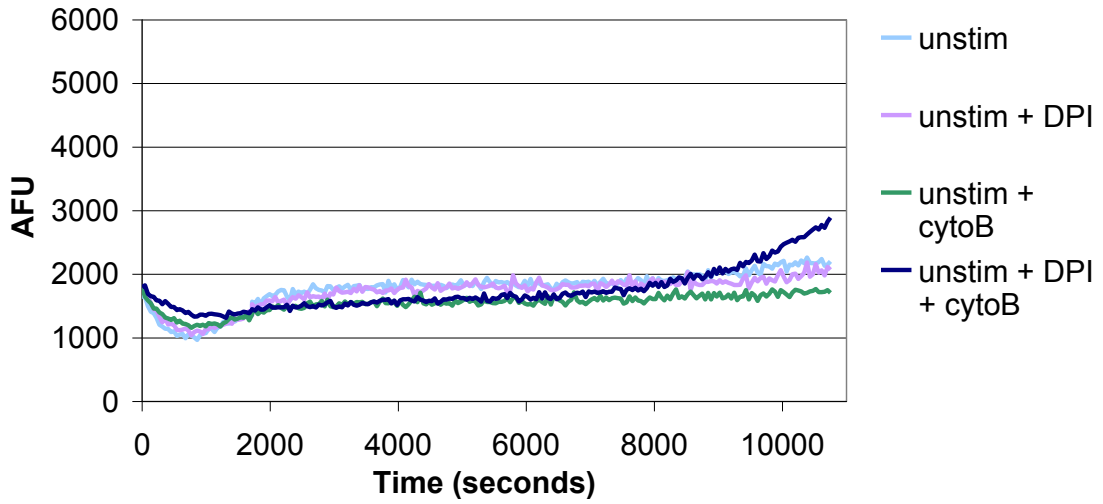
Figure 44. Analysis of cytochalasin B (10µg/ml) on NET production as determined by MNase assay in response to bacterial stimuli (MOI 1:150) or PMA 50nM. Results show mean of 4 experiments ± SD. * P<0.05 **P<0.01 by two-tailed paired T-test.

4.3 Effect of combination of ROS and phagocytosis inhibitors on NET release

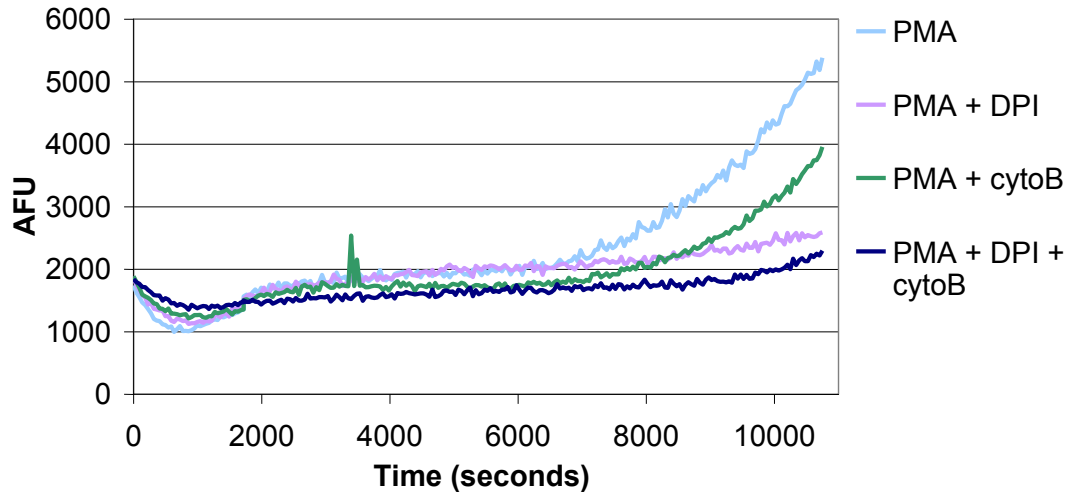
The NADPH oxidase inhibitor, DPI, and the phagocytosis inhibitor, cytochalasin B, were used alone and in combination as real-time fluorescence was recorded to monitor cell death and NET-DNA release (Figure 45). This treatment should act to inhibit the main killing mechanisms of neutrophils (phagocytosis and ROS/NET release) and help to elucidate the contributions of each mechanism in the NET response, as measured by fluorescence, when challenged with different stimuli.

With all stimuli used the absence of inhibitors resulted in the highest detected fluorescence. The largest reduction in fluorescence was observed using a combination of both inhibitors in response to all stimuli but not in unstimulated cells. Notably, singly cytochalasin B was the most effective inhibitor of NET production in bacteria-stimulated cells, whilst, DPI was more effective in reducing NET levels in PMA-stimulated cells.

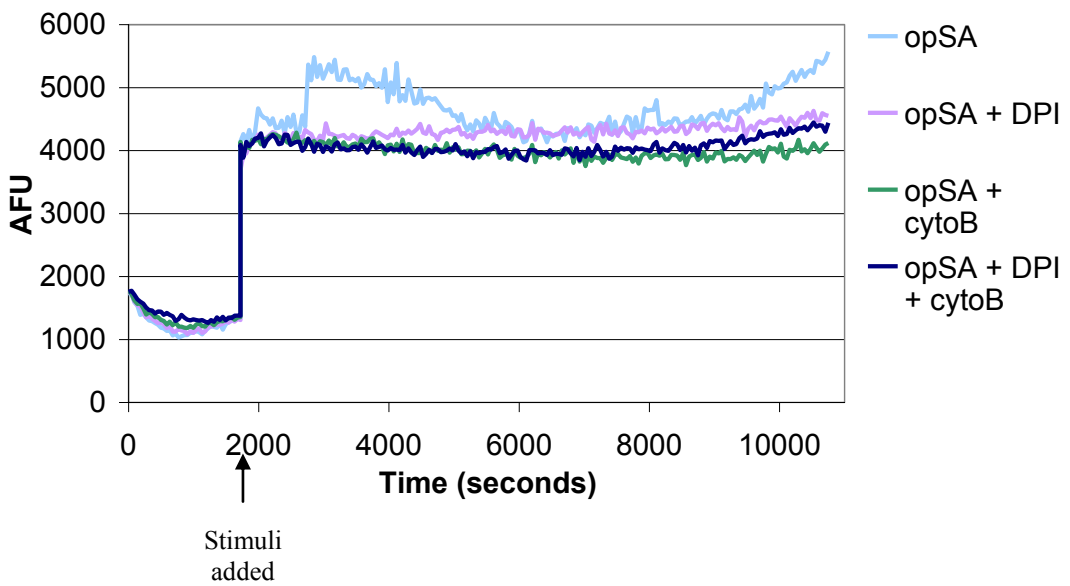
a) Unstimulated



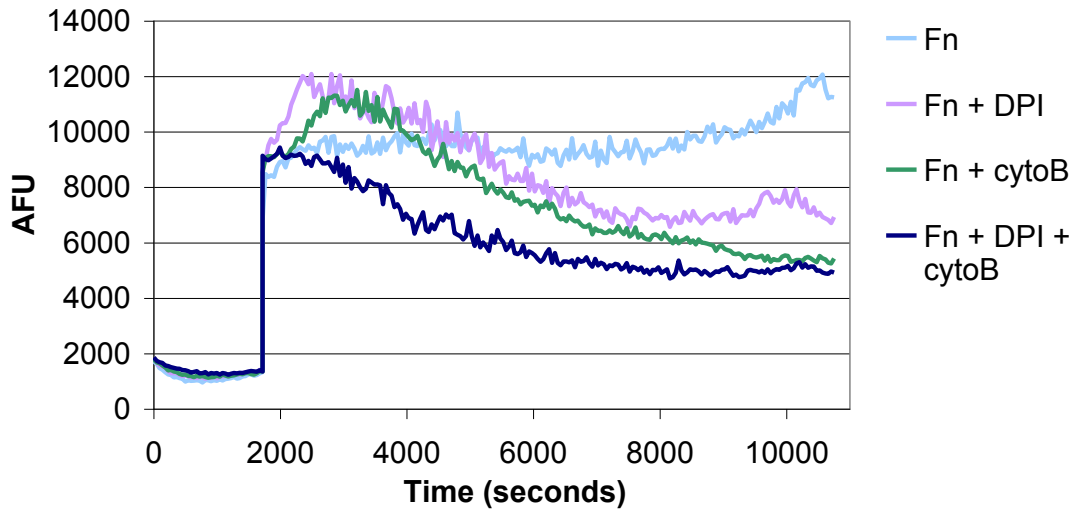
b) PMA stimulation



c) opsonised *S. aureus* stimulation



d) *F. nucleatum* stimulation



e) *T. forsythensis* stimulation

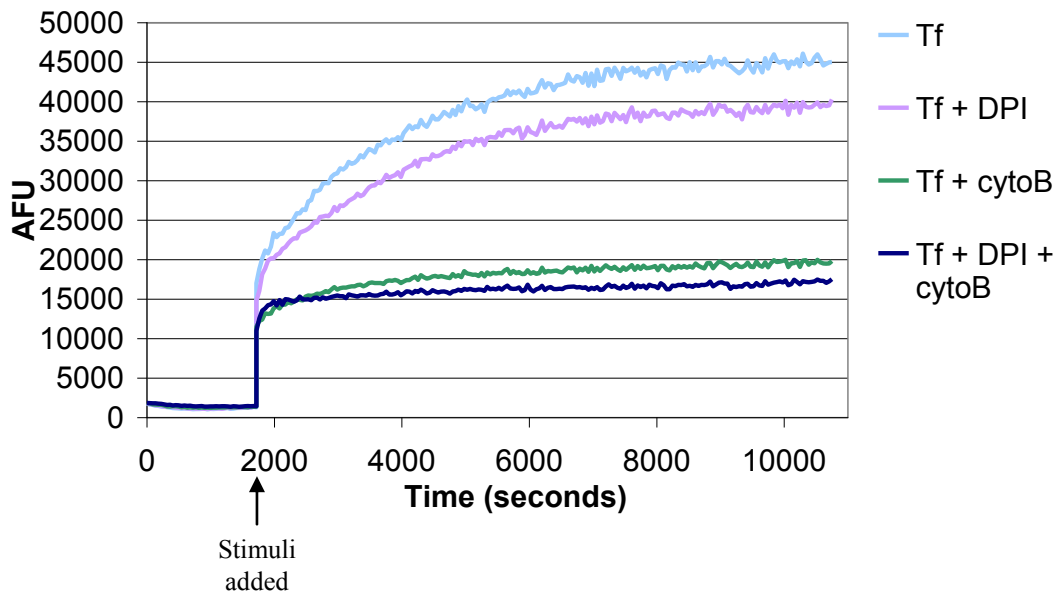


Figure 45. Effect of NADPH oxidase inhibitor (DPI 10 μ M) and/or phagocytosis inhibitor (cytochalasin B 10 μ g/ml) on NET release detected by real-time fluorescence. Fluorescent traces for a) unstimulated cells b) PMA 50nM c) opsonised *S. aureus* MOI 1:150 d) *F. nucleatum* MOI 1:150 e) *T. forsythensis* MOI 1:150. Results show mean of experiment performed in triplicate.

Data derived from subsequent MNase assay of cells incubated with DPI and/or cytochalasin B (Figure 46) demonstrated a similar trend to real-time fluorescence analysis (Figure 45). The absence of inhibitors generally exhibited the highest level of fluorescence and a combination

of both inhibitors resulted in the lowest DNA fluorescence detected. In PMA stimulated cells incubation with DPI alone or cytochalasin B alone caused a similar reduction in fluorescence. However, in bacterially stimulated cells cytochalasin B exposure resulted again in a greater reduction in detected fluorescence than following incubation with DPI.

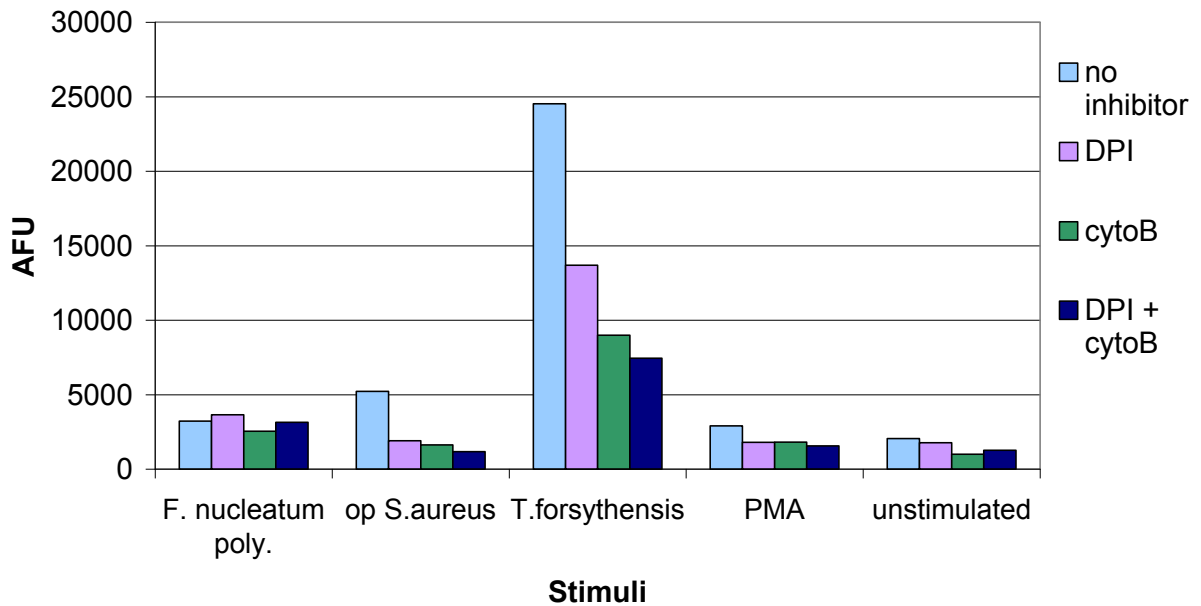


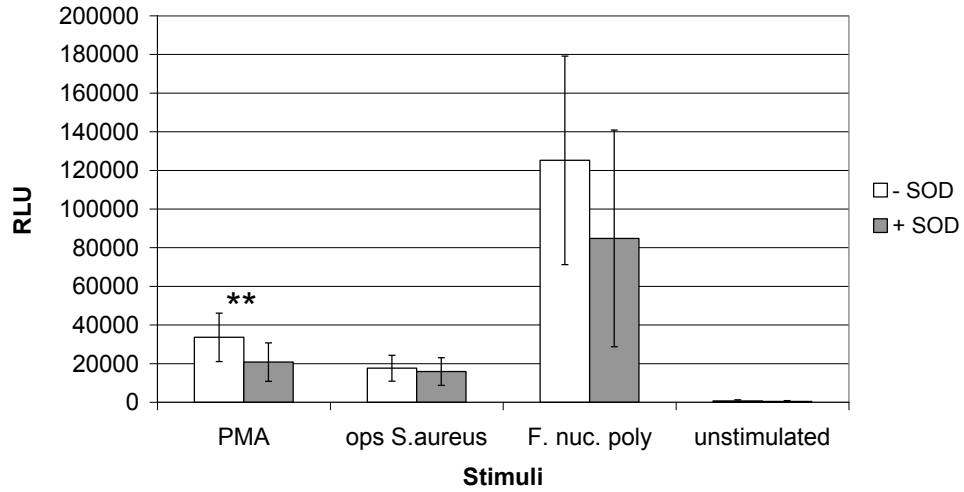
Figure 46. Effect of NADPH oxidase inhibitor (DPI 10 μ M) and/or phagocytosis inhibitor (cytochalasin B 10 μ g/ml) on NET release measured by MNase assay. A single well of cells used in Figure 45 were also assayed by MNase assay after 3 hours stimulation using bacterial stimuli (MOI 1:150) or PMA (50nM).

4.4 Superoxide dismutase (SOD)

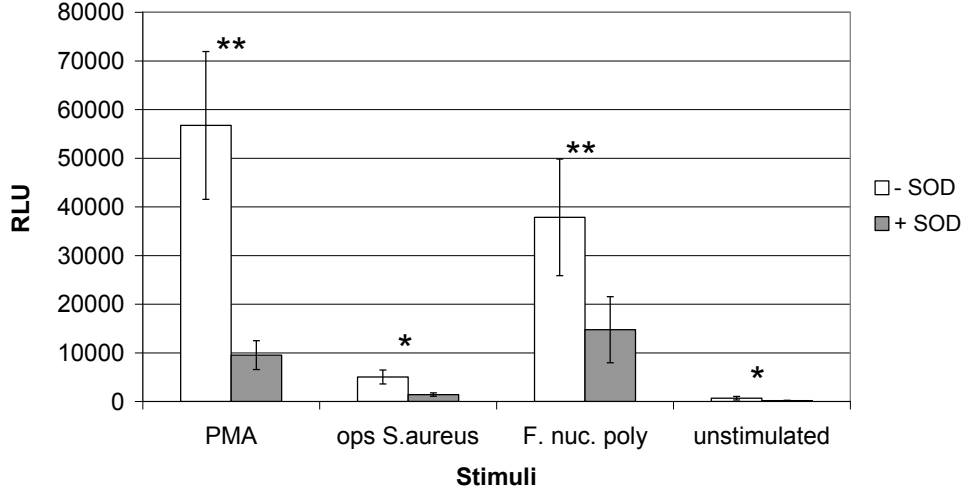
NET release has been demonstrated to be dependant on ROS generation (Fuchs et al. 2007, Figure 40), however, it was notable that cytochalasin B produced additional NET inhibition following DPI inhibition of NADPH-oxidase generated ROS (Figure 45 and 46). Therefore the relationship between ROS and NET production was further characterised using agents which modify the NADPH oxidase ROS generation pathway (Figure 8) in order to identify key steps necessary for induction of NETosis. Initially superoxide dismutase (SOD) which catalyses the conversion of the superoxide anion to hydrogen peroxide, was employed to ascertain whether either of these molecules were involved in NET induction.

Figure 47 demonstrates that the exposure of neutrophils to SOD was in general effective at reducing ROS production. Notably reduced levels of ROS production were primarily identified in isoluminol detected ROS ($P \leq 0.05$ under all stimuli conditions). Lucigenin detected ROS exhibited a minor reduction with SOD however this was not significant in *F. nucleatum* stimulated cells. The reduction in luminol detected ROS was only significant in PMA stimulated cells.

a) Luminol detection of peak ROS



b) Isoluminol detection of peak ROS



c) Lucigenin detection of peak ROS

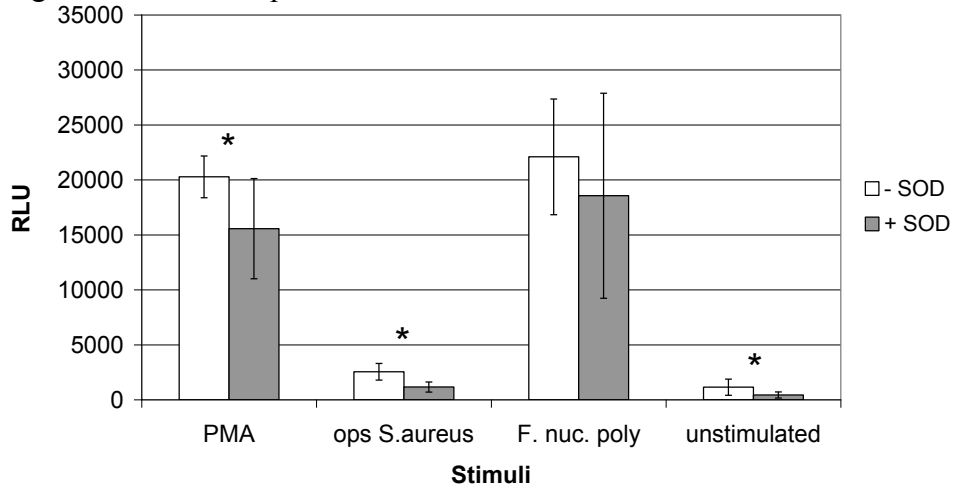


Figure 47. Effect of SOD 95U/ml on peak ROS production in response to PMA 50nM or bacterial stimulation (MOI 1:150). Detected by a) luminol b) isoluminol and c) lucigenin. Mean of 5 experiments performed in duplicate \pm SD. * $P \leq 0.05$ ** $P \leq 0.01$ by two tailed paired T-test.

Data presented in Figure 48 demonstrates that the addition of SOD resulted in increased NET release as measured by MNase assay. This increase was significant ($P \leq 0.01$) in both stimulated and unstimulated cells. This indicates that generation of the reaction product, i.e. hydrogen peroxide, facilitates NET release in concordance with previous data utilising catalase (Fuchs *et al.* 2007).

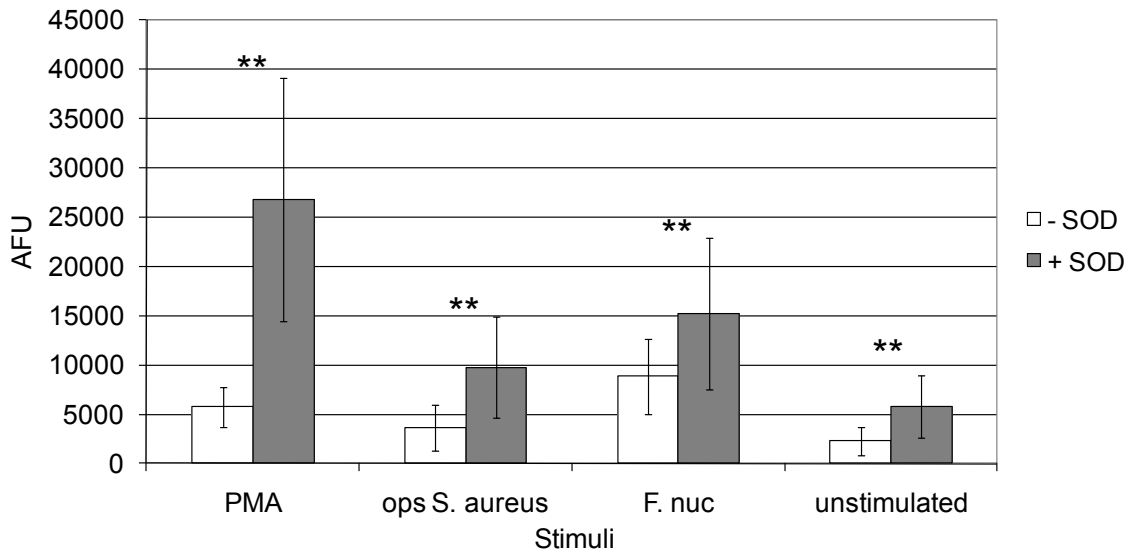
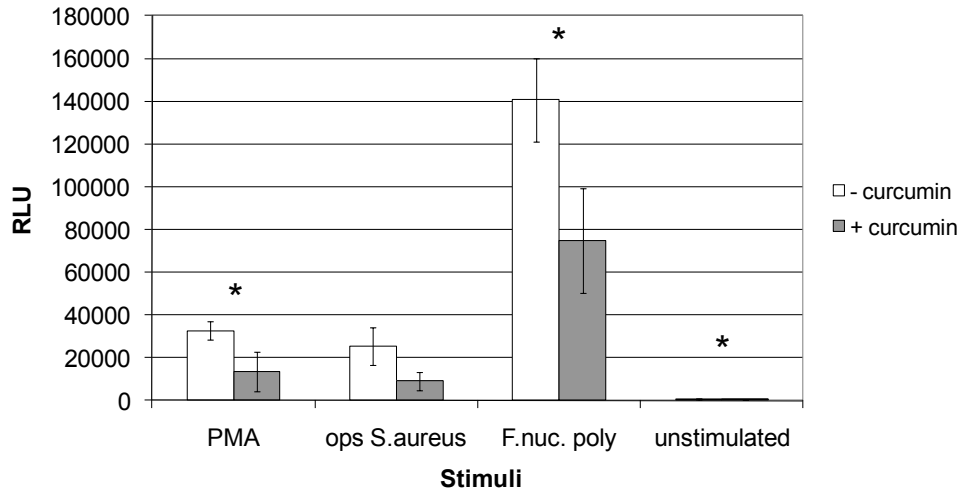


Figure 48. Effect of SOD (95U/ml) on MNase assay of NET production. Results show mean of 5 experiments performed in triplicate \pm SD. * $P < 0.05$ ** $P < 0.01$ by two-tailed paired T-test.

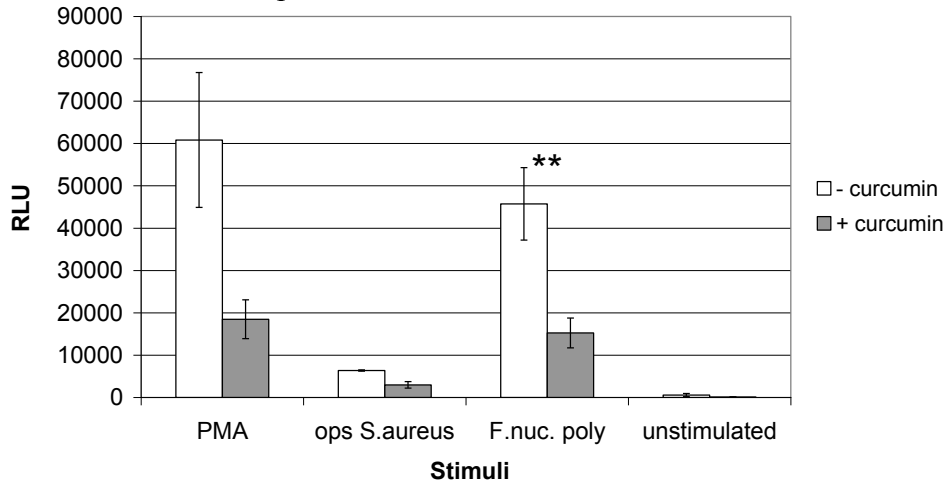
4.5 Antioxidant/radical scavenger, curcumin

Antioxidants remove or neutralise oxygen radicals therefore the ability of the antioxidant, curcumin, to reduce ROS production (Figure 49) and NET release (Figure 50) was examined. The addition of 5 μ M curcumin proved an effective concentration capable of reducing detected ROS under all conditions tested (Figure 49). A significant reduction in ROS was seen in luminol detected ROS in response to PMA, *F. nucleatum* and unstimulated cells ($P \leq 0.05$). Isoluminol and lucigenin detected ROS only reduced significantly in response to *F. nucleatum* stimulation ($P=0.01$ and $P=0.04$ respectively).

a) Luminol detection of peak ROS



b) Isoluminol detection of peak ROS



c) Lucigenin detection of peak ROS

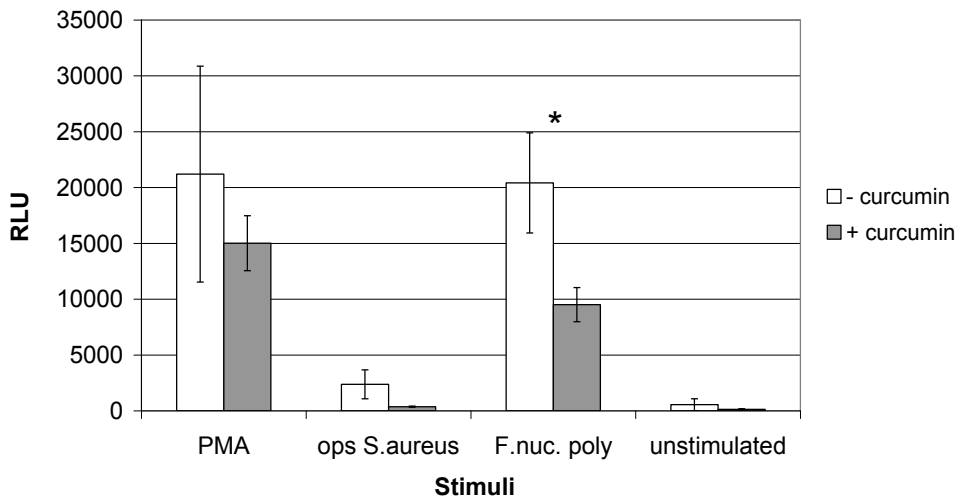


Figure 49. Effect of 5 μ M curcumin on peak ROS production in response to PMA 50nM and bacterial stimulation (MOI 1:150) detected by a) luminol b) isoluminol and c) lucigenin. Results show mean of 3 independent experiments performed in triplicate \pm SD.

MNase detection of NET release was reduced in the presence of curcumin in response to all stimuli (Figure 50) however this reduction was significant only in response to PMA exposure (P=0.01).

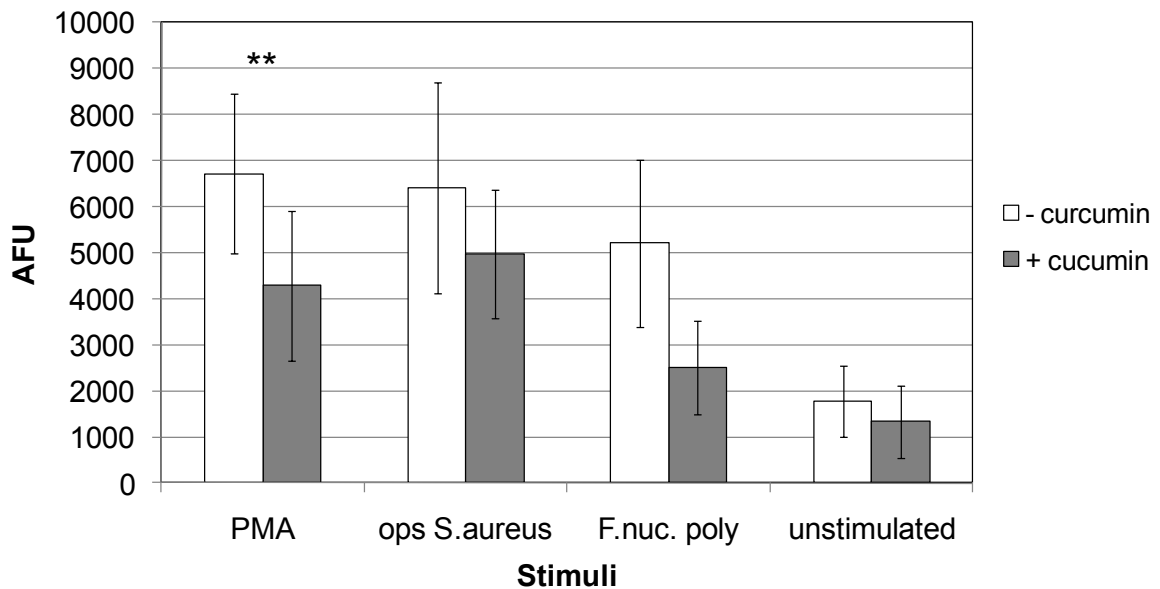


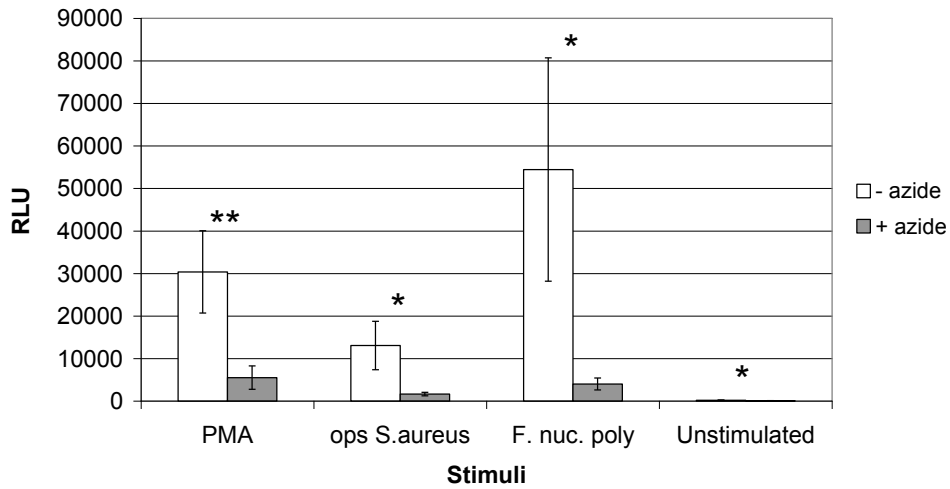
Figure 50. Effect of 5µM curcumin on NET release detected by MNase assay. Results show mean of 5 experiments performed in triplicate minus blanks (no cells) ± SD. ** P≤0.01 two-tailed paired T-test.

4.6 Myeloperoxidase inhibitor, sodium azide

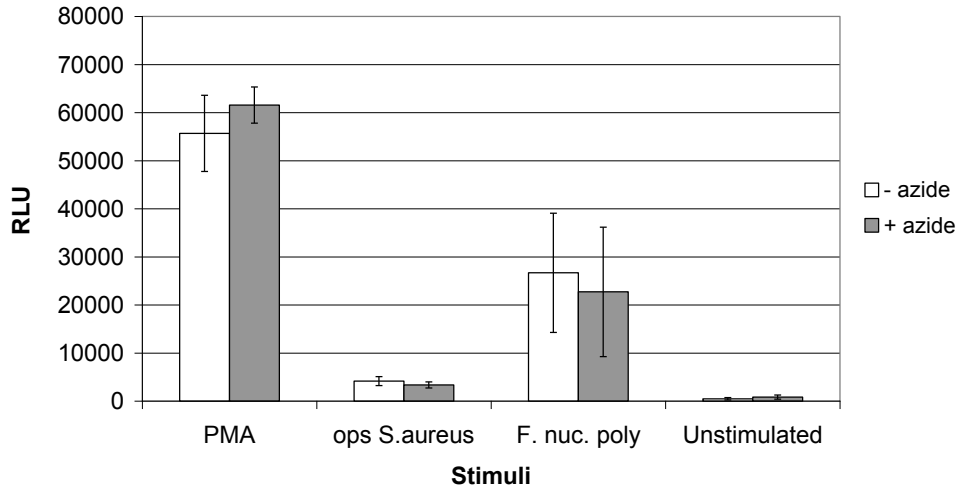
The conversion of hydrogen peroxide to hypochlorous acid by endogenous myeloperoxidase (MPO) can be inhibited by sodium azide. The effect of 2mM sodium azide was therefore tested on the generation of ROS (Figure 51) as well as NET release (Figure 52). The concentration of sodium azide applied was based on previous publications (Mundi *et al.* 1991; Dahlgren *et al.* 1999) in which 1mM sodium azide was used to inhibit MPO in the chemiluminescent assay of ROS production by neutrophils.

Sodium azide exposure caused a significant reduction in luminol detected ROS in response to all stimuli and in unstimulated cells (Figure 51a). Isoluminol and lucigenin detected ROS did not significantly change with the addition of sodium azide although minimal increases and decreases were observed (Figures 51b and c). This result was as expected as isoluminol only detects extracellular ROS and MPO is an intracellular enzyme, and lucigenin detects superoxide anion production which is upstream of MPO and also primarily detects extracellularly.

a) Luminol detection of peak ROS



b) Isoluminol detection of peak ROS



c) Lucigenin detection of peak ROS

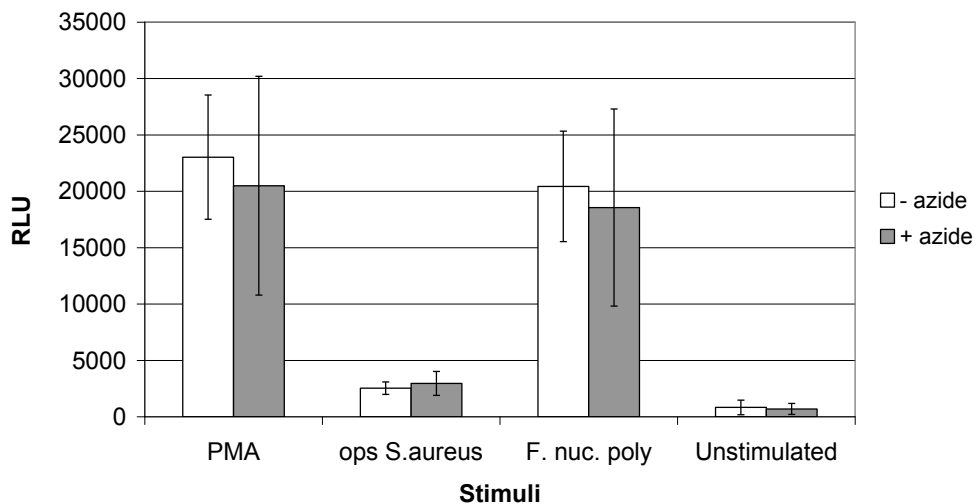


Figure 51. The effect of sodium azide (2mM) on peak ROS production in response to PMA (50nM) and bacterial stimulation (MOI 1:150). Detected by a) luminol b) isoluminol and c) lucigenin. Results show mean of 4 experiments performed in triplicate minus blanks (no cells) \pm SD. * $P \leq 0.05$ ** $P \leq 0.01$ by two-tailed paired T-test.

Data presented in Figure 52 demonstrates that MNase detected NET release was significantly decreased by the addition of sodium azide under all stimulatory conditions analysed ($P \leq 0.05$).

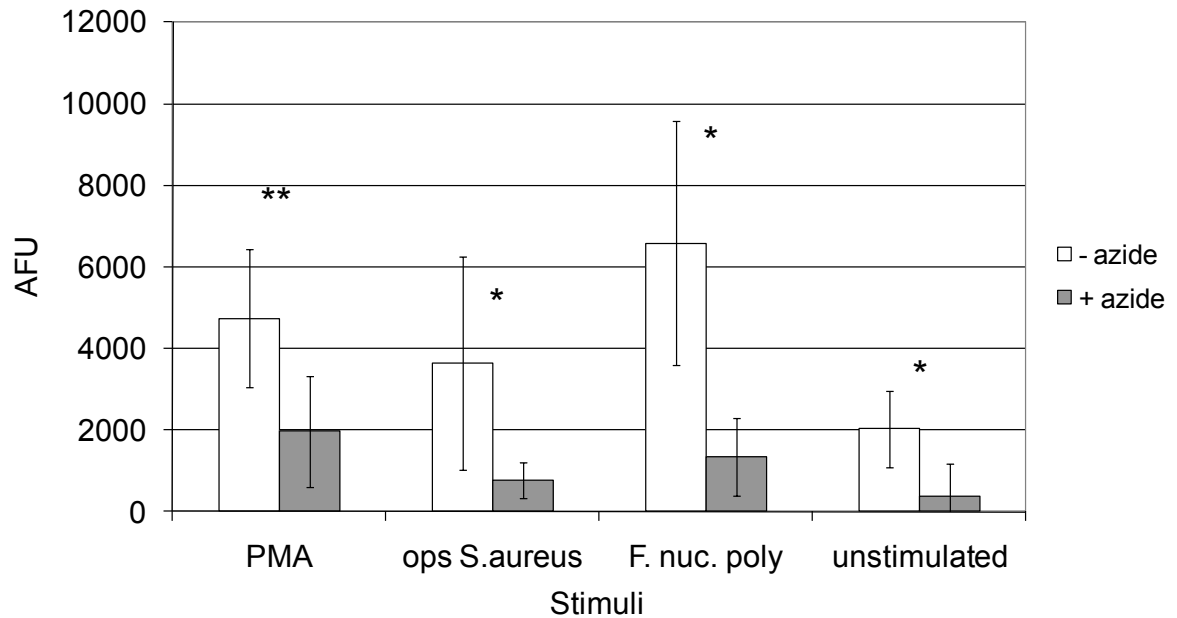


Figure 52. Effect of sodium azide (2mM) on NET production by MNase assay. Results show mean of 4 experiments performed in triplicate minus blanks (no cells) \pm SD. * $P \leq 0.05$ ** $P \leq 0.01$ by two-tailed paired T-test.

Discussion

NADPH oxidase inhibitor, DPI

Whilst DPI is a known inhibitor of NADPH oxidase, descriptions of its precise activity and mechanism of action are limited. It has been reported to have no effect on phagocytosis although degranulation of both azurophilic and specific granules in response to opsonised latex beads was inhibited (Ellis *et al.* 1988) indicating either more widespread non-specific effects of the inhibitor, or knock-on effects resulting from the inhibition of NADPH oxidase ROS production. It is suggested that DPI removes an electron as it is transferred between the redox centres of the oxidase enzyme to form a phenyl radical which covalently binds a 45kDa protein thought to be the reduced flavin, thereby inhibiting the enzyme (O'Donnell *et al.* 1993). The action DPI has on the activated enzyme may depend on the stimuli used to activate the enzyme because PMA induced superoxide production has been shown to be more sensitive to DPI inhibition than fMLP stimulated superoxide production (Ellis *et al.* 1988). DPI was first used in the study of NET release by Fuchs *et al.* (2007) and contributed to the conclusion that NET release was dependant on NADPH oxidase ROS generation. However, the relationship between NET release and ROS generation is subject to mixed reports. For example, the neutrophils of human neonates are reported to have the capacity for ROS generation but not for NET release (Yost *et al.* 2009) although more recently debate has arisen as to whether neonatal neutrophils are capable of severely delayed NET release (Marcos *et al.* 2009). In addition, milk proteins are reported to inhibit ROS generation but not NET release (Lippolis *et al.* 2004). In the chemiluminescent assay of ROS employed here, DPI was applied at a range of concentrations and significantly reduced the level of ROS

detected even at DPI concentrations as low as 0.6 μ M (Figure 39). However, ROS levels were reduced further up to the highest concentration of 25 μ M. As it is unknown as to whether the relationship between ROS generation and NET release is quantitative, or whether a small level of ROS generation is sufficient to trigger NET release under the correct stimulation conditions, it was decided to use the highest concentration of DPI (25 μ M) for subsequent experiments. In the presence of DPI, real time analysis of stimulated neutrophils over a 3 hour incubation period demonstrated a clear reduction in DNA fluorescence compared with values obtained in the absence of DPI (Figure 42a). This result may be attributable to DPI inhibition of NET release or simply due to the fact that DPI inhibited the generation of cytotoxic ROS resulting in increased cell survival. Subsequently a live-dead cytotoxicity assay was utilised (Promega), based on the fluorescent detection of proteases rather than DNA, allowing the detection of apoptosis independently of NETosis. The substrates are peptides which upon cleavage by cellular proteases emit fluorescence which is indicative of either live or dead cells. Data from the live cell stain indicated slightly fewer live cells in the presence of DPI, which was in contrast to the data generated simultaneously by the dead cell stain. The dead cell indicator is cell-impermeable and is only cleaved by proteases released from cells which have lost membrane integrity. As over 24 neutrophil proteins have been identified as components of NETs to date (Urban *et al.* 2009) and originate from the neutrophils nucleus, granules, cytoplasm and cytoskeleton, it is conceivable that proteases utilised in the cytotoxicity assay are released as part of NETs. However, the distinction between live cell fluorescence in the presence compared to the absence of DPI was only small and the experiment was only performed as a single preliminary experiment. The dead cell fluorescence showed a more marked difference over the 3 hour incubation period and when this data was examined, no cytotoxic effect of DPI was observed, in concordance with

previous publications (Ellis *et al.* 1988). Indeed, dead cell fluorescence data indicated increased survival of both unstimulated and PMA stimulated cells in the presence of DPI (Figure 41) which may be due to the reduced level of NADPH oxidase production of cytotoxic ROS, in addition to reduced NETosis. The MNase assay also allowed improved distinction between cells that had undergone NETosis from those that had undergone apoptosis. This data appeared to indicate that DPI did indeed reduce the level of NET release in stimulated cells. However, in unstimulated cells DPI consistently appeared to induce a small increase in NET release (Figures 40 and 42). The difference in unstimulated NET release was insignificant when the average of 16 independent assays of 16 different individuals were examined, this result was likely due to interpersonal and experimental day-to-day variation (Figure 40). However, when a single experiment was performed in triplicate, a statistically significant increase in unstimulated NET release was observed in the presence of DPI ($P=0.02$; Figure 42) and this finding was representative of observations throughout these studies. This implies that DPI stimulates a low level of NET release in unstimulated cells. In addition DPI may also cause a low level of NET release in stimulated cells which is insignificant in comparison to levels generated by the intended stimulus, and therefore the level of NADPH oxidase dependant NET release may be underestimated in studies employing DPI.

Phagocytosis inhibitor, cytochalasin b

Cytochalasin b is a cell permeable fungal metabolite that inhibits the polymerisation of actin and therefore inhibits phagocytosis. It has been utilised in a published method describing the inhibition of phagocytic killing so that NET-mediated killing could be measured independently (Beiter *et al.* 2006; Buchanan *et al.* 2006; Grinberg *et al.* 2008; Carlin *et al.*

2009; Katzenback *et al.* 2009). The actin cytoskeleton has been shown not to form part of the extruded NET (Palic *et al.* 2007). However this same study also utilised cytochalasin B and described a significant increase in PMA induced NET release in the presence of cytochalasin B. In contrast, NET release here was found to be dramatically reduced in the presence of cytochalasin B (Figure 44), and since completing this work, cytochalasin inhibition of the final stage of NET extrusion into the extracellular space has been described (Neeli *et al.* 2009) indicating that the actin cytoskeleton is necessary for NET release. This is unsurprising as all cell types so far listed as possessing extracellular trap capacity are also capable of phagocytosis and therefore possess an extensive cytoskeleton. The data presented here also indicates that cytochalasin B dramatically reduces neutrophil ROS generation (Figure 43) which is likely to indicate that phagolysosome formation was prevented and as such ROS generation not initiated on the phagolysosome membrane. Evidence in support of this theory is that the bacterially stimulated ROS response was reduced to a greater extent than the non-bacterial PMA stimulation. Taken together the data suggests there may be a two-fold inhibition of NET release by cytochalasin B, resulting from reduced initiation of post-phagocytic ROS generation within the phagosome and also the reported lack of actin cytoskeleton-mediated NET extrusion.

Superoxide dismutase

Superoxide dismutase is an enzyme endogenous to neutrophils responsible for converting superoxide to hydrogen peroxide. As the release of NETs is reported to be dependant on hydrogen peroxide (Fuchs *et al.* 2007) it was hypothesised that the addition of exogenous SOD and therefore, the increased generation of hydrogen peroxide would increase NET release. Whilst SOD is reported to be a hydrophobic glycoprotein (Marklund 1984), the

majority of publications describing the addition of exogenous SOD are concerned with only extracellular effects. SOD has been shown to have an affinity for the cell membrane although its migration through into the intracellular space is relatively slow (Emerit *et al.* 1996). This observation was supported here by the isoluminol detection of ROS (Figure 46). This represents extracellular ROS and was the only measure of ROS generation which was statistically significantly reduced under all 4 stimulatory conditions upon the addition of SOD.

Antioxidant and anti-inflammatory micronutrient, curcumin

Curcumin is a highly lipid soluble phenolic compound responsible for the yellow pigmentation of turmeric. Whilst it has wide ranging effects it is well known for its anti-inflammatory properties and the actions of interest here are those as a radical scavenger. Curcumin is a potent hydrogen peroxide and superoxide radical scavenger, to a similar if not superior level to established antioxidants such as α -tocopherol and Trolox (Ak *et al.* 2008). However, it was also found to act as a chelator of ferrous ions (Fe^{2+}) which may result in indirect antioxidant effects on radical production. In the studies described here, curcumin was found to reduce detected ROS in response to all stimuli, however this was most significant for luminol-dependant ROS which represented total radical production (Figure 49). Isoluminol and lucigenin-dependant ROS were only significantly reduced after *F. nucleatum* stimulation, with these data representing extracellular and superoxide radical production respectively. These results indicate that the antioxidant activity of curcumin likely occurs intracellularly, and later in the radical generation pathway than superoxide formation. NET release also appeared decreased upon the addition of curcumin following activation with all stimuli and basal levels in unstimulated cells were also decreased (Figure 50). Levels of reduction

however, were only significant upon PMA stimulation. This was unexpected as PMA-induced radical production only incurred a significant reduction with luminol detection. *F. nucleatum* stimulated radical production was significantly reduced when measured by all three chemiluminescent substrates, however, the detected NET release was not significantly reduced. It is understood that curcumin, as a highly lipophilic antioxidant, works best in conjunction with a water soluble antioxidant such as ascorbic acid (Jovanovic *et al.* 2001). Curcumin is able to insert into the cell membrane to intercept lipid radicals and form a phenoxyl radical which is then more able to move to the surface for repair by the water soluble antioxidant. Therefore further studies should be undertaken which utilise a combination of antioxidants for their efficacy in reducing the NET response.

Sodium azide

Azide molecules easily cross the cell membrane and therefore exert intracellular effects on endogenous enzymes such MPO. The enzyme specificity of this inhibitor is subject to mixed reports with reportedly sensitive enzymes being catalase (Lieber *et al.* 1970), SOD (Rigo *et al.* 1975) and MPO (Lundqvist *et al.* 1996a) and azide in-sensitive enzymes including glutathione peroxidase (Lundqvist *et al.* 1996b) and HRP (Dahlgren *et al.* 1987). Data from the chemiluminescent assay of ROS (Figure 51) demonstrated a significant decrease in only luminol (total) detected ROS. In contrast, lucigenin detected ROS did not significantly change in the presence of sodium azide. As this reagent is thought to primarily detect the superoxide radical (Williams *et al.* 1981), this suggests that the point of inhibition by sodium azide occurs following superoxide anion production in the radical generation pathway (Figure 8). In addition, no difference in isoluminol detected ROS was observed in the presence of sodium azide. As isoluminol is cell impermeable and therefore solely detects extracellular

ROS, this suggests that the point of inhibition at which sodium azide works is on an intracellular enzyme. Moreover, this data also indicates that the inhibition does not directly involve hydrogen peroxide as this radical is able to cross the cell membrane and as such alterations in its level are likely to be detected both intra- and extracellularly. Although either endogenous catalase or MPO could be inhibited, it is hypothesised here that MPO is the target of sodium azide. MPO is also the most relevant enzyme in terms of the antimicrobial response as it generates bactericidal hypochlorous acid, unlike catalase which generates water, and as such MPO is likely to take a primary role under stimulatory conditions. Sodium azide resulted in a significant reduction in detected NET release under all stimulatory conditions (Figure 52), and combined this data now implicates hypochlorous acid as a key molecule in the initiation of NET release. Previous research into the signalling pathway of NET release was unable to distinguish key molecules beyond hydrogen peroxide generation (Fuchs *et al.* 2007). Addition of exogenous catalase was found to decrease NET release which may be due to the removal of hydrogen peroxide as a substrate for MPO generation of hypochlorous acid. Inhibition of endogenous catalases induced increased NET release which again may have been due to the increased availability of hydrogen peroxide for MPO conversion, and further supports the hypothesis that sodium azide is inhibiting MPO rather than catalase as opposite effects were seen on NET release. Future work should therefore utilise taurine or 5-aminosalicylic acid (Dallegrì *et al.* 1990) as hypochlorous acid scavengers to assess whether this product of MPO is important for NET release. Interestingly, although CGD patients lacking in ROS generation suffer recurrent and life threatening infections, patients with complete MPO deficiency do not suffer from any increase in infection rate (Lanza 1998) indicating that if MPO is a key enzyme in NET release, this process is a last resort in antimicrobial defence after oxygen radical attack which appears to be essential.

CHAPTER 5 RESULTS

HL60 cells as a model system for NET release

Obtaining primary neutrophils for analysis of NET release from whole blood is time consuming and requires invasive procedures. In addition it has been shown here (Figure 66), and previously reported (Fuchs *et al.* 2007) that there is significant inter-individual and temporal variation in NET production levels. Therefore, use of a standardised human cell line as a model for primary neutrophils and NET release would be advantageous for future study. The well documented human promyelocytic HL60 cell line which can be differentiated into cells with a neutrophil-like phenotype using dimethyl sulphoxide (DMSO) may provide a suitable model system. Currently HL60 cells have been used by several groups to examine ROS release (Dahlgren 1989; Teufelhofer *et al.* 2003) however, one of only two papers reporting their use in the study of NET release described that >8% of differentiated cells extruded NETs upon stimulation with the calcium ionophore A23187 (Wang *et al.* 2009). Notably, within the literature there is also a large amount of variation in the reported differentiation conditions which can be used and the resultant characteristics of differentiated cells. Therefore, initially differentiation conditions were analysed and subsequently the differentiated cells were characterised prior to assay of NET production.

5.1 Differentiation of HL60 cells by DMSO

HL60 cells can be differentiated into a monocytic cell using vitamin D (Miyaura *et al.* 1981), a macrophage-like cell using PMA (Rovera *et al.* 1979) or a granulocytic cell using DMSO or retinoic acid (Gallagher *et al.* 1979; Breitman *et al.* 1980). Based on previous work from our group (Dias *et al.* 2008), DMSO was used for differentiation in this study. Initially the concentration required to achieve optimal differentiation after 3 days incubation was determined. Chemiluminescent detection of ROS production in response to PMA was used as

a surrogate marker of neutrophil phenotype and an indicator of functional differentiation (Figure 53).

As the applied concentration of DMSO increased, ROS production following PMA (50nM) stimulation increased in a dose-dependant manner, with the highest production of ROS observed in cells differentiated with 1.5% DMSO (Figure 53). Notably, the average peak luminol-detected ROS produced by 1.5% DMSO-differentiated cells was 1082 RLU which was significantly lower than ROS levels produced by the equivalent number of viable primary neutrophils (average peak PMA-induced luminol-detected ROS in excess of 30,000 RLU; see Figures 49 and 51). Notably there was also a high level of variation between cells of sequential passages differentiated in independent experiments (represented by the standard deviation; Figure 53). In addition, the number of viable cells obtained from cultures decreased as the concentration of DMSO increased resulting in insufficient cells for assay from 1.5% DMSO cultures. Therefore a concentration of 1.25% DMSO exposure for 3 days was used in all subsequent experiments to generate differentiated HL60 (dHL60) cells, in order to ensure effective differentiation without compromising cell survival.

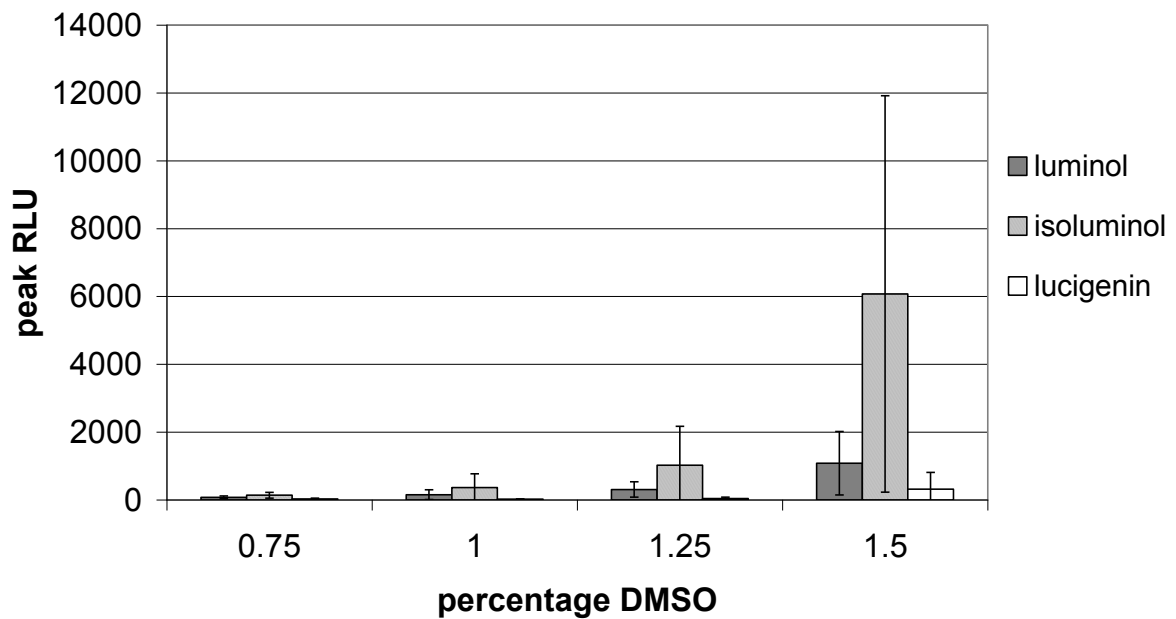


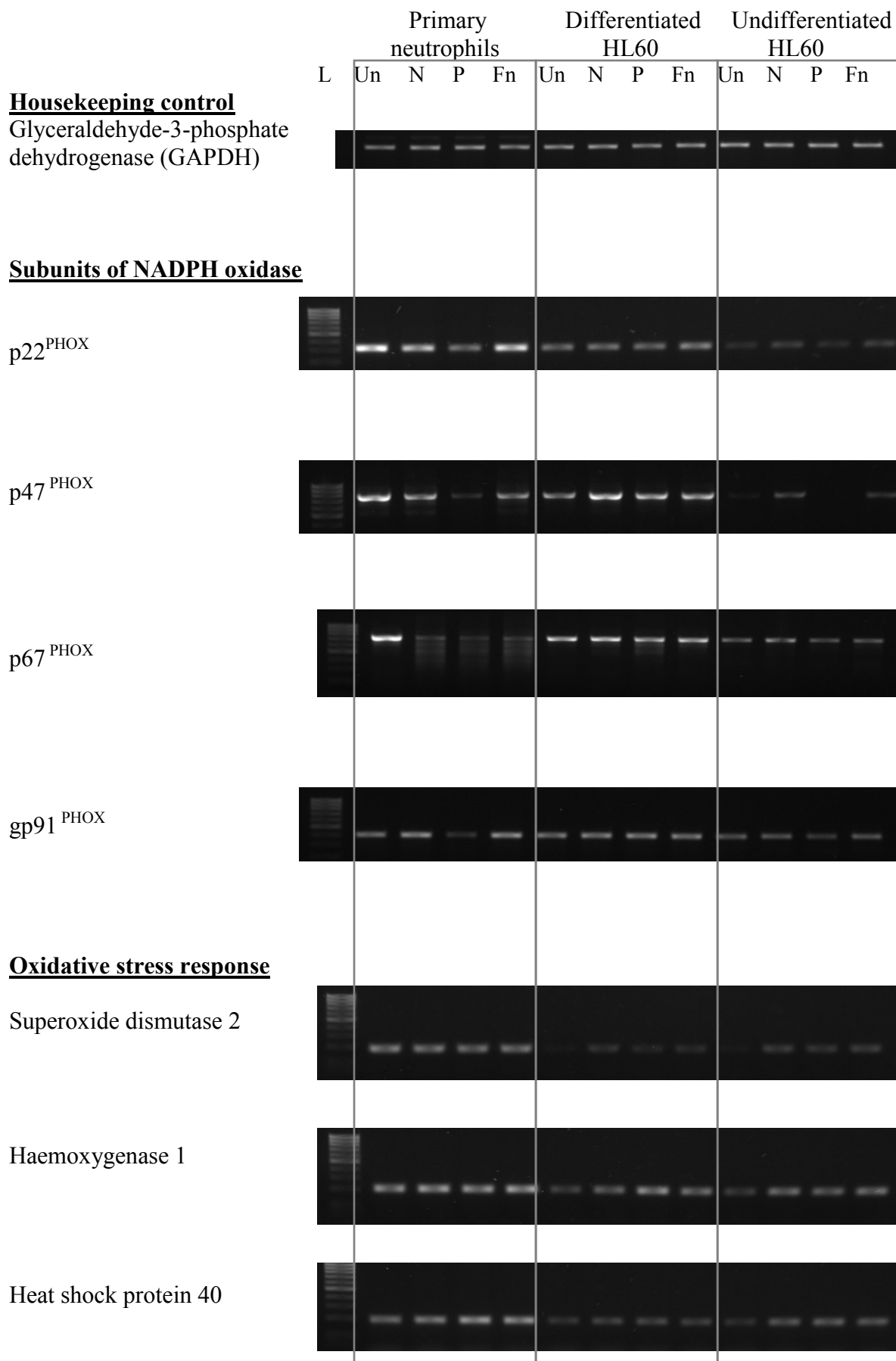
Figure 53. Peak ROS production detected by luminol, isoluminol and lucigenin from PMA (50nM) stimulated 3-day HL60 cells differentiated using 0.75%-1.5% DMSO concentrations. Results show mean of 3 independent experiments on cells from sequential passages \pm SD.

5.2 PCR characterisation of dHL60 cells

The functionality of cells is dependant upon the proteins expressed, which in turn depends on the transcriptional profile of the cell. Therefore selected transcripts were analysed by RT-PCR in dHL60 cells and compared to that of undifferentiated cells and primary neutrophils (Figure 54) with and without stimulation. The genes selected for analysis included those associated with the NADPH oxidase enzyme pathway, which is necessary for ROS production, genes responsive to oxidative stress, and enzymes involved in ROS metabolism. Transcript levels for several receptors and intracellular molecules involved in cytokine and bacterial component signalling were also assessed. The mRNA expression for these genes may indicate the ability of these cells to respond to appropriate stimulants of ROS and/or NET production.

Figure 54 provides data showing the PCR products of 13 transcripts and their responsiveness to changes in gene expression upon 3 hours bacterial (killed *F. nucleatum*) or PMA stimulation. Quantification of band intensity relative to normalised GAPDH levels is also shown (Figure 55). The expression levels of the 4 genes encoding subunits of the NADPH oxidase enzyme (p22^{PHOX}, p47^{PHOX}, p67^{PHOX} and gp91^{PHOX}) whose translated products are responsible for ROS generation, appeared up-regulated in dHL60 cells compared to undifferentiated cells, although levels remained relatively lower than those detected in primary neutrophils. After 3 hours incubation, dHL60 cells appeared to be less transcriptionally responsive to stimuli compared with primary neutrophils, as expression of the NADPH oxidase subunits were less dramatically affected by 3 hours incubation compared with the unstimulated cells. The exception was the p47^{PHOX} transcript which whilst its expression appeared altered, levels increased rather than decreased as seen in primary neutrophils. In general, PMA appeared to be the most effective stimuli with regard to down-regulating gene expression of NADPH oxidase subunits in primary neutrophils. However, in dHL60 cells there was either no observable change (e.g. p22^{PHOX} and p67^{PHOX}) or a relatively small increase in expression (e.g. p47^{PHOX} and gp91^{PHOX}) for these transcripts. Of the genes involved in oxidative stress responses, superoxide dismutase 2 (SOD2) was detected at relatively low levels in HL60 cells compared to primary neutrophils. After 3 hours incubation, SOD2 levels decreased in primary neutrophils, however, in dHL60 cells expression increased but did not reach levels detected in primary neutrophils. Heat shock protein 40 demonstrated relatively low expression levels in dHL60 cells compared to primary neutrophils and responded with a modest increase upon stimulation similar to primary neutrophils. The transcription factor NFκB2 showed reduced expression in dHL60 cells compared to primary neutrophils under all conditions tested except following PMA

stimulation in which a moderate increase in expression in dHL60 cells was detected. Conversely a notable decrease in NF κ B2 expression was observed in primary neutrophils. Of the cytokines analysed, CXCL3 was expressed at a relatively lower level in differentiated as compared to undifferentiated HL60 cells, however, the increases in expression upon stimulation were similar to that observed for primary neutrophils, although this was notably less dramatic. Colony stimulating factor 2 was also expressed at a higher level without DMSO induced differentiation in HL60 cells. Analysis of toll-like receptor (TLR) transcript levels revealed their expression levels to be relatively low in undifferentiated HL60 cells compared to primary neutrophils and expression appeared unaffected following DMSO differentiation. No consistent profile of stimulated TLR expression was observed in undifferentiated or differentiated HL60 cells as well as primary neutrophils.



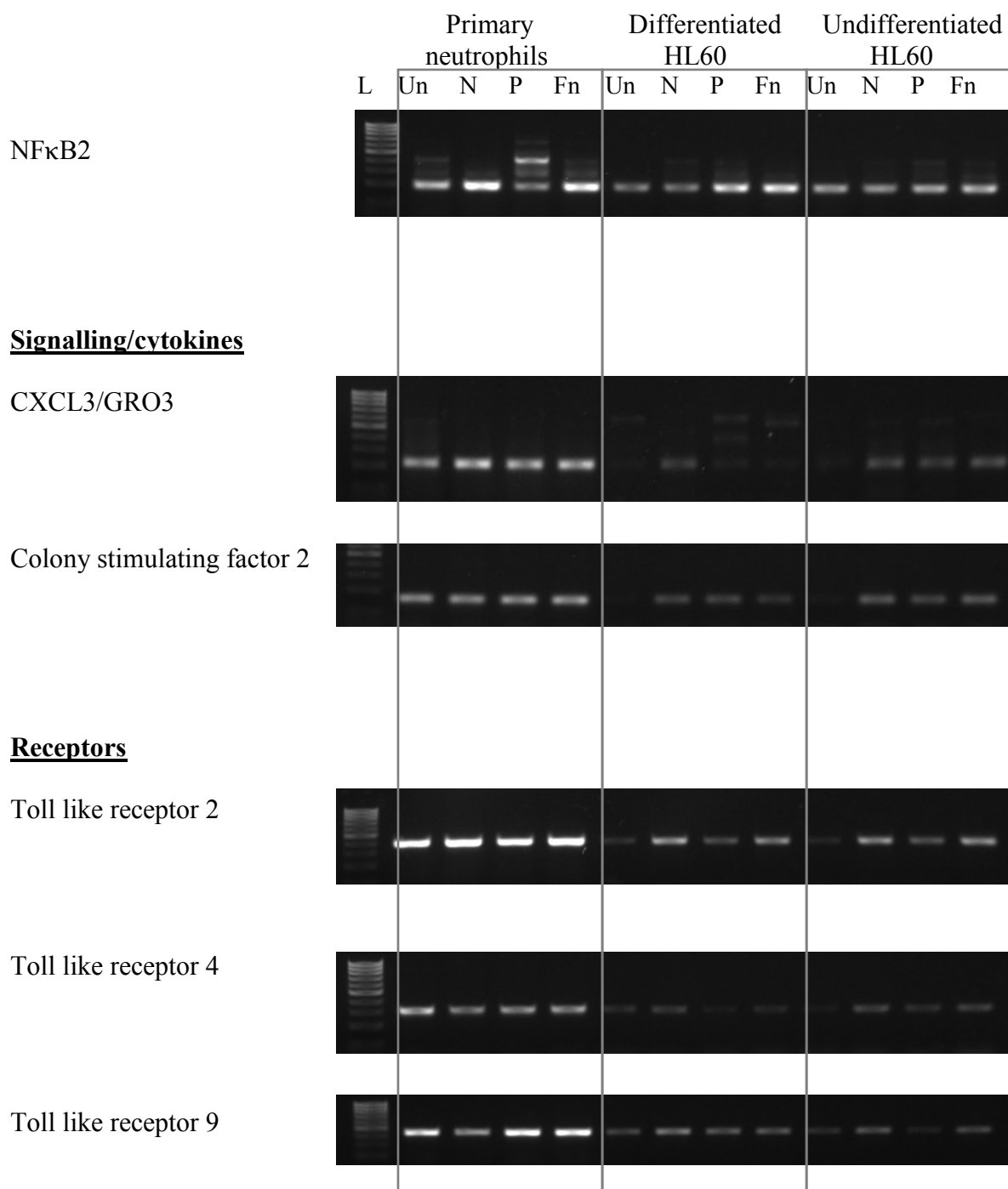
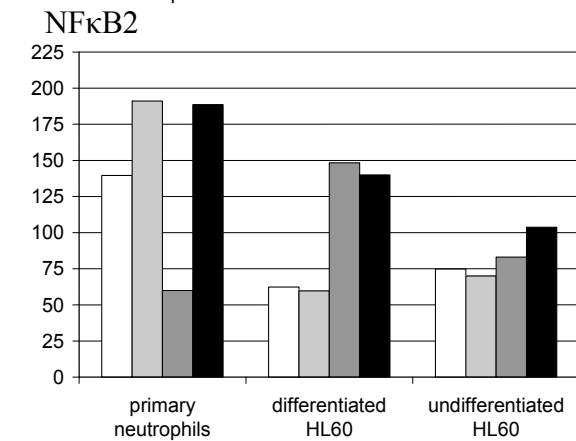
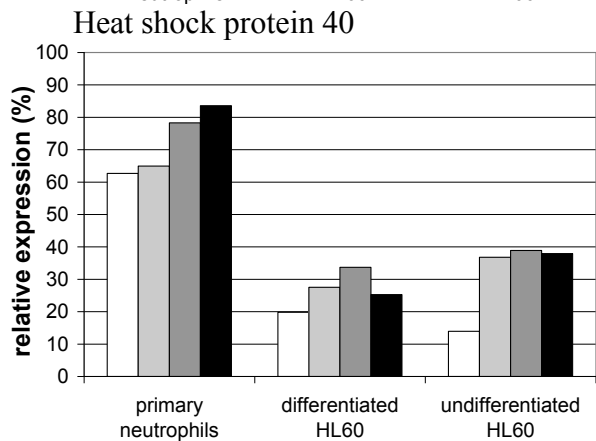
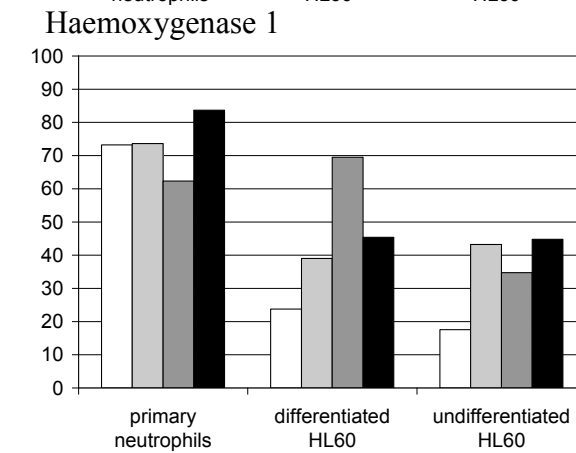
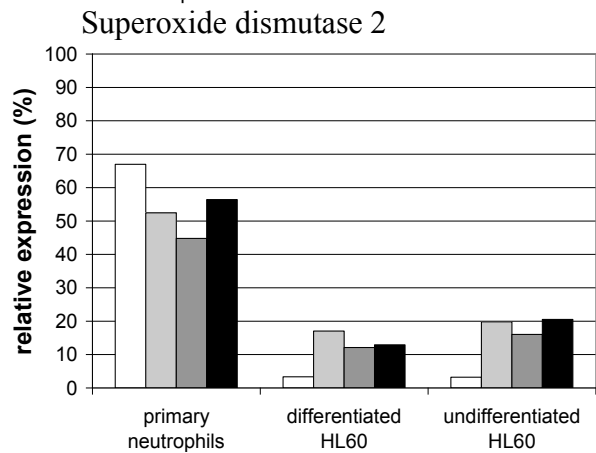
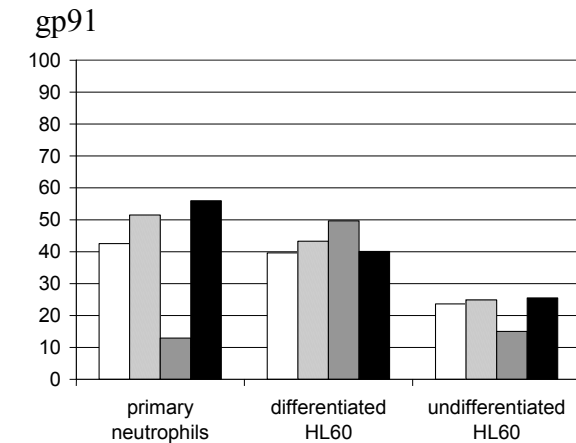
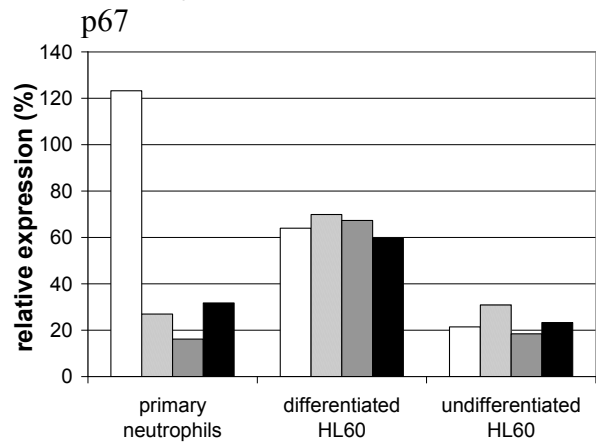
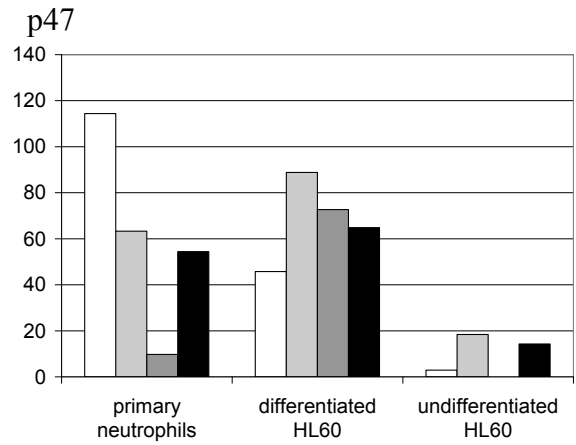
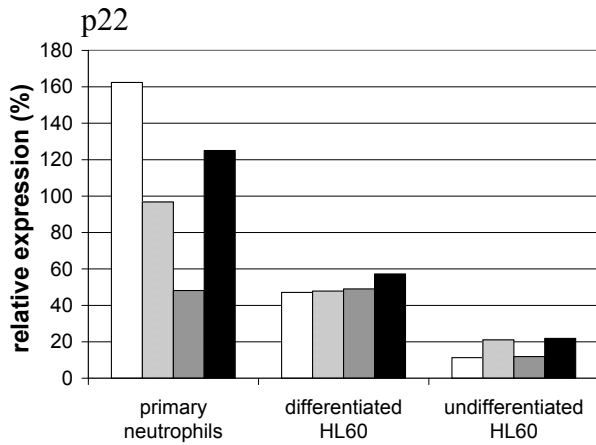


Figure 54. RT-PCR analysis of relative transcript levels in unstimulated and stimulated undifferentiated and DMSO differentiated HL60 cells compared to primary neutrophils. Key : L - ladder, Un – untreated time 0, N – no stimulation, P – PMA stimulation, Fn – *F. nucleatum* stimulation. Cells were incubated with or without stimulants for 3 hours prior to RNA isolation. The housekeeping gene GAPDH was used as a PCR normalisation control.



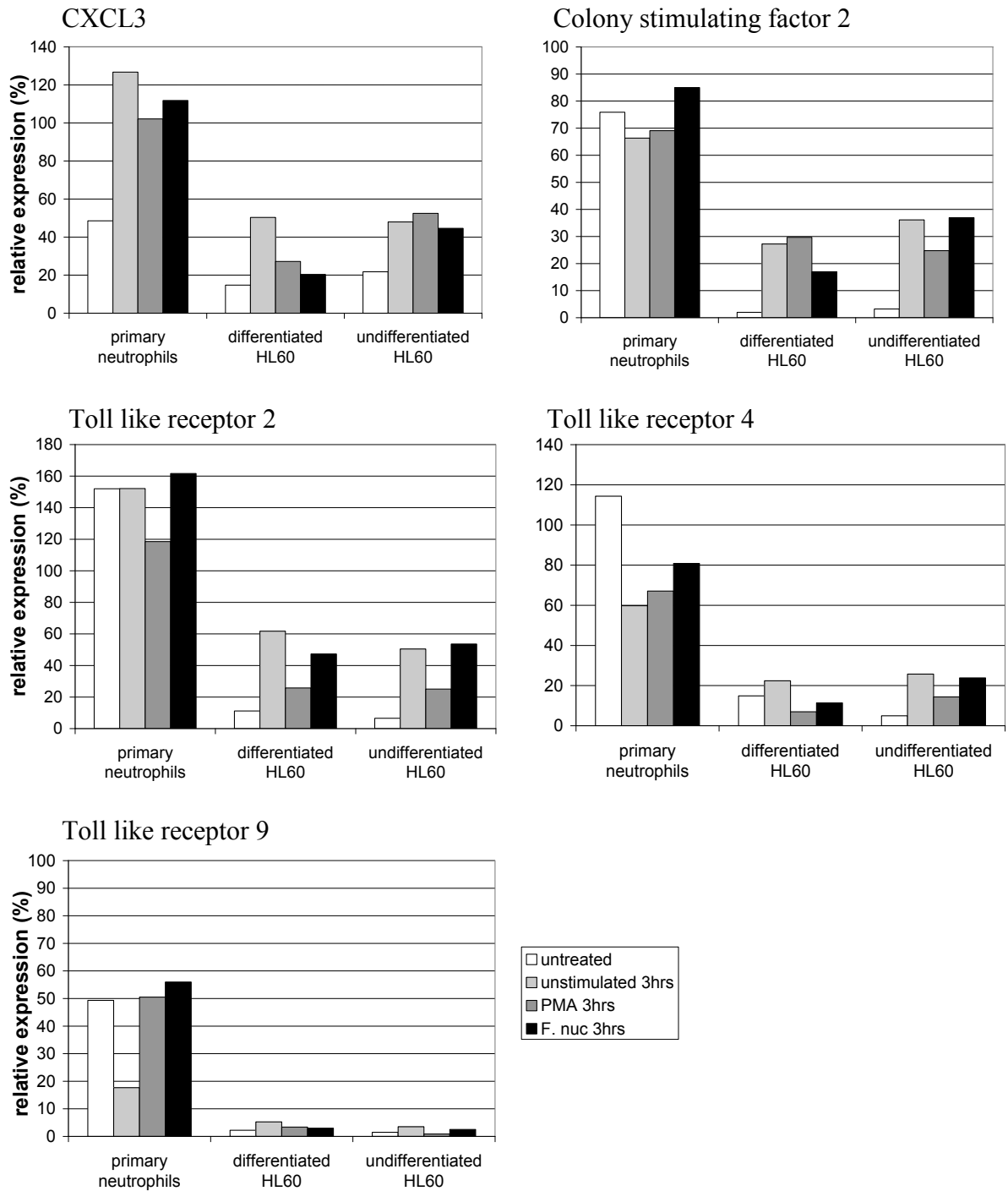


Figure 55. Densitometric profiles of RT-PCR transcript levels in unstimulated and stimulated undifferentiated and DMSO differentiated HL60 cells compared with primary neutrophils. Band intensity of gene products expressed as a percentage of GAPDH band intensity. White bars - untreated time 0, striped bars – no stimulation, grey bars - PMA stimulation, black bars - *F. nucleatum polymorphum* stimulation. Cells were incubated with or without stimulants for 3 hours prior to RNA isolation.

5.3 Cytological analysis of dHL60 cells

The functional assay (Figure 53) or gene expression analysis (Figures 54 and 55) does not distinguish the proportion of HL60 cells that may have differentiated. Therefore cell morphology was assessed by haematoxylin and eosin staining (Figure 56) as well as granule protein staining (Figure 57).

Both undifferentiated and differentiated HL60 cells stained more intensely than primary neutrophils following H+E staining (Figure 56). No differences were observed between undifferentiated and differentiated HL60 cells in terms of staining although differentiated cells did appear to display some spreading and cell adhesion whilst undifferentiated cells appeared rounded. Whilst primary neutrophils have a distinctive multi-lobulated nucleus this was not evident in dHL60 cell cultures. The overall morphology of neutrophils also appeared more irregular, in contrast to HL60 cells which exhibited a more regular and rounded morphology.

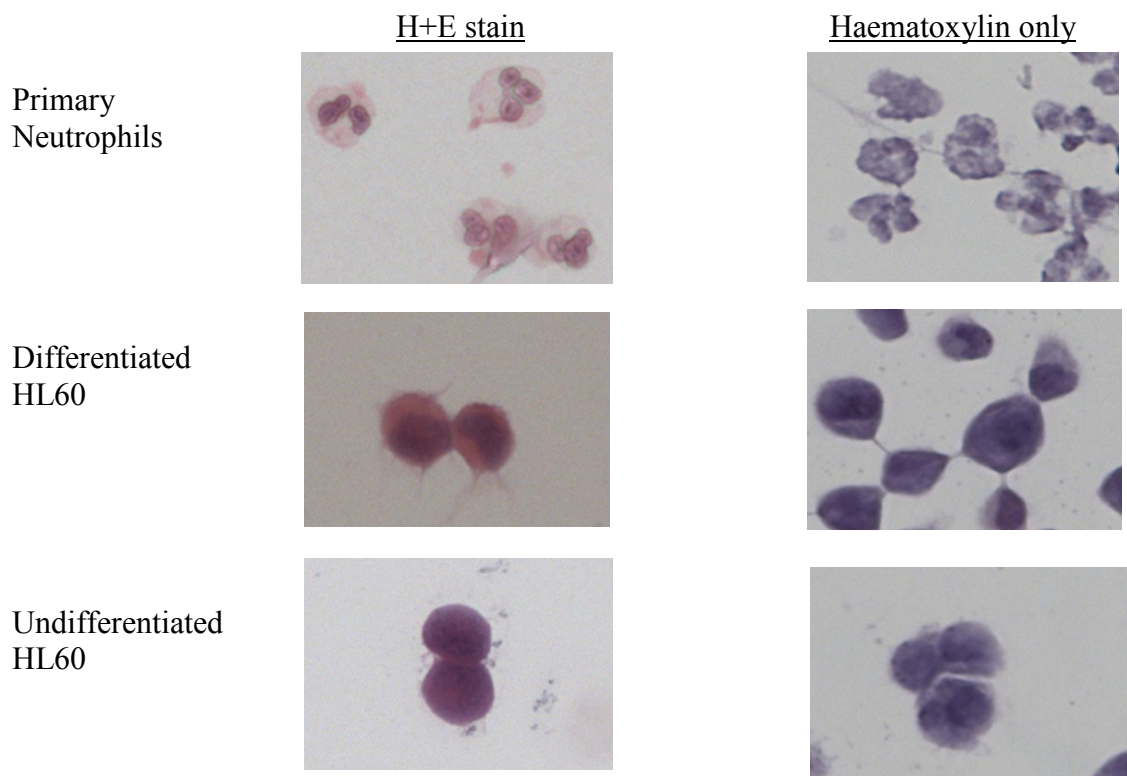


Figure 56. Haematoxylin (nucleic acid) and eosin (cytoplasmic) staining of undifferentiated and differentiated HL60 cells compared to primary neutrophils.

Whilst immunocytochemical staining indicated the presence of the neutrophil granule components neutrophil elastase and myeloperoxidase in HL60 cells (Figure 57), there appeared to be no difference in staining intensity or distribution between differentiated and undifferentiated HL60 cells. Immunostaining of primary neutrophils demonstrated the presence of neutrophil elastase and myeloperoxidase in spontaneously extruded NETs (Figure 57).

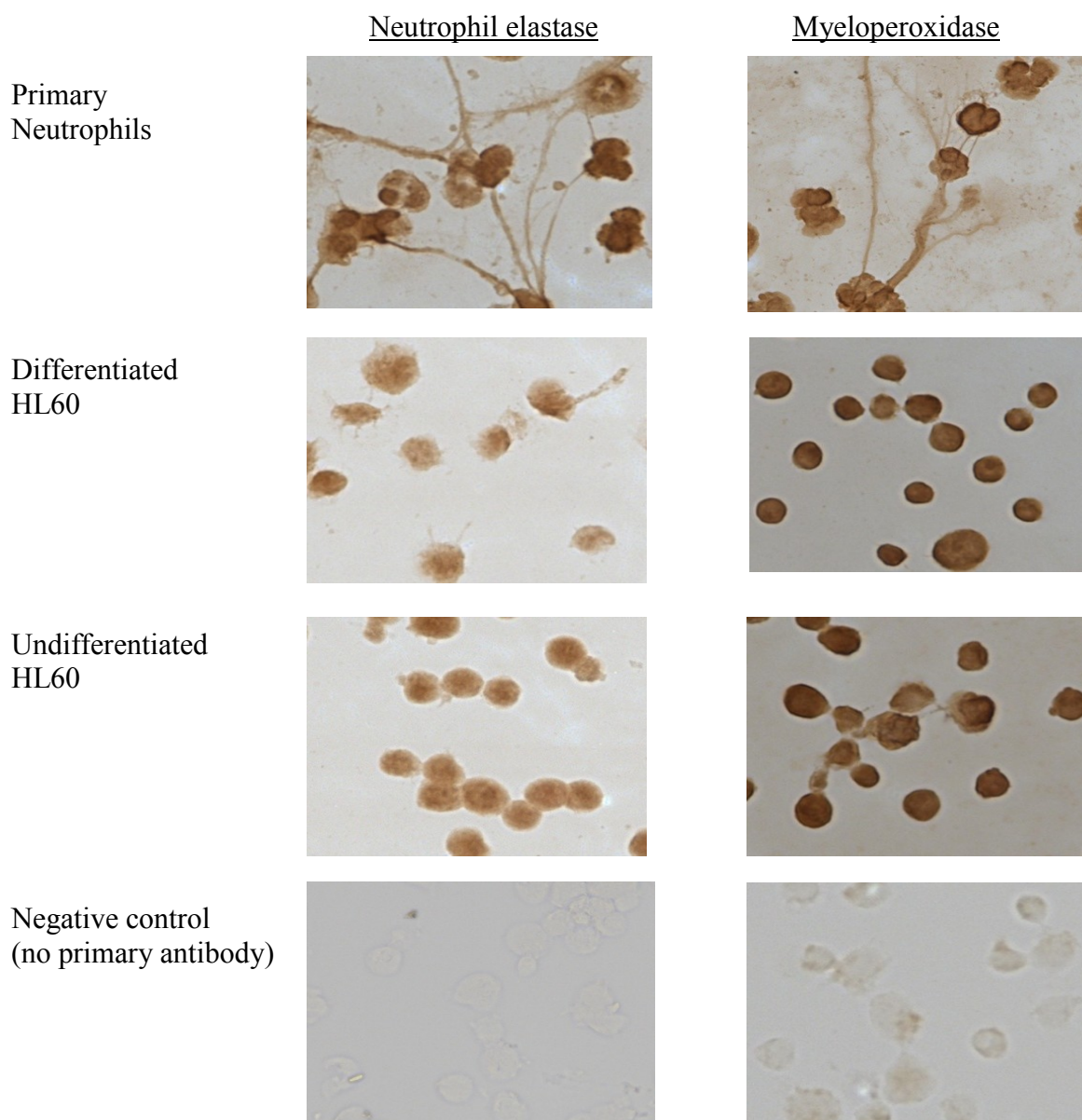


Figure 57. Immunocytochemical staining of undifferentiated and differentiated HL60 cells using primary antibodies against the neutrophil granule components - neutrophil elastase and myeloperoxidase. Negative controls (no primary antibody) show endogenous peroxidase activity. Primary neutrophils stained for comparison.

5.4 NET production in dHL60 cells

Following characterisation of differentiation for HL60 cells (1.25% DMSO for 3 days) their ability to produce NETs was assessed. The three techniques previously reported were applied

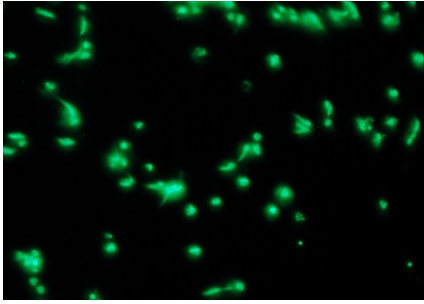
including direct visualisation by SYTOX[®] staining on slides (2.1.3), fluorometric real-time SYTOX[®] analysis (2.1.4), and MNase purification and fluorometric quantification of extracellular DNA (2.1.5). For NET induction several stimuli were used including PMA which is an effective stimulus of the respiratory burst in dHL60 cells (Newburger *et al.* 1979; Dahlgren 1989; Levy *et al.* 1990), fMLP which mimics bacterially-derived peptides and acts via the fMLP receptor (Snyderman *et al.* 1981), and the heat-killed gram negative periodontal bacteria *F. nucleatum polymorphum*, which likely acts via TLR2/4 binding of bacterial LPS (Remer *et al.* 2003). The calcium ionophore A23187 was also applied as this increases cytoplasmic free calcium and has been used to prime the respiratory burst in HL60 cells (Dahlgren 1989), as well as being reported to stimulate NET release from HL60 cells (Wang *et al.* 2009).

5.4.1 Visualisation of NETs in dHL60 cells

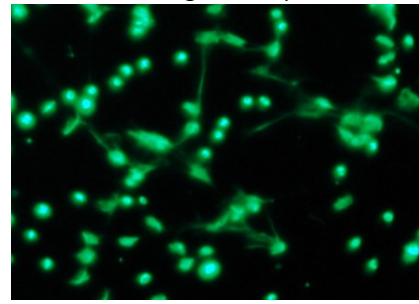
Initially dHL60 cells were seeded onto poly-L-lysine coated slides and incubated for 3 hours with NET stimuli and visualised using SYTOX[®] staining of the DNA (Figure 58).

Visualisation of dHL60 cells stimulated for NET production indicated relatively low level release (Figure 58). No extracellular NET-DNA release was evident following *F. nucleatum polymorphum* or fMLP stimulation. PMA exposure resulted in a minimal increase in the presence of extracellular DNA however, dHL60 cell stimulation using the calcium ionophore resulted in more apparent NET formation, though levels appeared minimal compared to NET levels released from primary neutrophils.

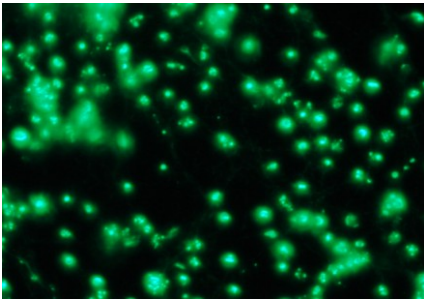
PMA 50nM



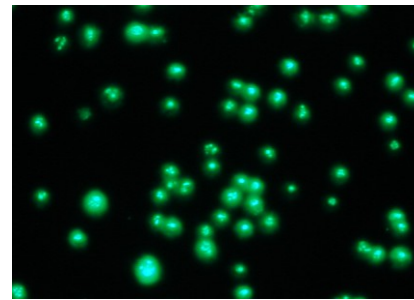
Calcium ionophore 4μM



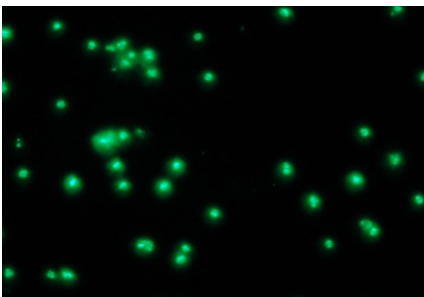
F. nucleatum MOI 150



fMLP 1000nM



Unstimulated



Positive control (primary neutrophils)

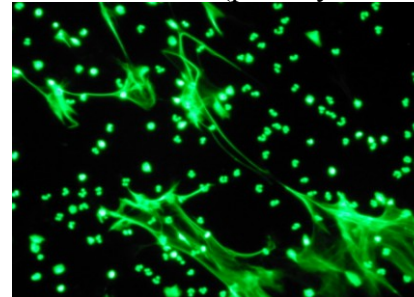


Figure 58. SYTOX[®] stained DNA in dHL60 cells. Representative images for dHL60 cells stimulated with PMA (50nM), calcium ionophore – A23187 (4μM), *F.nucleatum polymorphum* (MOI 1:150), fMLP (1000nM) or unstimulated control. Positive control shows primary neutrophils stimulated with PMA (50nM). Results are representative of 3 independent experiments.

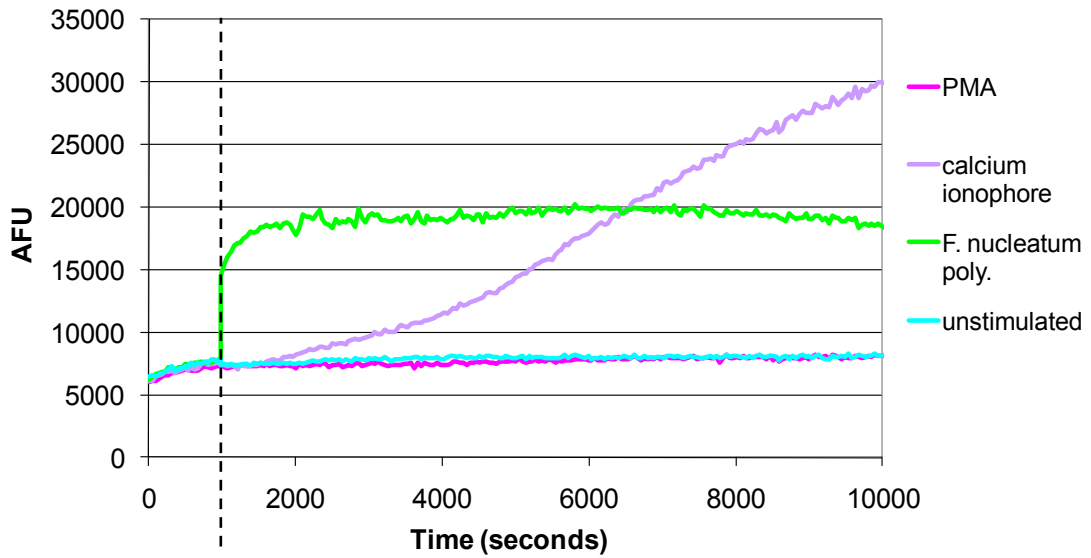
5.4.2 Fluorometric quantification of NET release from dHL60 cells

To quantify NET release, the fluorescence of dHL60 cells during the 3 hours stimulatory period was recorded (Figure 59). As has previously been described (Fuchs *et al.* 2007 and Section 4.1), the NADPH oxidase inhibitor, DPI, was included as a control within the analysis

to determine if increases in fluorescence after stimulation were ROS-dependant and therefore likely to be due to NET release.

With the addition of stimuli at 20 minutes (Figure 59a) PMA and *F. nucleatum* resulted in no detectable increase in fluorescence over the incubation time, however inclusion of the calcium ionophore A23187 stimulated DNA release and a marked increase in fluorescence with onset at 625 seconds (10 minutes) post-exposure. With the addition of the NADPH oxidase inhibitor, DPI (Figure 59b) the calcium ionophore induced fluorescence increased following the same pattern as that previously observed in the absence of DPI for the first 4065 seconds (67 minutes) after stimulation prior to reaching a plateau. DPI exposure resulted in only a marginal increase in the fluorescence of PMA and unstimulated cells beginning 1.5 hours post-stimulation.

a) Stimulated dHL60 cells



b) Stimuli dHL60 cells plus DPI exposure

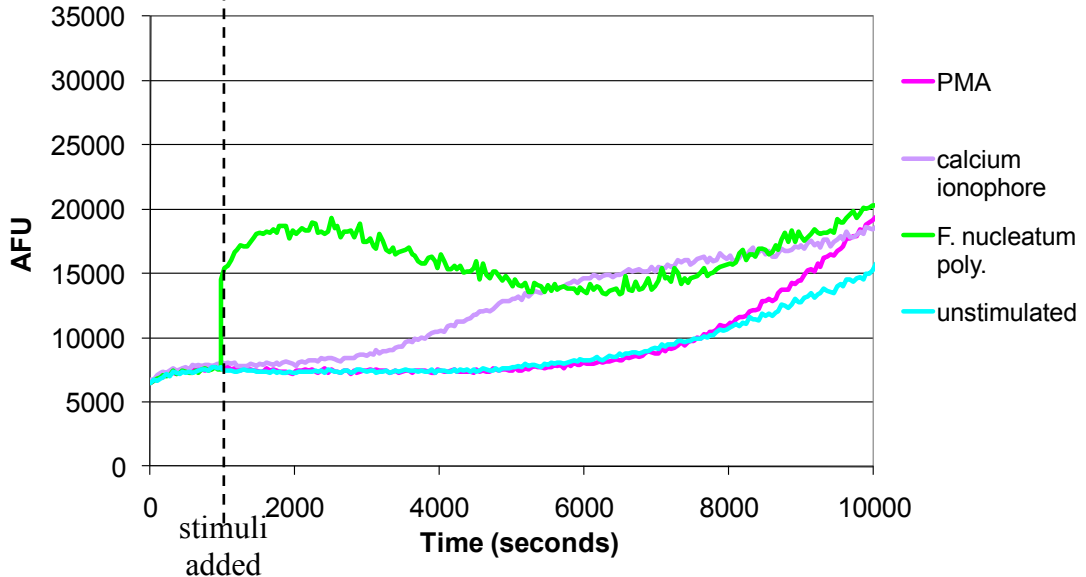


Figure 59. Real time fluorescence of differentiated HL60 cells a) without and b) with DPI (25 μ M). Cells stimulated after 20 minutes using PMA 50 μ M, calcium ionophore 4 μ M, *F. nucleatum polymorphum* MOI 1:150 or unstimulated. Results show mean of experiment performed in triplicate.

5.4.3 MNase assay of dHL60 cell NET production

Subsequently, NET release from dHL60 cells was quantified by MNase assay (Figure 60).

Data demonstrated minimal NET release from dHL60 cells following PMA or *F. nucleatum*

polymorphum exposure as the mean DNA-fluorescence detected did not significantly differ from that of unstimulated cells (indicated by dashed line). Calcium ionophore stimulation showed an increase in the extracellular DNA detected by MNase assay although this was not significant by two tailed T test when compared to unstimulated cells (P=0.11). Addition of the NADPH oxidase inhibitor DPI resulted in a minimal and statistically insignificant increase in the DNA-fluorescence of PMA stimulated (P=0.1) and bacterially-stimulated (*F. nucleatum*) cells (P=0.5) and had no effect on unstimulated cells. DPI addition to calcium ionophore stimulated dHL60 cells resulted in the only statistically significant reduction in detected DNA (P=0.04).

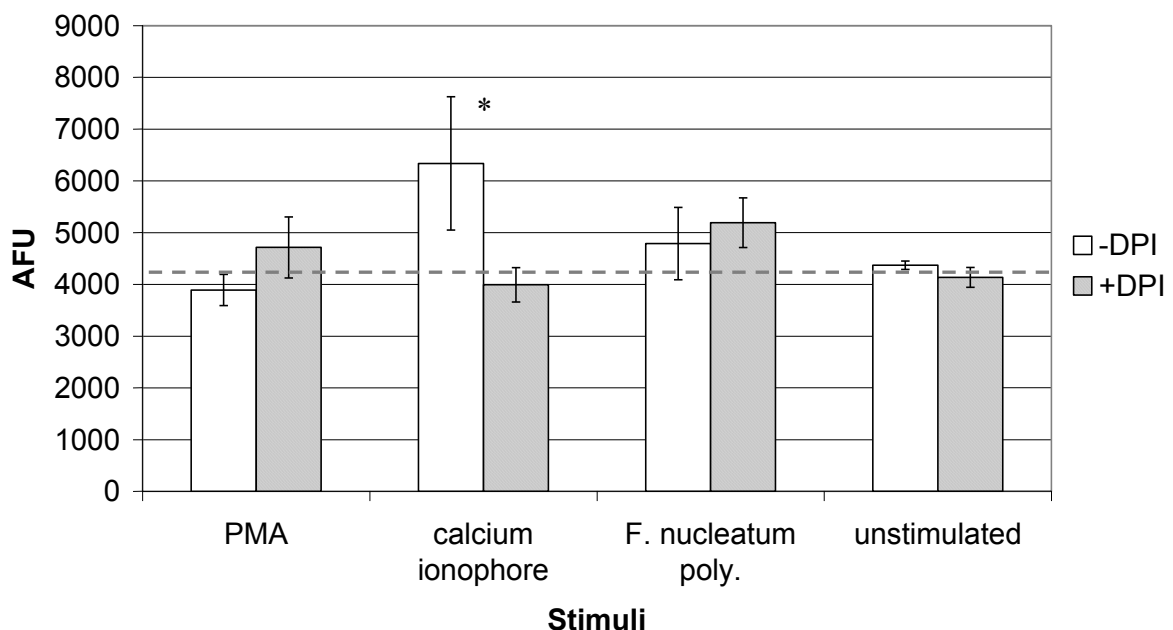
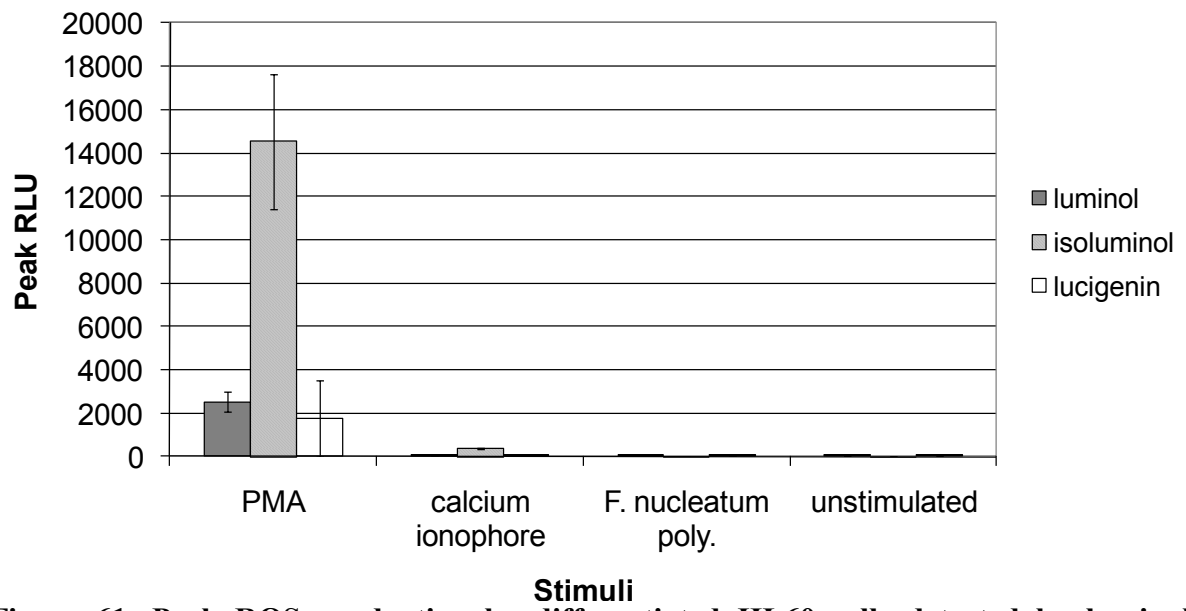


Figure 60. MNase assay of NET-DNA release from differentiated HL60 cells with and without DPI (25µM). Cells were stimulated at 20 minutes using PMA (50µM), calcium ionophore (4µM), *F. nucleatum polymorphum* (MOI 1:150) or were unstimulated (control). Results show mean experiments performed in triplicate ± SD. * P≤0.05 by two tailed unpaired T-test. Dashed line indicates fluorescence detected in unstimulated cell supernatant i.e. baseline NET release.

5.5 ROS production by dHL60 cells

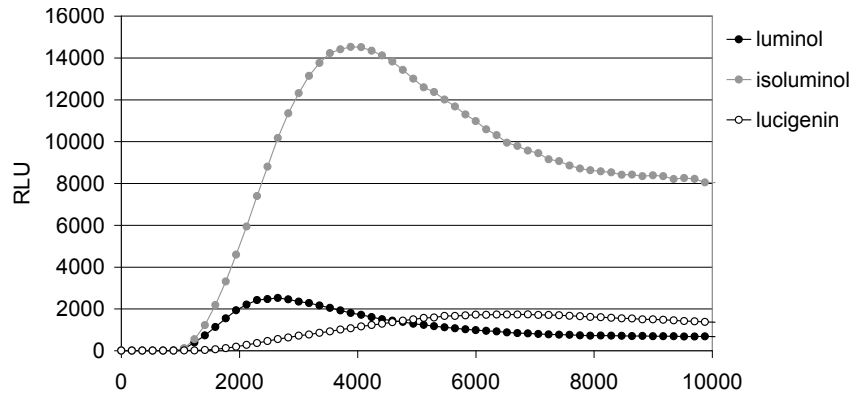
To compare ROS and NET production, ROS levels (Figure 61) were assayed simultaneously in the same dHL60 cell populations previously assayed for NET release (Figures 59 and 60). Calcium ionophore exposure resulted in low levels of ROS generation whilst *F. nucleatum polymorphum* stimulation resulted in no detectable effect (Figure 60). Notably only PMA stimulation resulted in significant ROS production.

Data presented in Figure 62 shows the kinetics from which the peak ROS generation was calculated for Figure 61. Notably the kinetics of PMA-induced ROS production were comparable to that observed for primary neutrophils (see appendix Figure 96). Calcium ionophore exposure caused an immediate and rapid increase in luminol and isoluminol dependent ROS production which may have continued to increase had the assay plate been read more frequently than the standard 3 minute intervals. Whereas PMA-induced luminol and isoluminol dependant ROS increased relatively rapidly and decreased more gradually, calcium ionophore induced ROS increased rapidly and decreased at the same rate to return to baseline levels only 40 minutes after exposure.

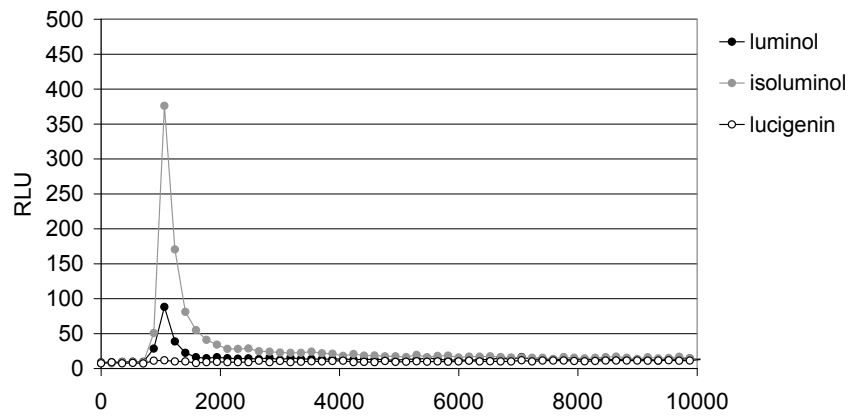


Stimuli
Figure 61. Peak ROS production by differentiated HL60 cells detected by luminol, isoluminol and lucigenin. Cells stimulated after 20 minutes using PMA 50 μ M, calcium ionophore 4 μ M, *F. nucleatum polymorphum* MOI 1:150 or unstimulated. Results show mean of experiment performed in triplicate \pm SD.

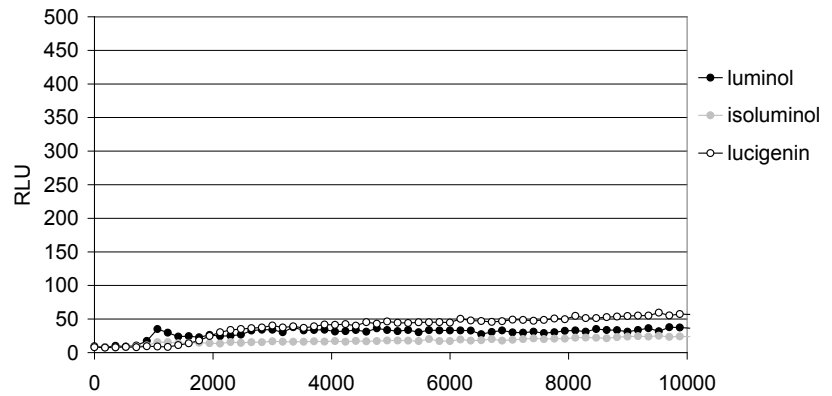
a) PMA



b) Calcium ionophore



c) *F. nucleatum polymorphum*



d) Unstimulated

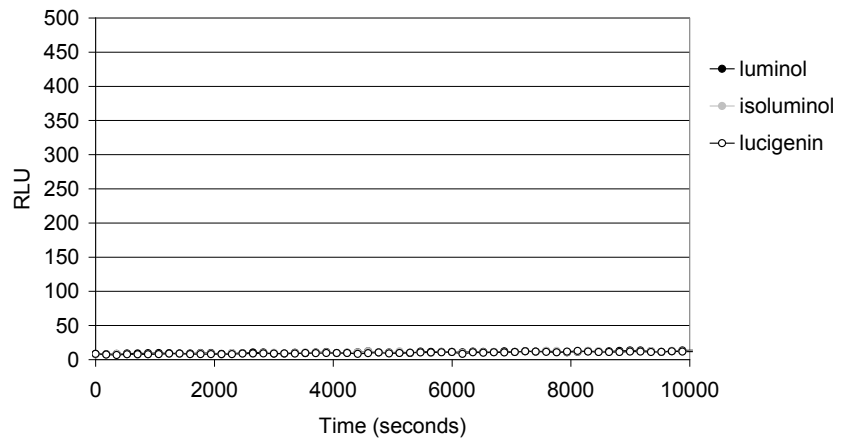


Figure 62. Time course of ROS production by dHL60 cells (1.25% DMSO 3 days) over time in response to stimulation using a) PMA 50nM b) calcium ionophore 4 μ M C) *F. nucleatum polymorphum* MOI 1:150 d) unstimulated.

Discussion

Differentiation of HL60 cells

The cytological (Figures 56 and 57) and molecular (Figure 55) data presented here indicated that the differentiation of HL60 cells using DMSO was relatively inefficient although the functional measure of differentiation, i.e. ROS generation (Figures 53 and 62) was more indicative of success. This is in agreement with previous publications in which day 1-3 HL60 cell cultures were described as morphologically immature but were capable of superoxide production, degranulation and bactericidal activity (Newburger *et al.* 1979). Whilst a key reason for using a cell line rather than primary cells was to eliminate day-to-day and person-to-person variation, data from the ROS assay indicated that this still varied greatly for each passage of the HL60 cells analysed (Figure 53). Notably whilst normal cell culture practice attempts to use only cells from relatively low passages, publications utilising HL60 cells have claimed that these cells were only used after 3 years continuous culture as responses to stimulation were increased (Preiss *et al.* 1987). Whilst transcriptional analysis indicated that HL60 cell DMSO exposure induced noticeable changes in the expression of genes encoding components of the NADPH oxidase enzyme, the expression of most other genes tested was not altered by treatment with DMSO (Figure 55). The expression of genes encoding the NADPH oxidase subunits in dHL60 cells was lower than in primary neutrophils, which is in agreement with the finding that ROS generation was also lower than in primary neutrophils (Figure 53). For the majority of genes studied, 3 hour stimulation with either *F. nucleatum* or PMA resulted in a change in gene expression indicating that the cells possessed the receptors and pathways to respond to these stimuli. The changes in gene expression however, were not

always consistent with those detected in primary neutrophils. For example, the relative level of SOD gene expression decreased over 3 hours incubation in primary neutrophils but increased in HL60 cells.

dHL60 cell responses

The most effective stimulus of dHL60 cells for evoking the generation of ROS was PMA (Figure 61), however, the most effective stimulus for evoking the release of NETs was the calcium ionophore A23187 (Figure 60). Interestingly however whilst the calcium ionophore was not the most effective stimulus for the generation of ROS, the NET release it evoked did appear to be dependent on ROS as the addition of the NADPH oxidase inhibitor, DPI, resulted in a significant reduction in detectable levels of NETs (Figure 60). The success of the calcium ionophore as a stimulus for NET production suggests that a short burst of ROS production is sufficient for the initiation of NET release. Whilst ROS release increased immediately upon stimulation, reached a peak within 10 minutes and returned to baseline within 40 minutes (Figure 62), in contrast, NET release was detectable from 30 minutes post-stimulation and increased for the duration of the 3 hour incubation period (Figure 59). An alternative form of calcium ionophore (ionomycin) has previously been reported to prime dHL60 cells resulting in increased ROS generation upon stimulation however, application of this alone was insufficient for ROS production (Dahlgren 1989). The ROS responses recorded here (Figure 62b) were relatively low in comparison to the PMA-induced response indicating that the assay previously described (Dahlgren 1989) may not have been sufficiently sensitive for the detection of calcium ionophore induced ROS. However, a ROS response was detected in primary neutrophils stimulated with calcium ionophore and displayed similar kinetics to those observed here, in that a peak was reached very rapidly within approximately

3 minutes (Dahlgren 1989). The efficacy of the calcium ionophore is consistent with evidence that NET release is dependent on calcium. Not only is the most widely reported stimulus of NET release an activator of a calcium dependant kinase, i.e. PMA, but increasing intracellular calcium concentrations (using calcium ionophore exposure) is demonstrated both here (Figures 59 and 60) and previously (Wang *et al.* 2009) to evoke NET release. Calcium is known to have widespread signalling roles within the cell so the mechanism by which this is able to elicit NET release requires further analysis. One possible mechanism however, is that the calcium ionophore is able to stimulate the generation of diacylglycerol as demonstrated in dHL60 cells by Preiss *et al.* (1987), which subsequently activates PKC, as previously reported in T-cells (Chatila *et al.* 1989) and the same mechanism stimulated by PMA.

Moreover the inconsistency between PMAs ability to stimulate ROS production and its ineffectiveness in triggering NET release may reflect the possibility that NET release is not entirely NADPH oxidase dependent, or alternatively may reflect phenotypic differences in biological pathways between dHL60 cells and primary neutrophils. Given the variation in functional responses between passages, the differences in gene expression and cellular appearance when compared to primary neutrophils, and the relative inability to extrude NETs, this cell line was considered unsuitable as a model for neutrophils in the further study of NET release.

CHAPTER 6 RESULTS

**Comparison between NET release in periodontitis patients and healthy controls
and the NET responses to periodontal pathogens**

It has previously been reported that the production of reactive oxygen species by peripheral blood neutrophils from periodontitis patients with untreated disease, differs from that of age and gender-matched periodontally healthy controls (Gustafsson *et al.* 1996; Fredriksson *et al.* 2003; Matthews *et al.* 2007a; Matthews *et al.* 2007b), particularly in response to Fc γ -receptor stimulation by opsonised *S. aureus*. As NET release has been reported to depend upon hydrogen peroxide generated during the respiratory burst (Fuchs *et al.* 2007), it was hypothesised that NET release by patient's peripheral blood neutrophils would also be higher than from controls. Subsequently 15 chronic periodontitis patients were recruited with at least 30% bone loss and a blood sample was collected before treatment was commenced. Neutrophils were isolated and assayed for ROS generation by chemiluminescent assay and for NET production by MNase assay. To further investigate the nature of NET release specific to the periodontally diseased state, peripheral blood neutrophils from control individuals self-reported as periodontally healthy were challenged with a panel of 11 periodontal pathogens and the same assays were again used to measure ROS and NET release. The NET release was also visualised by SYTOX[®] staining of the DNA and by scanning electron microscopy (SEM).

6.1 Comparison between NET release in periodontitis patients and self-reported healthy controls

6.1.1 Selection of test subjects

Periodontitis patients were selected according to the criteria previously detailed (2.2.1). Ages of volunteers at the time of sampling are documented in Table 9.

Table 9. Age of volunteers

Subject number	Sex	Patient age	Control age
01	F	60y 9m	58y 10m
02	F	53y 10m	50y 2m
03	F	48y 0m	48y 4m
04	F	58y 8m	61y 1m
05	F	53y 2m	55y 2m
06	F	46y 10m	48y 7m
07	M	40y 4m	40y 0m
08	F	39y 2m	46y 0m
09	F	30y 10m	30y 11m
10	M	42y 8m	47y 3m
11	M	63y 5m	59y 6m
12	F	35y 0m	33y 2m
13	M	48y 2m	46y 5m
14	F	49y 5m	55y 2m
15	F	58y 11m	57y 10m

Mean age: 48y 7m 49y 3m

Range: 30-63 years 30-61 years

Gender: 4 male : 11 female

6.1.2 ROS production

The rationale for this study was based on previous reports of peripheral blood neutrophil hyperactivity, i.e. unstimulated ROS production and hyper-reactivity i.e. stimulated ROS production, in periodontitis patients compared with those of healthy controls (Matthews *et al.* 2007a). A significant limitation of this study was that control patients were not examined to confirm their periodontal status, due to logistical reasons. The previous publications reported studies on Fc γ -receptor stimulation, therefore opsonised *S. aureus* was also used as a stimulus here, as well as a Gram negative periodontal pathogen (*F. nucleatum* subsp. *polymorphum*) and a well documented stimulator of NET release (PMA). These stimulatory conditions were assayed for their induction of ROS simultaneously with NET release.

Data from luminol dependant peak ROS generation by patient neutrophils paired with matched control neutrophils demonstrated that *F. nucleatum* was the most effective stimulant for evoking ROS generation, with the second most effective stimulus being PMA (Figure 63). *F. nucleatum* and PMA stimulation both demonstrated ROS generation to be generally higher in the patient group compared with the control group and this was statistically significant (P=0.02 and P=0.01 respectively) by paired T-test. Isoluminol (Figure 64) and lucigenin (Figure 65) dependant ROS generation did not appear to show any consistent or statistical differences between patient and control groups. PMA stimulation appeared to generate slightly higher levels of isoluminol-dependant ROS compared with *F. nucleatum* stimulation and both stimuli appeared equally effective at generating lucigenin-dependant ROS.

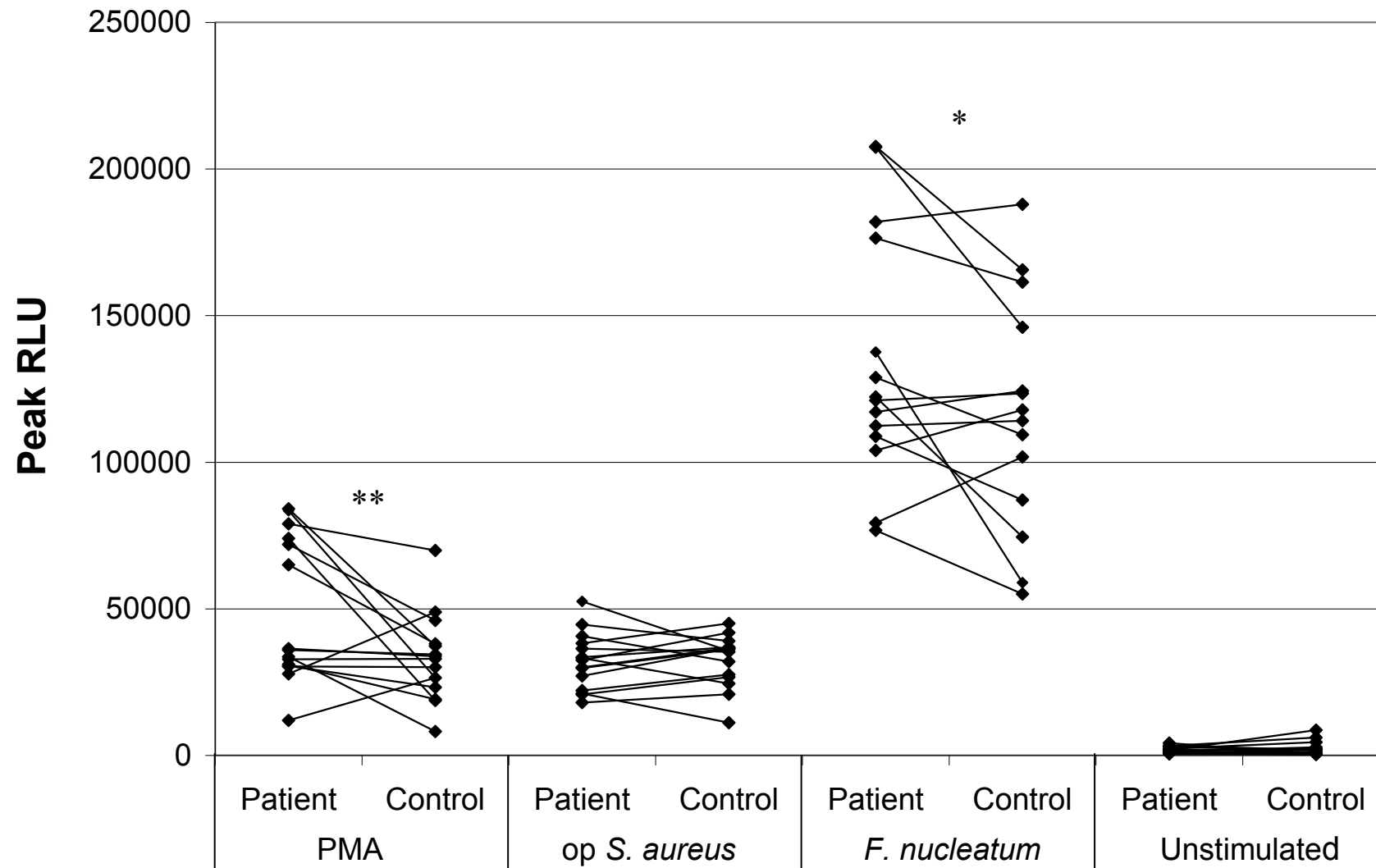


Figure 63. Luminol detected ROS production by the peripheral neutrophils of 15 patient-control pairs stimulated using PMA (50nM), opsonised *S. aureus* (MOI 1:150), *F. nucleatum polymorphum* or unstimulated (control). * $P \leq 0.05$. ** $P \leq 0.01$ using paired T-test.

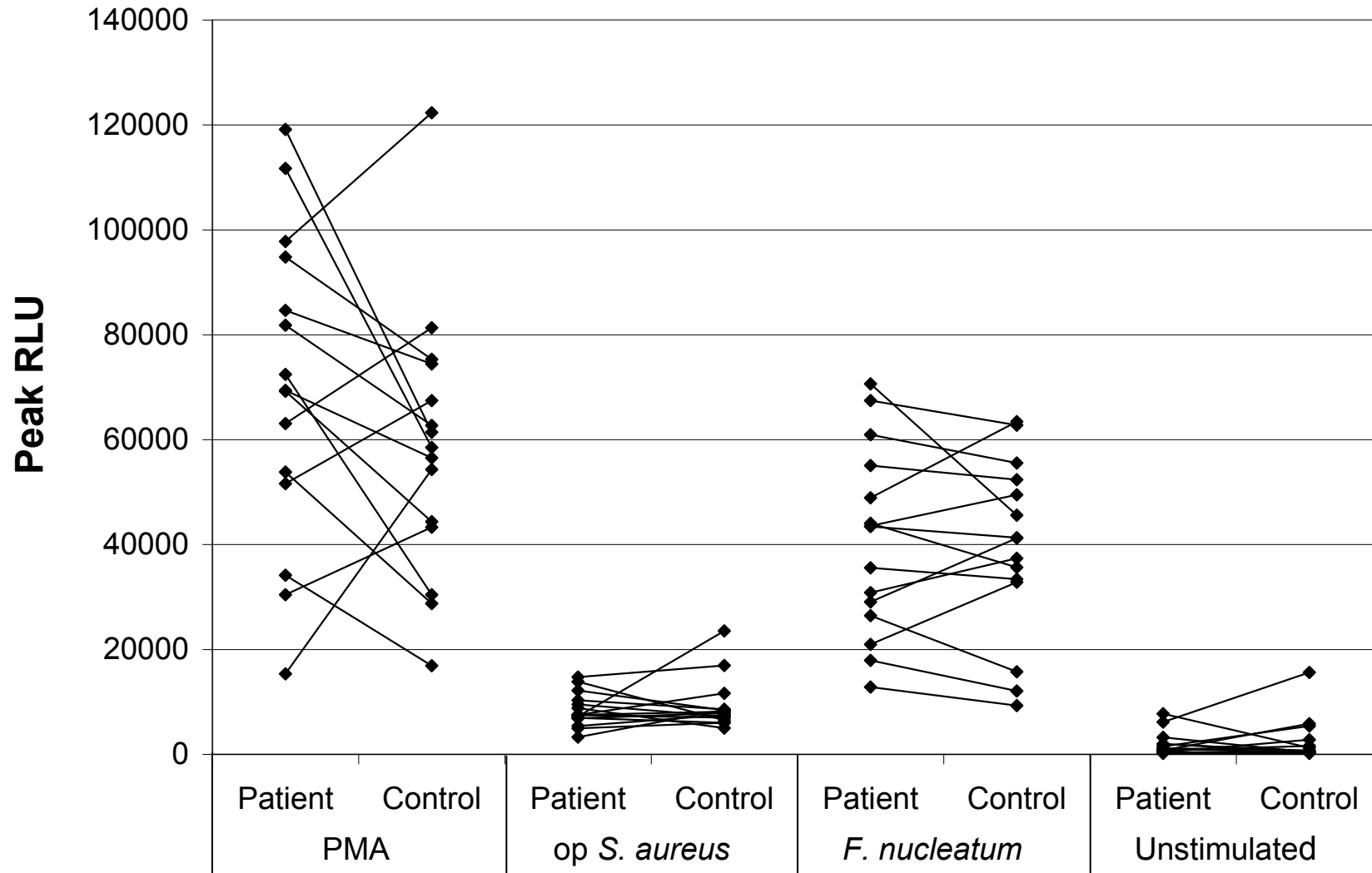


Figure 64. Isoluminol detected ROS production by the peripheral neutrophils of 15 patient-control pairs stimulated using PMA (50nM), opsonised *S. aureus* (MOI 1:150), *F. nucleatum polymorphum* or unstimulated (control). No significant differences were detected between patient and control groups using paired T-test.

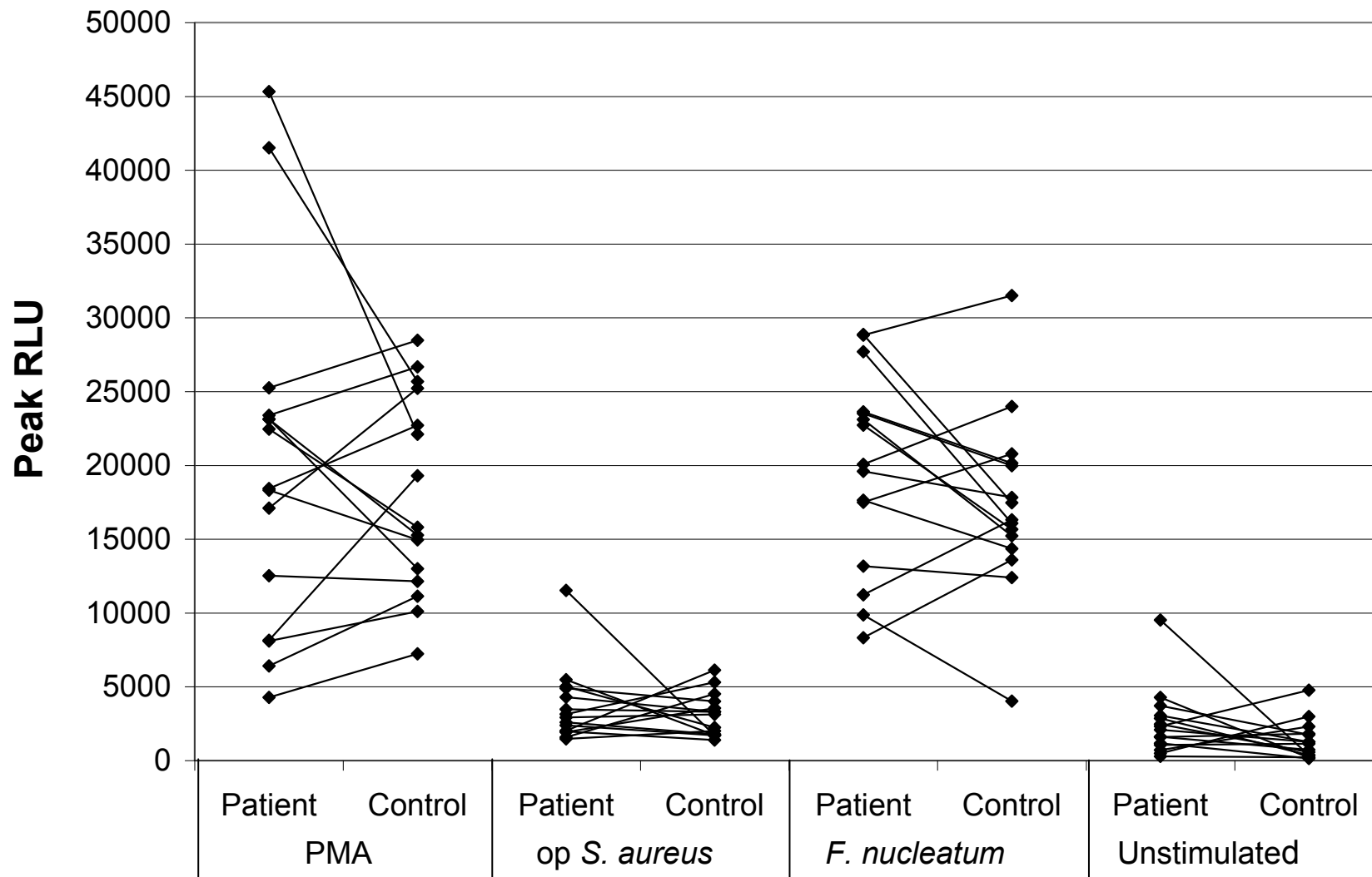


Figure 65. Lucigenin detected ROS production by the peripheral neutrophils of 15 patient-control pairs stimulated using PMA (50nM), opsonised *S. aureus* (MOI 1:150), *F. nucleatum polymorphum* or unstimulated (control). No significant differences were detected between patient and control groups using paired T-test.

6.1.3 NET release

The release of NETs was quantified by MNase assay and is displayed as 15 patient-control pairs (Figure 66). When examining the difference between the DNA-fluorescence from each patient and their matched control, paired T-test found no significant differences.

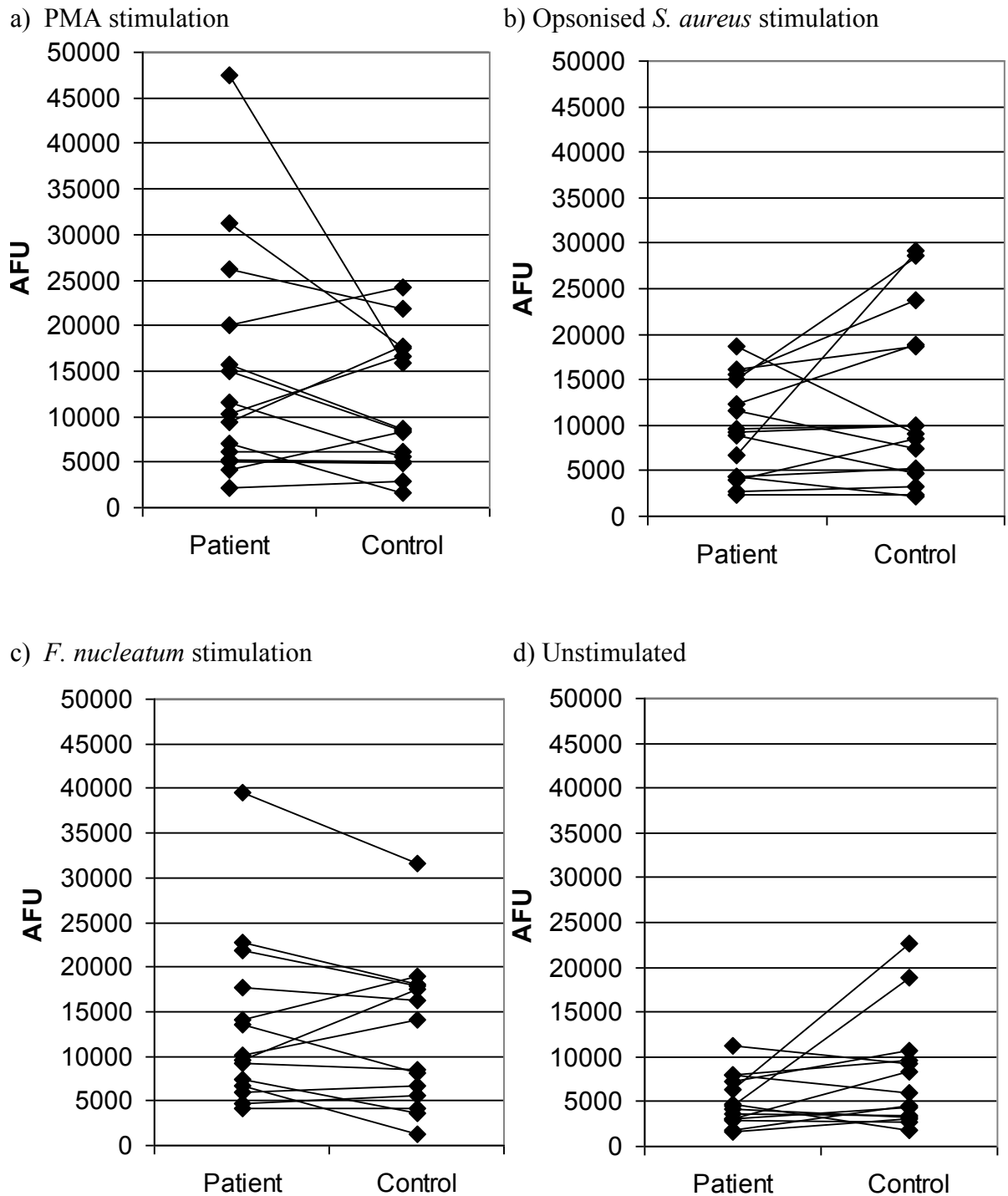
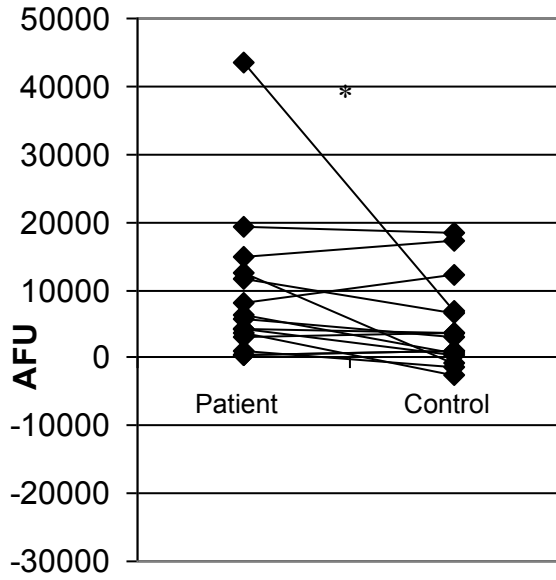


Figure 66. NET release from peripheral neutrophils of 15 patient-control pairs. Released DNA quantified by MNase assay. Results show 15 patient-control pairs assayed in triplicate. No significant differences were observed between patient and control groups by paired T-test.

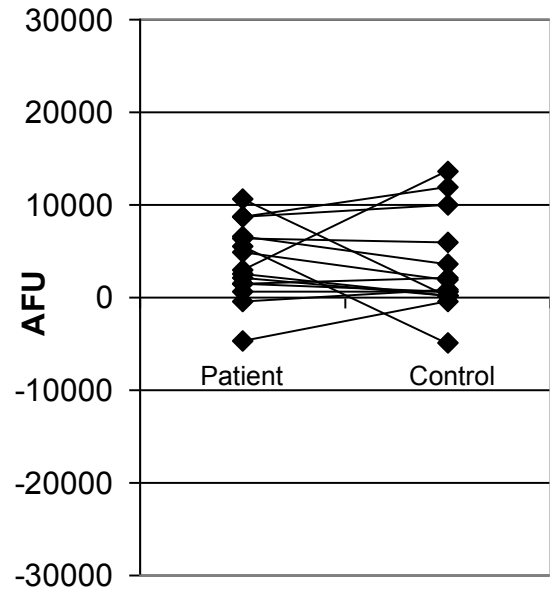
6.1.4 NADPH oxidase-dependant NET release

Previous publications have reported NET release to be dependant upon the NADPH oxidase generation of hydrogen peroxide and use of the NADPH oxidase inhibitor, DPI, here (Chapter 4) confirmed this finding. Notably however, a low level of NET formation was still present with DPI treatment which may represent NADPH oxidase independent NET release or cell death involving lysis. Therefore DPI (50 μ M) was used in the NET assay of neutrophils from patient-control pairs to elucidate the levels of ROS-dependant NET release in response to stimulation. The DPI-independent DNA fluorescence (i.e. in the presence of DPI) was subtracted from the total DNA fluorescence (i.e. in the absence of DPI) to give DPI-dependant (i.e. NADPH oxidase-dependant) DNA release (Figure 67). In some cases this yielded negative values suggesting that the addition of DPI resulted in an increase in NET release. Alternatively this may simply represent the inherent experimental variation of this assay method. Mean NET release was higher in patient groups compared to control groups in response to all 3 stimuli used although the mean NET release from unstimulated neutrophils was slightly higher in the control group than the patient group. The difference in NET release between patient-control pairs was statistically significant with PMA stimulation (P=0.04) and *F. nucleatum* stimulation (P=0.01) but was not statistically significant following opsonised *S. aureus* stimulation of neutrophils (P=0.3) by paired T-test.

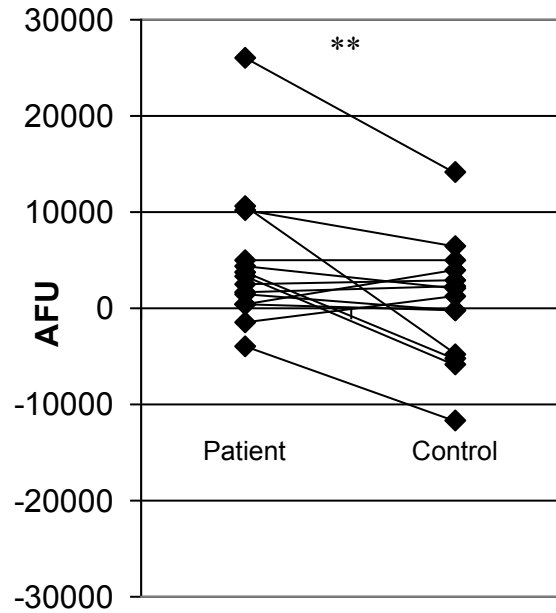
a) PMA stimulation



b) Oponised *S. aureus* stimulation



c) *F. nucleatum* stimulation



d) Unstimulated

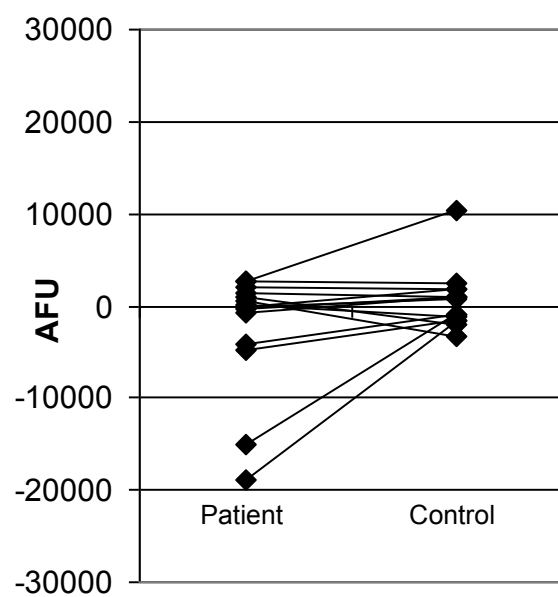
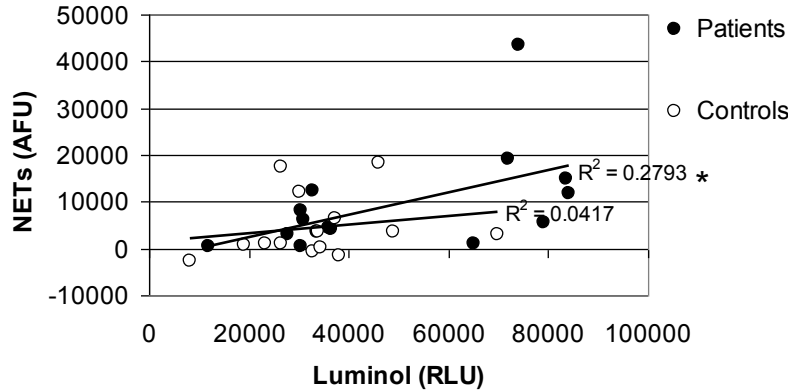


Figure 67. NADPH oxidase-dependant NET release from 15 patient-control pairs. Neutrophils stimulated with a) PMA (50nM) b) opsonised *S. aureus* (MOI 1:150) c) *F. nucleatum* (MOI 1:150) or d) unstimulated. Released DNA quantified by MNase assay with or without DPI (50 μ M). Results show results for 15 patient-control pairs assayed in triplicate. *P \leq 0.05 **P \leq 0.01 by paired T-test.

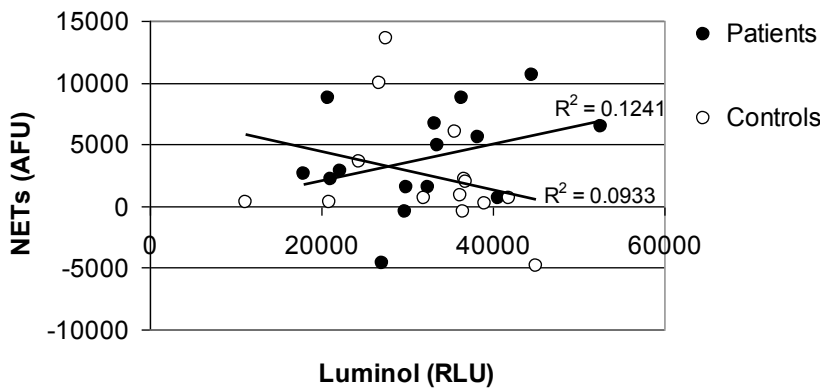
6.1.5 Comparison between ROS production and NADPH oxidase-dependant NET release

Generated ROS levels were compared to released NETs for each individual of the patient and control groups to analyse whether there was a link between the level of ROS and the level of NET release (Figure 68). Only PMA stimulation in the patient group resulted in a significant correlation between luminol-dependant ROS and NADPH oxidase-dependant NET release by Pearson test ($P=0.0428$; Figure 68a). When patient and control data points were combined to compare generated ROS levels to NET release independent of periodontal disease status, a correlation remained when examined by Pearson test ($R^2=0.2440$) with improved statistical significance ($P=0.0065$).

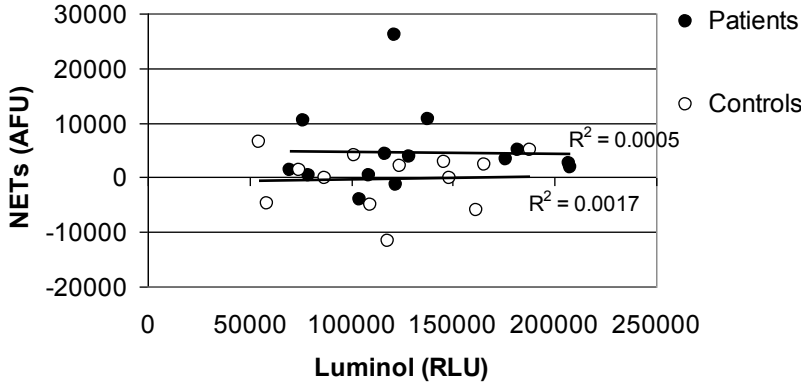
a) PMA stimulation



b) Opsonised *S. aureus*



c) *F. nucleatum* subsp. *polymorphum* stimulation



d) Unstimulated

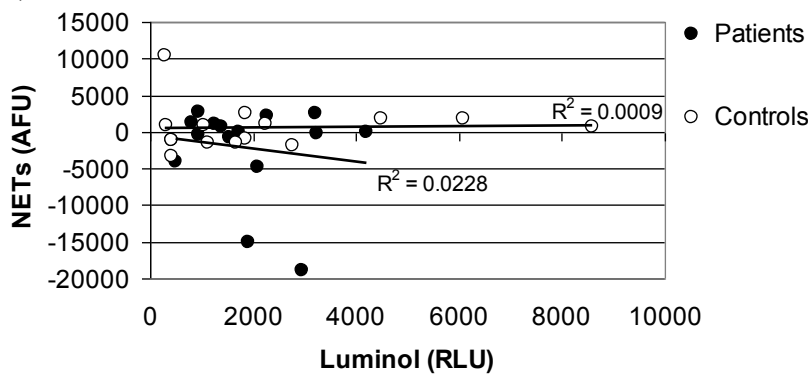


Figure 68. Comparison between luminol-dependent ROS and NADPH oxidase-dependent NET release in response to a) PMA (50nM) b) opsonised *S. aureus* (MOI 1:150) c) *F. nucleatum poly.* (MOI 1:150) and d) unstimulated neutrophils from patients and controls. * $P \leq 0.05$.

6.2 NET production by stimulation with periodontal pathogens and comparison with ROS production

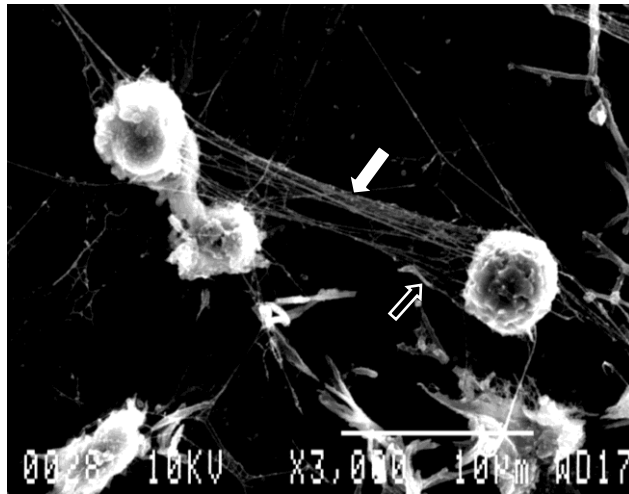
The periodontal diseased state is mediated by a balance between the host response (such as that of the neutrophil) and the bacteria present in the plaque biofilm (Section 1.1). Having investigated the responses of peripheral neutrophils from individuals suffering from periodontal disease, it was next investigated whether stimulation with periodontal pathogens associated with varying degrees of disease severity (Socransky *et al.* 1998; Figure 4) made a difference to the NET response. The NET response was assessed in the peripheral neutrophils from periodontally healthy individuals only, and was visualised by SYTOX[®] staining and scanning electron microscopy (SEM) as well as by quantitative MNase assay along with chemiluminescent assay of ROS generation.

6.2.1 SEM of periodontal pathogens interacting with NETs

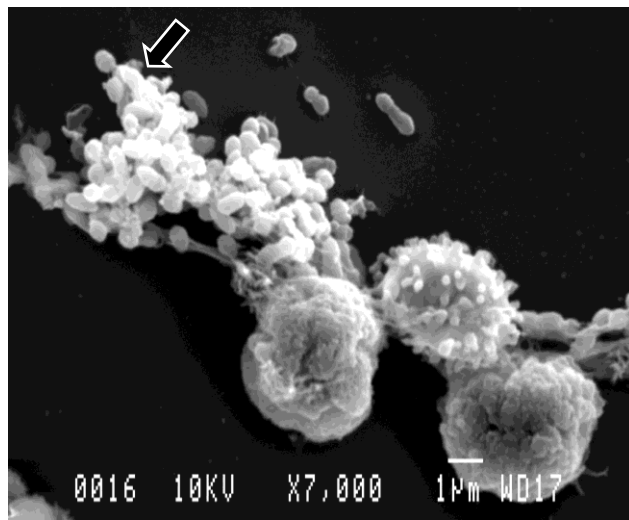
Neutrophils were seeded onto polylysine coated coverslips and stimulated with 6 periodontal pathogens to allow detailed analysis by SEM of the interaction between the bacteria and the NETs produced (Figure 69). Generally the NETs consisted of thin strand-like structures strung between neutrophils (white arrows) with the bacteria or clumps of bacteria (black arrows) associated with these strands (e.g. *T. forsythensis*, *S. constellatus*, *A. actinomycetemcomitans* and *P. gingivalis*). *A. actinomycetemcomitans* stimulated NETs also displayed a more diffuse structure which appeared to more effectively trap small groups of bacteria (black arrow). Opsonised *S. aureus* also appeared to be associated with smooth

diffuse strands (white arrow) which covered the neutrophil and surrounding bacteria. *F. nucleatum* stimulated NETs appeared more web-like, a phenomenon which had also been observed following SYTOX[®] staining of *F. nucleatum* stimulated NETs. These strands may represent thin NET filaments with the fusiform/rod shaped bacteria aligned along and adhered to these strands. There was an indication of the strands combining and twisting in a rope-like manner (white arrow), which had previously been described for the ultrastructure of NETs (Brinkmann *et al.* 2004; Brinkmann *et al.* 2007). SEM analysis of bacterially stimulated neutrophils also allowed high magnification visualisation of the bacteria which confirmed *T. forsythensis* to be fusiform, *S. constellatus* and *S. aureus* to be cocci, *A. actinomycetemcomitans* to be ovoid, *F. nucleatum* to be fusiform rods and *P. gingivalis* to be short rods.

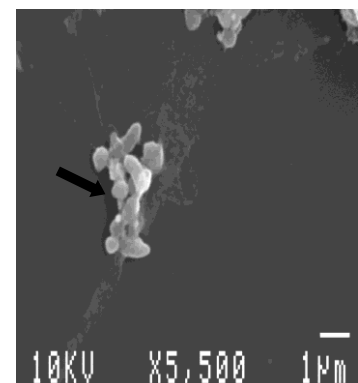
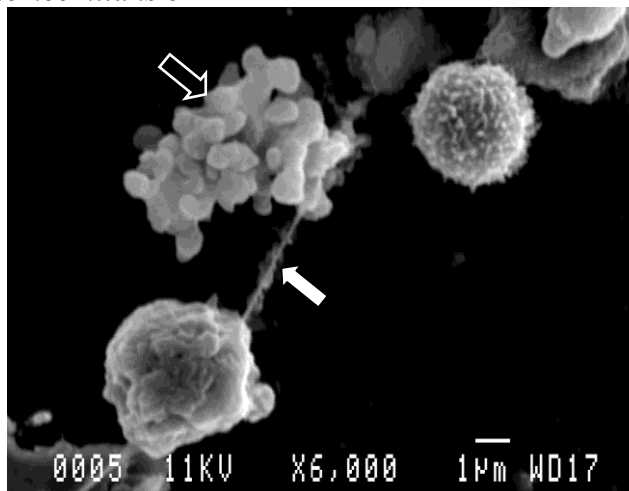
T. forsythensis



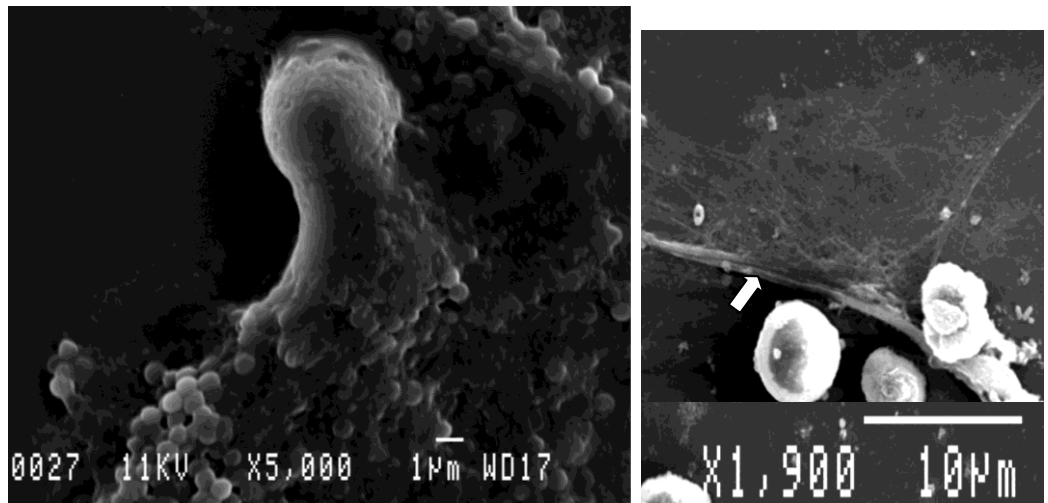
S. constellatus



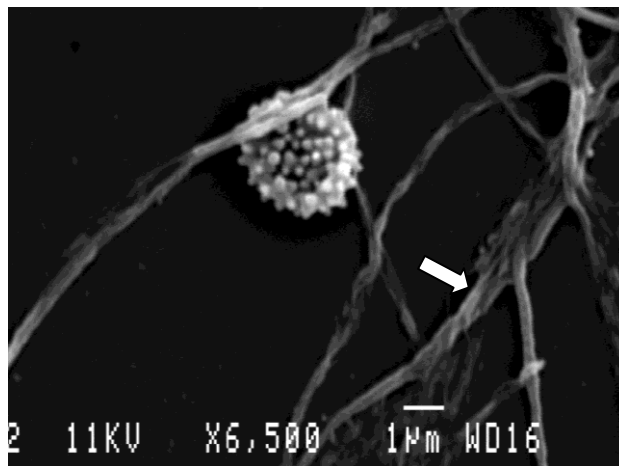
A. actinomycetemcomitans b



Oponised *S. aureus*



F. nucleatum



P. gingivalis

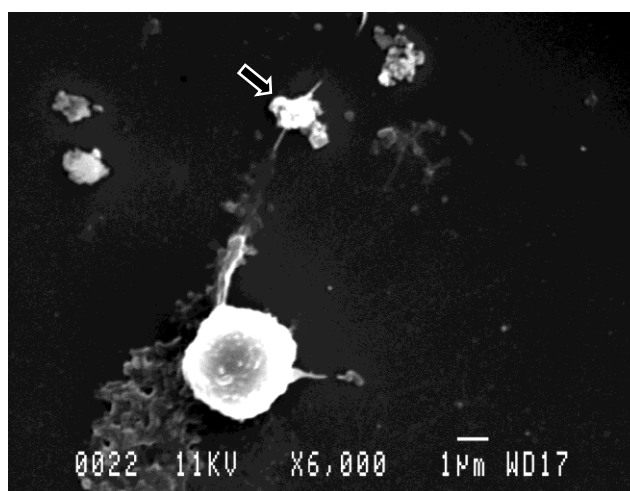


Figure 69. Scanning electron micrographs of peripheral blood neutrophils stimulated with periodontal pathogens (MOI 1:150). White arrows indicate NETs, black arrows indicate bacteria.

6.2.2 MNase assay of periodontal pathogen stimulated-NET release

The release of NETs in response to a panel of 9 periodontal pathogens in addition to opsonised and unopsonised *S. aureus* (all at an MOI of 150 bacteria per neutrophil) was quantified by MNase assay (Figure 70). Data show the mean NET release from 3 independent experiments performed on separate occasions using neutrophils from 3 different individuals. As a result there is a relatively large degree of variation in NET production, represented by the standard deviation, especially with those bacteria which evoked a higher level of NET release such as *T. forsythensis*, *A. actinomycetemcomitans* and *P. intermedia*. The extracellular DNA fluorescence detected after *S. constellatus* or unopsonised *S. aureus* stimulation was not increased in comparison to unstimulated cells.

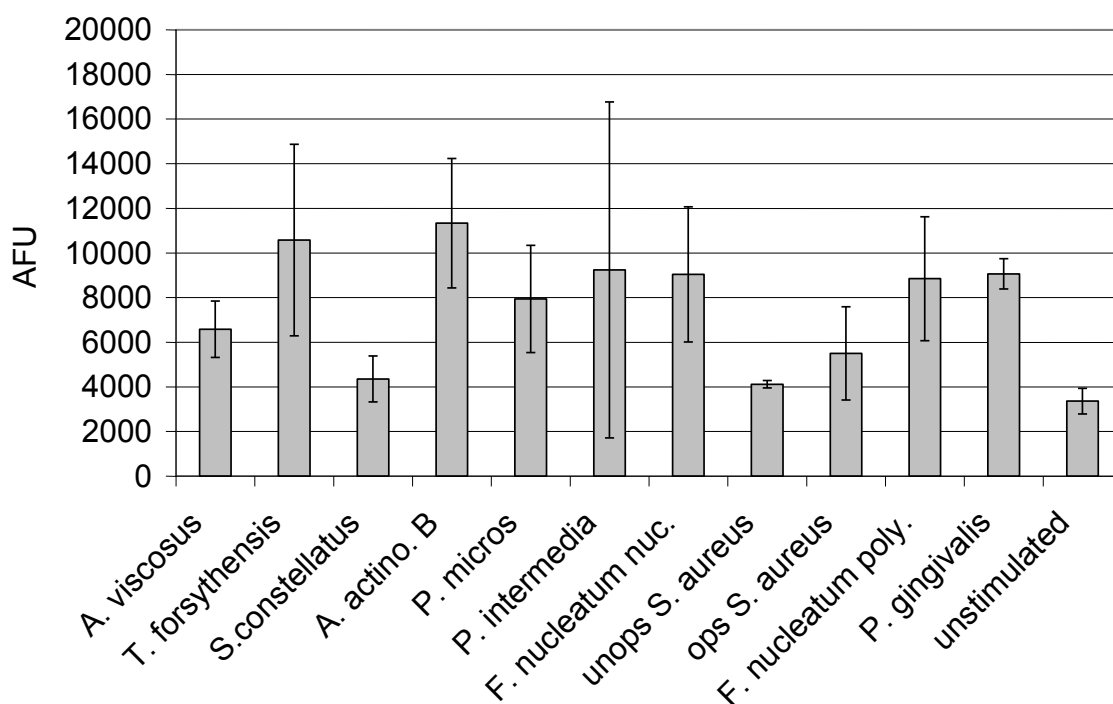
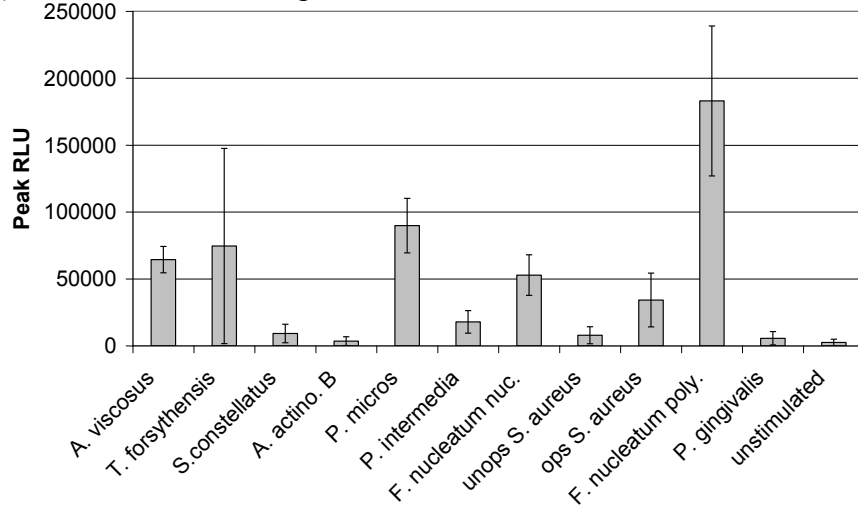


Figure 70. MNase assay of NET-DNA release from peripheral neutrophils of healthy individuals in response to periodontal pathogens (MOI 1:150). Results show mean of 3 independent experiments performed in triplicate \pm SD.

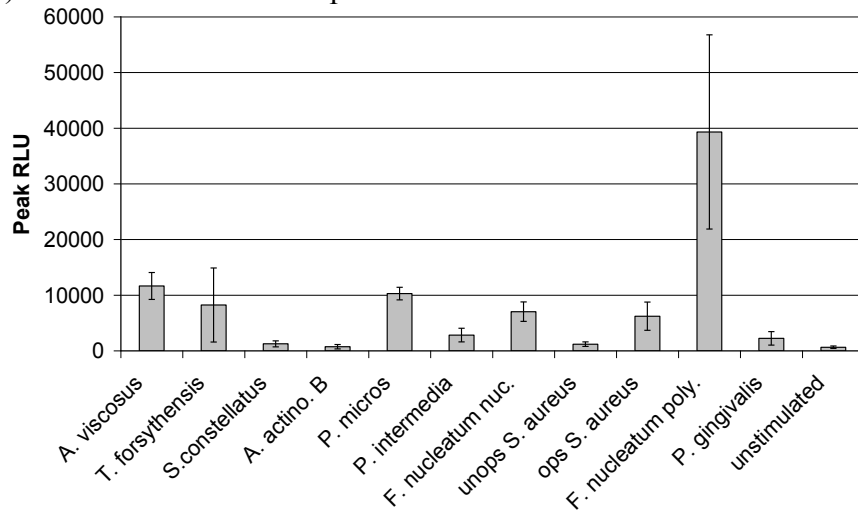
6.2.3 ROS production in response to periodontal pathogens

ROS production was quantified by chemiluminescent assay (Figure 71) simultaneously with the MNase assay of NET release previously described (Figure 70). All bacteria were again applied at equal concentrations (MOI 1:150) and were used to stimulate neutrophils on 3 independent occasions, resulting again in a large standard deviation particularly when readings were relatively high. *F. nucleatum* subsp. *polymorphum*, *P. micros* and *T. forsythensis* were the most effective stimuli at evoking luminol- and isoluminol-dependent ROS production. *F. nucleatum* subsp. *polymorphum*, *F. nucleatum* subsp. *nucleatum* and *P. micros* were the more effective stimuli at evoking lucigenin-dependent ROS generation.

a) Luminol detection of peak ROS



b) Isoluminol detection of peak ROS



c) Lucigenin detection of peak ROS

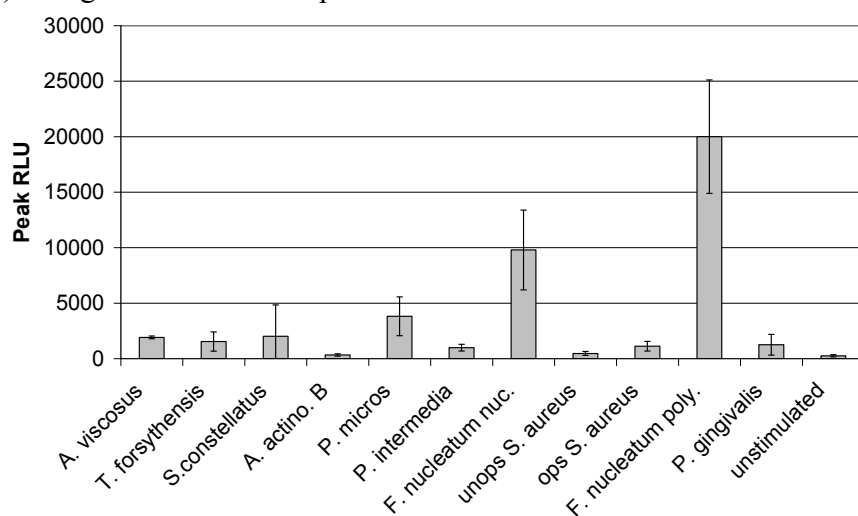
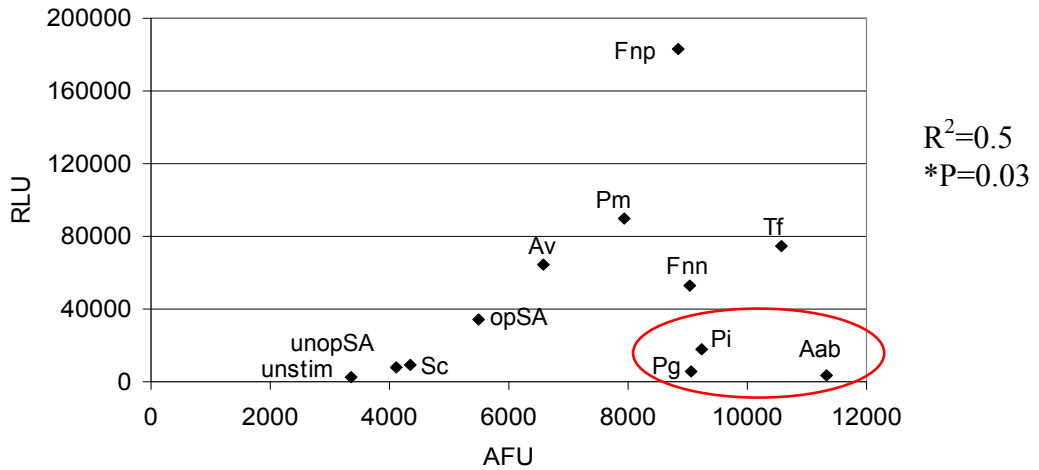


Figure 71. ROS production from peripheral neutrophils detected by a) luminol, b) isoluminol and c) lucigenin in response to periodontal pathogens MOI 1:150. Results represent mean of 3 independent experiments performed in triplicate \pm SD.

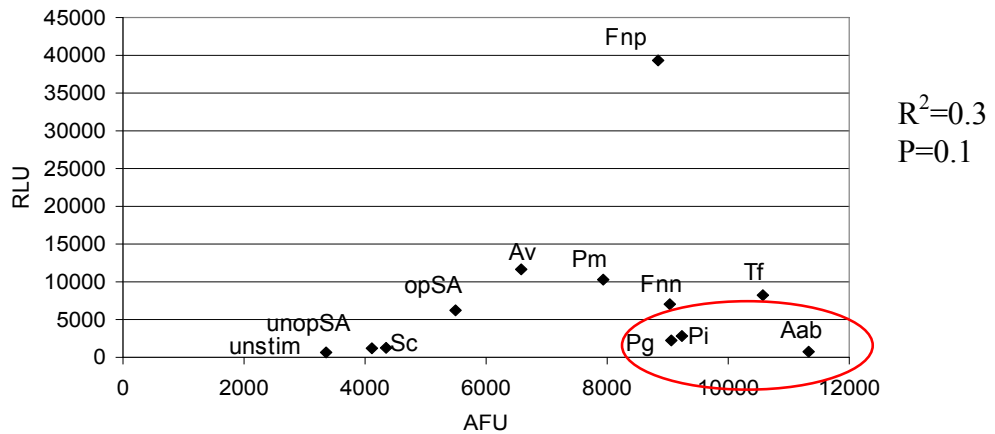
6.2.4 Correlation analysis between NET release and ROS generation in response to periodontal pathogens

To examine the relationship between the ROS generated and the level of NET release detected in response to the 11 bacteria, the data from Figures 70 and 71 were plotted against each other (Figure 72). No statistically significant correlation was observed by Pearson test between any measure of ROS generation (luminol, isoluminol or lucigenin) and the concurrent release of NETs. However, 3 bacteria consistently produced some of the highest levels of released DNA but produced extremely low levels of detected ROS. When these bacteria (*P. gingivalis*, *P. intermedia* and *A. actinomycetemcomitans* b) were excluded, Pearson test revealed a significant positive correlation between NET release and luminol-dependent ROS production ($R^2=0.5$; Figure 72a).

a) Correlation of NET release (AFU) with luminol detected ROS generation (RLU)



b) Correlation of NET release (AFU) with isoluminol detected ROS generation (RLU)



c) Correlation of NET release (AFU) with lucigenin detected ROS generation (RLU)

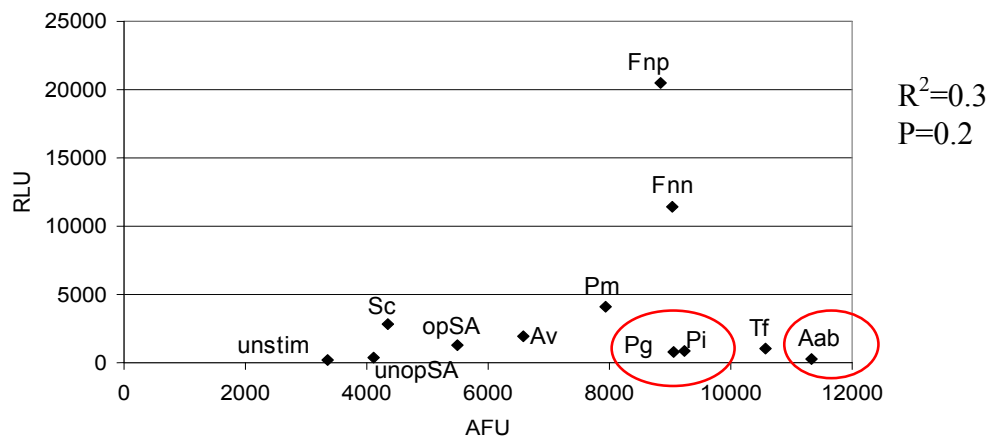


Figure 72. Correlation between NET-DNA detected by MNase assay and ROS detected by a) luminol b) isoluminol c) lucigenin. Bacterial stimuli used at MOI 1:150 *A. viscosus* (Av), *T. forsythensis* (Tf), *S. constellatus* (Sc), *A. actinomycetemcomitans* a (Aaa), *P. micros* (Pm), *P. intermedia* (Pi), *F. nucleatum nucleatum* (Fnn), unopsonised *S. aureus* (unopSA), opsonised *S. aureus* (opSA), *F. nucleatum polymorphum* (Fnp), *P. gingivalis* (Pg), unstimulated (unstim). Results show mean of 3 independent experiments performed in triplicate. R^2 values generated by Pearson test excluding circled data points.

Discussion

Differences in patient and control neutrophil responses

It is well established that peripheral blood neutrophil responses differ between individuals and even within the same individual assayed at different times and on different days (Chapple *et al.* 2007b; Fuchs *et al.* 2007). Two significant factors affecting interpersonal variation, age and gender were controlled for here. However, a major difference between the patient and control groups in the current study was that patients had blood samples taken following overnight fasting whilst controls had not previously fasted. This difference may have contributed to the fact that statistically significant differences between patient and control groups were only observed in the luminol detection of ROS (Figure 63) and the assay of NADPH oxidase-dependant NET release (Figure 67), since dietary glucose may result in an exaggerated NADPH oxidase respiratory burst (Chapple 2009). For the quantification of NET release, DPI was used to eliminate baseline (NADPH oxidase independent) DNA release which may have been due to cell necrosis and lysis induced by cell processing rather than active NET extrusion. When this approach was applied, patient responses were significantly higher than control responses in PMA and *F. nucleatum* stimulated cells (Figure 67). Whilst evidence exists that periodontitis is associated with elevated peripheral neutrophil activity in terms of chemotaxis (Van Dyke *et al.* 1980) and ROS generation (Gustafsson *et al.* 1996; Matthews *et al.* 2007a; Matthews *et al.* 2007b), the data presented here suggests that NETosis may also be elevated in peripheral neutrophils and may contribute to the pathology of this disease rather than protect against infection. When the stimulated NET values in the presence of DPI were subtracted from those in the absence of DPI some of the resultant data points were negative

(Figure 67). This suggests that DPI caused increased NET release, a phenomenon previously described in unstimulated and ineffectively stimulated cells (Chapter 4). Indeed, the negative values generated for NADPH oxidase-dependant NET release were most dramatic in the unstimulated cells. When ROS and NET production were compared no correlation was observed, only a weak correlation in PMA stimulated neutrophils (Figure 68). This suggests that the relationship between ROS generation and NET release may not be quantitative, that the quantitative relationship varies between individuals, or that NADPH oxidase independent mechanisms of NETosis also exist. Further investigation including the systematic and thorough study of periodontitis patients should therefore be performed. Moreover, newly emerging markers of NET activation could be utilised such as antibodies for the citrullination of histone H3 (Wang *et al.* 2009; Vitkov *et al.* 2010) which could provide greater specificity in the detection of NET release than those employed in this thesis.

NET release in response to periodontal pathogens

Numerous bacteria have been reported to associate with and be trapped by NETs such as *Staphylococcus aureus*, *Salmonella typhimurium*, *Shigella flexneri* (Brinkmann *et al.* 2004) and *Streptococcus pneumoniae* (Reid *et al.* 2009). As predicted, periodontal pathogens were also demonstrated to associate with NETs when analysed under SEM (Figure 69). Furthermore these NETs were produced in response to the bacteria, unlike in certain previous publications in which PMA or IL-8 were used to trigger NET release and the pathogen added subsequently. The morphology of the NETs observed also varied depending on the bacterial species associated with them. This observation may have arisen due to the different charges present on the bacterial surfaces which represents the current hypothesised mode of trapping (Brinkmann *et al.* 2007). For example, PMA is most commonly used to stimulate NET

release however the NETs produced often appear diffuse prior to mechanical stimulation (by SYTOX staining; Figure 26B). The presence of bacteria may provide a surface for NETs to adhere to and likewise, NETs are often observed to span between two neutrophils (Figure 69 *T. forsythensis*). Whilst in this study only dead bacteria were employed to stimulate NET production, previous work has demonstrated that live parasite sporozoites are more effective than dead ones at stimulating NET release (Behrendt *et al.* 2010). It might be expected that as dead bacteria have no motility then the release of NETs to trap the bacteria and prevent their dissemination is unnecessary, and therefore live bacteria may be more effective. Further work in this area could investigate whether live or dead periodontal bacteria of the same species result in different levels of NET release.

When ROS generation and NET release were quantified (Figures 71 and 72 respectively) a wide range of levels detected in response to different periodontal pathogens was evident with *F. nucleatum polymorphum* being amongst the highest producers and unopsonised *S. aureus* amongst the lowest. Therefore, although there is an ever increasing list of agents, microbes and molecules capable of stimulating NET release, these do not stimulate identical responses. Each bacterial species will exhibit a different combination of surface antigens which will result in variations in stimulation of host cells. Data presented here identified three bacteria as outliers when assayed simultaneously for ROS and NET generation (Figure 72). These bacteria exhibited low levels of ROS generation but surprisingly high levels of detected NET release. Highly variable levels of NET release were detected in response to *P. intermedia* over the three occasions tested (indicated by the standard deviation presented in Figure 70) making it difficult to draw any conclusions about the relationship between ROS and NET generation for this bacterium. Reasons for the relatively elevated NET readings in response to

the two remaining bacteria (*P. gingivalis* and *A. actinomycetemcomitans* b) may relate to bacterial DNase activity. If the majority of bacteria except these outliers expressed some level of DNase this may reduce the sensitivity of the NET detection assay relative to the outliers. Alternatively, *P. gingivalis* has been reported to express the PAD enzyme (Rodríguez *et al.* 2009), which is responsible for the citrullination of proteins, including histone H3, which has been demonstrated to be an essential step in NET release (Wang *et al.* 2009). It is possible that enhanced citrullination of histones within the neutrophil facilitates NET release even when levels of ROS are low. Whether any expressed PAD would remain bound to the bacteria and its activity preserved during the storage of the bacterial stimuli used here needs further investigation, although it has been reported that bacterial PADs do not require any cofactors for activity and are relatively robust, as whilst the enzyme aggregates upon storage at -20°C (also used here) activity was still subsequently detected following thawing (Rodríguez *et al.* 2009). If the experiments performed here were repeated utilising live bacteria which are more physiologically relevant, other outliers may also be identified. For example, catalase expression is a common characteristic amongst bacteria and this enzyme has previously been demonstrated to reduce NET release (Fuchs *et al.* 2007). It is therefore conceivable that bacterial catalase expression may exert the same effect *in vivo*. Although catalase is a large protein and therefore only able to act extracellularly (Dahlgren *et al.* 1999) it is possible that extracellular removal of hydrogen peroxide would maintain a gradient promoting its diffusion into the extracellular space and maintaining a reduced intracellular hydrogen peroxide concentration.

In conclusion, there are likely to be certain bacterial species with particular virulence or susceptibility in terms of their interaction with host neutrophils. However, if in general the

potency of any given species to stimulate ROS generation correlates with the level of NET release, this evidence suggests that where there exists a pathology involving the release of ROS, NETs are also likely to play a role. Indeed a statistically significant correlation was observed between luminol-dependant ROS production and NET release (Figure 72a) when the panel of periodontal pathogens were used as stimuli. This is in agreement with the periodontitis patient data, in which the same two stimuli (PMA and *F. nucleatum*) resulted in a significant difference between the two groups for both luminol-dependant ROS and NADPH oxidase-dependant NET release (Figure 63 and 67).

CHAPTER 7 RESULTS

Characterisation of periodontal pathogens and their susceptibility to killing by histone

A panel of 34 anaerobic periodontal pathogens (Table 6) which were all American Type Culture Collection (ATCC) strains obtained from cultures maintained at the Forsyth Institute, Boston, USA (kind gift by Professor S. Socransky), were utilised in this project. Members of this panel were used to i) stimulate NET release from peripheral blood neutrophils, ii) assay for their *in vitro* DNase activity and iii) test their susceptibility to killing by histones. Given the duration of maintenance and likely phenotypic changes induced by repeated culture, it was deemed important to confirm their validity for use. The bacteria were therefore identified and characterised using several complementary approaches including morphological and biochemical analysis, and species specific PCR where appropriate.

7.1 Characterisation of periodontal pathogens

Prior to experimental analysis of the bacteria, their identity was established using PCR of species specific genes, morphological and biochemical testing.

7.1.1 PCR identification of bacteria

Twenty-four primers were obtained from the existing literature and four were additionally designed in-house to amplify gene sequences specific to each bacterial species (Table 7). Commonly, the target DNA sequences was the small ribosomal subunit (16s rRNA) which differs in nucleotide sequence between species but is highly conserved, i.e. not subject to significant change between strains of the same species (Woese 1987). For certain bacteria however, 16s rRNA assays were not reported and therefore alternative genomic sequences were utilised. For the purpose of a screening for identification, and to minimise the number

of PCR assays performed, a rows and columns approach was utilised (Table 10). Equal volumes of the 6 bacteria in each row and column were combined and 12 PCR assays performed on samples of these pooled bacteria (C1-6 and R1-6). Thereby for any single species specific gene, one column (C) and one row (R) should enable detection of a positive result, the intersection of which indicates the bacterial species (Table 10).

Table 10. Bacterial mixes used for PCR analysis

Bacterial species identified by ATCC number.

<u>Columns:</u>	C1	C2	C3	C4	C5	C6
<u>Rows:</u> R1	33277	43037	10953	25586	25611	27823
R2	33270	33238	33563	51146	33236	10556
R3	10558*	27335	35037	49456*	33612	29523
R4	33624	10790	17929	43718	43146	12104
R5	11827	11828	14201	19696	25175	25845
R6	27824*	33397	35308	12102	-	-

*No PCR assay currently reported for these bacterial species

PCR products generated using the 28 species specific primer pairs available were visualised using agarose gel electrophoresis (Figure 73). No primers were identified from the literature or successfully designed for three of the bacterial species (10558 *S. gordonii*, 27824 *G. morbillorum* and 49456 *S. mitis*). These bacteria were still included in the PCR analysis to ensure there was no primer cross-hybridisation with these species or that these bacterial

cultures were not contaminated with any species for which primers were available. The 28 PCR assays utilised gave positive identification of the bacterial species which they were designed to identify. Exceptions were observed for the primer for the fimbrial protein of *A. naeslundii* which only successfully amplified from *A. viscosus* DNA. These two bacterial species are very closely related and when the primers taken from literature (Tran *et al.* 1996) were aligned with the gene sequences for fimbrial proteins from *A. naeslundii* and *A. viscosus* the primer sequences appeared more specific for *A. viscosus* than for *A. naeslundii*, and would predictively yield a PCR product only 6 base pairs shorter (for sequence alignments see appendix Figure 97). The PCR assay for the 16s rRNA DNA sequence of *P. denticola* not only amplified DNA from this bacterial culture but also that from *P. melaninogenica*, indicating the potential for the *P. melaninogenica* culture being contaminated with *P. denticola*. However, these two bacterial species are both species of *Prevotella* and share 91% homology in their 16s rRNA gene sequence resulting in the primers designed for the 16s rRNA gene assay in *P. denticola* also reacting with the *P. melaninogenica* 16s rRNA sequence. Subsequently, under the PCR conditions applied a PCR product of identical size was generated. Similarly, for the identification of the two *Campylobacter* species (*C. showae* and *C. rectus*) and also the two subspecies of *Fusobacterium nucleatum* (subsp. *polymorphum* and *nucleatum*), a single primer pair for 16s rRNA was identified from the literature and used. Therefore, these assays were only able to confirm genera/species and were unable to distinguish between the species/subspecies, respectively. Finally, the primer specific to the 16s rRNA of *P. acnes* successfully amplified product from the culture of ATCC 11828 but not 11827, and also appeared to amplify DNA from the culture of *C. sputigena*, suggesting that the culture of *C. sputigena* may be contaminated with *P. acnes* (see below for further characterisation of this potentially mixed culture – section 7.1.2).

10556 *S. sanguis* (glucosyltransferaseP)

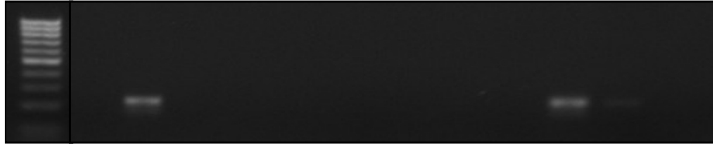
L C1 C2 C3 C4 C5 C6 R1 R2 R3 R4 R5 R6



positive identification C6/R2

10790 *V. parvula* (16s rRNA)

L C1 C2 C3 C4 C5 C6 R1 R2 R3 R4 R5 R6



positive identification C2/R4

10953 *F. nucleatum* subsp. *polymorphum* and
25586 *F. nucleatum* subsp. *nucleatum* (16srRNA)

L C1 C2 C3 C4 C5 C6 R1 R2 R3 R4 R5 R6

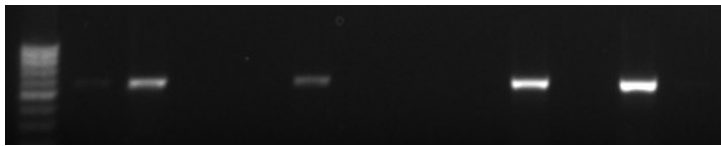


positive identification
C3/R1 and C4/R1

11827 *P. acnes* and

11828 *P. acnes* (16s rRNA)

L C1 C2 C3 C4 C5 C6 R1 R2 R3 R4 R5 R6



positive identification C1/R5 and
C2/R5. Also detects C5/R3 (33612
C. sputigena)

12102 *A. israelii* (16s rRNA)

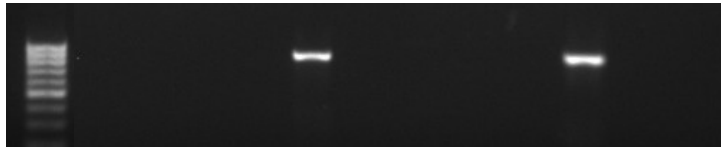
L C1 C2 C3 C4 C5 C6 R1 R2 R3 R4 R5 R6



positive identification C4/R6
also detects C6/R4 (12104
A. naeslundii)

12104 *A. naeslundii* (fimbrial protein)

L C1 C2 C3 C4 C5 C6 R1 R2 R3 R4 R5 R6



positive identification C6/R4
Detects C5/R4 (12102 *A. viscosus*)
instead

14201 *L. buccalis* (16s rRNA)

L C1 C2 C3 C4 C5 C6 R1 R2 R3 R4 R5 R6



positive identification C3/R5

17929 *A. odontolyticus* (16s rRNA)

L C1 C2 C3 C4 C5 C6 R1 R2 R3 R4 R5 R6



positive identification C3/R4

19696 *N. mucosa* (penicillin binding protein A)

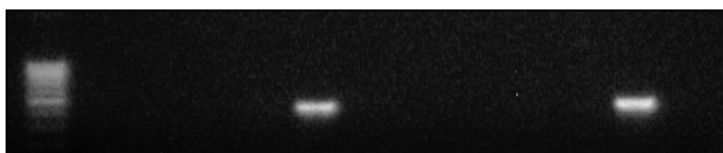
L C1 C2 C3 C4 C5 C6 R1 R2 R3 R4 R5 R6



positive identification C4/R5

25175 *S. mutans* (glucosyltransferase)

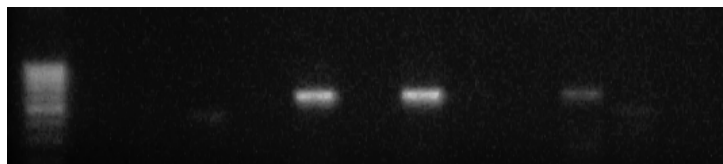
L C1 C2 C3 C4 C5 C6 R1 R2 R3 R4 R5 R6



positive identification C5/R5

25611 *P. intermedia* (16s rRNA)

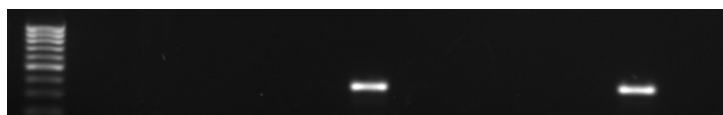
L C1 C2 C3 C4 C5 C6 R1 R2 R3 R4 R5 R6



positive identification C5/R1

25845 *P. melaninogenica* (haemolysin)

L C1 C2 C3 C4 C5 C6 R1 R2 R3 R4 R5 R6



positive identification C6/R5

27335 *S. intermedius* (intermedilysin)

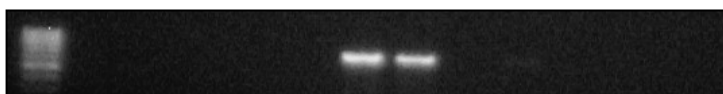
L C1 C2 C3 C4 C5 C6 R1 R2 R3 R4 R5 R6



positive identification C2/R3

27823 *S. constellatus* (hyaluronate lyase)

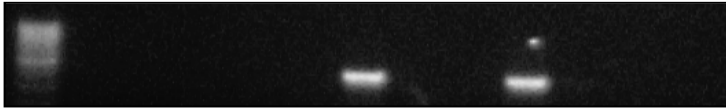
L C1 C2 C3 C4 C5 C6 R1 R2 R3 R4 R5 R6



positive identification C6/R1

29523 *A. actinomycetemcomitans* serotype a (mannosyltransferase)

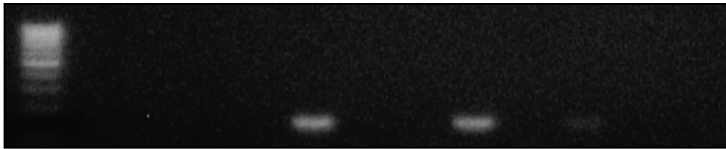
L C1 C2 C3 C4 C5 C6 R1 R2 R3 R4 R5 R6



positive identification C6/R3

33236 *C. gracilis* (16s rRNA)

L C1 C2 C3 C4 C5 C6 R1 R2 R3 R4 R5 R6

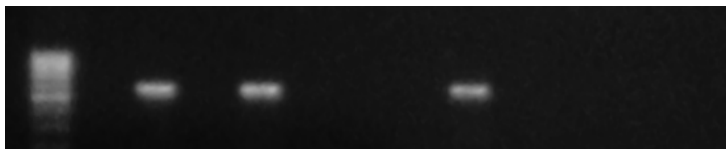


positive identification C5/R2

33238 *C. rectus* and

51146 *C. showae* (16s rRNA)

L C1 C2 C3 C4 C5 C6 R1 R2 R3 R4 R5 R6



positive identification C2/R2 and C4/R2

33270 *P. micros* (16s rRNA)

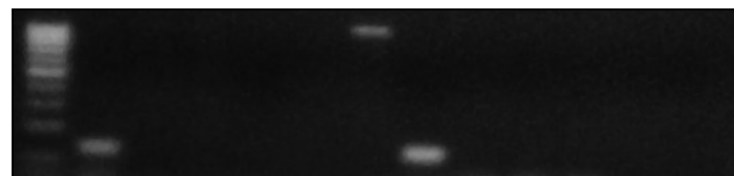
L C1 C2 C3 C4 C5 C6 R1 R2 R3 R4 R5 R6



positive identification C1/R2

33277 *P. gingivalis* (fimbrial protein)

L C1 C2 C3 C4 C5 C6 R1 R2 R3 R4 R5 R6



positive identification C1/R1

33397 *S. anginosus* (16s rRNA)

L C1 C2 C3 C4 C5 C6 R1 R2 R3 R4 R5 R6



positive identification C2/R6

33563 *P. nigrescens* (16s rRNA)

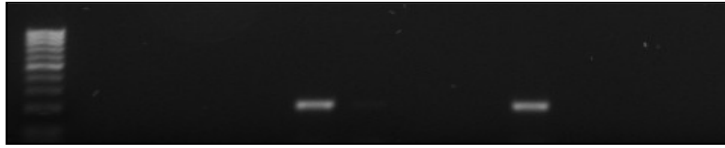
L C1 C2 C3 C4 C5 C6 R1 R2 R3 R4 R5 R6



positive identification C3/R2

33612 *C. sputigena* (16s rRNA)

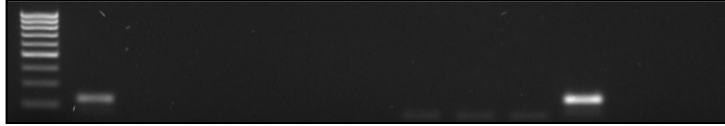
L C1 C2 C3 C4 C5 C6 R1 R2 R3 R4 R5 R6



positive identification C5/R3

33624 *C. gingivalis* (16s rRNA)

L C1 C2 C3 C4 C5 C6 R1 R2 R3 R4 R5 R6



positive identification C1/R4

35037 *S. oralis* (glucosyltransferase)

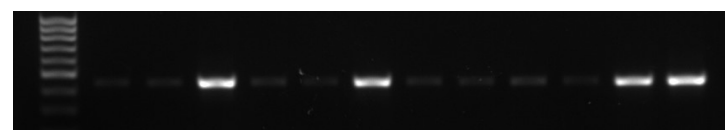
L C1 C2 C3 C4 C5 C6 R1 R2 R3 R4 R5 R6



positive identification C3/R3

35308 *P. denticola* (16s rRNA)

L C1 C2 C3 C4 C5 C6 R1 R2 R3 R4 R5 R6



positive identification C3/R6
also detects C6/R5 (25845
P. melaninogenica)

43037 *T. forsythensis* (16s rRNA)

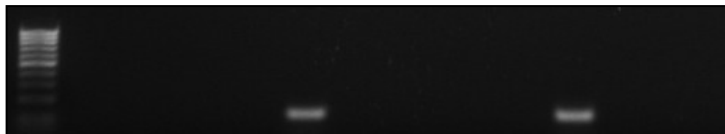
L C1 C2 C3 C4 C5 C6 R1 R2 R3 R4 R5 R6



positive identification C2/R1

43146 *A. viscosus* (unknown protein)

L C1 C2 C3 C4 C5 C6 R1 R2 R3 R4 R5 R6



positive identification C5/R4

43718 *A. actinomycetemcomitans* serotype b (mannosyltransferase)

L C1 C2 C3 C4 C5 C6 R1 R2 R3 R4 R5 R6



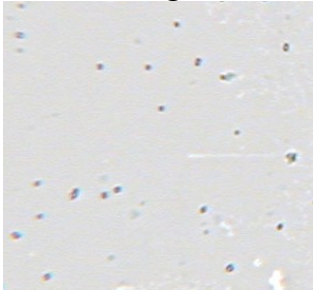
positive identification C4/R4

Figure 73. PCR amplification of species specific genomic sequences in bacterial mixes. Target bacteria identified by ATCC number followed by name and target gene shown in parenthesis. 6 μ l of PCR product was electrophoresed on a 1.5% ethidium bromide stained agarose gel. L = ladder (PCR ranger 100bp DNA ladder, Bioline).

7.1.2 Gram stain and cell morphology analysis

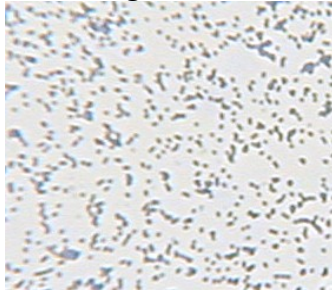
Having previously provided positive evidence for the identity of 23 of the 34 bacterial species by PCR assay, along with a further 6 positively identified but not specific to a single bacterial species, Gram staining was also applied. This analysis would provide further evidence regarding the identity of the bacteria based on the composition of their cell wall and their morphology (descriptions from Bergey's Manual of Determinative Bacteriology 9th Edition; (Holt 1994). Grams iodine stains the thick peptidoglycan layer of Gram positive bacteria purple, whereas Gram negative bacteria exhibit only a thin peptidoglycan layer which is covered by an additional outer membrane that is removed by the acetone rinsing step and results in pink counterstaining using carbol fuchsin. Gram stains generally provided further data supporting the identity of the bacteria (Figure 74), although due to the variable nature of these characteristics this analysis cannot be applied alone. Indeed, literature indicated that for some bacteria, e.g. *V. parvula*, the Gram stain was uninformative due to these bacteria appearing Gram negative or positive under certain culture conditions. In addition, for morphological characterisation certain bacteria e.g. *Fusobacterium* are pleomorphic and therefore morphological characterisation alone can also be misleading. Data generated using these cytological approaches was however useful in the analysis of the *C. sputigena* cultures in which PCR results indicated that cultures may be contaminated with *P. acnes*. Visualisation confirmed the culture to consist of a mixed population of the desired Gram negative rods and also Gram positive cocci bacteria likely to be *P. acnes*. Therefore a fresh vial of stock bacteria was re-cultured and characterised by molecular and cytological approaches to ensure the correct homogenous culture was utilised in future experiments.

10556 *S. sanguis*



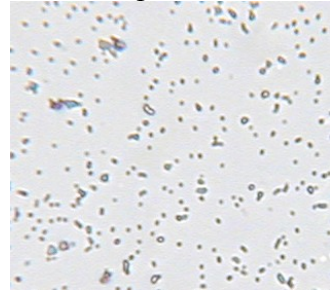
Gram positive
Cocci/ovoid

10558 *S. gordonii*



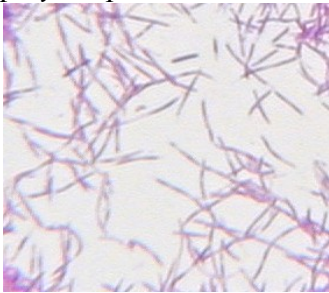
Gram positive
Cocci/ovoid

10790 *V. parvula*



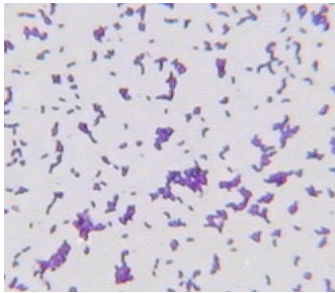
Gram negative
Cocci

10953 *F. nucleatum* subsp.
polymorphum



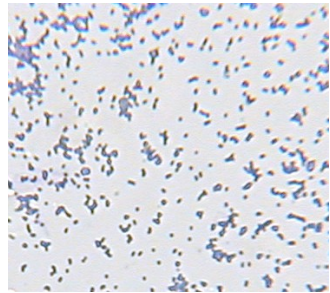
Gram negative
Fusiform/rods

11827 *P. acnes*



Gram positive
Irregular rods/cocci

11828 *P. acnes*



Gram positive
Irregular rods/cocci

12102 *A. israelii*



Gram positive
Rods

12104 *A. naeshlundii*



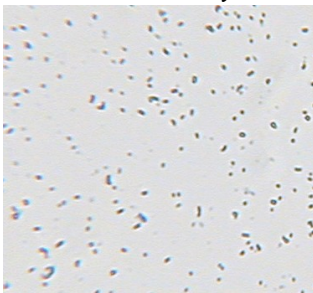
Gram positive
Rods

14201 *L. buccalis*



Gram positive
Fusiform rods

17929 *A. odontolyticus*



Gram positive
Rods

19696 *N. mucosa*



Gram negative
Cocci

25175 *S. mutans*



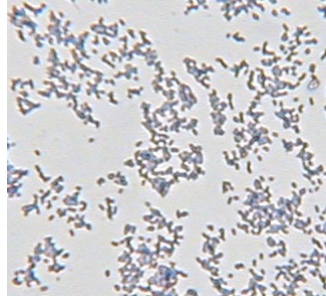
Gram positive
Cocci/ovoid

25586 *F. nucleatum* subsp. *nucleatum*



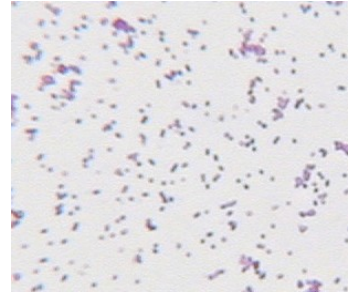
Gram negative
Rods/spindles

25611 *P. intermedia*



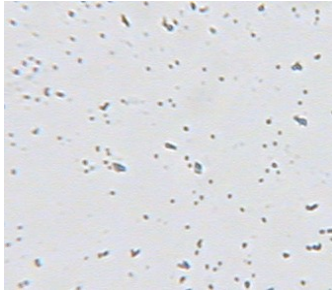
Gram negative
Pleomorphic rods

25845 *P. melaninogenica*



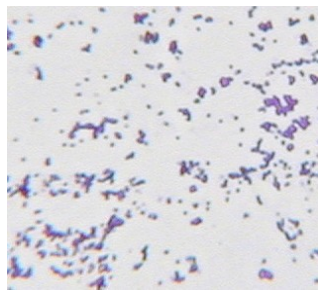
Gram negative
Pleomorphic rods

27335 *S. intermedius*



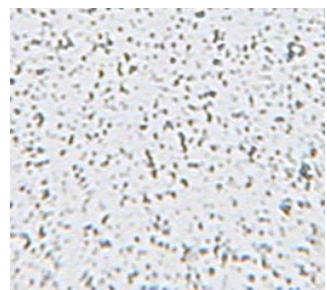
Gram positive
Cocci/ovoid

27823 *S. constellatus*



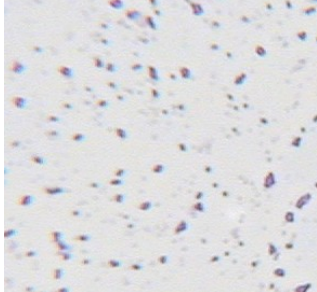
Gram positive
Cocci/ovoid

27824 *G. morbillorum*



Gram positive/variable
Cocci/elongate

29523 *A. actinomycetemcomitans*



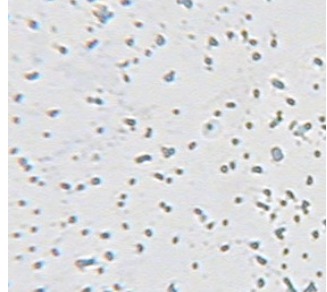
Gram negative
Rods/ovoid

33236 *C. gracilis*



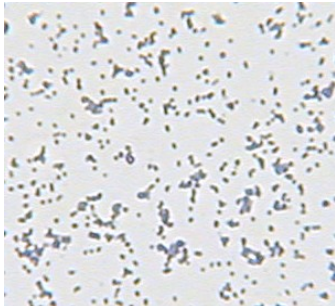
Gram negative
Rods

33238 *C. rectus*



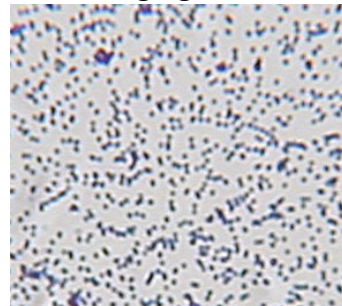
Gram negative
Rods

33270 *P. micros*



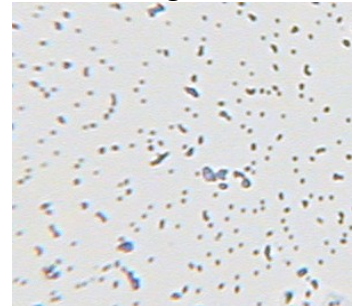
Gram positive
Cocci

33277 *P. gingivalis*



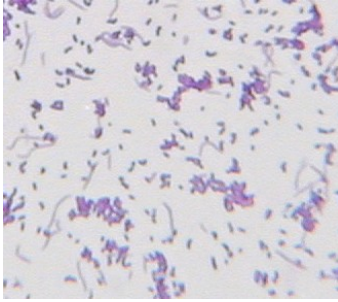
Gram negative
Short rods

33397 *S. anginosus*



Gram positive
Cocci/ovoid

33612 *C. sputigena*



Gram negative
Rods

33563 *P. nigrescens*



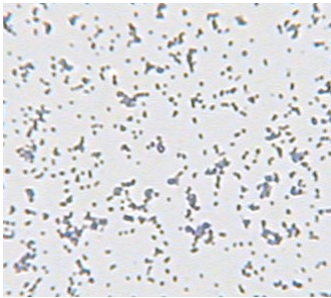
Gram negative
Pleomorphic rods

33624 *C. gingivalis*



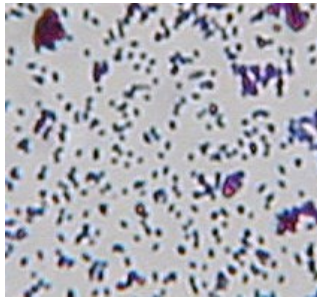
Gram negative
Rods

35037 *S. oralis*



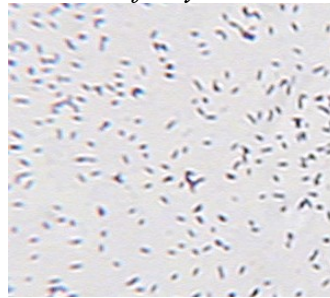
Gram positive
Cocci/ovoid

35038 *P. denticola*



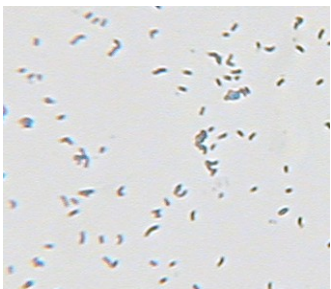
Gram negative
Pleomorphic rods

43037 *T. forsythensis*



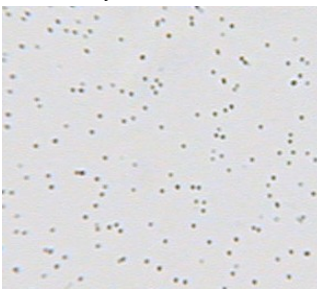
Gram negative
Fusiform

43146 *A. viscosus*



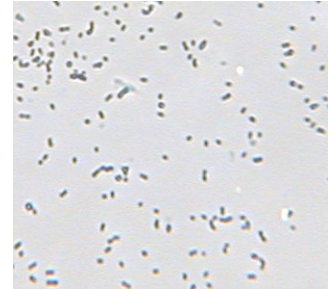
Gram positive
Short rods

43718 *A. actinomycetemcomitans*



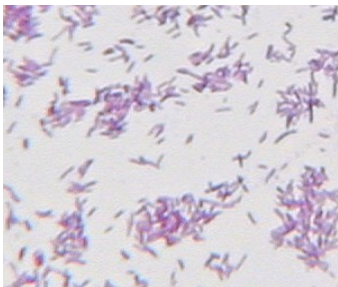
Gram negative
Rods/ovoid

49456 *S. mitis*



Gram positive
Cocci/ovoid

51146 *C. showae*



Gram negative
Rods

Figure 74. Gram stains of bacterial cultures obtained from agar plates and emulsified in saline on glass slides. Visualisation by oil immersion microscopy. Gram negative bacteria stained pink and Gram positive bacteria stained a deeper purple. Cell morphology was either cocci (spherical), ovoid, rods (bacilli) or fusiform (spindle shaped). ATCC number and bacterial species are provided.

7.1.3 Haemolysis and colony morphology

When bacteria are cultured on blood agar they can exhibit three types of haemolysis (α , β or γ) depending on the species analysed. This is a variable characteristic and is not described for many species, therefore only the bacteria for which this effect was reported as a significant characteristic in Bergeys Manual (Holt 1994) were analysed (Figure 75). In addition, the type of haemolysis can depend on the type of media and blood used, which for these experiments consisted of tryptone soya agar supplemented with whole horse blood. All bacteria tested showed the expected form of haemolysis.

Certain bacteria obtain iron from the heme group in blood agar and produce porphyrin resulting in a distinctive black/brown colony pigmentation. This characteristic allowed positive identification of *P. intermedia* (Figure 75), *P. nigrescens* (Figure 75), *P. melaninogenica* and *P. gingivalis*. In addition *P. denticola* appeared marginally pigmented and the colonies of *C. sputigena* appeared yellow/orange.

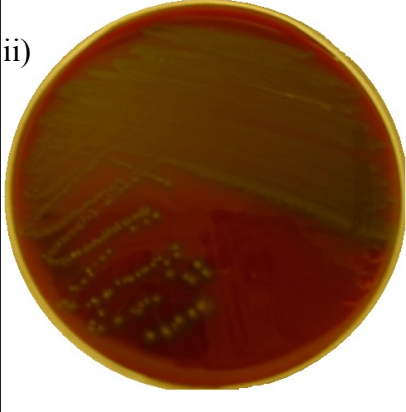
<p>i) <u>α-haemolysis</u> Partial lysis of red blood cells resulting in greenish discolouration of agar.</p>	<p><u>β-haemolysis</u> Complete lysis of red blood cells resulting in clearing of the blood in the agar.</p>	<p><u>γ-haemolysis</u> No haemolysis</p>
<p>ii) </p>	<p></p>	<p></p>
<p>iii)</p> <ul style="list-style-type: none"> • <i>S. gordonii</i>* • <i>S. oralis</i> • <i>G. morbillorum</i> 	<ul style="list-style-type: none"> • <i>P. intermedia</i>* • <i>P. acnes</i> • <i>P. melaninogenica</i> • <i>A. actinomycetemcomitans</i> 	<ul style="list-style-type: none"> • <i>P. nigrescens</i>* • <i>S. mutans</i> • <i>N. mucosa</i> • <i>T. forsythensis</i>

Figure 75. Haemolysis by periodontal pathogens. i) Description of 3 types of haemolysis ii) Photographs of 5 days bacterial growth on agar plates supplemented with whole horse blood (α -haemolysis *S. gordonii*, β -haemolysis *P. intermedia*, γ -haemolysis *P. nigrescens*) and iii) Bacteria listed for which haemolysis is a reported characteristic (Bergey's Manual). *indicates bacteria shown in example photograph.

7.1.4 Catalase testing

The production of catalase by bacteria is tested by exposing them to hydrogen peroxide and observing the liberation of oxygen bubbles. This is only a significant characteristic for certain bacteria present in the test panel and these are shown in Table 11. Notably, catalase production is one of the only phenotypic characteristics that distinguishes *C. showae* from *C. rectus* (Etoh *et al.* 1993). The catalase test also distinguishes catalase negative streptococci from catalase positive staphylococci which can appear very similar by cellular morphology. All bacteria tested displayed the expected catalase activity listed in Table 11.

Table 11. Catalase production by periodontal bacteria used in this study

Negative	Positive
<i>T. forsythensis</i>	<i>P. acnes</i>
<i>S. sanguis</i>	<i>N. mucosa</i>
<i>S. gordonii</i>	<i>A. actinomycetemcomitans</i>
<i>S. mutans</i>	<i>C. showae</i>
<i>S. intermedius</i>	
<i>S. constellatus</i>	
<i>S. anginosus</i>	
<i>S. oralis</i>	
<i>S. mitis</i>	
<i>V. parvula</i>	
<i>G. morbillorum</i>	
<i>C. gracilis</i>	
<i>C. rectus</i>	
<i>C. sputigena</i>	
<i>C. gingivalis</i>	

7.1.5 Summary of identification

To summarise the results of all 6 identification tests a positive (✓) or negative (✗) outcome is indicated in Table 12. Where no result is indicated the test was not performed or not relevant. All 34 strains were positively identified by 2-4 of the 6 identifying characteristics with the exception of bacteria *C. sputigena* (ATCC 33612). Where identification was initially negative an archived culture was obtained from storage (-80°C) and re-tested to confirm identity before use in further experiments.

Table 12. Summary of identification tests

ATCC number	Bacterial strain	PCR	Gram stain	Cell morphology	Haemolysis	Colony morphology	Catalase
10556	<i>S. sanguis</i>	✓	✓	✓			✓
10558	<i>S. gordonii</i>		✓	✓	✓		✓
10790	<i>V. parvula</i>	✓		✓			✓
10953	<i>F. nucleatum polymorphum</i>	✓	✓	✓			
11827	<i>P. acnes</i>	✗	✗	✓	✓		✓
11828	<i>P. acnes</i>	✓	✓	✓	✓		✓
12102	<i>A. israelii</i>	✓	✓	✓			
12104	<i>A. naeslundii</i>		✓	✓			
14201	<i>L. buccalis</i>	✓	✓	✓			
17929	<i>A. odontolyticus</i>	✓	✓				
19696	<i>N. mucosa</i>	✓	✓	✓	✓		✓
25175	<i>S. mutans</i>	✓	✓		✓		✓
25586	<i>F. nucleatum nucleatum</i>	✓		✓			
25611	<i>P. intermedia</i>	✓		✓	✓	✓	
25845	<i>P. melaninogenica</i>	✓	✓		✓	✓	
27335	<i>S. intermedius</i>	✓	✓	✓			✓
27823	<i>S. constellatus</i>	✓	✓	✓			✓
27824	<i>G. morbillorum</i>		✓	✓	✓		✓
29523	<i>A. actinomycetemcomitans a</i>	✓	✓	✓	✓		✓
33236	<i>C. gracilis</i>	✓	✓	✓			✓
33238	<i>C. rectus</i>	✓		✗			✓
33270	<i>P. micros</i>	✓	✓	✓			
33277	<i>P. gingivalis</i>	✓		✗		✓	
33397	<i>S. anginosus</i>	✓	✓	✓			✓
33612	<i>C. sputigena</i>	✗	✗	✗		✗	✓
33563	<i>P. nigescens</i>	✓		✓	✓	✓	
33624	<i>C. gingivalis</i>	✓		✓			✓
35037	<i>S. oralis</i>		✓	✓	✓		
35308	<i>P. denticola</i>	✓	✓	✓		✓	
43037	<i>T. forsythensis</i>	✓	✓	✓	✓		✓
43146	<i>A. viscosus</i>	✓	✓	✓			
43718	<i>A. actinomycetemcomitans b</i>	✓		✓	✓		✓
49456	<i>S. mitis</i>		✓	✓			✓
51146	<i>C. showae</i>	✓	✓	✓			✓

7.2 Susceptibility of periodontal pathogens to killing by histones

Following the provision of data supporting the identity of all 34 ATCC periodontal pathogens they were tested for their susceptibility to killing by histones as this has not previously been reported for this group of bacteria. Histones are core chromatin proteins present within NETs, which have previously been reported to exert an antimicrobial effect (Brinkmann *et al.* 2004). The effectiveness of purified mixed histone to inhibit growth of the periodontal pathogens was assessed using several methods which included spectrophotometric analysis, colony counting and fluorometric analysis in order to identify a robust method with high accuracy and throughput suitable for the assay of this panel of anaerobic bacteria. Methods were initially validated using a combination of known antibiotics (penicillin-streptomycin) prior to testing the histones.

7.2.1 Spectrophotometric analysis

The turbidity and hence concentration of bacterial cultures can be assessed spectrophotometrically using absorbance at 600nm (or 630nm when using automated plate reader). An advantage of this approach is that it can be performed at relatively high-throughput using a small amount of reagents in a 96-well plate format. In addition, bacterial growth can be assessed at multiple time points. Two bacteria including *S. mutans* (ATCC 25175) which has previously been reported to be susceptible to killing by histone H2A (Park *et al.* 1998b), in addition to *E. faecalis* (ATCC 29212) which has also been reported susceptible to histone H1 killing (Rose *et al.* 1998), were incubated with penicillin-streptomycin overnight and absorbance at 600nm measured (Figure 76). Optical density

readings displayed a dose-dependent reduction in detected bacterial growth as the concentration of penicillin-streptomycin was increased up to 0.5µg/ml.

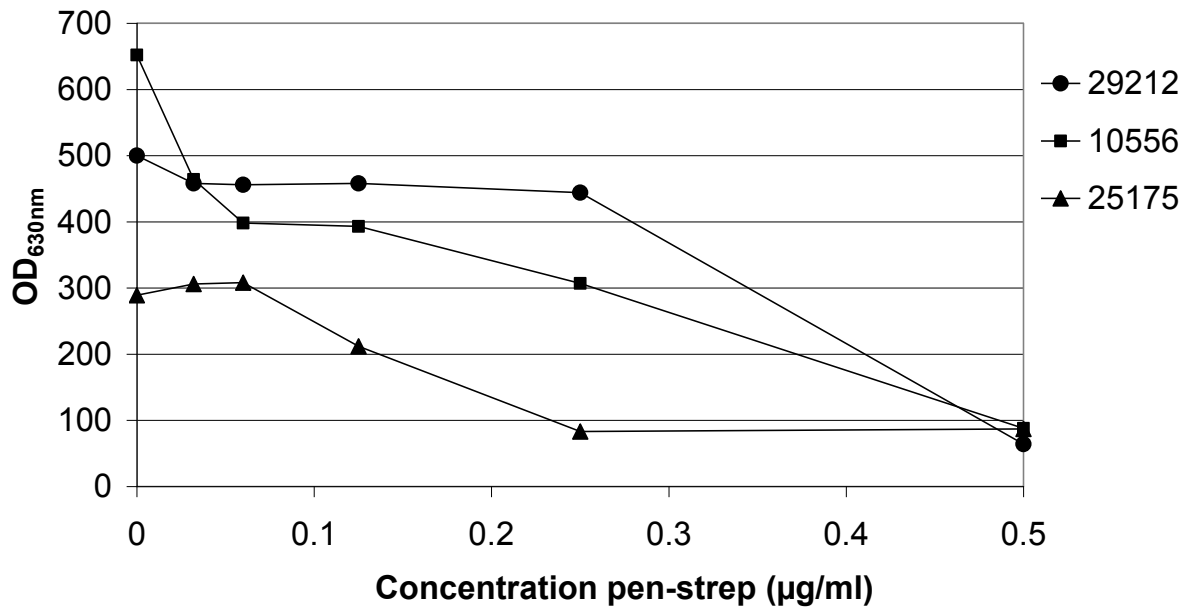


Figure 76. Spectrophotometric analysis of overnight growth of three bacteria in the presence of pen-strep (0-0.5 units penicillin and 0-0.5 µg streptomycin per ml). Bacteria (29212 *E. faecalis*, 10556 *S. sanguis*, 25175 *S. mutans*) were incubated anaerobically overnight prior to measurement of absorbance at 630nm. Results show analysis from a single preliminary experiment.

However, when the test substance (mixed histone) was used in place of the positive control (pen-strep), a significant increase in turbidity was immediately observed and obscured any changes in bacterial growth which could be assayed using this approach. The increased optical density of un-inoculated (negative control) bacterial broth upon the addition of histone is demonstrated in Figure 77 and displays a dose dependant increase, indicating that the turbidity was due to the histone proteins present.

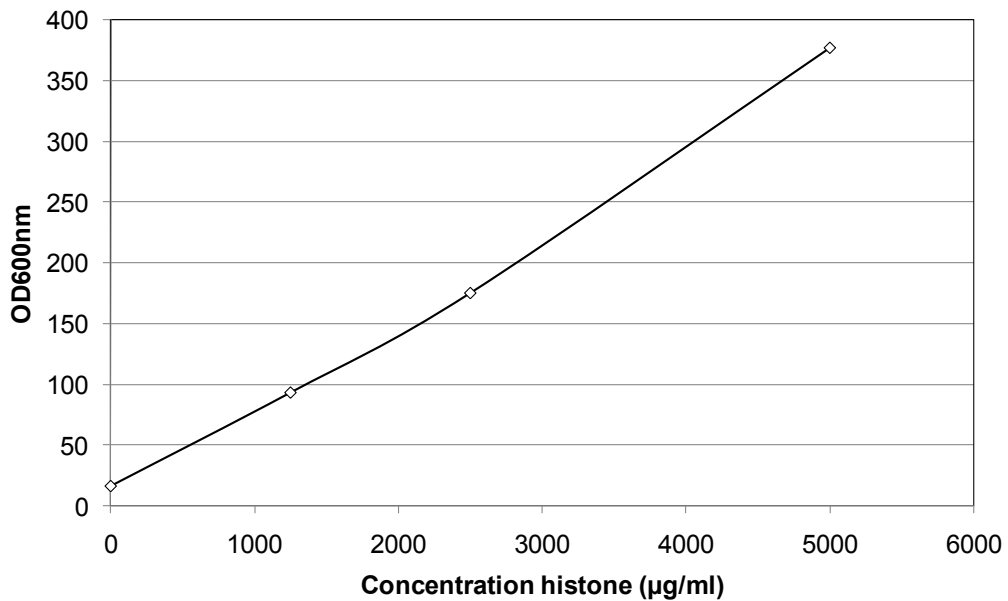


Figure 77. Spectrophotometric analysis of histone (0-5000µg/ml) in un-inoculated bacterial broth incubated overnight. Optical density measured at 630nm. Results show analysis from a single preliminary experiment.

7.2.2 Plating method (colony count)

As the addition of histone caused significant increases in turbidity measurements, bacterial growth from overnight cultures in microtitre plates could not be determined by absorbance measurements. Therefore a sample of overnight broth culture was obtained and serial dilutions were made for plating onto agar to enable colony counts for bacterial cell number determination. Inoculated plates were incubated anaerobically prior to colony counts being performed.

Incubation with penicillin-streptomycin and subsequent colony count analysis (Figure 78) of bacterial cultures used for spectrophotometric analysis (Figure 76) demonstrated a similar dose-dependent reduction in detected bacterial growth. The highest concentration of

penicillin-streptomycin used (0.5 µg streptomycin and 0.5 units penicillin per ml) resulted in no detectable growth of the 3 test bacteria

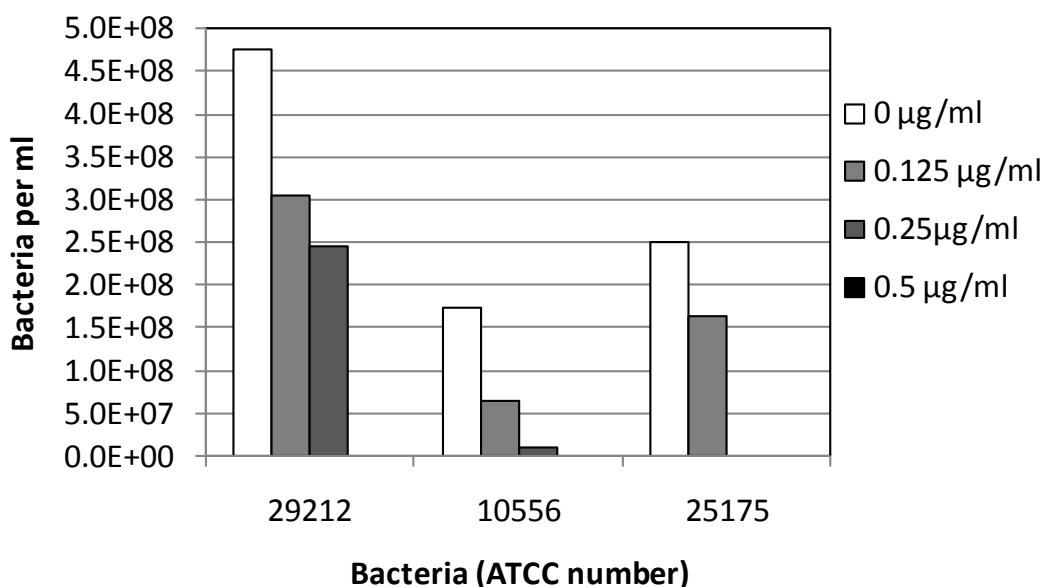


Figure 78. Colony count analysis of overnight cultures of three bacteria exposed to pen-strep (0-0.5units penicillin and 0-0.5µg streptomycin per ml). Bacteria (29212 *E. faecalis*, 10556 *S. sanguis*, 25175 *S. mutans*) were incubated anaerobically overnight in 96-well microtitre plates and a sample used to make 3 serial dilutions for plating onto agar. Results are derived from a single preliminary experiment.

As data indicated that a colony count approach was able to accurately determine the effect of antibiotics on bacterial growth (Figure 77), bacteria were subsequently grown in the presence of histones prior to plating. As previous publications have analysed the antimicrobial effect of purified histone H2A at concentrations up to 30µg/ml (Brinkmann *et al.* 2004) and as multiple histones are associated with genomic DNA, mixed histone was used here comprising all 4 core histone nucleosome subunits (H2A, H2B, H3 and H4) at a concentration of 100µg/ml. The three bacteria previously analysed (*S. mutans*, *E. faecalis* and *S. sanguis*) were initially tested in this assay in addition to two further periodontal pathogens (*F. nucleatum* and *S. oralis*). Results were expressed as a percentage of growth detected in the absence of the antimicrobial agent (Figure 79). Data represents 7 independent experiments although data was only obtained on 2-5 occasions for each bacterial strain (Figure 79). This

relatively low success rate and large spread of data points (represented by the standard deviation) for certain bacteria was likely due to the variability in oxygen exposure incurred during processing.

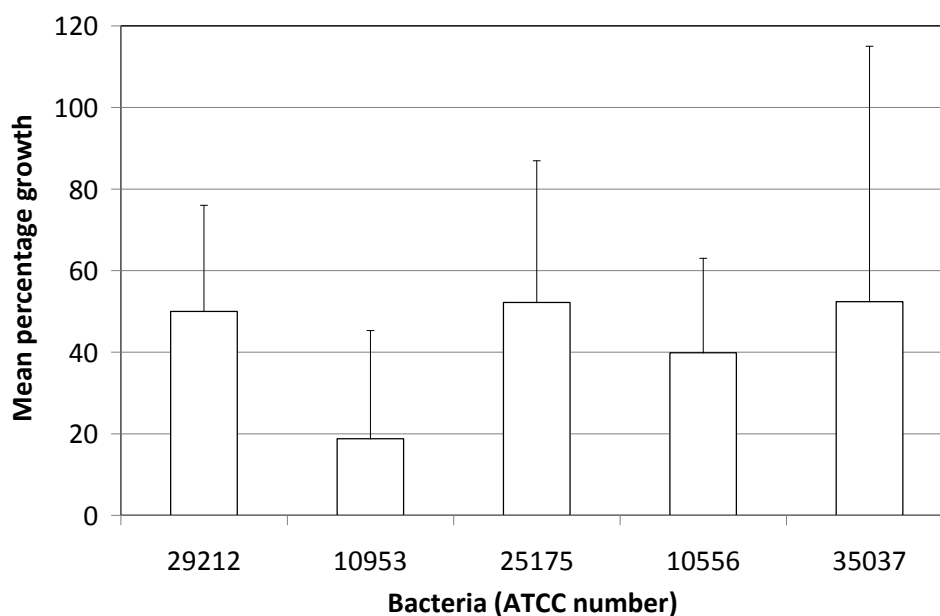


Figure 79. Percentage growth of periodontal pathogens with mixed histone (100µg/ml) measured by plating out method. A panel of 5 bacteria (29212 *E. faecalis*, 10953 *F. nucleatum*, 25175 *S. mutans*, 10556 *S. sanguis*, 35037 *S. oralis*) were incubated overnight with mixed histone in a 96 well plate before serial dilution and plating out. Results expressed as percentage of growth in the absence of histone and represent mean of up to 5 independent experiments \pm SD.

7.2.3 Fluorometric quantification of bacterial growth

The SYTOX[®] green fluorescent nucleic acid stain (Invitrogen) can be used to indicate the presence of dead cells and can therefore be used in conjunction with fluorometric analysis to quantify the number of dead bacteria in a culture. Bacteria were cultured in microtitre plates overnight and the plate was subsequently processed by freeze-thawing, which in addition to the exposure to oxygen, ensured bacterial killing. Initially the sensitivity of this method for bacterial quantification was tested using a culture of a single strain of bacteria (*F. nucleatum*)

stained with 5µM SYTOX[®] green (Figure 80). Data demonstrated a dose-dependant increase in fluorescence as bacterial concentration increased. A plateau phase within the graph was observed at concentrations above 5×10^5 bacteria/ml indicating saturation of the assay system. Bacterial concentrations below this displayed a linear range of fluorescence and therefore this range was used in subsequent assays for antimicrobial activity (range is indicated by dashed box, Figure 80).

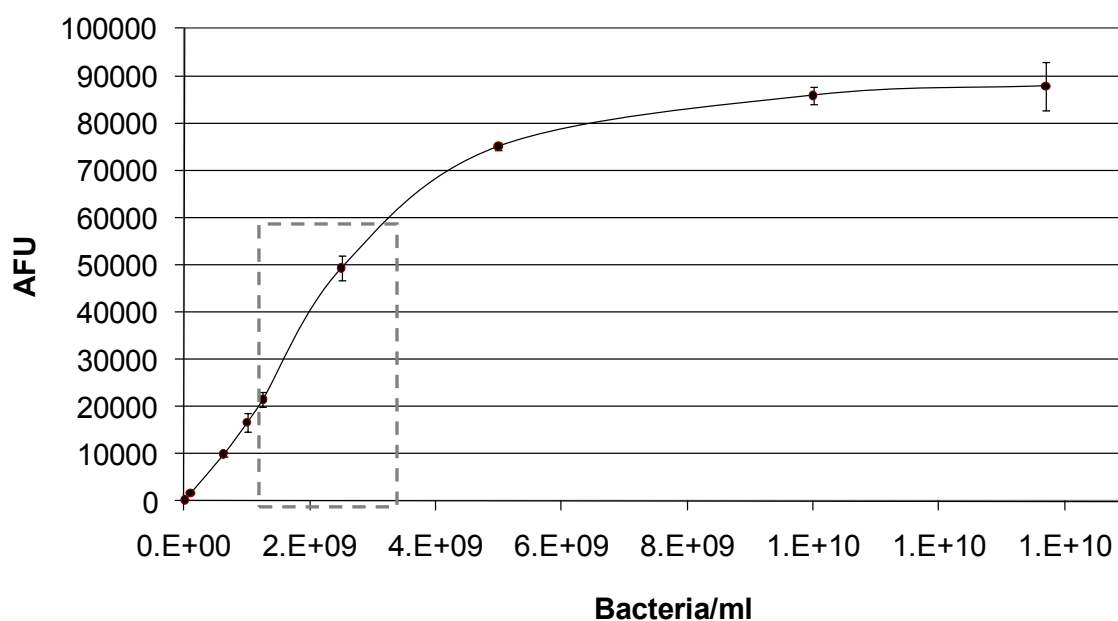
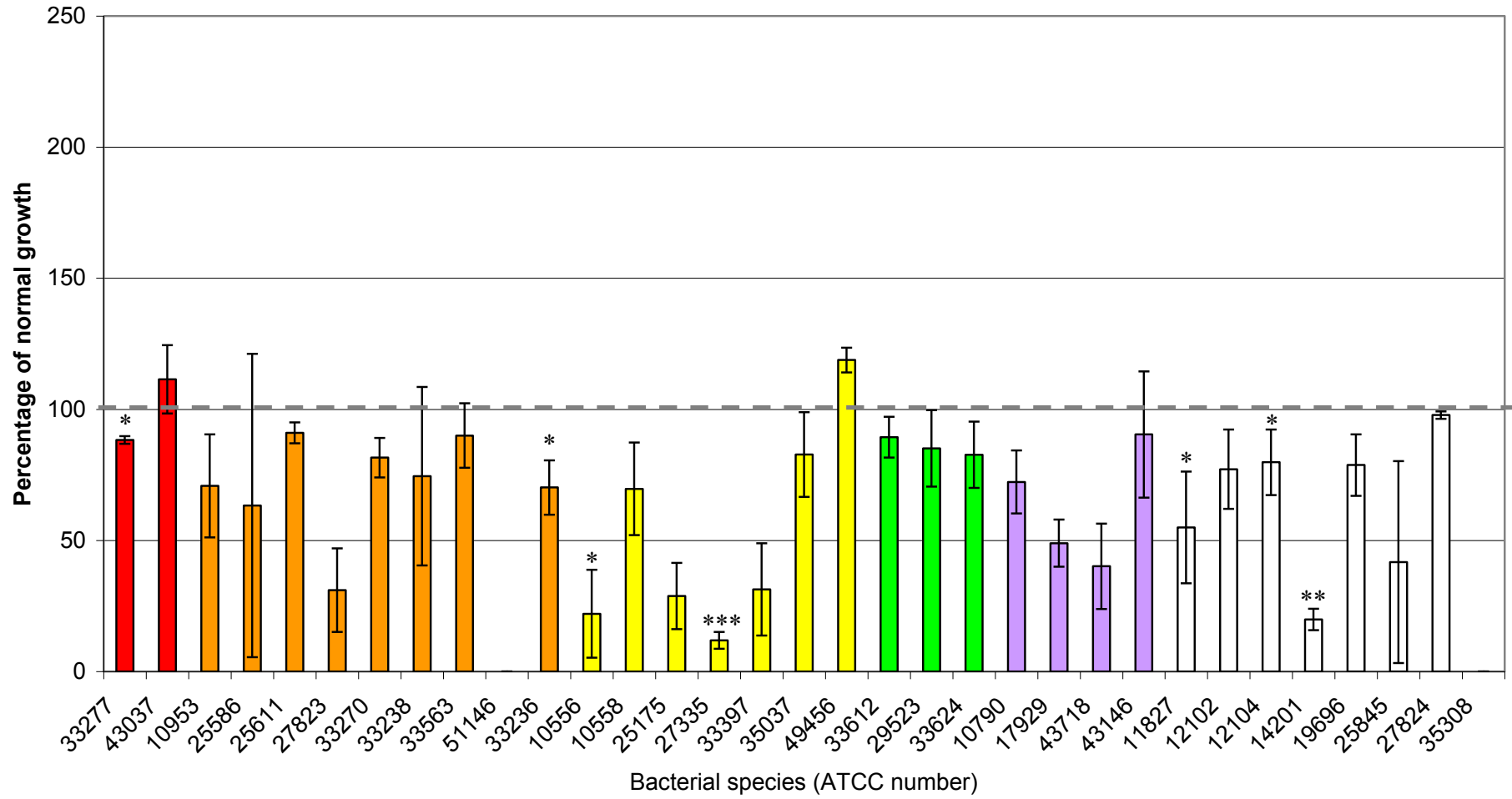


Figure 80. Standard curve of SYTOX[®] detection of *F. nucleatum* subsp. *polymorphum*. Concentration of bacteria estimated by spectrophotometry and diluted to concentrations displayed on x-axis. 25µl sample then stained with SYTOX[®] 5µM in 200µl total volume, and fluorometer reading taken at 10mins. Results show mean of experiment performed in triplicate \pm SD. Dashed box represents range of fluorescence in antimicrobial assay, Figure 81.

2×10^4 bacteria per well were incubated overnight with no antimicrobial (negative control), 10units/ml penicillin-streptomycin (positive control) or the test agent (mixed histone 100µg/ml). Subsequent fluorometric quantification of a 25µl sample was used to assess growth in the presence of the antimicrobial and test agents, and represented as a percentage of bacterial growth in the absence of any antimicrobial (Figure 81). Two bacteria proved difficult to routinely culture in broth and therefore no data were obtained for 35308 *P*.

denticola and 51146 *C. Showae*, and only a single strain of *P. acnes* (11827) was assayed. The remaining 31 bacteria were successfully grown in broth culture and the majority appeared susceptible to killing by the positive control agent (penicillin-streptomycin) with the exception of 27824 *G. morbillorum*, 43037 *T. forsythensis* and 49456 *S. mitis* (Figure 81a). The addition of mixed histone also appeared to cause a reduction in the growth of 21 out of the 31 bacteria (Figure 81b). Notably 13 of these bacteria exhibited $\leq 50\%$ growth in the presence of mixed histone compared to normal bacterial growth. However, a small selection of bacteria (6 out of 31) exhibited increased growth in the presence of histones. This increased growth was most dramatic for 33277 *P. gingivalis*, 10558 *S. gordonii* and 33397 *S. anginosus*, followed by 10556 *S. sanguis*, 27823 *S. constellatus* and 27335 *S. intermedius*. The growth of a further 4 out of 31 bacteria appeared unaffected by the addition of histone. Interestingly, all 10 bacteria which appeared resistant to killing by histone (unaffected or increased growth) were from the red, orange and yellow microbial complexes associated with increased disease severity in periodontitis. All bacteria tested from the green, purple or non-colour coded complexes appeared susceptible to killing by histone.

a) penicillin-streptomycin



b) mixed histone

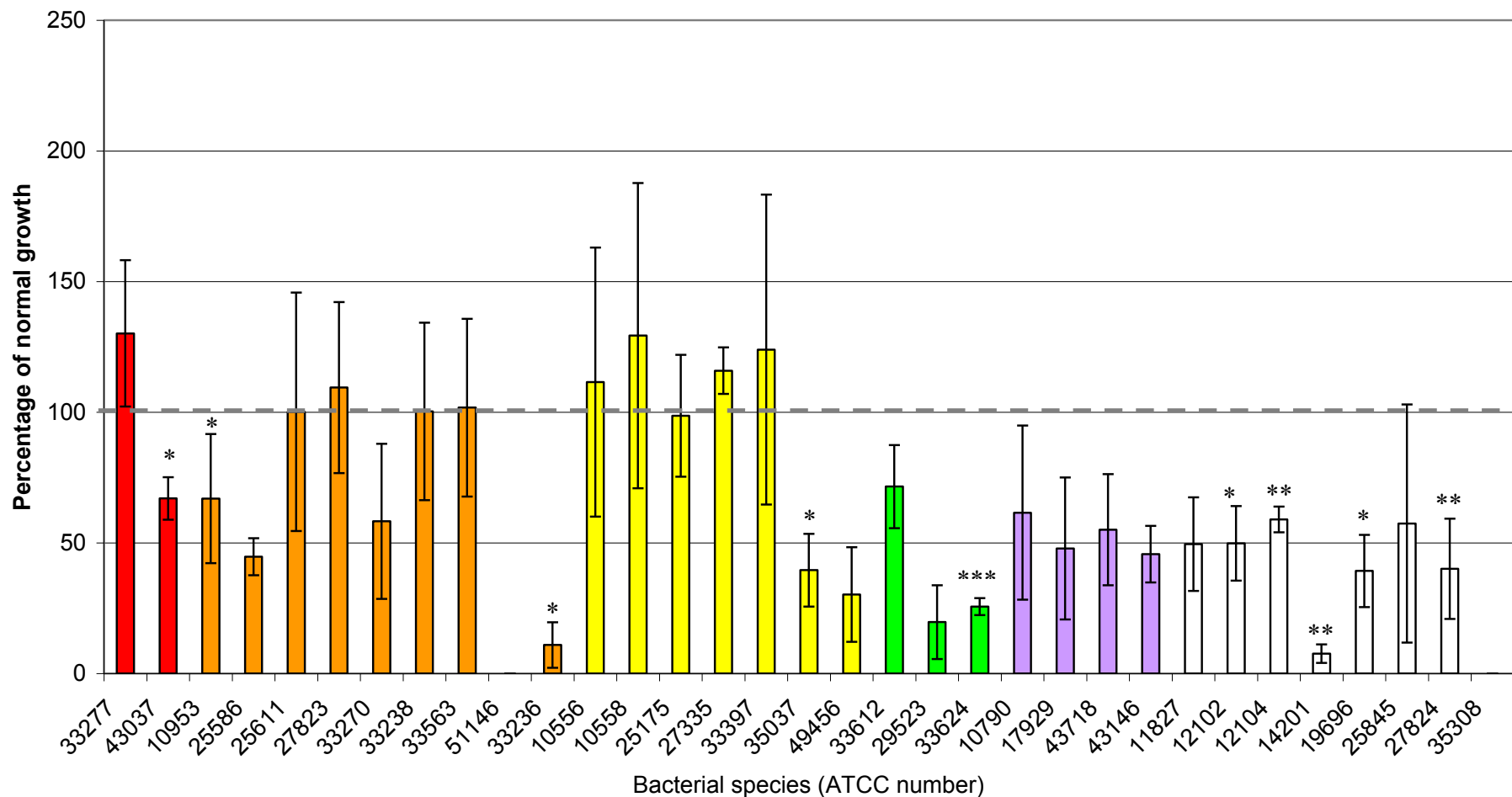


Figure 81. Fluorometric quantification of the antimicrobial activity of a) penicillin-streptomycin (10units penicillin and 10µg streptomycin per ml) and b) mixed histone (100µg/ml) against 33 periodontal pathogens grouped by colour complex (Socransky *et al.* 1998). Results show mean of 3 independent experiments performed in triplicate ± SD. Fluorescence of wells not containing bacteria were subtracted and fluorescence expressed as percentage of normal overnight growth (i.e. in the absence of pen-strep). Dashed line indicates 100% of normal growth i.e. no change. * P≤0.05, ** P≤0.01, * P≤0.001 by paired T-test of non-transformed data.**

Discussion

Identification of bacteria

When utilising a large panel of different bacterial strains it is appropriate to characterise them to provide evidence of their identity. Combined the data presented here supported the identity of the majority of the bacteria used in this study (Table 12). A variety of complementary tests were chosen which utilise diverse characteristics and properties of the bacteria. For example the genotype of the bacteria were examined by species specific PCR (Figure 73) which was a preferred method for identification as this characteristic is highly conserved and therefore generally robust; however this approach was not available for all bacteria. The phenotype of the bacteria was examined by the catalase test (Table 11) and Gram stain (Figure 74), although these characteristics are known to be variable, subject to change and can be influenced by factors such as the pH, temperature or nutrient availability of the growth conditions. Indeed even aging of the bacterial culture can result in an alteration in phenotypic appearance (Holt 1994). Although phenotypic characterisation is the most commonly used method in diagnostic laboratories for the identification of bacterial strains, this approach relies upon a range of tests specific to each bacteria (Duerden *et al.* 1998). When screening a large panel of bacteria it is more practical to use tests which could be applied to the entire panel of bacteria. The final mode of identification used here was morphological characterisation which, whilst being highly subjective, is useful for the discrimination of particular bacteria such as the black pigmented strains.

Susceptibility to killing by histone

The degranulation of neutrophils as an antimicrobial defence mechanism is well known, however, the more recently described phenomenon of NET release involves the release of not only antimicrobial proteins but also nuclear chromatin. A proposed reason for the presence of chromatin within the NETs is to provide a scaffold on which the antimicrobial proteins can adhere along with the trapped microorganisms. However, an antimicrobial activity of the chromatin core has been demonstrated based on the apparent increased survival of microorganisms in NETs treated with anti-histone antibodies (Brinkmann *et al.* 2004; Guimaraes-Costa *et al.* 2009). Experiments here initially attempted to use a spectrophotometric approach to determine relative bacterial growth in the presence and absence of histone proteins. However, when the histone protein was combined with the culture media a visible 'cloudy' precipitate was apparent even in the absence of bacteria. The acid solubility of histones is commonly exploited for their extraction and therefore the precipitate may be due to a sub-optimal pH of the culture media (Shechter *et al.* 2007). Therefore, bacterial growth was subsequently quantified fluorometrically based on staining of total bacterial DNA which revealed a reduction in growth of 21 out of the 31 bacteria tested. It is hypothesised that histones function in a similar way to other cationic neutrophil-derived AMPs such as defensins, in that they permeabilise the bacterial membrane resulting in cell lysis (Birkemo *et al.* 2003). Alternatively, it has been reported that a peptide related to histone H2A (Bforin I) exerts its effect by crossing the bacterial membrane and binding intracellularly to the bacterial DNA (Park *et al.* 1998a). Significantly however, the data presented here also revealed the growth of 7 bacterial strains to be increased in the presence of mixed histone. In addition, the positive control antimicrobials used did not inhibit the growth of all bacteria tested to the same degree, and appeared to have no effect on the growth

of 3 of the bacteria at the concentrations applied here. This data is in concordance with widespread research indicating that every bacterial strain has a different minimal inhibitory concentration (MIC) when tested with the same antimicrobial (Al-Haroni *et al.* 2006).

The findings presented here (Figure 81) and previously (Brinkmann *et al.* 2004) were obtained using purified histones which are proposed to exert their effect via the strong cationic charge of the proteins resulting from the relative abundance of lysine and arginine residues. This positive charge is vital to its function in the packaging of negatively charged DNA, however, in NETs where the histone protein is found complexed with DNA, the opposing charges may neutralise each other casting doubt on the *in vivo* relevance of histone microbicidal activity. Indeed, one of the earliest reports of the antimicrobial activity of histone described a reduction in the killing efficacy of histone in the presence of nucleic acid (Hirsch 1958). An *in vivo* antimicrobial role within NETs was identified by the use of anti-histone (H2A/H2B) antibodies which allowed increased survival of microorganisms (Brinkmann *et al.* 2004; Guimaraes-Costa *et al.* 2009), although whether this effect was due to neutralisation of direct antimicrobial activity of the histone proteins or due to physical obstruction of microorganism immobilisation and killing by the granule proteins instead, is unclear. As the other core component of NETs is DNA, future work could examine the antimicrobial potential of this molecule. Indeed, reports exist describing an antimicrobial action of extracellular DNA against *P. aeruginosa*, *S. aureus* and *E. coli* (Mulcahy *et al.* 2008). This is thought to function via chelation of oppositely charged ions (cations in this case) which removes LPS-associated Mg^{2+} from its stabilising role in the outer membrane of the bacteria. When this membrane becomes unstable cell lysis occurs. Furthermore, it is reported that certain bacteria such as *P. aeruginosa* possess virulence factors, triggered by low

Mg²⁺ concentrations resulting from chelation by DNA, to modify the LPS structure and protect against membrane disruption (Mulcahy *et al.* 2008).

CHAPTER 8 RESULTS

DNase expression by periodontal pathogens and in dental plaque

8.1 DNase expression by periodontal pathogens

The pathogenic microbial subgingival flora of periodontal disease is characterised by a predominance of Gram negative anaerobes which have also been reported to exhibit significant DNase activity (Porschen and Sonntag 1974). As the function of NETs can be destroyed by bacterial DNases which leads to increased pathogenic activity of the bacteria *in vivo* (Beiter *et al.* 2006; Buchanan *et al.* 2006), 34 anaerobic and facultative anaerobic bacteria reported to be important in periodontal disease pathogenesis were screened for extracellular DNase expression using two complementary approaches,

- i) DNase test plates
- ii) Assay by agarose gel.

DNase test plate analysis enabled detection of culminative DNase expression by bacteria grown in a solid biofilm state, i.e. on agar plates. Assay of DNase activity by agarose gel electrophoresis analysis following broth culture enabled determination of DNase expression by bacteria grown planktonically, i.e. in broth culture.

8.1.1 DNase test plate assay

DNase test plates are commercially available agar plates supplemented with mammalian DNA as the substrate for the DNase enzyme. Hydrolysis of the DNA is detected by flooding the plate with hydrochloric acid, or the metachromatic dye, toluidine blue O (TBO) as applied here. DNase test plates are used diagnostically for the detection of pathogenic staphylococci and therefore *Staphylococcus aureus* was used as a positive control when screening the 34 periodontal pathogens. As each bacteria grows at a different rate which is also dependant on

the size of the initial spot inoculum, for comparison of activity the area of DNA hydrolysis was normalised to the area of bacterial growth (mm² of hydrolysis per mm² bacterial growth).

8.1.1.1 Duration of incubation of test plates

Previous reports using DNase test agar to grow and assay for DNase activity in anaerobic pathogens involved bacterial incubations for between 48 hours and 5 days prior to assay (Porschen *et al.* 1974; Rudek *et al.* 1976; Brailsford *et al.* 1999). Therefore, initially a preliminary experiment was performed to determine the necessary incubation time for periodontal bacteria on the DNase test agar plates using a randomly selected panel of 6 pathogens. TBO staining was performed at days 2 to 6 post-inoculation (Figure 82). Three of the bacteria demonstrated detectable DNase activity after 2 days growth (*P. melaninogenica*, *S. anginosus* and *S. intermedius*), however, *S. sanguis* and *C. gingivalis* only exhibited detectable activity from day 4 onwards, whilst *S. constellatus* exhibited DNase positivity at day 5. The zone of DNA hydrolysis generated by *S. intermedius* continued to increase throughout the incubation period which may reflect increased DNase production or simply the radial diffusion of the DNase secreted at an earlier time-point during bacterial growth. The zone of DNA hydrolysis produced by *S. anginosus* and *P. melaninogenica* peaked on days 4 and 5 respectively, although levels appeared reduced on subsequent days. This result was likely due to the increased spread of the bacterial colony which may be advancing at a greater rate than the area of DNA hydrolysis at this culture time-point. As DNase expression was evident in all bacterial strains tested by day 5, this time-point was selected as the duration of incubation for all subsequent DNase test plate assays for the anaerobic pathogens.

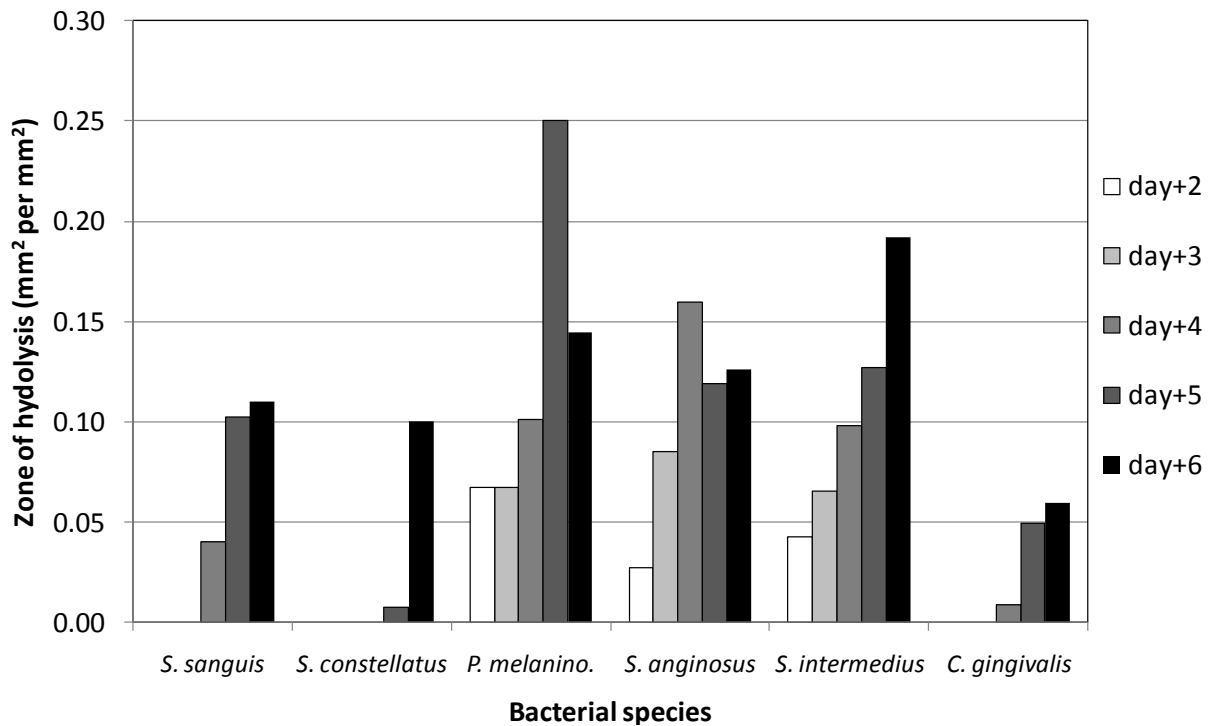


Figure 82. Time-course analysis of the DNase activity of 6 periodontal pathogens detected by DNase test agar plates. Separate plates were incubated anaerobically for 2 to 6 days prior to staining for DNA hydrolysis using TBO. Results presented as mm² hydrolysis per mm² bacterial colony growth and are derived from a single preliminary experiment.

8.1.1.2 Plate-based assay of periodontal pathogens

Subsequently, the panel of 34 periodontal pathogens were incubated for a standard 5 day period on DNase test agar plates, which were stained and the zone of DNA hydrolysis quantified as described (Figure 83). Thirteen of the 34 bacteria tested exhibited positive DNase activity. Notably the majority of these DNase positive pathogens (10 out of 13) represented the colour-coded groups previously associated with periodontitis pathogenesis (Socransky *et al.* 1998).

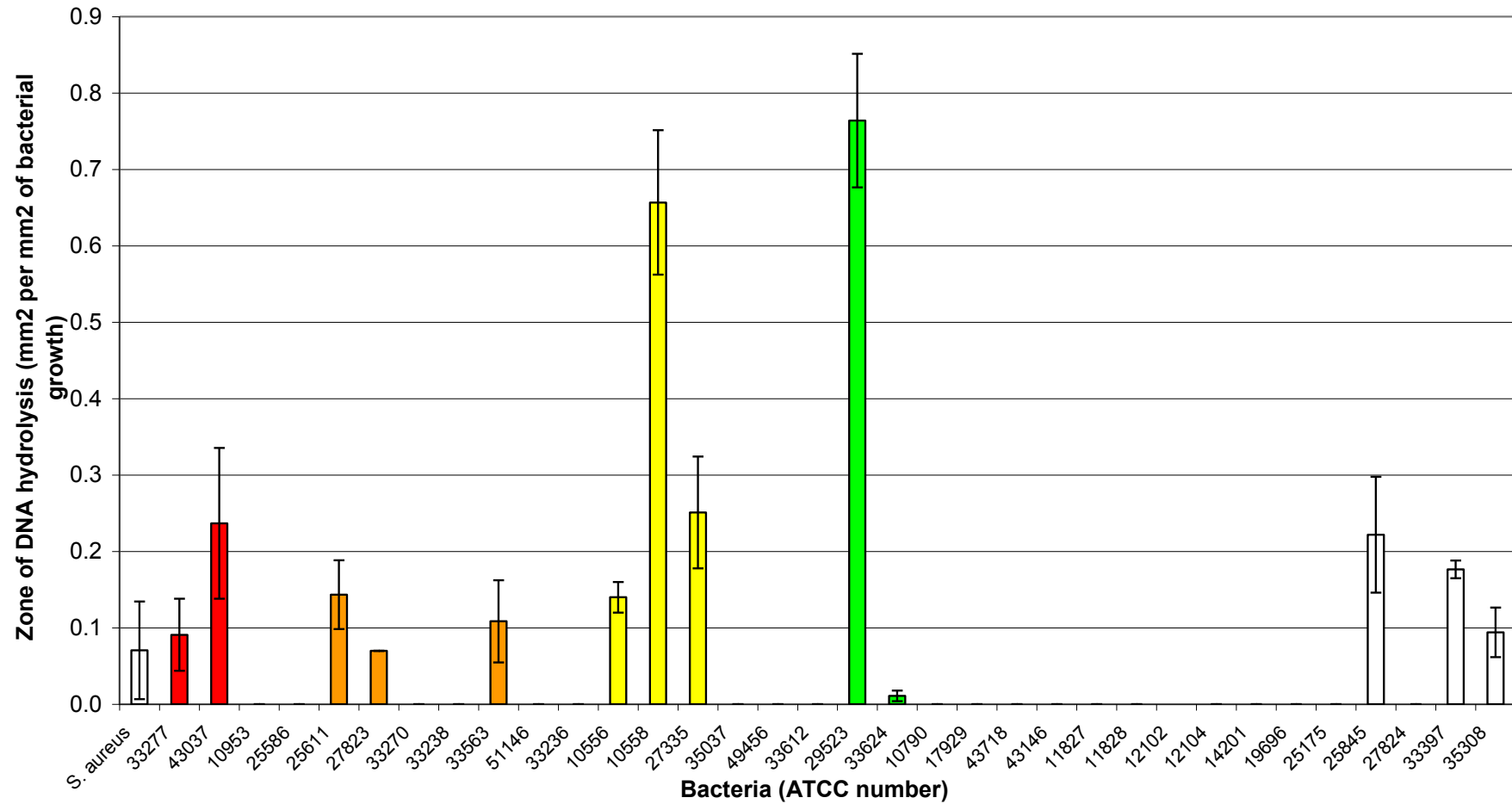


Figure 83. Zone ratio of DNA hydrolysis after 5 days growth on DNase test agar plates. Thirty-four periodontal pathogens identified by ATCC number and grouped by colour complex (Socransky *et al.* 1998). Digital photographs were analysed to provide the area of TBO stained hydrolysed DNA per area of bacterial growth. Results show mean of 3 independent experiments \pm SD.

8.1.2 ‘Gel-based assay’ of DNase activity in bacterial broth culture

To assay DNase activity of planktonically grown bacteria a sample (supernatant or pellet; 2.7.2.1) was incubated with mammalian DNA for 2 hours before visualisation on agarose gel to assess the extent of DNA degradation.

8.1.2.1 Optimum duration of ‘gel-based assay’

To enable the comparison of DNase activity levels between bacterial species, the duration of incubation needed to be standardised so that DNA digestion was visibly detectable. Therefore one DNase positive bacteria (*P. intermedia* ATCC 25611) and one DNase negative bacteria (*C. gracilis* ATCC 33236), as demonstrated by DNase test plate assay (Figure 83), were incubated with calf thymus DNA for between 30 minutes and 4 hours (Figure 84). A control ‘no DNase’ sample was also assayed to demonstrate intact DNA of a high molecular weight. The reaction containing the DNase negative bacteria, *C. gracilis*, indicated visible undigested high molecular weight DNA, demonstrating no DNase contamination of the bacterial broth. The resultant DNA from both of the DNase negative reactions (*C. gracilis* and blank) remained unchanged throughout the incubation period at 37°C. The DNase positive bacteria displayed DNA degradation as early as 30 minutes and was visualised as smearing of the DNA on the gel. After 1 hour incubation the DNA exhibited decreased intensity indicating partial DNA digestion, whilst after 2 hours DNA was not visible indicating complete digestion. Therefore, a 2 hour incubation period was chosen to provide the greatest sensitivity to detect DNase activity in bacteria producing levels equivalent to, and lower than, *P. intermedia*.

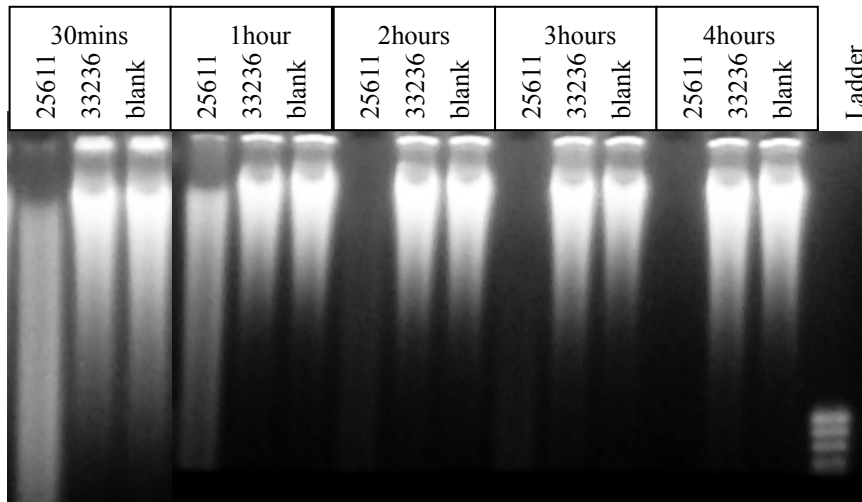


Figure 84. Time-course analysis of DNA degradation visualised by ethidium bromide stained agarose gel electrophoresis. DNase positive bacteria (ATCC 25611), DNase negative bacteria (ATCC 33236) and blank containing no bacterial sample. Ladder - PCR ranger 100bp DNA ladder (Bioline). High molecular weight calf thymus genomic DNA was used for assay.

8.1.2.2 DNase standards

The 34 periodontal bacteria available were grown in broth cultures for 6 days and subsequently the bacteria were pelleted and washed whilst a sample of the broth culture supernatant was collected. For this approach the pellet and supernatant were assayed separately to distinguish between membrane bound DNase and secreted DNase activity respectively. For this assay the pellet was suspended in PBS whilst the supernatant was composed of bacterial broth. To determine if the diluent affected the detected DNase activity, DNase standards (bovine pancreatic DNase) were suspended in either PBS or sterile tryptone soya broth and assayed.

Bovine pancreatic DNase (Sigma) was used as positive control for this assay and by using a range of known concentrations a standard curve was generated based on the distance migrated

on gel electrophoresis by the DNA digestion front, to enable estimation of DNase concentration in test samples. A range of between 0.5 and 250 Kunitz/L bovine pancreatic DNase was diluted in PBS (the diluent of bacterial pellet samples) and also diluted in media (the diluent of bacterial supernatant samples) (Figure 85). DNase in media resulted in visibly increased digestion of the DNA within the 2 hour assay period as compared with the equivalent concentration diluted in PBS (Figure 85a). Gel images were binarised using ImageJ and the distance the DNA migrated from the well was measured in pixels (Figure 85b) to enable the generation of a standard curve (Figure 85c), from which the DNase activity of test samples could be estimated. As the composition of the bacterial media allowed more rapid DNase enzymatic activity compared with the PBS diluent, the DNase assay for bacterial supernatant samples was subsequently more sensitive than the assay of bacterial pellets. For example, 4Kunitz/L DNase in PBS showed no detectable digestion of DNA in the 2 hour incubation period, however, 4Kunitz/L DNase diluted in sterile media demonstrated considerable degradation of the DNA as no fragments remained visibly intact.

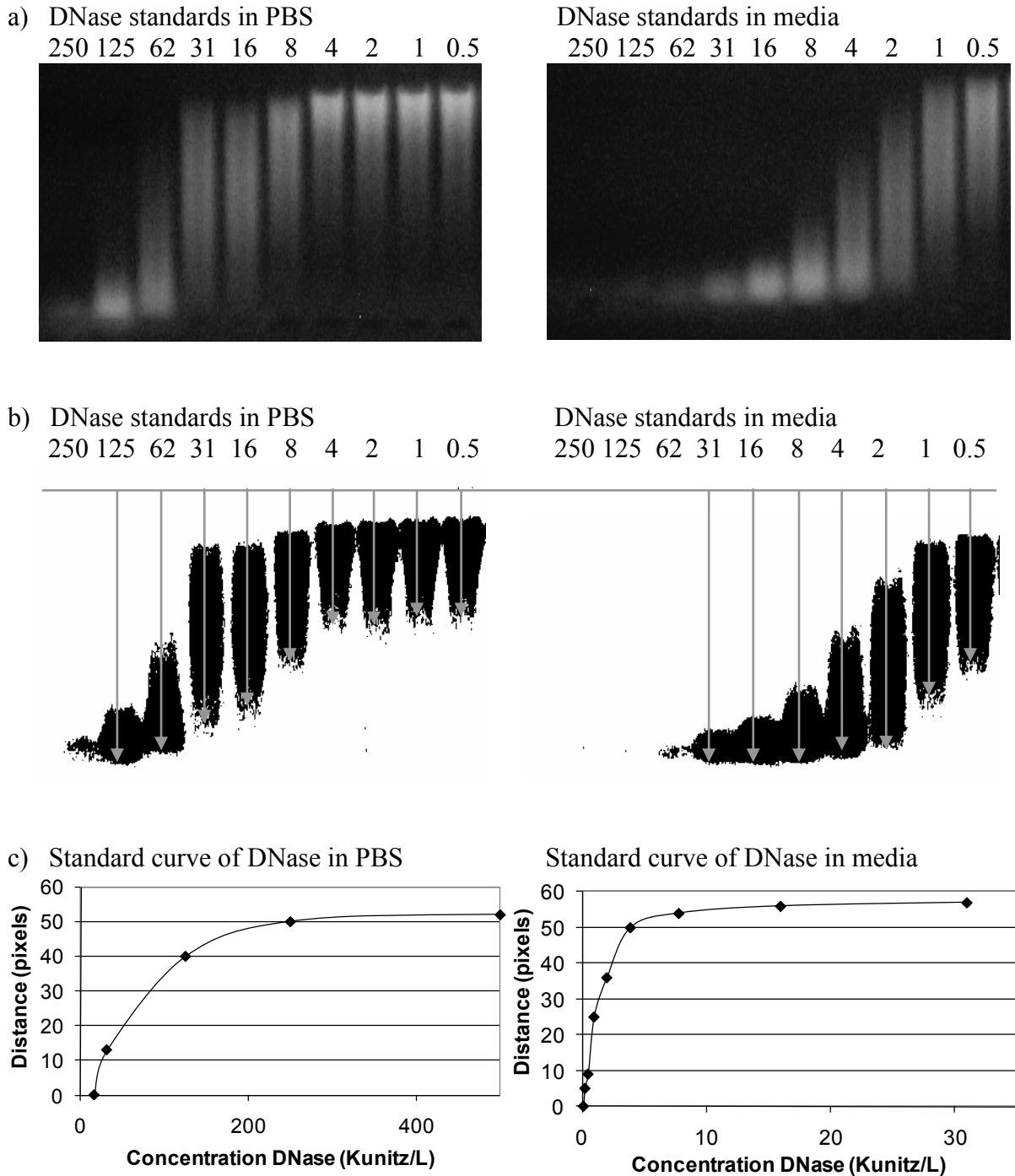
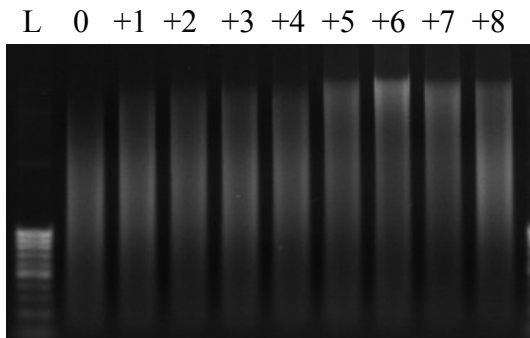


Figure 85. DNA degradation by bovine pancreatic DNase standards (0.5-250 Kunitz/L) in PBS or culture media. a) Visualisation of DNA degradation by ethidium bromide gel electrophoresis, Kunitz/L values are shown above each lane, b) Binarised image of agarose gel (using ImageJ), red arrows show distance measured in pixels from well to front of DNA band c) Standard curve of distance migrated in pixels plotted against concentration of bovine pancreatic DNase.

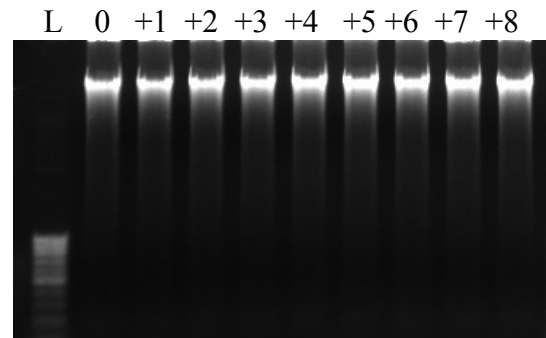
8.1.2.3 Stability of DNase

It is recommended that purified bovine pancreatic DNase (D4263 Sigma) is stored at -20°C as reportedly storage at 4°C at a concentration of 10mg/ml can result in a loss of ~20% activity per week (Sigma). It was therefore hypothesised that if bacteria were cultured in broth for 6 days at 37°C, DNase that was secreted early in the culture period may have lost significant activity prior to time of assay. To investigate whether the gel-based assay of broth cultures of bacteria was likely to detect only DNase produced immediately prior to harvest or detect cumulative DNase expression throughout bacterial growth, bovine pancreatic DNase was diluted into sterile culture media, incubated anaerobically at 37°C and an aliquot taken daily for gel-based assay of DNase activity (Figure 86). No reduction in the potency of DNase degradation of DNA was detectable between DNase at day 0 compared to DNase following 8 days incubation at 37°C. This data therefore indicated that it was reasonable to culture bacteria for 6 days prior to harvest and subsequently assay of DNase.

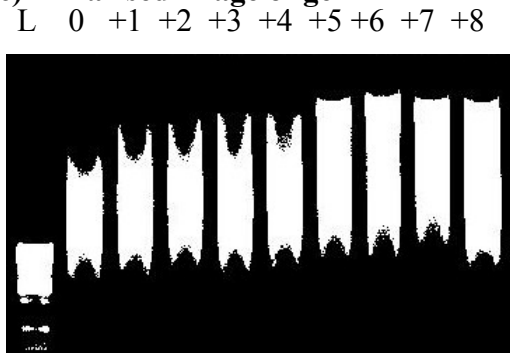
a) 10 Kunitz/ml DNase in media



b) 0 kunitz/ml DNase (media only)



c) Binarised image of gel



d) Distance migrated

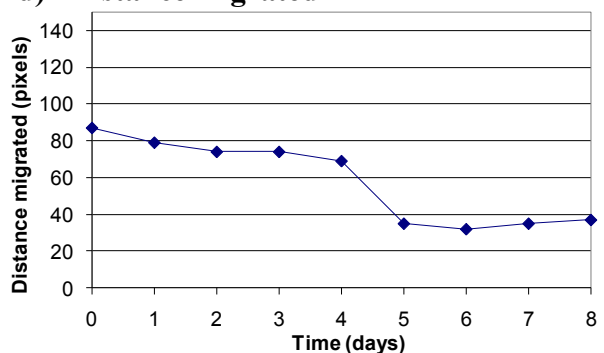


Figure 86. Degradation of bovine pancreatic DNase at 37°C anaerobic incubation in sterile media. **a)** 10 Kunitz/ml DNase in media **b)** no DNase (negative control), **c)** Image analysis of DNase positive gel, and **d)** graphical data showing distance migrated. Samples of DNase were collected daily for 8 days (time points shown above gel images a-c) and assayed by gel-based DNase assay. DNA end products were visualised following electrophoresis on ethidium bromide stained agarose gel. L = PCR ranger 100bp DNA ladder (Bioline).

8.1.2.4 Gel-based assay of periodontal pathogen DNase activity

Gel-based assay of DNase activity in the bacterial pellet (Figure 87) and supernatant (Figure 88) samples from 34 periodontal pathogens demonstrated that a high number of strains (21 out of 34) exhibited significant activity. All samples were previously adjusted by dilution to 1×10^9 bacteria per ml and supernatants were diluted by the same factor prior to assay of a $10 \mu\text{l}$ aliquot, and subsequently enzymatic activity was expressed in Kunitz per bacteria. The positive control bacterial strain, *S. aureus*, displayed the highest detected DNase activity in both the pellet and supernatant, although the levels detected in the supernatant were

significantly higher (232 Kunitz/bacteria) than those in the pellet (42 Kunitz/bacteria) potentially indicating that DNase is primarily secreted. DNase activity was higher in the supernatant than the pellets for all DNase positive bacteria detected except three which were amongst the lowest producers (including *C. rectus* ATCC 33238, *S. sanguis* ATCC 10556 and *C. sputigena* ATCC 33612). DNase activity in the bacterial pellet was particularly common amongst orange and yellow complex bacteria (Figure 87) (Socransky *et al.* 1998). However, DNase activity of bacterial supernatants did not demonstrate such a clear pattern and the highest DNase producer, *P. melaninogenica* (ATCC 25845), was not from a reported colour complex (Figure 88).

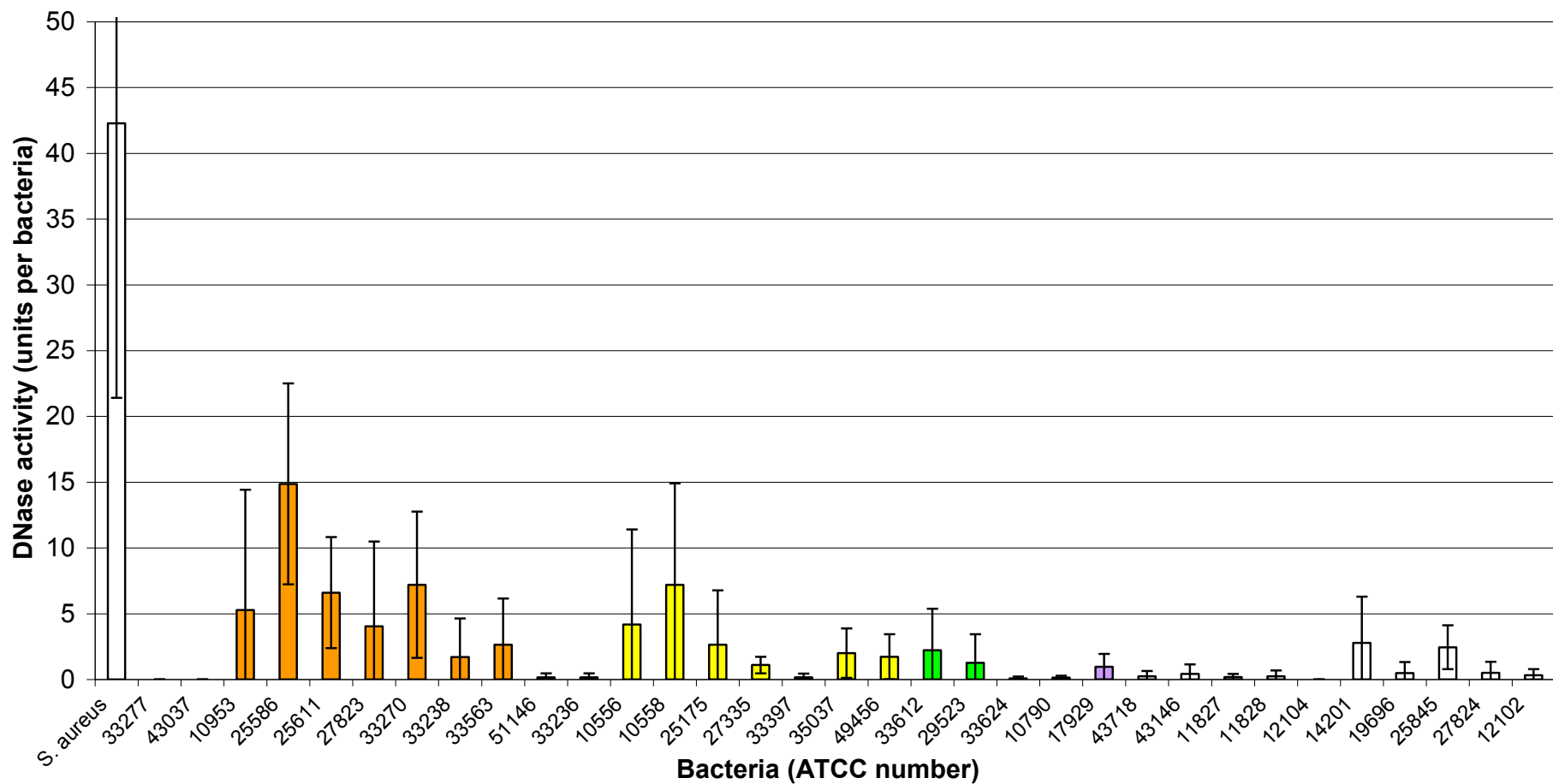


Figure 87. Gel-based assay of membrane bound (bacterial pellet) DNase activity in 34 periodontal pathogens. Bacteria are identified by ATCC number and grouped by colour complex (Socransky *et al.* 1998). *S. aureus* is shown as a positive control for bacterial DNase activity. Bovine pancreatic DNase standards were used to estimate DNase in enzymatic units and is expressed per bacteria. Results show mean of 3 independent experiments \pm SD.

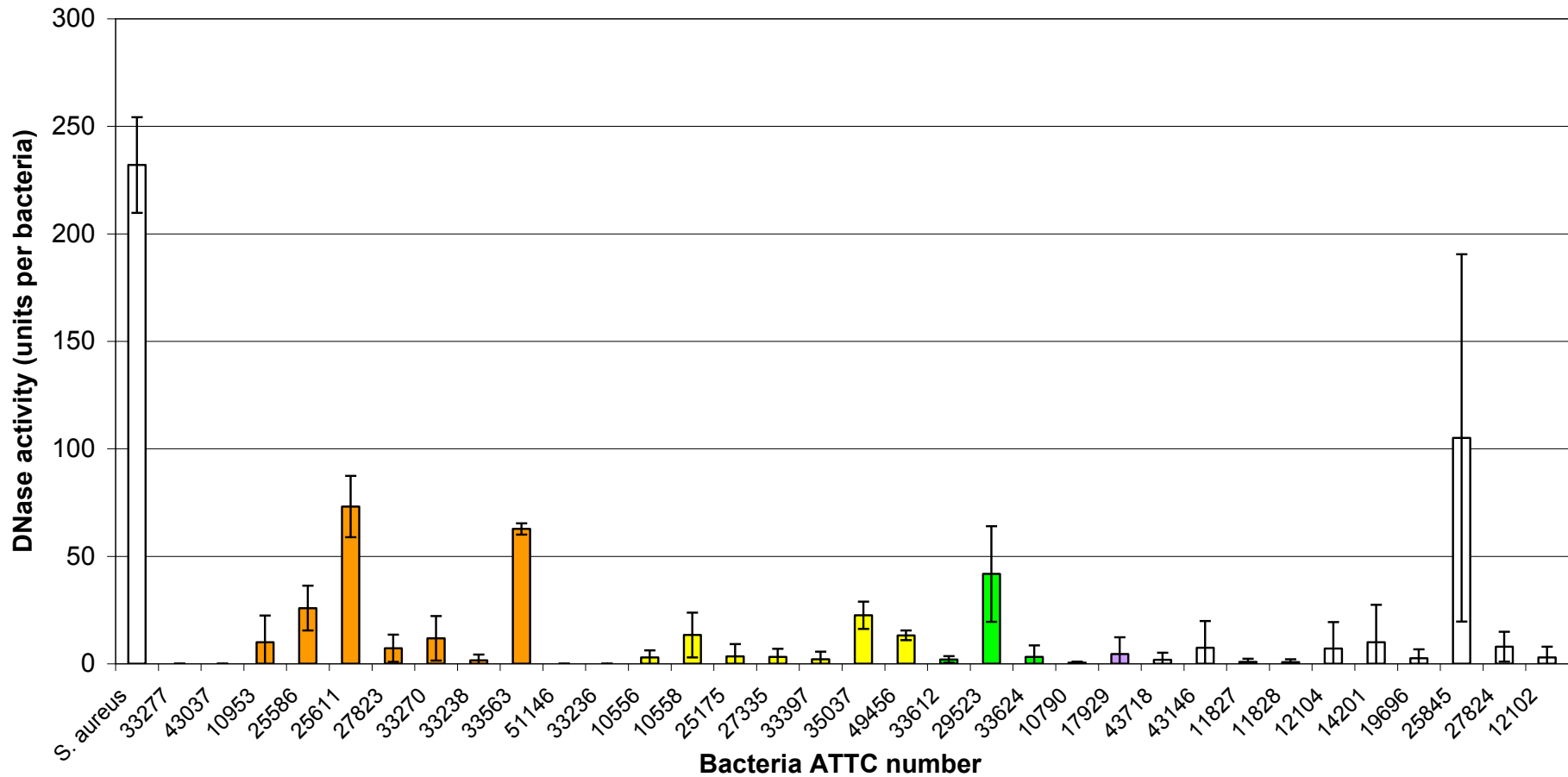


Figure 88. Gel-based assay of secreted (supernatant) DNase expression in 34 periodontal pathogens. Bacteria are identified by ATCC number and grouped by colour complex (Socransky *et al.* 1998). *S. aureus* is shown as positive control for bacterial DNase activity. Bovine pancreatic DNase standards were used to estimate DNase activity in enzymatic units which is expressed per bacteria in the original bacterial culture prior to their removal for separate assay. Results show mean of 3 independent experiments \pm SD.

8.1.3 Summary of DNase expression by periodontal pathogens by both methods

Bacterial DNase activity detected by the two assay methods is summarised in Table 13. A threshold of DNase activity was nominally set at 1 Kunitz/bacteria for the bacterial pellet and 5 Kunitz/bacteria for the supernatant to distinguish 'DNase positive' bacteria from 'DNase negative' bacteria.

Table 13. Summary of detected bacterial DNase expression

ATCC	Bacterial species	Plate-based assay	Gel-based assay	
			Pellet	Supernatant
RED COMPLEX				
33277	<i>P. gingivalis</i>	+	-	-
43037	<i>T. forsythensis</i>	+	-	-
ORANGE COMPLEX				
10953	<i>F. nuc. poly.</i>	-	++	+
25586	<i>F. nuc. nuc.</i>	-	++	++
25611	<i>P. intermedia</i>	+	++	+++
27823	<i>S. constellatus</i>	+	++	+
33270	<i>P. micros</i>	-	++	++
33238	<i>C. rectus</i>	-	+	-
33563	<i>P. nigrescens</i>	+	+	+++
51146	<i>C. showae</i>	-	-	-
33236	<i>C. gracilis</i>	-	-	-
YELLOW COMPLEX				
10556	<i>S. sanguis</i>	+	++	-
10558	<i>S. gordonii</i>	++	++	++
25175	<i>S. mutans</i>	-	+	-
27335	<i>S. intermedius</i>	+	+	-
33397	<i>S. anginosus</i>	+	-	-
35037	<i>S. oralis</i>	-	+	++
49456	<i>S. mitis</i>	-	+	++
GREEN COMPLEX				
33612	<i>C. sputigena</i>	-	+	-
29523	<i>A. actino. a</i>	++	+	+++
33624	<i>C. gingivalis</i>	+	-	-
PURPLE COMPLEX				
10790	<i>V. parvula</i>	-	-	-
17929	<i>A. odontolyticus</i>	-	+	-
43718	<i>A. actino. b</i>	-	-	-
43146	<i>A. viscosus</i>	-	-	+
OTHER BACTERIA				
11827	<i>P. acnes</i>	-	-	-
11828	<i>P. acnes</i>	-	-	-
12102	<i>A. israeli</i>	-	-	-
12104	<i>A. naeslundii</i>	-	-	+
14201	<i>L. buccalis</i>	-	+	+
19696	<i>N. mucosa</i>	-	-	-
25845	<i>P. melanino.</i>	+	+	+++
27824	<i>G. morbillorum</i>	-	-	+
35308	<i>P. denticola</i>	+	-	-

Bacteria grouped by colour coded complex associated with periodontitis pathogenesis (Socransky *et al.* 1998). For the plate-based assay of DNase: + 0-0.5 mm²/mm², ++ >0.5 mm²/mm²; for gel-based assay of bacterial pellets: + 1-4 Kunitz/bacteria, ++ >4 Kunitz/bacteria; for gel-based assay of bacterial supernatant: + 5-10 Kunitz/bacteria, ++ 10-20 Kunitz/bacteria, +++ >20 Kunitz/bacteria.

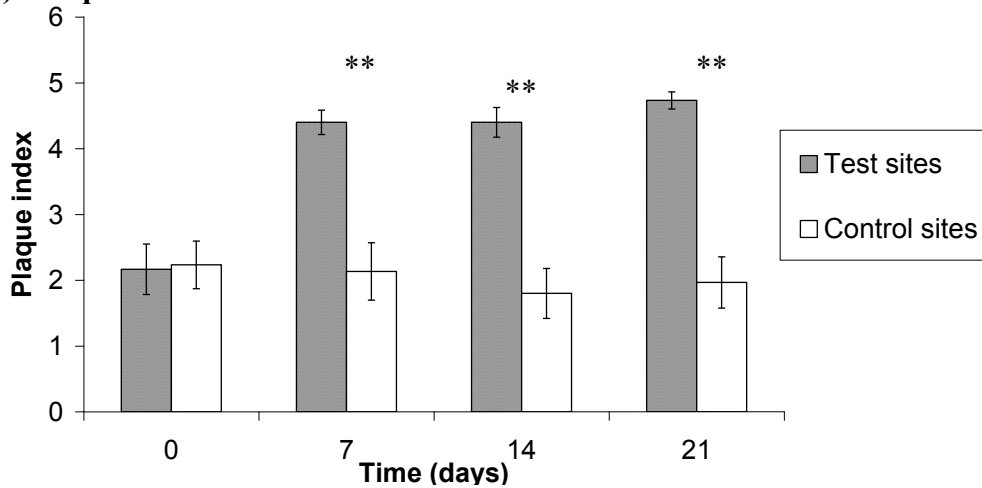
8.2 *In vivo* DNase activity in gingival inflammation

Having established that DNase expression is a relatively common characteristic within a panel of 34 bacterial strains associated with periodontal disease, it was appropriate to investigate whether DNase was present *in vivo* in the plaque biofilm and in GCF. This study was performed utilising a 21 day model of gingivitis in which 4 teeth were shielded during tooth brushing to allow for plaque accumulation and providing ‘test sites’ and non-guarded teeth on the opposite side of the mouth were brushed normally and providing ‘control sites’ (2.8). Plaque and GCF samples were collected and assayed for DNase activity.

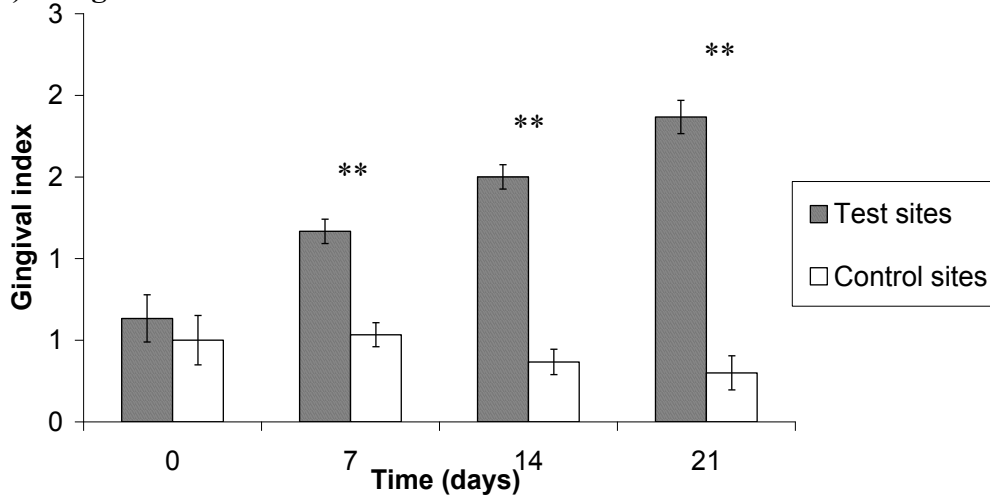
8.2.1 Clinical measure of inflammation

To record successful induction of gingivitis during the 21 day study period 3 clinical parameters were measured (Figure 89). These were i) the plaque index to record plaque accumulation, ii) the gingival index to record gingival inflammation and iii) GCF volume. At baseline (day 0) there was no significant difference in plaque index, gingival index or GCF volume ($P=0.7$, 0.7 and 0.95 , respectively) at test sites compared to control sites. All 3 parameters significantly increased as expected in test sites compared to control sites in the first 7 days ($P=0.002$, 0.002 and 0.007 , respectively) and remained elevated when compared to control sites throughout the 21 day study period. No increase was observed in any parameter at control sites over the study period indicating the maintenance of gingival health.

a) Plaque index



b) Gingival index



c) GCF volume

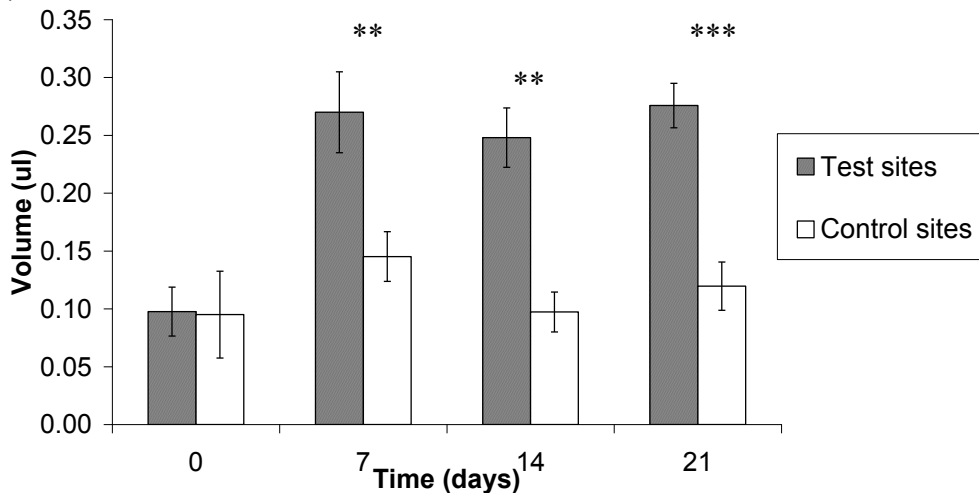


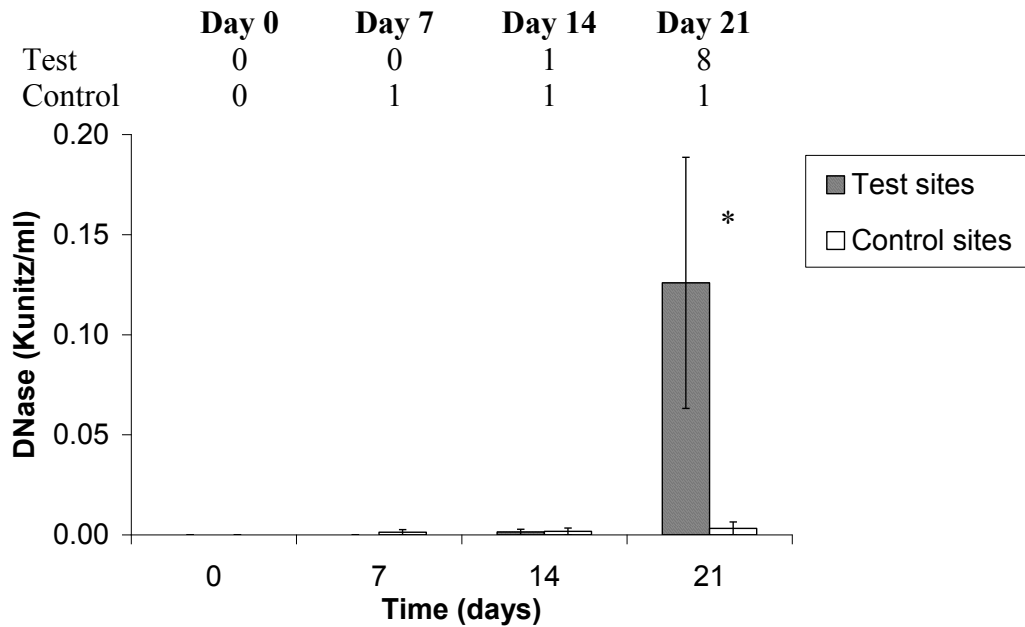
Figure 89. Clinical measures of inflammation during the 21 day experimental model of gingivitis. a) Plaque index, b) gingival index, and c) GCF volume. Results show mean measures from test and control sites in 10 individuals \pm SEM. ** $P \leq 0.01$ *** $P \leq 0.001$ by Wilcoxon test for plaque and gingival index or by paired T-test for GCF volume.

8.2.2 DNase activity within biological samples

Samples of plaque and GCF were collected on days 0, 7, 14 and 21 of the study period and stored until assay by gel-based assay. GCF samples were diluted according to GCF flow rate (volume collected per unit time) so that any increased DNase activity did not simply reflect increased volume but was due to increased concentration or activity. It was not possible to quantify the plaque collected at each sample site so plaque samples were not normalised. GCF samples were diluted in PBS-BSA and plaque samples were suspended in PBS, therefore standard curves were generated using bovine pancreatic DNase suspended in PBS-BSA and PBS separately for estimation of DNase activity in Kunitz/ml. The addition of BSA was found to cause the DNase-dependant degradation of DNA to progress further in the 2 hour assay period, and therefore the assay of DNase activity in GCF samples was more sensitive than that used for the assay of plaque samples. No detectable DNase activity was found in plaque samples from test sites on days 0 or +7, and only 1 individual out of 10 displayed detectable DNase activity on day +14 (Figure 90a). By day +21 the majority of individuals (8 out of 10) demonstrated DNase activity in plaque samples from test sites. Plaque samples from control sites demonstrated no detectable DNase activity throughout the study period, with only a single individual on each day exhibiting any DNase activity. The difference in DNase activity on day +21 between test and control sites was statistically significant by paired T-test ($P=0.04$). DNase assay of normalised GCF samples found no detectable DNase activity in the majority of samples from control sites throughout the study period (Figure 90b) and also no detectable activity in samples from test sites on day 0 i.e. before any inflammation had developed. However, on days +7, +14 and +21 DNase activity

was seen in the majority of individuals and was significantly elevated in comparison to samples from control sites (P=0.05, 0.04 and 0.03 respectively by paired T-test).

a) DNase activity in plaque samples



b) DNase activity in GCF samples

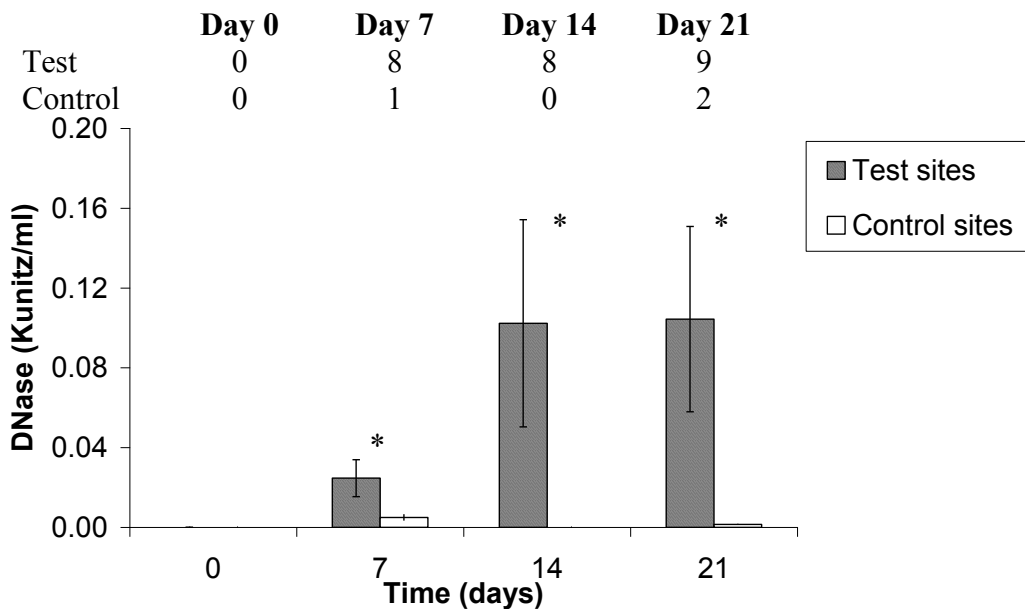


Figure 90. Gel-based assay of DNase activity in samples collected on days 0, 7, 14 and 21. a) assay of plaque samples, and **b)** assay of normalised GCF samples. Results show mean of DNase activity in samples from test and control sites of 10 individuals \pm SEM. *P \leq 0.05 by paired T-test. Tables indicate the number of individuals testing DNase positive (n=10).

Discussion

Bacterial DNase detection

DNase diluted in media resulted in more complete DNA digestion in the 2 hour incubation period compared with DNase diluted in PBS (Figure 85). This may be due to the high availability of divalent cations within the media which are known to be necessary for the activity of DNase (Pan *et al.* 1999). Collation of bacterial DNase expression data (Table 13) indicated that detection of DNase activity varied depending on the assay type. The gel-based assay likely detected both secreted and membrane bound DNase activity whereas the plate-based assay was only able to effectively detect secreted DNase able to diffuse through the agar from the bacterial colony. Subsequently, the positive control strain (*S. aureus*) displayed greater levels of DNase activity in the supernatant than the pellet when assayed by gel-based method (Figures 87 and 88) and moderate levels by the plate-based assay (Figure 83), indicating a primarily secreted DNase as previously reported (Cunningham *et al.* 1956). Of particular interest are the test bacteria that were found to be DNase negative by DNase test plate but positive by gel-based assay of the bacterial pellet such as *C. rectus*, *S. mutans*, *C. sputigena* and *A. odontolyticus*, indicating that the DNase may be membrane bound in these organisms. Also of interest are the bacteria that were found to be DNase positive by plate-based assay but negative by gel-based assay of broth cultures and this group included several streptococci spp. (*S. constellatus*, *S. sanguis*, *S. gordonii* and *S. intermedius*). It is conceivable that this phenomenon could be due to DNase test agar containing the DNA substrate which may induce DNase expression over the 6 days of bacterial growth. In contrast, in broth culture bacteria are not exposed to DNA until after harvest and freezing of

the samples. The two assays applied also utilised bacteria cultured in different states (solid state on agar or planktonic in broth), a factor which is known to affect gene transcription and phenotype (Donlan *et al.* 2002; Mikkelsen *et al.* 2007). Differences in DNase expression depending upon the growth state would be consistent with previous findings in which *P. acnes* and *F. nucleatum* were found to be DNase positive when grown on test agar but DNase negative when grown in broth culture prior to transfer to the test agar, which may also relate to the inducibility of DNase activity (Dahlen *et al.* 1983). Alternative theories to explain the occurrence of DNase expression in the panel of periodontal pathogens are that subgingival bacteria may have a greater necessity for DNase expression and NET evasion than supragingival pathogens due to the closer proximity to host tissues and host defences. Indeed, it has been reported that co-incubation of *S. pyogenes* with human pharyngeal cells induces the expression of an extracellular DNase (Broudy *et al.* 2002). Another agent found to induce the gene expression of an extracellular DNase in GAS was hydrogen peroxide (Banks *et al.* 2003), a membrane permeable ROS produced by neutrophil NADPH oxidase. It has been demonstrated that functional NADPH oxidase is present in NETs but inactivated by DNase treatment (Munafò *et al.* 2009) and therefore bacterial DNase expression may protect against killing by extracellular ROS. However, no such pattern in DNase expression based on localisation of the bacteria to the sub- or supragingival plaque (Ximénez-Fyvie *et al.* 2000) was observed in the panel of pathogens assayed here. This may be attributable to the reported inconsistency of DNase expression amongst bacteria of a given species, as only a single strain of each bacterial species was tested here. Indeed previous publications have assayed multiple strains of the same bacteria and found for example 8 out of 10 strains of *P. melaninogenica* to be DNase positive (Whaley *et al.* 1995), 3 out of 6 strains of *S. intermedius* to be DNase

positive (Marshall *et al.* 1981), and 28 out of 31 strains of *A. naeslundii* to be DNase positive (Whaley *et al.* 1995).

In vivo DNase detection

Recently it has been hypothesised that the increased flow of GCF in periodontal disease functions to remove bacterially produced DNase leaving NETs intact (Vitkov *et al.* 2009). Therefore the increased concentration of DNase detected in GCF may represent a host response that is successfully ‘rinsing’ bacterial DNase out of the gingival crevice. Conversely, as GCF is derived from plasma, the DNase detected may originate from host cells and tissues. In a similar way that host production of serpins functions to limit the inappropriate destruction of host tissue by serine proteinases released from neutrophils (Henson *et al.* 1987), or glutathione acts as an antioxidant to neutralise ROS (Iwasaki *et al.* 2009), it could be expected that a similar mechanism exists to terminate the function of NETs. This would be necessary to prevent immobilisation of host immune cells and also prevent possible autoimmune reactions triggered by an accumulation of extracellular neutrophil components comprising the NETs. Alternatively it is possible that DNase expression is a physiological antimicrobial response by the host as DNase I has been demonstrated to strongly inhibit biofilm formation by *P. aeruginosa* (Whitchurch *et al.* 2002). Evidence in support of this host derived DNase is given by the fact that activity was detectable in GCF earlier (day +7) than in plaque samples (day +21). Alternatively, detection of DNase activity in GCF prior to plaque may indicate that the majority of DNase produced by the plaque bacteria is secreted rather than membrane bound. If secreted DNase is removed by increased GCF flow during the development of inflammation, those bacteria expressing membrane bound DNase may display more virulence and comprise a greater proportion of the dental

plaque later in the development of inflammation. This may explain why DNase activity retained within the dental plaque samples was only detectable on day 21 (Figure 90a) and GCF-DNase activity had reached a plateau by day 21 in this study (Figure 90b). Additionally, the difference in the detection pattern of DNase activity in GCF and plaque samples may have been influenced by the fact that the assay for GCF-DNase was more sensitive than plaque-DNase due to the diluent used, and in addition, GCF samples were normalised and this approach was not possible for plaque samples, therefore direct comparisons between the two sample types cannot easily be made. Regardless of the origins of the DNase, levels were significantly increased in test sites compared to healthy sites by the end of the study period indicating a role for DNase activity in the inflamed tissue, possibly in the regulation of NETs. As to whether regulation of DNase activity is to the advantage of the host or the bacteria remains to be elucidated, and future work should aim to identify the origin of the detected DNase within the GCF. Indeed, discrimination between mammalian and bacterial DNase should be possible as bacterial and mammalian DNases are significantly different, for example the nuclease of *S. aureus* is approximately half the molecular weight (~16.9kDa) (Taniuchi *et al.* 1967) of mammalian DNase I (~31kDa) (Lindberg 1967).

CHAPTER 9 CONCLUDING REMARKS

9.1 Mechanism of NET release

Described in this thesis are four NET detection methods, including SEM, fluorescent staining, fluorometric time course analysis and end point separation of the extracellular DNA by MNase digestion (Chapters 3 and 6). The latter method, based on those previously reported (Fuchs *et al.* 2007; Ramos-Kichik *et al.* 2009; Wang *et al.* 2009), provided a high throughput and reproducible assay for comparison of NET responses under different experimental conditions. Utilisation of this approach also enabled the application of a range of ROS pathway inhibitors and whilst it is established that NET release is associated with NADPH oxidase dependant hydrogen peroxide production (Fuchs *et al.* 2007), data presented here now indicates that the key step may lie downstream of hydrogen peroxide and implicates hypochlorous acid generated by myeloperoxidase activity (Chapter 4).

HL60 cells were also utilised to study NET formation, and whilst they did not provide a robust model of neutrophil activity, they did add further to our understanding of the mechanisms involved in NET release. Currently, only two publications exist documenting the analysis of NETs in HL60 cells (Munafò *et al.* 2009; Wang *et al.* 2009) in which combinations of stimuli e.g. IL-8 plus *S. flexneri*, or calcium ionophore stimulation resulted in only 3.2% and 8% NET release, respectively (Wang *et al.* 2009). In this study, whilst calcium ionophore successfully induced NET release in dHL60 cells, only a short and relatively small burst of associated ROS production was detected. In contrast, PMA stimulated dHL60 cells exhibited significant and sustained production of ROS, although no NET release was detected indicating that there may be other mechanisms, independent of NADPH oxidase, that result in NET release from dHL60 cells. In further support of this

finding is the observation that although the NADPH oxidase inhibitor DPI, used both here (Chapters 4 and 6) and previously (Fuchs *et al.* 2007; von Kockritz-Blickwede *et al.* 2008; Yost *et al.* 2009), demonstrated the dependency of NET release on ROS production, DPI exposure did not result in complete NET inhibition and residual levels, thought to be NADPH oxidase-independent, were detectable. Notably whilst DPI exposure caused a significant reduction in stimulated NET levels, in contrast where a stimulus was ineffective at evoking NET release (e.g. unstimulated primary neutrophils; or PMA stimulated, *F. nucleatum* stimulated or unstimulated dHL60 cells), exposure to DPI variably invoked an increase in NET release (Figures 40 and 42). To further characterise the dependency of NET release on ROS production, attempts were made to correlate induced levels of these two responses. Notably a quantitative relationship has previously been demonstrated in murine neutrophils (Ermert *et al.* 2009) and the data presented here also indicated a positive correlation when neutrophils were stimulated with various periodontal pathogens (assuming exclusion of outliers; Figure 72). Interestingly, this association was only detected when ROS production was measured by luminol detection, confirming that the key NET-associated ROS are intracellular molecules synthesised late in the ROS-metabolic pathway. In addition, a weak correlation between luminol detected ROS and NET levels was also observed when neutrophils were stimulated with PMA ($R^2=0.24$, $P=0.007$; 6.1.5). It is notable that the data presented here was obtained using peripheral blood neutrophils which are exposed to a multitude of influencing factors prior to the point of assay. In contrast, the previous report of a positive correlation between ROS and NET production utilised bone marrow derived neutrophils (Ermert *et al.* 2009) which are relatively naïve cells and potentially provide a ‘cleaner’ assay of cellular responses to stimulation.

Previous studies have also demonstrated an important role for calcium in the synthesis of NETs, with evidence indicating that increasing intracellular calcium levels alone, induced through the use of a calcium ionophore, evokes NET release (Palic *et al.* 2007; Wang *et al.* 2009). Notably, of the 4 stimuli tested (Palic *et al.* 2007) this was the only one which displayed a dose dependant increase in NET release. Combined, this data along with that presented here demonstrating that calcium ionophore was the only stimuli capable of evoking significant NET release in dHL60 cells (Figures 59 and 60), suggests that calcium levels activate a direct and essential step in the process of NET release, likely a calcium dependant enzyme. Further support for the role of calcium in the NET process is derived from results demonstrating: i) activation of a calcium dependant protein kinase (i.e. PMA) is the most effective stimulus of NET release in primary neutrophils and ii) that histone citrullination by calcium dependant PAD is necessary for NET release (Wang *et al.* 2009).

9.2 Microbial interactions with NETs

For the first time, a sub-panel of periodontal pathogens were demonstrated as being capable of stimulating the release of, and interacting with, NETs (Chapter 6). In addition, an extensive panel of periodontal pathogens were screened for potential virulence traits which may confer a survival advantage when challenged with NETs, namely resistance to killing by histones (Chapter 7) and DNase expression (Chapter 8). Both the antimicrobial action of histones and bacterial DNase expression have been documented, since 1958 (Hirsch) and 1974 (Porschen and Sonntag), respectively, although their *in vivo* relevance was then not realised. Now however, the role of host derived NETs may go some way to explaining a role for both these bacterial properties.

Histones reportedly represent 70% of NET associated proteins (Urban *et al.* 2009) therefore the previously demonstrated antimicrobial role of NETs may, at least in part, be attributed to histone molecules. Antimicrobial susceptibility to histone proteins has recently been described in several types of bacteria with regard to NETs (Brinkmann *et al.* 2004), however, the yeast *C. albicans* has been demonstrated to be resistant to killing by histone, although it is effectively killed by complete NETs (Urban *et al.* 2006b). The variability in susceptibility of the 32 different bacteria tested here to the antimicrobial activity of histones is therefore consistent with the current literature. Interestingly, all 10 bacteria which appeared resistant to killing by mixed histone (Figure 81b) were derived from the red, orange and yellow colour complexes associated with more severe periodontitis (Socransky *et al.* 1998). This could potentially result in their survival within periodontal tissues and the development of a more chronic and dysregulated inflammation.

Bacterial DNase expression has previously been demonstrated to be directly linked to both bacterial survival *in vitro* and *in vivo* when challenged with NETs, and this property associates with increased disease severity (Beiter *et al.* 2006). Therefore the panel of periodontal pathogens were also assayed for DNase activity by two independent methods and a large proportion (76% of strains tested) were found to exhibit some degree of activity (Table 13). In order to examine any relationship that may exist between DNase expression and disease severity in periodontitis, the test bacteria were grouped according to colour coded complexes (Socransky *et al.* 1998). A higher proportion of the bacteria from the colour complexes (55% on average) were DNase positive compared with bacteria not associated with a complex (33% on average) when tested using all three methods (plate-based assay, gel-

based assay of the pellet and gel-based assay of the supernatant). This data potentially indicates the importance of DNase expression as a bacterial virulence determinant associated with periodontitis. As these bacteria exist within a biofilm *in vivo* DNase expression by members of this complex will therefore likely contribute to a mutually beneficial environment whereby other non-DNase producing bacteria are afforded survival advantages.

It is interesting to speculate that there may be a necessary association between the two virulence factors examined here, as following DNase digestion of NETs, histones may subsequently be liberated thereby creating a requirement for resistance to killing by these molecules. Comparison of DNase activity detected in the bacterial pellet and resistance to histones lends support to this hypothesis as both appear to be a more common characteristic amongst bacteria of the orange and yellow colour complexes with 8 out of the 10 bacteria exhibiting resistant to killing by histone (Figure 81b) also producing significant membrane bound DNase activity (Figure 87).

In addition to the virulence traits examined here, it has been hypothesised that bacterially produced catalase may be able to modulate the NET response of host neutrophils as *in vitro* addition of exogenous catalase decreases NET release (Fuchs *et al.* 2007). Therefore future work could also examine the constitutive and inducible catalase production by periodontal pathogens as an anti-NET strategy. Whilst catalase production by bacteria was assessed in a small panel of the bacteria for identification purposes (Table 11), this assay was a relatively insensitive visual test and was only performed for those bacteria for which catalase production was considered a key characteristic. In addition, investigations could assess whether the levels produced were sufficient to play a patho-physiological role. Bacterial PAD expression

is another bacterial property which may influence NET release as histone H3 citrullination by the endogenous PAD enzyme has been shown to be essential for NET release (Wang *et al.* 2009). The only bacterium currently known to express this enzyme is *P. gingivalis* (Rodríguez *et al.* 2009) which is one of the most pathogenic periodontal organisms, and also an intracellular pathogen (Lamont *et al.* 1995), implicating *P. gingivalis* derived PAD enzymatic activity a possible modulator of NET release. Further investigations could examine bacterial PAD regulation of NET release and determine whether other periodontal bacteria also possess this property.

9.3 NETs in periodontitis

Research into the phenomenon of NET release has increased significantly since they were first reported in 2004 (Brinkmann *et al.*). Although at the outset of this work a role in periodontitis was only hypothesised based on its neutrophil driven pathology, a recent publication has now identified NETs in pus derived from the gingival crevice and gingival pocket surface (Vitkov *et al.* 2009). The data presented here comparing NET responses from the peripheral blood neutrophils of periodontitis patients and age and gender matched healthy controls suggests a relationship may exist between periodontitis and elevated NET release (Chapter 6). In addition to investigating the NET production associated with periodontitis, DNase activity in the disease state was also examined in a 21-day model of gingivitis. This revealed a significant increase in DNase activity during the development of gingival inflammation potentially indicating an *in vivo* role for the previously described bacterial DNase expression (Table 13) and is in concordance with previous reports that bacterial DNase expression affects disease severity (Beiter *et al.* 2006). It is however interesting to note that

pure cultures of 3 of the most pathogenic periodontal bacteria (*P. gingivalis*, *T. forsythensis* and *A. actinomycetemcomitans* serotype b) whilst able to stimulate NET release (Figure 70), exhibited a low occurrence of detectable DNase activity (Table 13), suggesting that a high presence of NETs may be detrimental to the host in periodontitis. It is also conceivable that the *in vivo* increases in DNase activity may be of host origin rather than being bacterially derived, as activity was detectable in plaque at a later stage of clinical inflammation compared to levels detected in GCF samples (Figure 90). Therefore host DNase expression may be a physiological rather than pathological response to increased NETs as a result of disease progression. Indeed the presence of DNase has previously been demonstrated to be an essential counter-NET mechanism present in equine semen to enable effective fertilisation (Alghamdi *et al.* 2005). DNase may be functioning to not only prevent trapping of host immune cells required to combat infiltrating bacteria but also prevent generation of auto-antigens due to the presence of extracellular neutrophil components. Indeed, it is known that circulating levels of self-nucleosomes are associated with the autoimmune disease, systemic lupus erythmatosus (Amoura *et al.* 1997), and it has been demonstrated in small vessel vasculitis that circulating DNA-MPO complexes proposed to be NET fragments are also elevated in active disease but not in remission (Kessenbrock *et al.* 2009). Therefore effective removal of NETs may be essential to prevent the triggering of an autoimmune response due to excessive and prolonged accumulation of NETs within the tissues. Conversely, if this does not occur efficiently NET release may contribute to propagation of the local inflammatory reaction and subsequently contribute to the association of periodontitis with other systemic diseases which exhibit an autoimmune component. Therefore it is proposed that a strict balance between the presence of NETs and host-derived DNase activity exists to effectively combat bacterial infiltration and also bring about NET removal at the appropriate time thereby

maintaining a state of health within the tissues (Figure 91). This dynamic may be subverted by excess DNase production by bacteria, which may confer survival advantages on those species, or excess host DNase production, although data on the latter in relation to disease pathogenesis is absent in the literature. Moreover, excess NET production within tissues is likely to have pathogenic consequences by inhibiting immune surveillance mechanisms, and inadequate NET formation is also likely to have pathogenic consequences by facilitating pathogen survival.

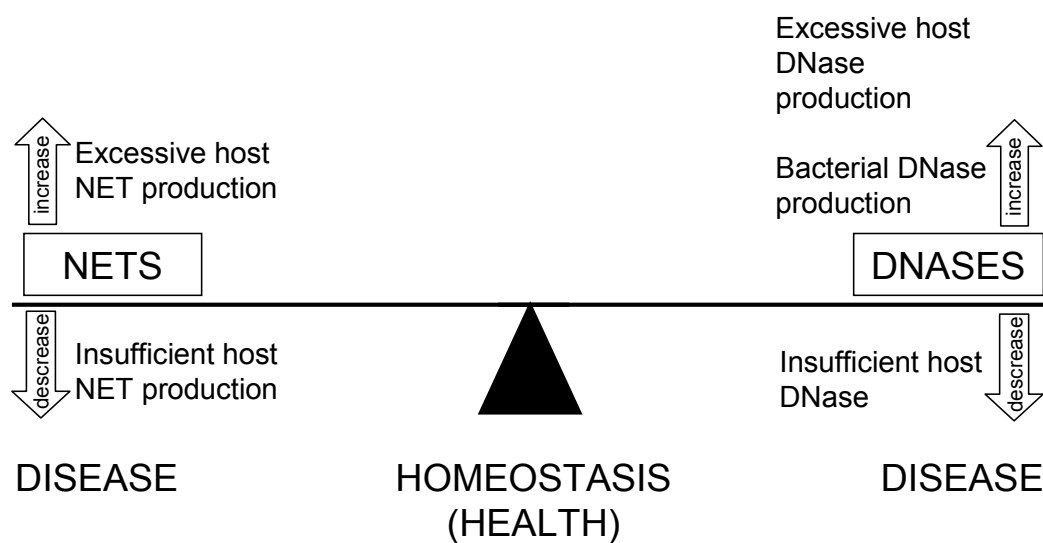


Figure 91. Schematic of relationship that may exist between NET production and DNase production in inflammation such as periodontitis.

To further characterise the role of NETs in the pathogenesis of periodontitis a study of peripheral neutrophil NET responses should be carried out in more strictly phenotyped patients and matched controls. The use of antibodies to citrullinated histone H3 could also be utilised as this histone modification has been demonstrated to be an early and necessary step in NET activation and may indicate the level of peripheral neutrophils in a primed state for heightened NET release. Similarly the expression levels of the PAD enzyme responsible for this citrullination may also be examined. As inhibition of PAD suppresses NET release

(Wang *et al.* 2009), it is hypothesised that increased levels of PAD may promote NET release. Preliminary microarray data obtained in our laboratory indicates that PAD levels in patient neutrophils may be 1.5 times those of healthy controls (Personal communication, Dr H Wright) and this too could be further investigated in a patient group with appropriately matched healthy controls. Future experiments could also harvest neutrophils directly from the gingival crevice to assess the effect the local environment within the periodontal tissues has on their capacity for NET release.

References

- Abachin, E., C. Poyart, E. Pellegrini, E. Milohanic, F. Fiedler, P. Berche and P. Trieu-Cuot (2002).** Formation of D-alanyl-lipoteichoic acid is required for adhesion and virulence of *Listeria monocytogenes*. *Molecular Microbiology* 43(1): 1-14.
- Ahluwalia, J., A. Tinker, L. H. Clapp, M. R. Duchon, A. Y. Abramov, S. Pope, M. Nobles and A. W. Segal (2004).** The large-conductance Ca²⁺-activated K⁺ channel is essential for innate immunity. *Nature* 427(6977): 853-858.
- Ak, T. and I. Gulcin (2008).** Antioxidant and radical scavenging properties of curcumin. *Chemico-Biological Interactions* 174(1): 27-37.
- Al-Haroni, M. H., N. Skaug and N. N. Al-Hebshi (2006).** Prevalence of subgingival bacteria resistant to aminopenicillins and metronidazole in dental patients from Yemen and Norway. *International Journal of Antimicrobial Agents* 27(3): 217-223.
- Alberts, B., A. Johnson, J. Lewis, M. Raff, K. Roberts and P. Walter (2002).** *Molecular Biology of the Cell*. New York, Garland Science.
- Alghamdi, A. S. and D. N. Foster (2005).** Seminal DNase Frees Spermatozoa Entangled in Neutrophil Extracellular Traps. *Biology of Reproduction* 73(6): 1174-1181.
- Alghamdi, A. S., B. J. Lovaas, S. L. Bird, G. C. Lamb, A. K. Rendahl, P. C. Taube and D. N. Foster (2009).** Species-specific interaction of seminal plasma on sperm-neutrophil binding. *Animal Reproduction Science* 114(4): 331-344.
- Amoura, Z., J. C. Piette, H. Chabre, P. Cacoub, T. Papo, B. Wechsler, J. F. Bach and S. Koutouzov (1997).** Circulating plasma levels of nucleosomes in patients with systemic lupus erythematosus - Correlation with serum antinucleosome antibody titers and absence of clear association with disease activity. *Arthritis and Rheumatism* 40(12): 2217-2225.
- Ashimoto, A., C. Chen, I. Bakker and J. Slots (1996).** Polymerase chain reaction detection of 8 putative periodontal pathogens in subgingival plaque of gingivitis and advanced periodontitis lesions. *Oral Microbiology and Immunology* 11(4): 266-273.
- Assuma, R., T. Oates, D. Cochran, S. Amar and D. T. Graves (1998).** IL-1 and TNF Antagonists Inhibit the Inflammatory Response and Bone Loss in Experimental Periodontitis. *Journal of Immunology* 160(1): 403-409.
- Baehni, P., C. C. Tsai, W. P. McArthur, B. F. Hammond and N. S. Taichman (1979).** Interaction of inflammatory cells and oral microorganisms. VIII. Detection of leukotoxic activity of a plaque-derived gram-negative microorganism. *Infection and Immunity* 24(1): 233-243.
- Baharin, B., R. M. Palmer, P. Coward and R. F. Wilson (2006).** Investigation of periodontal destruction patterns in smokers and non-smokers. *Journal of Clinical Periodontology* 33(7): 485-490.
- Baker, P. J. (2000).** The role of immune responses in bone loss during periodontal disease. *Microbes and Infection* 2(10): 1181-1192.
- Baker, V., G. Imade, N. Molta, P. Tawde, S. Pam, M. Obadofin, S. Sagay, D. Egah, D. Iya, B. Afolabi, M. Baker, K. Ford, R. Ford, K. Roux and T. Keller (2008).** Cytokine-associated neutrophil extracellular traps and antinuclear antibodies in *Plasmodium falciparum* infected children under six years of age. *Malaria Journal* 7(1): 41.

- Baltacioglu, E., F. A. Akalin, A. Alver, F. Balaban, M. Unsal and E. Karabulut (2006).** Total antioxidant capacity and superoxide dismutase activity levels in serum and gingival crevicular fluid in post-menopausal women with chronic periodontitis. *Journal of Clinical Periodontology* 33(6): 385-392.
- Banks, D. J., B. Lei and J. M. Musser (2003).** Prophage Induction and Expression of Prophage-Encoded Virulence Factors in Group A Streptococcus Serotype M3 Strain MGAS315. *Infection and Immunity* 71(12): 7079-7086.
- Bax, B. E., A. S. M. T. Alam, B. Banerji, C. M. R. Bax, P. J. R. Bevis, C. R. Stevens, B. S. Moonga, D. R. Blake and M. Zaidi (1992).** Stimulation of osteoclastic bone resorption by hydrogen peroxide. *Biochemical and Biophysical Research Communications* 183(3): 1153-1158.
- Beck, J. D., G. G. Koch and S. Offenbacher (1995).** Incidence of Attachment Loss over 3 Years in Older Adults - New and Progressing Lesions. *Community Dentistry and Oral Epidemiology* 23(5): 291-296.
- Behrendt, J. H., A. Ruiz, H. Zahner, A. Taubert and C. Hermosilla (2010).** Neutrophil extracellular trap formation as innate immune reactions against the apicomplexan parasite *Eimeria bovis*. *Veterinary Immunology and Immunopathology* 133(1): 1-8.
- Beiter, K., F. Wartha, B. Albiger, S. Normark, A. Zychlinsky and B. Henriques-Normark (2006).** An Endonuclease Allows *Streptococcus pneumoniae* to Escape from Neutrophil Extracellular Traps. *Current Biology* 16(4): 401-407.
- Bensaci, M. F. and J. Y. Takemoto (2007).** Syringopeptin SP25A-mediated killing of gram-positive bacteria and the role of teichoic acid d-alanylation. *FEMS Microbiology Letters* 268(1): 106-111.
- Bianchi, M., A. H. Rahmathullah, V. Brinkmann, U. Siler, R. A. Seger, A. Zychlinsky and J. Reichenback (2009).** Restoration of NET formation by gene therapy in CGD controls aspergillosis. *Blood* 114(13): 2619-2622.
- Birkemo, G. A., T. Luders, O. Andersen, I. F. Nes and J. Nissen-Meyer (2003).** Hippusin, a histone-derived antimicrobial peptide in Atlantic halibut (*Hippoglossus hippoglossus* L.). *Biochimica et Biophysica Acta (BBA) - Proteins & Proteomics* 1646(1-2): 207-215.
- Bland, J. M. and D. G. Altman (1986).** Statistical-Methods for Assessing Agreement between 2 Methods of Clinical Measurement. *Lancet* 1(8476): 307-310.
- Borregaard, N. and J. B. Cowland (1997).** Granules of the Human Neutrophilic Polymorphonuclear Leukocyte. *Blood* 89(10): 3503-3521.
- Boyd, D. A., D. G. Cvitkovitch, A. S. Bleiweis, M. Y. Kiriukhin, D. V. Debabov, F. C. Neuhaus and I. R. Hamilton (2000).** Defects in D-Alanyl-Lipoteichoic Acid Synthesis in *Streptococcus mutans* Results in Acid Sensitivity. *Journal of Bacteriology* 182(21): 6055-6065.
- Brailsford, S. R., R. B. Tregaskis, H. S. Leftwich and D. Beighton (1999).** The predominant *Actinomyces* spp. isolated from infected dentin of active root caries lesions. *Journal of Dental Research* 78(9): 1525-1534.
- Breitman, T. R., S. E. Selonick and S. J. Collins (1980).** Induction of Differentiation of the Human Promyelocytic Leukemia-Cell Line (HL-60) by Retinoic Acid. *Proceedings of the National Academy of Sciences of the United States of America-Biological Sciences* 77(5): 2936-2940.
- Brinkmann, V., U. Reichard, C. Goosmann, B. Fauler, Y. Uhlemann, D. S. Weiss, Y. Weinrauch and A. Zychlinsky (2004).** Neutrophil Extracellular Traps Kill Bacteria. *Science* 303(5663): 1532-1535.

- Brinkmann, V. and A. Zychlinsky (2007).** Beneficial suicide: why neutrophils die to make NETs. *Nature Reviews Microbiology* 5(8): 577-582.
- Buchanan, J. T., A. J. Simpson, R. K. Aziz, G. Y. Liu, S. A. Kristian, M. Kotb, J. Feramisco and V. Nizet (2006).** DNase Expression Allows the Pathogen Group A Streptococcus to Escape Killing in Neutrophil Extracellular Traps. *Current Biology* 16(4): 396-400.
- Busch, H. (1971).** *Methods in Cancer Research* New York, Academic Press.
- Cao, M. and J. D. Helmann (2004).** The Bacillus subtilis Extracytoplasmic-Function {sigma}X Factor Regulates Modification of the Cell Envelope and Resistance to Cationic Antimicrobial Peptides. *Journal of Bacteriology* 186(4): 1136-1146.
- Carlin, A. F., S. Uchiyama, Y. C. Chang, A. L. Lewis, V. Nizet and A. Varki (2009).** Molecular mimicry of host sialylated glycans allows a bacterial pathogen to engage neutrophil Siglec-9 and dampen the innate immune response. *Blood* 113(14): 3333-3336.
- Chapple, I. L. C. (2009).** Potential Mechanisms Underpinning the Nutritional Modulation of Periodontal Inflammation. *The Journal of the American Dental Association* 140(2): 178-184.
- Chapple, I. L. C., G. R. Brock, M. R. Milward, N. Ling and J. B. Matthews (2007a).** Compromised GCF total antioxidant capacity in periodontitis: cause or effect? *Journal of Clinical Periodontology* 34(2): 103-110.
- Chapple, I. L. C. and A. D. Gilbert (2002).** *Understanding Periodontal Diseases: Assessment and Diagnostic Procedures in Practice*. London, Quintessence Publishing Co. Ltd.
- Chapple, I. L. C., G. Landini, G. S. Griffiths, N. C. Patel and R. S. N. Ward (1999).** Calibration of the Periotron 8000 (R) and 6000 (R) by polynomial regression. *Journal of Periodontal Research* 34(2): 79-86.
- Chapple, I. L. C., G. I. Mason, I. Garner, J. B. Matthews, G. H. Thorpe, S. R. J. Maxwell and T. P. Whitehead (1997).** Enhanced chemiluminescent assay for measuring the total antioxidant capacity of serum, saliva and crevicular fluid. *Annals of Clinical Biochemistry* 34: 412-421.
- Chapple, I. L. C. and J. B. Matthews (2007b).** The role of reactive oxygen and antioxidant species in periodontal tissue destruction. *Periodontology 2000* 43: 160-232.
- Chapple, I. L. C., M. R. Milward and T. Dietrich (2007c).** The Prevalence of Inflammatory Periodontitis Is Negatively Associated with Serum Antioxidant Concentrations. *Journal of Nutrition* 137(3): 657-664.
- Chapple, I. L. C., S. S. Socransky, S. Dibart, D. H. Glenwright and J. B. Matthews (1996).** Chemiluminescent assay of alkaline phosphatase in human gingival crevicular fluid: investigations with an experimental gingivitis model and studies on the source of the enzyme within crevicular fluid. *Journal of Clinical Periodontology* 23(6): 587-594.
- Chatila, T., L. Silverman, R. Miller and R. Geha (1989).** Mechanisms of T-Cell Activation by the Calcium Ionophore Ionomycin. *Journal of Immunology* 143(4): 1283-1289.
- Chuammitri, P., J. Ostojic, C. B. Andreasen, S. B. Redmond, S. J. Lamont and D. Palic (2009).** Chicken heterophil extracellular traps (HETs): Novel defense mechanism of chicken heterophils. *Veterinary Immunology and Immunopathology* 129(1-2): 126-131.
- Clark, S. R., A. C. Ma, S. A. Tavener, B. McDonald, Z. Goodarzi, M. M. Kelly, K. D. Patel, S. Chakrabarti, E. McAvoy, G. D. Sinclair, E. M. Keys, E. Allen-Vercoe, R.**

- DeVinney, C. J. Doig, F. H. Y. Green and P. Kubes (2007).** Platelet TLR4 activates neutrophil extracellular traps to ensnare bacteria in septic blood. *Nature Medicine* 13(4): 463-469.
- Clemans, D. L., P. E. Kolenbrander, D. V. DeBabov, Q. Zhang, R. D. Lunsford, H. Sakone, C. J. Whittaker, M. P. Heaton and F. C. Neuhaus (1999).** Insertional Inactivation of Genes Responsible for the D-Alanylation of Lipoteichoic Acid in *Streptococcus gordonii* DL1 (Challis) Affects Intrageneric Coaggregations. *Infect. Immun.* 67(5): 2464-2474.
- Clerehugh, V., M. A. Lennon and H. V. Worthington (1990).** 5-year results of a longitudinal study of early periodontitis in 14- to 19-year-old adolescents. *Journal of Clinical Periodontology* 17(10): 702-708.
- Clerehugh, V., H. V. Worthington, M. A. Lennon and R. Chandler (1995).** Site progression of loss of attachment over 5 years in 14-to 19-year-old adolescents. *Journal of Clinical Periodontology* 22(1): 15-21.
- Cole, J. N., J. D. McArthur, F. C. McKay, M. L. Sanderson-Smith, A. J. Cork, M. Ranson, M. Rohde, A. Itzek, H. Sun, D. Ginsburg, M. Kotb, V. Nizet, G. S. Chhatwal and M. J. Walker (2006).** Trigger for group A streptococcal M1T1 invasive disease. *FASEB* 20(10): 1745-1747.
- Collins, S. J., R. C. Gallo and R. E. Gallagher (1977).** Continuous Growth and Differentiation of Human Myeloid Leukemic-Cells in Suspension Culture. *Nature* 270(5635): 347-349.
- Conrads, G., S. E. Gharbia, K. Gulabivala, F. Lampert and H. N. Shah (1997).** The use of a 16S rDNA directed PCR for the detection of endodontopathogenic bacteria. *Journal of Endodontics* 23(7): 433-438.
- Cuatrecasas, P., S. Fuchs and C. B. Anfinsen (1967).** Catalytic Properties and Specificity of the Extracellular Nuclease of *Staphylococcus aureus*. *Journal of Biological Chemistry* 242(7): 1541-1547.
- Cunningham, L., B. W. Catlin and M. P. de Garihe (1956).** A Deoxyribonuclease of *Micrococcus pyogenes* 1. *Journal of the American Chemical Society* 78(18): 4642-4645.
- Dahlen, G., M. Wikstrom and A. Moller (1983).** Production of Histolytic Enzymes by a Combination of Oral Bacteria with Known Pathogenicity. *Journal of Dental Research* 62(10): 1041-1044.
- Dahlgren, C. (1989).** The calcium ionophore ionomycin can prime, but not activate, the reactive oxygen generating system in differentiated HL-60 cells. *Journal of Leukocyte Biology* 46(1): 15-24.
- Dahlgren, C., T. Andersson and O. Stendahl (1987).** Chemotactic factor binding and functional capacity: a comparison between human granulocytes and differentiated HL-60 cells. *Journal of Leukocyte Biology* 42(3): 245-252.
- Dahlgren, C. and A. Karlsson (1999).** Respiratory burst in human neutrophils. *Journal of Immunological Methods* 232(1-2): 3-14.
- Dale, B. A. (2002).** Periodontal epithelium: a newly recognized role in health and disease. *Periodontology 2000* 30(1): 70-78.
- Dallegrì, F., L. Ottonello, A. Ballestrero, F. Bogliolo, F. Ferrando and F. Patrone (1990).** Cytoprotection against Neutrophil Derived Hypochlorous Acid - a Potential Mechanism for the Therapeutic Action of 5-Aminosalicylic Acid in Ulcerative-Colitis. *Gut* 31(2): 184-186.

- de Haas, C. J. C., K. E. Veldkamp, A. Peschel, F. Weerkamp, W. J. B. Van Wamel, E. C. J. M. Heezius, M. J. J. G. Poppelier, K. P. M. Van Kessel and J. A. G. van Strijp (2004).** Chemotaxis Inhibitory Protein of *Staphylococcus aureus*, a Bacterial Antiinflammatory Agent. *Journal of Experimental Medicine* 199(5): 687-695.
- Dias, I. H. K., L. Marshall, P. A. Lambert, I. L. C. Chapple, J. B. Matthews and H. R. Griffiths (2008).** Gingipains from *Porphyromonas gingivalis* Increase the Chemotactic and Respiratory Burst-Priming Properties of the 77-Amino-Acid Interleukin-8 Variant. *Infection and Immunity* 76(1): 317-323.
- Dinauer, M. C. (2005).** Chronic Granulomatous Disease and Other Disorders of Phagocyte Function. *Hematology: The American Society of Hematology Education Program Book* 2005(1): 89-95.
- Donlan, R. M. and J. W. Costerton (2002).** Biofilms: Survival Mechanisms of Clinically Relevant Microorganisms. *Clinical Microbiology Reviews* 15(2): 167-193.
- Duerden, B. I., K. J. Towner and J. T. Magee (1998).** Isolation, description and identification of bacteria. *Systematic Bacteriology*. L. Collier, A. Balows and M. Sussman. London, Arnold. Volume 2: 65-84.
- Ellis, J. A., S. J. Mayer and O. T. G. Jones (1988).** The Effect of the NADPH Oxidase Inhibitor Diphenyleneiodonium on Aerobic and Anaerobic Microbicidal Activities of Human-Neutrophils. *Biochemical Journal* 251(3): 887-891.
- Elwell, C. A. and L. A. Dreyfus (2000).** DNase I homologous residues in CdtB are critical for cytolethal distending toxin-mediated cell cycle arrest. *Molecular Microbiology* 37(4): 952-963.
- Emerit, I., F. Garban, J. Vassy, A. Levy, P. Filipe and J. Freitas (1996).** Superoxide-mediated clastogenesis and anticlastogenic effects of exogenous superoxide dismutase. *Proceedings of the National Academy of Sciences of the United States of America* 93(23): 12799-12804.
- Ermert, D., C. F. Urban, B. Laube, C. Goosmann, A. Zychlinsky and V. Brinkmann (2009).** Mouse Neutrophil Extracellular Traps in Microbial Infections. *Journal of Innate Immunity* 1(3): 181-193.
- Etoh, Y., F. E. Dewhirst, B. J. Paster, A. Yamamoto and N. Goto (1993).** *Campylobacter showae* sp. nov., Isolated from the Human Oral Cavity. *International Journal of Systematic Bacteriology* 43(4): 631-639.
- Falk, R. J., R. S. Terrell, L. A. Charles and J. C. Jennette (1990).** Anti-neutrophil cytoplasmic autoantibodies induce neutrophils to degranulate and produce oxygen radicals in vitro. *Proceedings of the National Academy of Sciences* 87(11): 4115-4119.
- Faurschou, M. and N. Borregaard (2003).** Neutrophil granules and secretory vesicles in inflammation. *Microbes and Infection* 5(14): 1317-1327.
- Figueredo, C. M. S., R. G. Fischer and A. Gustafsson (2005).** Aberrant Neutrophil Reactions in Periodontitis. *Journal of Periodontology* 76(6): 951-955.
- Figueredo, C. M. S., A. Gustafsson, B. Åsman and K. Bergström (2000).** Expression of intracellular elastase activity in peripheral neutrophils from patients with adult periodontitis. *Journal of Clinical Periodontology* 27(8): 572-577.
- Forsyth, K. D., V. Talbot and I. Beckman (1994).** Endothelial Serpins - Protectors of the Vasculature. *Clinical and Experimental Immunology* 95(2): 277-282.
- Fox, J. B. and D. F. Holtman (1968).** Effect of Anaerobiosis on Staphylococcal Nuclease Production. *Journal of Bacteriology* 95(5): 1548-1550.

- Fredriksson, M. I., A. K. Gustafsson, K. G. Bergstrom and B. E. Asman (2003).** Constitutionally Hyperreactive Neutrophils in Periodontitis. *Journal of Periodontology* 74(2): 219-224.
- Fuchs, H. J., D. S. Borowitz, D. H. Christiansen, E. M. Morris, M. L. Nash, B. W. Ramsey, B. J. Rosenstein, A. L. Smith and M. E. Wohl (1994).** Effect of Aerosolized Recombinant Human Dnase on Exacerbations of Respiratory Symptoms and on Pulmonary-Function in Patients with Cystic-Fibrosis. *New England Journal of Medicine* 331(10): 637-642.
- Fuchs, T. A., U. Abed, C. Goosmann, R. Hurwitz, I. Schulze, V. Wahn, Y. Weinrauch, V. Brinkmann and A. Zychlinsky (2007).** Novel cell death program leads to neutrophil extracellular traps. *Journal of Cell Biology* 176(2): 231-241.
- Gaffen, S. L. and G. Hajishengallis (2008).** A New Inflammatory Cytokine on the Block: Re-thinking Periodontal Disease and the Th1/Th2 Paradigm in the Context of Th17 Cells and IL-17. *Journal of Dental Research* 87(9): 817-828.
- Gallagher, R., S. Collins, J. Trujillo, K. McCredie, M. Ahearn, S. Tsai, R. Metzgar, G. Aulakh, R. Ting, F. Ruscetti and R. Gallo (1979).** Characterization of the continuous, differentiating myeloid cell line (HL-60) from a patient with acute promyelocytic leukemia. *Blood* 54(3): 713-733.
- Garcia-Garcia, E. (2005).** *Molecular Mechanisms of Phagocytosis*. Georgetown, Texas, Landes Bioscience.
- Garrett, I. R., B. F. Boyce, R. O. C. Oreffo, L. Bonewald, J. Poser and G. R. Mundy (1990).** Oxygen-Derived Free-Radicals Stimulate Osteoclastic Bone-Resorption in Rodent Bone Invitro and Invivo. *Journal of Clinical Investigation* 85(3): 632-639.
- Gera, J. F. and A. Lichtenstein (1991).** Human Neutrophil Peptide Defensins Induce Single Strand DNA Breaks in Target Cells. *Cellular Immunology* 138(1): 108-120.
- Goto, T., H. Nagamune, A. Miyazaki, Y. Kawamura, O. Ohnishi, K. Hattori, K. Ohkura, K. Miyamoto, S. Akimoto, T. Ezaki, K. Hirota, Y. Miyake, T. Maeda and H. Kourai (2002).** Rapid identification of *Streptococcus intermedius* by PCR with the *ily* gene as a species marker gene. *Journal of Medical Microbiology* 51(2): 178-186.
- Grinberg, N., S. Elazar, I. Rosenshine and N. Y. Shpigel (2008).** beta-hydroxybutyrate abrogates formation of bovine neutrophil extracellular traps and bactericidal activity against mammary pathogenic *Escherichia coli*. *Infection and Immunity* 76(6): 2802-2807.
- Grosdent, N., I. Maridonneau-Parini, M.-P. Sory and G. R. Cornelis (2002).** Role of Yops and Adhesins in Resistance of *Yersinia enterocolitica* to Phagocytosis. *Infection and Immunity* 70(8): 4165-4176.
- Grossi, S. G., J. J. Zambon, A. W. Ho, G. Koch, R. G. Dunford, E. E. Machtei, O. M. Norderyd and R. J. Genco (1994).** Assessment of Risk for Periodontal-Disease 1. Risk Indicators for Attachment Loss. *Journal of Periodontology* 65(3): 260-267.
- Guimaraes-Costa, A. B., M. T. C. Nascimento, G. S. Froment, R. P. P. Soares, F. N. Morgado, F. Conceicao-Silva and E. M. Saraiva (2009).** *Leishmania amazonensis* promastigotes induce and are killed by neutrophil extracellular traps. *PNAS* 106(16): 6748-6753.
- Gunn, J. S., S. S. Ryan, J. C. Van Velkinburgh, R. K. Ernst and S. I. Miller (2000).** Genetic and Functional Analysis of a PmrA-PmrB-Regulated Locus Necessary for Lipopolysaccharide Modification, Antimicrobial Peptide Resistance, and Oral Virulence of *Salmonella enterica* Serovar Typhimurium. *Infect. Immun.* 68(11): 6139-6146.

- Gupta, A. K., P. Hasler, W. Holzgreve, S. Gebhardt and S. Hahn (2005).** Induction of Neutrophil Extracellular DNA Lattices by Placental Microparticles and IL-8 and Their Presence in Preeclampsia. *Human Immunology* 66(11): 1146-1154.
- Gustafsson, A. and B. Asman (1996).** Increased release of free oxygen radicals from peripheral neutrophils in adult periodontitis after Fc gamma-receptor stimulation. *Journal of Clinical Periodontology* 23(1): 38-44.
- Hadjigogos, K. (2003).** The role of free radicals in the pathogenesis of rheumatoid arthritis. *Panminerva Medica* 45(1): 7-13.
- Haffajee, A. D., S. S. Socransky, C. Smith and S. Dibart (1991).** Microbial Risk Indicators for Periodontal Attachment Loss. *Journal of Periodontal Research* 26(3): 293-296.
- Hamada, S. and H. D. Slade (1980).** Biology, immunology, and cariogenicity of *Streptococcus mutans*. *Microbiology and Molecular Biology Reviews* 44(2): 331-384.
- Harris, P. and P. Ralph (1985).** Human Leukemic Models of Myelomonocytic Development - a Review of the HL-60 and U937 Cell Lines. *Journal of Leukocyte Biology* 37(4): 407-422.
- Hayashi, F., M. Okada, X. Zhong and K. Miura (2001).** PCR detection of Capnocytophaga species in dental plaque samples from children aged 2 to 12 years. *Microbiology and Immunology* 45(1): 17-22.
- Henson, P. M. and R. B. Johnston (1987).** Tissue-Injury in Inflammation - Oxidants, Proteinases, and Cationic Proteins. *Journal of Clinical Investigation* 79(3): 669-674.
- Hirsch, J. G. (1958).** Bactericidal Action of Histone. *Journal of Experimental Medicine* 108(6): 925-944.
- Hitchcock, S. E. (1980).** Actin deoxyribonuclease I interaction. Depolymerization and nucleotide exchange. *Journal of Biological Chemistry* 255(12): 5668-5673.
- Hoeben, D., R. Heyneman and C. Burvenich (1997).** Elevated levels of beta-hydroxybutyric acid in periparturient cows and in vitro effect on respiratory burst activity of bovine neutrophils. *Veterinary Immunology and Immunopathology* 58(2): 165-170.
- Holdenrieder, S., P. Eichhorn, U. Beuers, W. Samtleben, U. Schoenermarck, R. Zchoval, D. Nagel and P. Stieber (2006).** Nucleosomal DNA Fragments in Autoimmune Diseases. *Annals of the New York Academy of Sciences* 1075: 318-327.
- Holt, J. G. (1994).** *Bergey's Manual of Determinative Bacteriology*. Baltimore, Williams and Wilkins.
- Hong, W. Z., R. A. Juneau, B. Pang and W. E. Swords (2009).** Survival of Bacterial Biofilms within Neutrophil Extracellular Traps Promotes Nontypeable *Haemophilus influenzae* Persistence in the Chinchilla Model for Otitis Media. *Journal of Innate Immunity* 1(3): 215-224.
- Hoshino, T., M. Kawaguchi, N. Shimizu, N. Hoshino, T. Ooshima and T. Fujiwara (2004).** PCR detection and identification of oral streptococci in saliva samples using GTF genes. *Diagnostic Microbiology and Infectious Disease* 48(3): 195-199.
- Huizinga, T. W., F. van Kemenade, L. Koenderman, K. M. Dolman, A. E. von dem Borne, P. A. Tetteroo and D. Roos (1989).** The 40-kDa Fc gamma receptor (FcRII) on human neutrophils is essential for the IgG-induced respiratory burst and IgG-induced phagocytosis. *Journal of Immunology* 142(7): 2365-2369.
- Ishii, K. J., K. Suzuki, C. Coban, F. Takeshita, Y. Itoh, H. Matoba, L. D. Kohn and D. M. Klinman (2001).** Genomic DNA Released by Dying Cells Induces the Maturation of APCs. *Journal of Immunology* 167(5): 2602-2607.

- Iwasaki, Y., Y. Saito, Y. Nakano, K. Mochizuki, O. Sakata, R. Ito, K. Saito and H. Nakazawa (2009).** Chromatographic and mass spectrometric analysis of glutathione in biological samples. *Journal of Chromatography B* 877(28): 3309-3317.
- Jaillon, S., G. Peri, Y. Delneste, I. Fremaux, A. Doni, F. Moalli, C. Garlanda, L. Romani, H. Gascan, S. Bellocchio, S. Bozza, M. A. Cassatella, P. Jeannin and A. Mantovani (2007).** The humoral pattern recognition receptor PTX3 is stored in neutrophil granules and localizes in extracellular traps. *Journal of Experimental Medicine* 204(4): 793-804.
- Johnson, W. M. and H. Lior (1988a).** A New Heat-Labile Cytolethal Distending Toxin (Cldt) Produced by Campylobacter Spp. *Microbial Pathogenesis* 4(2): 115-126.
- Johnson, W. M. and H. Lior (1988b).** A New Heat-Labile Cytolethal Distending Toxin (Cldt) Produced by Escherichia-Coli Isolates from Clinical Material. *Microbial Pathogenesis* 4(2): 103-113.
- Jones, S. A., V. B. O'Donnell, J. D. Wood, J. P. Broughton, E. J. Hughes and O. T. Jones (1996).** Expression of phagocyte NADPH oxidase components in human endothelial cells. *American Journal of Physiology: Heart and Circulatory Physiology* 271: H1626-1634.
- Jovanovic, S. V., C. W. Boone, S. Steenken, M. Trinoga and R. B. Kaskey (2001).** How curcumin works preferentially with water soluble antioxidants. *Journal of the American Chemical Society* 123(13): 3064-3068.
- Kalfas, S., G. Svensater, D. Birkhed and S. Edwardsson (1990).** Sorbitol Adaptation of Dental Plaque in People with Low and Normal Salivary-secretion Rates. *Journal of Dental Research* 69(2): 442-446.
- Katzenback, B. A. and M. Belosevic (2009).** Isolation and functional characterization of neutrophil-like cells, from goldfish (*Carassius auratus* L.) kidney. *Developmental and Comparative Immunology* 33(4): 601-611.
- Kessenbrock, K., M. Krumbholz, U. Schonermarck, W. Back, W. L. Gross, Z. Werb, H.-J. Grone, V. Brinkmann and D. E. Jenne (2009).** Netting neutrophils in autoimmune small-vessel vasculitis. *Nature Medicine* 15(6): 623-625.
- Kinane, D. F. and R. Attstrom (2005).** Advances in the pathogenesis of periodontitis - Group B consensus report of the fifth European workshop in periodontology. *Journal of Clinical Periodontology* 32: 130-131.
- Kobayashi, S. D., K. R. Braughton, A. R. Whitney, J. M. Voyich, T. G. Schwan, J. M. Musser and F. R. DeLeo (2003).** Bacterial pathogens modulate an apoptosis differentiation program in human neutrophils. *Proceedings of the National Academy of Sciences of the United States of America* 100(19): 10948-10953.
- Kristian, S. A., V. Datta, C. Weidenmaier, R. Kansal, I. Fedtke, A. Peschel, R. L. Gallo and V. Nizet (2005).** D-alanylation of teichoic acids promotes group A Streptococcus antimicrobial peptide resistance, neutrophil survival, and epithelial cell invasion. *Journal of Bacteriology* 187(19): 6719-6725.
- Kristian, S. A., M. Durr, J. A. G. Van Strijp, B. Neumeister and A. Peschel (2003).** MprF-mediated lysinylation of phospholipids in Staphylococcus aureus leads to protection against oxygen-independent neutrophil killing. *Infection and Immunity* 71(1): 546-549.
- Kulekci, G., S. Ciftci, F. Keskin, A. O. Kilic, S. Turkoglu, S. Badur, O. N. Develioglu, B. Leblibicioglu and M. Kulekci (2001).** PCR analysis of *Actinobacillus actinomycetemcomitans*, *Porphyromonas gingivalis*, *Treponema denticola* and *Fusobacterium nucleatum* in middle ear effusion. *Anaerobe* 7: 241-246.

- Kunitz, M. (1950).** Crystalline Desoxyribonuclease: I. Isolation and General Properties Spectrophotometric Method for the Measurement of Desoxyribonuclease Activity. *Journal of General Physiology* 33(4): 349-362.
- Lamont, R., A. Chan, C. Belton, K. Izutsu, D. Vasel and A. Weinberg (1995).** *Porphyromonas gingivalis* invasion of gingival epithelial cells. *Infection and Immunity* 63(10): 3878-3885.
- Lande, R., J. Gregorio, V. Facchinetti, B. Chatterjee, Y.-H. Wang, B. Homey, W. Cao, Y.-H. Wang, B. Su, F. O. Nestle, T. Zal, I. Mellman, J.-M. Schroder, Y.-J. Liu and M. Gilliet (2007).** Plasmacytoid dendritic cells sense self-DNA coupled with antimicrobial peptide. *Nature* 449(7162): 564-569.
- Lanza, F. (1998).** Clinical manifestation of myeloperoxidase deficiency. *Journal of Molecular Medicine* 76(10): 676-681.
- Lara-Tejero, M. and J. E. Galan (2002).** Cytolethal distending toxin: limited damage as a strategy to modulate cellular functions. *Trends in Microbiology* 10(3): 147-152.
- Larkin, M. A., G. Blackshields, N. P. Brown, R. Chenna, P. A. McGettigan, H. McWilliam, F. Valentin, I. M. Wallace, A. Wilm, R. Lopez, J. D. Thompson, T. J. Gibson and D. G. Higgins (2007).** Clustal W and Clustal X version 2.0. *Bioinformatics* 23(21): 2947-2948.
- Lauth, X., M. von Kockritz-Blickwede, C. W. McNamara, S. Myskowski, A. S. Zinkernagel, B. Beall, P. Ghosh, R. L. Gallo and V. Nizet (2009).** M1 Protein Allows Group A Streptococcal Survival in Phagocyte Extracellular Traps through Cathelicidin Inhibition. *Journal of Innate Immunity* 1(3): 202-214.
- Lee, W. L. and S. Grinstein (2004).** The tangled webs that neutrophils weave. *Science* 303(5663): 1477-1478.
- Levy, R., D. Rotrosen, O. Nagauker, T. L. Leto and H. L. Malech (1990).** Induction of the Respiratory Burst in HL-60 Cells - Correlation of Function and Protein Expression. *Journal of Immunology* 145(8): 2595-2601.
- Lichtenstein, A. (1991).** Mechanism of mammalian cell lysis mediated by peptide defensins. Evidence for an initial alteration of the plasma membrane. *The Journal of Clinical Investigation* 88(1): 93-100.
- Lieber, C. S. and L. M. Decarli (1970).** Hepatic Microsomal Ethanol-Oxidizing System: in Vitro Characteristics and Adaptive Properties in Vivo. *Journal of Biological Chemistry* 245(10): 2505-&.
- Lindberg, U. (1967).** Molecular Weight and Amino Acid Composition of Deoxyribonuclease I. *Biochemistry* 6(1): 335.
- Lingstrom, P., T. Imfeld and D. Birkhed (1993).** Comparison of Three Different Methods for Measurement of Plaque-pH in Humans after Consumption of Soft Bread and Potato Chips. *Journal of Dental Research* 72(5): 865-870.
- Linzer, R. and F. C. Neuhaus (1973).** Biosynthesis of Membrane Teichoic Acid - Role for D-Alanine-Activating Enzyme. *Journal of Biological Chemistry* 248(9): 3196-3201.
- Lippolis, J. D., T. A. Reinhardt, J. P. Goff and R. L. Horst (2006).** Neutrophil extracellular trap formation by bovine neutrophils is not inhibited by milk. *Veterinary Immunology and Immunopathology* 113(1-2): 248-255.
- Loe, H., A. Anerud, H. Boysen and E. Morrison (1986).** Natural history of periodontal disease in man. Rapid, moderate and no loss of attachment in Sri Lankan laborers 14 to 46 years of age. *Journal of Clinical Periodontology* 13(5): 431-440.
- Loe, H., E. Theilade and S. B. Jensen (1965).** Experimental Gingivitis in Man. *Journal of Periodontology* 36(3): 177.

- Loesche, W. J. (1976).** Chemotherapy of dental plaque infections. *Oral Sciences Reviews* 9: 65-107.
- Lögters, T., A. Paunel-Görgülü, C. Zilkens, J. Altrichter, M. Scholz, S. Thelen, R. Krauspe, S. Margraf, T. Jeri, J. Windolf and M. Jäger (2009).** Diagnostic accuracy of neutrophil-derived circulating free DNA (cf-DNA/NETs) for septic arthritis. *Journal of Orthopaedic Research* 27(11): 1401-1407.
- Lundqvist, H. and C. Dahlgren (1996a).** Isoluminol-enhanced chemiluminescence: A sensitive method to study the release of superoxide anion from human neutrophils. *Free Radical Biology and Medicine* 20(6): 785-792.
- Lundqvist, H., P. Follin, L. Khalfan and C. Dahlgren (1996b).** Phorbol myristate acetate-induced NADPH oxidase activity in human neutrophils: only half the story has been told. *Journal of Leukocyte Biology* 59(2): 270-279.
- Macanovic, M., D. Sinicropi, S. Shak, S. Baughman, S. Thiru and P. J. Lachmann (1996).** The treatment of systemic lupus erythematosus (SLE) in NZB/W F-1 hybrid mice; Studies with recombinant murine DNase and with dexamethasone. *Clinical and Experimental Immunology* 106(2): 243-252.
- Marcos, V., C. Nussbaum, L. Vitkov, A. Hector, E.-M. Wiedenbauer, D. Roos, T. Kuijpers, W. D. Krautgartner, O. Genzel-Boroviczeny, M. Sperandio and D. Hartl (2009).** Delayed but functional neutrophil extracellular trap formation in neonates. *Blood* 114(23): 4908-4911.
- Margraf, S., T. Lögters, J. Reipen, J. Altrichter, M. Scholz and J. Windolf (2008).** Neutrophil-derived circulating free DNA (cf-DNA-NETs): A potential prognostic marker for posttraumatic development of inflammatory second hit and sepsis. *Shock* 30(4): 352-358.
- Marklund, S. L. (1984).** Extracellular Superoxide Dismutase in Human Tissues and Human Cell Lines. *Journal of Clinical Investigation* 74(4): 1398-1403.
- Marsh, P. D. and V. M. Martin (2009).** *Oral Microbiology*. London, Churchill Livingstone Elsevier.
- Marshall, R. and A. K. Kaufman (1981).** Production of deoxyribonuclease, ribonuclease, coagulase, and hemolysins by anaerobic gram-positive cocci. *Journal of Clinical Microbiology* 13(4): 787-788.
- Martinelli, S., M. Urosevic, A. Daryadel, P. A. Oberholzer, C. Baumann, M. F. Fey, R. Dummer, H. U. Simon and S. Yousefi (2004).** Induction of genes mediating interferon-dependent extracellular trap formation during neutrophil differentiation. *Journal of Biological Chemistry* 279(42): 44123-44132.
- Matarasso, S., V. Daniele, V. Iorio Siciliano, M. D. Mignogna, G. Andreuccetti and C. Cafiero (2009).** The effect of recombinant granulocyte colony-stimulating factor on oral and periodontal manifestations in a patient with cyclic neutropenia: a case report. *International Journal of Dentistry* 2009: 654239.
- Matthews, J. B., H. J. Wright, A. Roberts, P. R. Cooper and I. L. C. Chapple (2007a).** Hyperactivity and reactivity of peripheral blood neutrophils in chronic periodontitis. *Clinical and Experimental Immunology* 147(2): 255-264.
- Matthews, J. B., H. J. Wright, A. Roberts, N. Ling-Mountford, P. R. Cooper and I. L. C. Chapple (2007b).** Neutrophil Hyper-responsiveness in Periodontitis. *Journal of Dental Research* 86(8): 718-722.
- Mayadas, T. N., G. C. Tsokos and N. Tsuboi (2009).** Mechanisms of Immune Complex-Mediated Neutrophil Recruitment and Tissue Injury. *Circulation* 120(20): 2012-2024.

- McCoy, A. J., H. J. Liu, T. J. Falla and J. S. Gunn (2001).** Identification of *Proteus mirabilis* mutants with increased sensitivity to antimicrobial peptides. *Antimicrobial Agents and Chemotherapy* 45(7): 2030-2037.
- McLachlan, J. L., A. J. Sloan, A. J. Smith, G. Landini and P. R. Cooper (2004).** S100 and cytokine expression in caries. *Infection and Immunity* 72(7): 4102-4108.
- Mealey, B. L. and T. W. Oates (2006).** Diabetes mellitus and periodontal diseases. *Journal of Periodontology* 77(8): 1289-1303.
- Mehrzad, J., H. Dosogne, F. Vangroenweghe and C. Burvenich (2001).** A comparative study of bovine blood and milk neutrophil functions with luminol-dependent chemiluminescence. *Luminescence* 16(6): 343-356.
- Michalowicz, B. S., D. Aeppli, J. G. Virag, D. G. Klump, J. E. Hinrichs, N. L. Segal, T. J. Bouchard and B. L. Pihlstrom (1991).** Periodontal Findings in Adult Twins. *Journal of Periodontology* 62(5): 293-299.
- Mikkelsen, H., Z. Duck, K. S. Lilley and M. Welch (2007).** Interrelationships between colonies, biofilms, and planktonic cells of *Pseudomonas aeruginosa*. *Journal of Bacteriology* 189(6): 2411-2416.
- Miller, B. F., R. Abrams, A. Dorfman and M. Klein (1942).** Antibacterial properties of protamine histone. *Science* 96: 428-430.
- Milward, M. R., I. L. C. Chapple, H. J. Wright, J. L. Millard, J. B. Matthews and P. R. Cooper (2007).** Differential activation of NF- κ B and gene expression in oral epithelial cells by periodontal pathogens. *Clinical & Experimental Immunology* 148(2): 307-324.
- Miyakawa, Y., T. Yamada, M. Shitara and Y. Fukazawa (1985).** Electrophoretic Patterns of Extracellular Deoxyribonuclease (Dnase) and Their Correlation with T-Type in Group-a Streptococci. *Microbiology and Immunology* 29(3): 195-204.
- Miyaura, C., E. Abe, T. Kuribayashi, H. Tanaka, K. Konno, Y. Nishii and T. Suda (1981).** 1- α , 25-Dihydroxyvitamin-D₃ Induces Differentiation of Human Myeloid-Leukemia Cells. *Biochemical and Biophysical Research Communications* 102(3): 937-943.
- Monboisse, J. C., L. Rittie, H. Lamfarraj, R. Garnotel and P. Gillery (2000).** In vitro glycoxidation alters the interactions between collagens and human polymorphonuclear leukocytes. *Biochemical Journal* 350: 777-783.
- Morris, A. J., J. Steele and D. A. White (2001).** The oral cleanliness and periodontal health of UK adults in 1998. *British Dental Journal* 191(4): 186-192.
- Moseley, R., R. J. Waddington and G. Embery (1997).** Degradation of glycosaminoglycans by reactive oxygen species derived from stimulated polymorphonuclear leukocytes. *Biochimica et Biophysica Acta - Molecular Basis of Disease* 1362(2-3): 221-231.
- Mulcahy, H., L. Charron-Mazenod and S. Lewenza (2008).** Extracellular DNA Chelates Cations and Induces Antibiotic Resistance in *Pseudomonas aeruginosa* Biofilms. *PLoS Pathogens* 4(11): e1000213.
- Munafò, D. B., J. L. Johnson, A. A. Brzezinska, B. A. Ellis, M. R. Wood and S. D. Catz (2009).** DNase I Inhibits a Late Phase of Reactive Oxygen Species Production in Neutrophils. *Journal of Innate Immunity* 1(6): 527-542.
- Mundi, H., B. Bjorksten, C. Svanborg, L. Ohman and C. Dahlgren (1991).** Extracellular release of reactive oxygen species from human neutrophils upon interaction with *Escherichia coli* strains causing renal scarring. *Infection and Immunity* 59(11): 4168-4172.

- Napirei, M., H. Karsunky, B. Zevnik, H. Stephan, H. G. Mannherz and T. Moroy (2000).** Features of systemic lupus erythematosus in DNase1-deficient mice. *Nature Genetics* 25(2): 177-181.
- Neeli, I., N. Dwivedi, S. Khan and M. Radic (2009).** Regulation of Extracellular Chromatin Release from Neutrophils. *Journal of Innate Immunity* 1(3): 194-201.
- Neeli, I., S. N. Khan and M. Radic (2008).** Histone Deimination As a Response to Inflammatory Stimuli in Neutrophils. *Journal of Immunology* 180(3): 1895-1902.
- Newburger, P. E., M. E. Chovaniec, J. S. Greenberger and H. J. Cohen (1979).** Functional-Changes in Human-Leukemic Cell-Line HL-60 - Model for Myeloid Differentiation. *Journal of Cell Biology* 82(2): 315-322.
- Newton, A. C. (1995).** Protein Kinase C: Structure, Function and Regulation. *Journal of Biological Chemistry* 270(48): 28495-28498.
- Nguyen, T. D., F.-X. Maquart and J.-C. Monboisse (2005).** Ionizing radiations and collagen metabolism: from oxygen free radicals to radio-induced late fibrosis. *Radiation Physics and Chemistry* 72(2-3): 381-386.
- Nichols, B. A., D. F. Bainton and M. G. Farquhar (1971).** Differentiation of Monocytes: Origin, Nature, and Fate of Their Azurophil Granules. *Journal of Cell Biology* 50(2): 498-515.
- Noga, E. J., Z. Fan and U. Silphaduang (2001).** Histone-like proteins from fish are lethal to the parasitic dinoflagellate *Amyloodinium ocellatum*. *Parasitology* 123: 57-65.
- Noll, M. (1974).** Subunit Structure of Chromatin. *Nature* 251(5472): 249-251.
- O'Donnell, V. B., D. G. Tew, O. T. G. Jones and P. J. England (1993).** Studies on the Inhibitory Mechanism of Iodonium Compounds with Special Reference to Neutrophil NADPH Oxidase. *Biochemical Journal* 290: 41-49.
- Oehmcke, S., M. Morgelin and H. Herwald (2009).** Activation of the Human Contact System on Neutrophil Extracellular Traps. *Journal of Innate Immunity* 1(3): 225-230.
- Page, R. C. and K. S. Kornman (1997).** The pathogenesis of human periodontitis: an introduction. *Periodontology* 2000 14(1): 9-11.
- Page, R. C. and H. E. Schroeder (1976).** Pathogenesis of inflammatory periodontal disease. A summary of current work. *Laboratory Investigation* 34(3): 235-249.
- Palic, D., J. Ostojic, C. B. Andreasen and J. A. Roth (2007).** Fish cast NETs: Neutrophil extracellular traps are released from fish neutrophils. *Developmental & Comparative Immunology* 31(8): 805-816.
- Pan, C. Q. and R. A. Lazarus (1999).** Ca²⁺-dependent activity of human DNase I and its hyperactive variants. *Protein Science* 8(9): 1780-1788.
- Papapanou, P. (1999).** Epidemiology of Periodontal Diseases: an update. *Journal of the International Academy of Periodontology* 1: 110-116.
- Park, C. B., H. S. Kim and S. C. Kim (1998a).** Mechanism of Action of the Antimicrobial Peptide Buforin II: Buforin II Kills Microorganisms by Penetrating the Cell Membrane and Inhibiting Cellular Functions. *Biochemical and Biophysical Research Communications* 244(1): 253-257.
- Park, C. B., M. S. Kim and S. C. Kim (1996).** A Novel Antimicrobial Peptide from *Bufo bufo gargarizans*. *Biochemical and Biophysical Research Communications* 218(1): 408-413.
- Park, I. Y., C. B. Park, M. S. Kim and S. C. Kim (1998b).** Parasin I, an antimicrobial peptide derived from histone H2A in the catfish, *Parasilurus asotus*. *FEBS Letters* 437(3): 258-262.

- Paster, B. J. and F. E. Dewhirst (2009).** Molecular microbial diagnosis. *Periodontology* 2000 51: 38-44.
- Patat, S. A., R. B. Carnegie, C. Kingsbury, P. S. Gross, R. Chapman and K. L. Schey (2004).** Antimicrobial activity of histones from hemocytes of the Pacific white shrimp. *European Journal of Biochemistry* 271(23-24): 4825-4833.
- Peschel, A., R. W. Jack, M. Otto, L. V. Collins, P. Staubitz, G. Nicholson, H. Kalbacher, W. F. Nieuwenhuizen, G. Jung, A. Tarkowski, K. P. M. van Kessel and J. A. G. van Strijp (2001).** Staphylococcus aureus resistance to human defensins and evasion of neutrophil killing via the novel virulence factor MprF is based on modification of membrane lipids with L-lysine. *Journal of Experimental Medicine* 193(9): 1067-1076.
- Peschel, A., M. Otto, R. W. Jack, H. Kalbacher, G. Jung and F. Gotz (1999).** Inactivation of the dlt operon in Staphylococcus aureus confers sensitivity to defensins, protegrins, and other antimicrobial peptides. *Journal of Biological Chemistry* 274(13): 8405-8410.
- Petersen, S. V., T. D. Oury, L. Ostergaard, Z. Valnickova, J. Wegrzyn, I. B. Thogersen, C. Jacobsen, R. P. Bowler, C. L. Fattman, J. D. Crapo and J. J. Enghild (2004).** Extracellular Superoxide Dismutase (EC-SOD) Binds to Type I Collagen and Protects Against Oxidative Fragmentation. *Journal of Biological Chemistry* 279(14): 13705-13710.
- Porschen, R. K. and S. Sonntag (1974).** Extracellular Deoxyribonuclease Production by Anaerobic Bacteria. *Applied Microbiology* 27(6): 1031-1033.
- Poyart, C., E. Pellegrini, M. Marceau, M. Baptista, F. Jaubert, M. C. Lamy and P. Trieu-Cuot (2003).** Attenuated virulence of Streptococcus agalactiae deficient in D-alanyl-lipoteichoic acid is due to an increased susceptibility to defensins and phagocytic cells. *Molecular Microbiology* 49(6): 1615-1625.
- Preiss, J. E., R. M. Bell and J. E. Niedel (1987).** Diacylglycerol Mass Measurements in Stimulated HL-60 Phagocytes. *Journal of Immunology* 138(5): 1542-1545.
- Ramos-Kichik, V., R. Mondragón-Flores, M. Mondragón-Castelán, S. Gonzalez-Pozos, S. Muñoz-Hernandez, O. Rojas-Espinosa, R. Chacón-Salinas, S. Estrada-Parra and I. Estrada-García (2009).** Neutrophil extracellular traps are induced by Mycobacterium tuberculosis. *Tuberculosis* 89(1): 29-37.
- Rebecchi, I. M. M., N. F. Novo, Y. Julian and A. Campa (2000).** Oxidative metabolism and release of myeloperoxidase from polymorphonuclear leukocytes obtained from blood sedimentation in a ficoll-hypaque gradient. *Cell Biochemistry and Function* 18(2): 127-132.
- Reid, S D., W. Hong, K E. Dew, D R. Winn, B. Pang, J. Watt, D T. Glover, S K. Hollingshead and W. E. Swords (2009).** Streptococcus pneumoniae forms surface-attached communities in the middle ear of experimentally infected chinchillas. *The Journal of Infectious Diseases* 199(6): 786-794.
- Remer, K. A., M. Brcic and T. W. Jungi (2003).** Toll-like receptor-4 is involved in eliciting an LPS-induced oxidative burst in neutrophils. *Immunology Letters* 85(1): 75-80.
- Riggio, M. P., A. Lennon and A. Smith (2001).** Detection of Peptostreptococcus micros DNA in clinical samples by PCR. *Journal of Medical Microbiology* 50(3): 249-254.
- Rigo, A., P. Viglino and G. Rotilio (1975).** Polarographic Determination of Superoxide Dismutase. *Analytical Biochemistry* 68(1): 1-8.
- Roberts, P. J., A. R. Cross, O. T. G. Jones and A. W. Segal (1982).** Development of Cytochrome-B and an Active Oxidase System in Association with Maturation of a Human Promyelocytic (HL-60) Cell-Line. *Journal of Cell Biology* 95(3): 720-726.

- Robinson, J. M. (2008).** Reactive oxygen species in phagocytic leukocytes. *Histochemistry and Cell Biology* 130(2): 281-297.
- Rôças, I. N. and J. J. F. Siqueira (2006).** Culture-Independent Detection of *Eikenella corrodens* and *Veillonella parvula* in Primary Endodontic Infections. *Journal of Endodontics* 32(6): 509-512.
- Rodríguez, S. B., B. L. Stitt and D. E. Ash (2009).** Expression of peptidylarginine deiminase from *Porphyromonas gingivalis* in *Escherichia coli*: Enzyme purification and characterization. *Archives of Biochemistry and Biophysics* 488(1): 14-22.
- Rose, F. R. A. J., K. Bailey, J. W. Keyte, W. C. Chan, D. Greenwood and Y. R. Mahida (1998).** Potential Role of Epithelial Cell-Derived Histone H1 Proteins in Innate Antimicrobial Defense in the Human Gastrointestinal Tract. *Infection and Immunity* 66(7): 3255-3263.
- Roth, B. L., M. Poot, S. T. Yue and P. J. Millard (1997).** Bacterial viability and antibiotic susceptibility testing with SYTOX Green nucleic acid stain. *Applied and Environmental Microbiology* 63(6): 2421-2431.
- Rovera, G., D. Santoli and C. Damsky (1979).** Human promyelocytic leukemia cells in culture differentiate into macrophage-like cells when treated with a phorbol diester. *PNAS* 76(6): 2779-2783.
- Rudek, W. and R. U. Haque (1976).** Extracellular enzymes of the genus *Bacteroides*. *Journal of Clinical Microbiology* 4(5): 458-460.
- Sabroe, I., L. R. Prince, E. C. Jones, M. J. Horsburgh, S. J. Foster, S. N. Vogel, S. K. Dower and M. K. B. Whyte (2003).** Selective Roles for Toll-Like Receptor (TLR)2 and TLR4 in the Regulation of Neutrophil Activation and Life Span. *Journal of Immunology* 170(10): 5268-5275.
- Samaranayake, L. P. (2002).** *Essential Microbiology for Dentistry*. Edinburgh, Churchill Livingstone.
- Sfanos, K. S. and W. B. Isaacs (2008).** An evaluation of PCR primer sets used for detection of *Propionibacterium acnes* in prostate tissue samples. *The Prostate* 68(14): 1492-1495.
- Shechter, D., H. L. Dormann, C. D. Allis and S. B. Hake (2007).** Extraction, purification and analysis of histones. *Nature Protocols* 2(6): 1445-1457.
- Shuto, T., T. Furuta, J. Cheung, D. C. Gruenert, Y. Ohira, S. Shimasaki, M. A. Suico, K. Sato and H. Kai (2007).** Increased responsiveness to TLR2 and TLR4 ligands during dimethylsulfoxide-induced neutrophil-like differentiation of HL-60 myeloid leukemia cells. *Leukemia Research* 31(12): 1721-1728.
- Sierig, G., C. Cywes, M. R. Wessels and C. D. Ashbaugh (2003).** Cytotoxic Effects of Streptolysin O and Streptolysin S Enhance the Virulence of Poorly Encapsulated Group A Streptococci. *Infection and Immunity* 71(1): 446-455.
- Siqueira Júnior, J. F. and I. d. N. Rôças (2003).** A 16S rDNA-based nested PCR protocol to detect *Campylobacter gracilis* in oral infections. *Pesquisa Odontológica Brasileira* 17: 142-146.
- Slots, J. (1999).** *Actinobacillus actinomycetemcomitans* and *Porphyromonas gingivalis* in periodontal disease: introduction. *Periodontology* 2000 20(1): 7-13.
- Slots, J., A. Ashimoto, M. J. Flynn, G. L. Li and C. Chen (1995).** Detection of Putative Periodontal Pathogens in Subgingival Specimens by 16s Ribosomal DNA Amplification with the Polymerase Chain-Reaction. *Clinical Infectious Diseases* 20: S304-S307.

- Snyderman, R. and E. J. Goetzel (1981).** Molecular and cellular mechanisms of leukocyte chemotaxis. *Science* 213(4510): 830-837.
- Socransky, S. S., A. D. Haffajee, M. A. Cugini, C. Smith and R. L. Kent (1998).** Microbial complexes in subgingival plaque. *Journal of Clinical Periodontology* 25(2): 134-144.
- Socransky, S. S., A. D. Haffajee, J. M. Goodson and J. Lindhe (1984).** New Concepts of Destructive Periodontal-Disease. *Journal of Clinical Periodontology* 11(1): 21-32.
- Spatafora, G. A., M. Sheets, R. June, D. Luyimbazi, K. Howard, R. Hulbert, D. Barnard, M. El Janne and M. C. Hudson (1999).** Regulated expression of the Streptococcus mutans dlt genes correlates with intracellular polysaccharide accumulation. *Journal of Bacteriology* 181(8): 2363-2372.
- Squier, M. K. T., A. J. Sehnert and J. J. Cohen (1995).** Apoptosis in Leukocytes. *Journal of Leukocyte Biology* 57(1): 2-10.
- Steinckwich, N., J.-P. Fripiat, M.-J. Stasia, M. Erard, R. Boxio, C. Tankosic, I. Doignon and O. Nusse (2007).** Potent inhibition of store-operated Ca²⁺ influx and superoxide production in HL60 cells and polymorphonuclear neutrophils by the pyrazole derivative BTP2. *Journal of Leukocyte Biology* 81(4): 1054-1064.
- Stendahl, O., T. Andersson, C. Dahlgren and K. E. Magnusson (1986).** Defective Chemiluminescence Response in Differentiated HL60-Cells Due to Impaired Degranulation. *Biochimica Et Biophysica Acta* 881(3): 430-436.
- Sugai, M., T. Kawamoto, S. Y. Peres, Y. Ueno, H. Komatsuzawa, T. Fujiwara, H. Kurihara, H. Suginaka and E. Oswald (1998).** The cell cycle-specific growth-inhibitory factor produced by Actinobacillus actinomycetemcomitans is a cytolethal distending toxin. *Infection and Immunity* 66(10): 5008-5019.
- Sumby, P., K. D. Barbican, D. J. Gardner, A. R. Whitney, D. M. Welty, R. D. Long, J. R. Bailey, M. J. Parnell, N. P. Hoe, G. G. Adams, F. R. DeLeo and J. M. Musser (2005).** Extracellular deoxyribonuclease made by group A Streptococcus assists pathogenesis by enhancing evasion of the innate immune response. *Proceedings of the National Academy of Sciences of the United States of America* 102(5): 1679-1684.
- Suzuki, N., Y. Nakano, A. Yoshida, Y. Yamashita and Y. Kiyoura (2004).** Real-Time TaqMan PCR for Quantifying Oral Bacteria during Biofilm Formation. *Journal of Clinical Microbiology* 42(8): 3827-3830.
- Suzuki, N., Y. Nakano, Y. Yoshida, D. Ikeda and T. Koga (2001).** Identification of Actinobacillus actinomycetemcomitans Serotypes by Multiplex PCR. *Journal of Clinical Microbiology* 39(5): 2002-2005.
- Takao, A., H. Nagamune and N. Maeda (2004).** Identification of the anginosus group within the genus Streptococcus using polymerase chain reaction. *FEMS Microbiology Letters* 233(1): 83-89.
- Takei, H., A. Araki, H. Watanabe, A. Ichinose and F. Sendo (1996).** Rapid killing of human neutrophils by the potent activator phorbol 12-myristate 13-acetate (PMA) accompanied by changes different from typical apoptosis or necrosis. *Journal of Leukocyte Biology* 59(2): 229-240.
- Taniuchi, H., C. B. Anfinsen and A. Sodja (1967).** Amino Acid Sequence of an Extracellular Nuclease of Staphylococcus Aureus III. Complete Amino Acid Sequence. *Journal of Biological Chemistry* 242(20): 4752-4758.
- Tapper, H. (1996).** The secretion of preformed granules by macrophages and neutrophils. *Journal of Leukocyte Biology* 59(5): 613-622.
- Teufelhofer, O., R.-M. Weiss, W. Parzefall, R. Schulte-Hermann, M. Micksche, W. Berger and L. Elbling (2003).** Promyelocytic HL60 Cells Express NADPH Oxidase

- and Are Excellent Targets in a Rapid Spectrophotometric Microplate Assay for Extracellular Superoxide. *Toxicological Sciences* 76(2): 376-383.
- Tew, J. G., D. R. Marshall, J. A. Burmeister and R. R. Ranney (1985).** Relationship between Gingival Crevicular Fluid and Serum Antibody-Titers in Young-Adults with Generalized and Localized Periodontitis. *Infection and Immunity* 49(3): 487-493.
- Theilade, E. (1986).** The Nonspecific Theory in Microbial Etiology of Inflammatory Periodontal-Diseases. *Journal of Clinical Periodontology* 13(10): 905-911.
- Tran, S. D. and J. D. Rudney (1996).** Multiplex PCR using conserved and species-specific 16S rRNA gene primers for simultaneous detection of Actinobacillus actinomycetemcomitans and Porphyromonas gingivalis. *Journal of Clinical Microbiology* 34(11): 2674-2678.
- Urban, C. F., D. Ermert, M. Schmid, U. Abu-Abed, C. Goosmann, W. Nacken, V. Brinkmann, P. R. Jungblut and A. Zychlinsky (2009).** Neutrophil Extracellular Traps Contain Calprotectin, a Cytosolic Protein Complex Involved in Host Defense against *Candida albicans*. *PLoS Pathogens* 5(10): e1000639.
- Urban, C. F., S. Lourido and A. Zychlinsky (2006a).** How do microbes evade neutrophil killing? *Cellular Microbiology* 8(11): 1687-1696.
- Urban, C. F., U. Reichard, V. Brinkmann and A. Zychlinsky (2006b).** Neutrophil extracellular traps capture and kill *Candida albicans* yeast and hyphal forms. *Cellular Microbiology* 8(4): 668-676.
- Van Dyke, T. E., H. U. Horoszewicz, L. J. Cianciola and R. J. Genco (1980).** Neutrophil Chemotaxis Dysfunction in Human Periodontitis. *Infection and Immunity* 27(1): 124-132.
- Vitkov, L., M. Klappacher, M. Hannig and W. D. Krautgartner (2009).** Extracellular neutrophil traps in periodontitis. *Journal of Periodontal Research* 44(5): 664-672.
- Vitkov, L., M. Klappacher, M. Hannig and W. D. Krautgartner (2010).** Neutrophil Fate in Gingival Crevicular Fluid. *Ultrastructural Pathology* 34(1): 25-30.
- von Kockritz-Blickwede, M., O. A. Chow and V. Nizet (2009).** Fetal calf serum contains heat-stable nucleases that degrade neutrophil extracellular traps. *Blood* 114(25): 5245-5246.
- von Kockritz-Blickwede, M., O. Goldmann, P. Thulin, K. Heinemann, A. Norrby-Teglund, M. Rohde and E. Medina (2008).** Phagocytosis-independent antimicrobial activity of mast cells by means of extracellular trap formation. *Blood* 111(6): 3070-3080.
- Voyich, J. M., D. E. Sturdevant, K. R. Braughton, S. D. Kobayashi, B. Lei, K. Virtaneva, D. W. Dorward, J. M. Musser and F. R. DeLeo (2003).** Genome-wide protective response used by group A Streptococcus to evade destruction by human polymorphonuclear leukocytes. *Proceedings of the National Academy of Sciences of the United States of America* 100(4): 1996-2001.
- Walker, M. J., A. Hollands, M. L. Sanderson-Smith, J. N. Cole, J. K. Kirk, A. Henningham, J. D. McArthur, K. Dinkla, R. K. Aziz, R. G. Kansal, A. J. Simpson, J. T. Buchanan, G. S. Chhatwal, M. Kotb and V. Nizet (2007).** DNase Sda1 provides selection pressure for a switch to invasive group A streptococcal infection. *Nature Medicine* 13(8): 981-985.
- Wang, Y., M. Li, S. Stadler, S. Correll, P. Li, D. Wang, R. Hayama, L. Leonelli, H. Han, S. A. Grigoryev, C. D. Allis and S. A. Coonrod (2009).** Histone hypercitullination mediates chromatin decondensation and neutrophil extracellular trap formation. *Journal of Cell Biology* 184(2): 205-213.

- Wannamaker, L. W. (1958).** The Differentiation of 3 Distinct Desoxyribonucleases of Group-a Streptococci. *Journal of Experimental Medicine* 107(6): 797-812.
- Wardini, A. B., A. B. Guimaraes-Costa, M. T. Nascimento, N. R. Nadaes, M. d. G. M. Danelli, C. Mazur, C. F. Benjamim, E. M. Saraiva and L. H. Pinto-da-Silva (2010).** Characterization of neutrophil extracellular traps in cats naturally-infected with the feline leukemia virus (FeLV). *Journal of General Virology* 91(1): 259-264.
- Wartha, F., K. Beiter, B. Albiger, J. Fernebro, A. Zychlinsky, S. Normark and B. Henriques-Normark (2007).** Capsule and d-alanylated lipoteichoic acids protect *Streptococcus pneumoniae* against neutrophil extracellular traps. *Cellular Microbiology* 9(5): 1162-1171.
- Watanabe, K. and T. O. Frommel (1993).** Detection of *Porphyromonas gingivalis* in oral plaque samples by use of the polymerase chain reaction. *Journal of Dental Research* 72(6): 1040-1044.
- Watson, R. W. G., H. P. Redmond, J. H. Wang, C. Condron and D. Bouchier-Hayes (1996).** Neutrophils undergo apoptosis following ingestion of *Escherichia coli*. *Journal of Immunology* 156(10): 3986-3992.
- Weinrauch, Y., D. Drujan, S. D. Shapiro, J. Weiss and A. Zychlinsky (2002).** Neutrophil elastase targets virulence factors of enterobacteria. *Nature* 417(6884): 91-94.
- Whaley, D. N., L. S. Wiggs, P. H. Miller, P. U. Srivastava and J. M. Miller (1995).** Use of Presumptive Plates to identify anaerobic bacteria. *Journal of Clinical Microbiology* 33(5): 1196-1202.
- Whitchurch, C. B., T. Tolker-Nielsen, P. C. Ragas and J. S. Mattick (2002).** Extracellular DNA Required for Bacterial Biofilm Formation. *Science* 295(5559): 1487.
- Williams, A. J. and P. J. Cole (1981).** Investigation of Alveolar Macrophage Function Using Lucigenin-Dependent Chemiluminescence. *Thorax* 36(11): 866-869.
- Woese, C. R. (1987).** Bacterial evolution. *Microbiological Reviews* 51(2): 221-271.
- Wright, H. J., J. B. Matthews, I. L. C. Chapple, N. Ling-Mountford and P. R. Cooper (2008).** Periodontitis Associates with a Type 1 IFN Signature in Peripheral Blood Neutrophils. *Journal of Immunology* 181(8): 5775-5784.
- Ximénez-Fyvie, L. A., A. D. Haffajee and S. S. Socransky (2000).** Microbial composition of supra- and subgingival plaque in subjects with adult periodontitis. *Journal of Clinical Periodontology* 27(10): 722-732.
- Yoshida, A., M. Tachibana, T. Ansai and T. Takehara (2005).** Multiplex polymerase chain reaction assay for simultaneous detection of black-pigmented *Prevotella* species in oral specimens. *Oral Microbiology and Immunology* 20(1): 43-46.
- Yost, C. C., M. J. Cody, E. S. Harris, N. L. Thornton, A. M. McInturff, M. L. Martinez, N. B. Chandler, C. K. Rodesch, K. H. Albertine, C. A. Petti, A. S. Weyrich and G. A. Zimmerman (2009).** Impaired neutrophil extracellular trap (NET) formation: A novel innate immune deficiency of human neonates. *Blood* 113(25): 6419-6427.
- Yousefi, S., J. A. Gold, N. Andina, J. J. Lee, A. M. Kelly, E. Kozlowski, I. Schmid, A. Straumann, J. Reichenbach, G. J. Gleich and H.-U. Simon (2008).** Catapult-like release of mitochondrial DNA by eosinophils contributes to antibacterial defense. *Nature Medicine* 14(9): 949-953.
- Yousefi, S., C. Mihalache, E. Kozlowski, I. Schmid and H. U. Simon (2009).** Viable neutrophils release mitochondrial DNA to form neutrophil extracellular traps. *Cell Death and Differentiation* 16(11): 1438-1444.
- Zhou, Z. M., A. A. Ribeiro, S. H. Lin, R. J. Cotter, S. I. Miller and C. R. H. Raetz (2001).** Lipid A modifications in polymyxin-resistant *Salmonella typhimurium* - PMRA-

dependent 4-amino-4-deoxy-L-arabinose, and phosphoethanolamine incorporation.
Journal of Biological Chemistry 276(46): 43111-43121.

APPENDIX

Fnuenuc16sRNA	AAGTCTACTTGAATTTGGGTTTTTAACTTCGATTTGGGTGGCGGACGGGTGAGTAAACGC	120	Fnuenuc16sRNA	GTAGTCCACGCCGTAACCGATGATTACTAGGTGGTGGGG-GTCGAACCTCAGCGCCCAAG	837
Fnuvinceti116sRNA	AAGTCAACTTGAATTTGGGTTTTT-AACTTAGGTTGGGTGGCGGACGGGTGAGTAAACGC	119	Fnuvinceti116sRNA	GTAGTCCACGCCGTAACCGATGATTACTAGGTGGTGGGG-GTCGAACCTCAGCGCCCAAG	836
Lbuccalis16sRNA	-----CNNAAGCGGACGGGTGAGTAAACGC	24	Lbuccalis16sRNA	GTAGTCCCGCCGTAACCGATGATTACTAGGTGGTGGGCATGAAGAGTGTCCGTTCGGAAG	740
	*****			reverse primer site	
Fnuenuc16sRNA	GTAAGAATTTGCCCTCACACCTAGGGACACACATTTGAAACGAATGCTAATACCTGATAT	180	Fnuenuc16sRNA	CRAACGCGATAAGTAAATCCGCTGGGGAGTACGTAACGAGTATGAAACTCAAAGGAAT	897
Fnuvinceti116sRNA	GTAAGAACTTGCCTCACACCTAGGGACACACATTTGAAACGAATGCTAATACCTAATAT	179	Fnuvinceti116sRNA	CRAACGCGATAAGTAAATCCGCTGGGGAGTACGTAACGAGTATGAAACTCAAAGGAAT	896
Lbuccalis16sRNA	GTAAAGAACTTGCCTGCACAGGGATAACAGACGGAAACGACTGATNATNCTNATNC	84	Lbuccalis16sRNA	CTAANGCGATAAGTAAATCCGCTGGGGAGTACGGCCGCAAGGCTNAAACTCAAAGGAAT	800
	*****			*****	
Fnuenuc16sRNA	TAIGATTATAGGSCATCC-TAGAATTGAAAGCTATATGCGCTGTGAGAGAGCTTTGCG	239	Fnuenuc16sRNA	GACGGGGACCCGCACAAGCGGTGGAGCATGTGGTTTAAATCGACGCAACGCGAGGAACCT	957
Fnuvinceti116sRNA	TATGATTAATAGGSCATCC-TATAATTGAAAGCTATAAGCGCTGTGAGAGAGCTTTGCG	238	Fnuvinceti116sRNA	GACGGGGACCCGCACAAGCGGTGGAGCATGTGGTTTAAATCGACGCAACGCGAGGAACCT	956
Lbuccalis16sRNA	TATGCCAGCACGCATGTGCCCGGCAATGAAA--AGNNATGCTGCAGGAGAGCTTTGCG	141	Lbuccalis16sRNA	GACGGGGACC-CCACAAGCGGTGGAGCATGTGGTTTAAATCGACGCAACGCGAGGAACCT	859
	*****			*****	
	forward primer site				
Fnuenuc16sRNA	TCOCATTAGCTAGTTGGAGAGGTAAACGGCTCACCAAGGCGATGATGGGTAGCCGGCCTGA	299	Fnuenuc16sRNA	TACCAGGTTTGACATCTTAGGAATGAGACAGAGATGTTTTCAGTGTCCCTTCGGGGAAC	1017
Fnuvinceti116sRNA	TCOCATTAGCTAGTTGGAGAGGTAAACGGCTCACCAAGGCGATGATGGGTAGCCGGCCTGA	298	Fnuvinceti116sRNA	TACCAGGTTTGACATCTTAGGAATGAGATAGAGATATTTTCAGTGTCCCTTCGGGGAAC	1016
Lbuccalis16sRNA	TCCTNTTAGCTTGTGGTGAAGTAAACGGCTCACCAAGGCGATGATGNGTGGTGGCCTGA	201	Lbuccalis16sRNA	TCCAGATCTTGACATCTTAGGAATGCGCTNTGAGAA--CAGNNGTGCTTCGGG--AAC	915
	*****			*****	
Fnuenuc16sRNA	GAGGGTGAACGCCACAGGGGACTGAGACACGGCCCTTACTCCTACGGGAGGCGAGCAGT	359	Fnuenuc16sRNA	CTAAGACAGGTGGTGCATGGCTGTCTGCTCAGCTCGTGTCTGTGAGATGTTGGGTTAAGTCC	1077
Fnuvinceti116sRNA	GAGGGTGAATCGGCCACAGGGGACTGAGACACGGCCCTTACTCCTACGGGAGGCGAGCAGT	358	Fnuvinceti116sRNA	CTAAGACAGGTGGTGCATGGCTGTCTGCTCAGCTCGTGTCTGTGAGATGTTGGGTTAAGTCC	1076
Lbuccalis16sRNA	GAGGGTGAACGCCACAGGGGACTGAGATCCGGCCCTTACTCCTACGGGAGGCGCGCT	261	Lbuccalis16sRNA	GTAGACAGGTGGTGCATGGCTGTCTGACAGCTCGTGTCTGTGAGATGTTGGGTTAAGTCC	975
	*****			*****	
Fnuenuc16sRNA	GGGGAATATTGGACAATGGACCGAGAGTCTGATCCAGCAATTCGTGTGCACGATGACGT	419	Fnuenuc16sRNA	CGCAACGAGCGCAACCCCTTTCGTATGTTACCATCATTAAAGTGGGGACTCATGCGATAC	1137
Fnuvinceti116sRNA	GGGGAATATTGGACAATGGACCGAGAGTCTGATCCAGCAATTCGTGTGCACGATGAAGT	418	Fnuvinceti116sRNA	CGCAACGAGCGCAACCCCTTTCGTATGTTACCATCATTAAAGTGGGGACTCATGCGATAC	1136
Lbuccalis16sRNA	GGGGAATATTGGACAATGGGG--GCAACCTGATCCAGCAATTCGTGTGCACGAAAGG	320	Lbuccalis16sRNA	CGCAACGAGCGCAACCCCNATCGTATGTTGCCATCATTNAGTGGGGACTCATGCGGAGAC	1038
	*****			*****	
Fnuenuc16sRNA	TTTTCGGAATGTAAGTGCCTTCAGTTGGGAAGAAAAAATGACGGTACCAACAGAGAA	479	Fnuenuc16sRNA	TGCTACGATGAGTAGGAGGAAGTGGGGATGACGTCAGTCAATCATGCCCCCTTATACGC	1197
Fnuvinceti116sRNA	TTTTCGGAATGTAAGTGCCTTCAGTTGGGAAGAAAAAATGACGGTACCAACAGAGAA	478	Fnuvinceti116sRNA	TGCTACGATGAGTAGGAGGAAGTGGGGATGACGTCAGTCAATCATGCCCCCTTATACGC	1196
Lbuccalis16sRNA	TTTTCGGATGTAAGTGCCTTCAGCAGGGAAAGAAAGTGTGACGCTACCTGCAAGAA	380	Lbuccalis16sRNA	TGCTGCGAAGAGCAGGAGGAAGTGGGGATGACGTCAGTCAATCATGCCCCCTTATGATC	1098
	*****			*****	
Fnuenuc16sRNA	GTGACGGCTAAATACGTTGCCAGCAGCCGCGGTAATACGATGTCACGAGCGTTATCCGGA	539	Fnuenuc16sRNA	TGGGTACACACGTTGCTACAATGGTGAACAGAGAGTTGCAAAAGCGGTGAGGTGGAGCT	1257
Fnuvinceti116sRNA	GTGACGGCTAAATACGTTGCCAGCAGCCGCGGTAATACGATGTCACGAGCGTTATCCGGA	538	Fnuvinceti116sRNA	TGGGTACACACGTTGCTACAATGGTGAACAGAGAGTTGCAAAAGCGGTGAGGTGGAGCT	1256
Lbuccalis16sRNA	GCGACGGCTAAATACGTTGCCAGCAGCCGCGGTAATACGATGTCGCGNAGCGTTATCCGGA	440	Lbuccalis16sRNA	TGGGTACACACGTTGCTACAATGGCCGGTACAAGAGAGTGCAAAAGCGGTGAGGTGGAGCT	1158
	*****			*****	
Fnuenuc16sRNA	TTTATTGGGCGTAAAGCGGCTAGGTTGGTTATGTAAGTCTGATGTGAAAAATGCAGGGCT	599	Fnuenuc16sRNA	AATCTCAGAAAATCTATTCTTAGTTCGGATTGTAAGTCTGCAACTCGAGTACATGAAGTTGG	1317
Fnuvinceti116sRNA	TTTATTGGGCGTAAAGCGGCTAGGTTGGTTATGTAAGTCTGATGTGAAAAATGCAGGGCT	598	Fnuvinceti116sRNA	AATCTCAGAAAATCTATTCTTAGTTCGGATTGTAAGTCTGCAACTCGAGTACATGAAGTTGG	1316
Lbuccalis16sRNA	ATTATTGGGCATAAAGGGCATCTAGGCGCCAGACAAAGTCTGGGGTGAAGAACTNGCGGCT	500	Lbuccalis16sRNA	AATCTTTNAAAG--CGGTCGCGATTGCAAGTCTGCAACTCGACTNCAATGAAGCGGG	1214
	*****			*****	
Fnuenuc16sRNA	CAACT-CTGATTTGCGTTGGAAACTGTGTAACCTAGAGTACTGGAGAGGTAAGCGGAAC	658	Fnuenuc16sRNA	AATCGTAGTAATCGCGAATCAGCAATGTCGCGGTGAATACGTTCTCGGGTCTGTGACAC	1377
Fnuvinceti116sRNA	CAACT-CTGATTTGCGTTGGAAACTGTATAACCTAGAGTACTGGAGAGGTAAGCGGAAC	657	Fnuvinceti116sRNA	AATCGTAGTAATCGCGAATCAGCAATGTCGCGGTGAATACGTTCTCGGGTCTGTGACAC	1376
Lbuccalis16sRNA	CAACCGNAGCCTGCGCTGGAAACTGTTNNCTNAGAGTCTGGAGAGTGTGNCGGAAGT	560	Lbuccalis16sRNA	AATCGTAGTAATCGCAGATCAGCAATGCTGCGGTGAATACGTTCTCGGGTCTGTGACAC	1274
	*****			*****	
Fnuenuc16sRNA	CAAGTGTAGAGGTGAAATTCGTAGATATTTGTAGGAATGCCGATGGGGAAGCCAGCTTAC	718	Fnuenuc16sRNA	ACGCGCGCTCACACCACGAGAGTTGGTTGCACCTGAAGTAGCAGGCTAACCGTAAGGAG	1437
Fnuvinceti116sRNA	CAAGTGTAGAGGTGAAATTCGTAGATATTTGTAGGAATGCCGATGGGGAAGCCAGCTTAC	717	Fnuvinceti116sRNA	ACGCGCGCTCACACCACGAGAGTTGGTTGCACCTGAAGTAGCAGGCTAACCGTAAGGAG	1436
Lbuccalis16sRNA	CACGAGTAGAGGTGAAATTCGTAGATATGTCAGGAATGCCGATGGGGAAGGAAAGATAGTTCAC	620	Lbuccalis16sRNA	ACGCGCGCTCACACCACGAGAGTTNTNGCACCTGAAGCCGCGGTCGCAACCG-----	1327
	*****			*****	
Fnuenuc16sRNA	TGSACAGATACTGACGCTGAAGCGCGAAAGCGTGGGTAGCAACAGGATTAGATACCCTG	778	Fnuenuc16sRNA	GGATGTTCCGAGGGTGTGATTAGCGATTGGGGTGAAGTCTGTAACAGGATCCGTCAGGG	1497
Fnuvinceti116sRNA	TGSACAGATACTGACGCTGAAGCGCGAAAGCGTGGGTAGCAACAGGATTAGATACCCTG	777	Fnuvinceti116sRNA	GGATGTTCCGAGGGTGTGATTAGCGATTGGGGTGAAGTCTGTAACAGGATCCGTCAGGG	1496
Lbuccalis16sRNA	TGGACGGTACTGACGCTGAAGTCCGAAAGCTGGGGAGCGCAACAGGATTAGATACCCTG	680	Lbuccalis16sRNA	-----	
	*****			*****	

Figure 92. Gene alignments for design of primers: a) *L. buccalis* (16s rRNA; accession number X90831). 83% sequence match to *F. nucleatum* subsp. *nucleatum* 16s rRNA and 83% sequence match to *F. nucleatum* subsp. *vincetii* 16s rRNA.

Aodontolyticus16srRNA	-----CGGGCGTCTTAACACATGCAAGTCGAAC	29	Aodontolyticus16srRNA	GAATTATTGGGCGTAAAGGGCTTGTAGGCGGTINGTGCCTCTGCCGTGA	561
Mcurtisii	CCTGGCTCAGGACGAACGCTGGCGCGTCTTAACACATGCAAGTCGAAC	240	Mcurtisii	GATTTATTGGGCGTAAAGAGCTCGTAGTGGTTCCTCGCCTCTGTCTGTA	773
Aviscosus	CCTGGCTCAG-ACGAACGCTGGCGCGTCTTAACACATGCAAGTCGAAC	59	Aviscosus	GAATTATTGGGCGTAAAGAGCTCGTAGGCGGTGTTGCCTCTGTCTGTA	608
Aurogenitalis	CCTGGCTCAGGACGAACGCTGGCGCGTCTTAACACATGCAAGTCGAAC	300	Aurogenitalis	GAATTATTGGGCGTAAAGAGCTCGTAGGCGGTGTTGCCTCTGTCTGTA	837
	*****			** *****	
Aodontolyticus16srRNA	GCTGAAGCC--CAGCTTGCTG-GG-TGGATGAGTGGCGAACGGGTGAGTA	75	Aodontolyticus16srRNA	AATCCTCTGGCTTAACCTGGGCGCTGCGGTGGGTACGGGCTNACTTGAGT	611
Mcurtisii	GATGAAGCC-CCAGCTTGCTGTTGG-TGGATTAGTGGCGAACGGGCGAGTA	288	Mcurtisii	AAGCCAGCAGCTTAACCTGTTGGCTGCGGTGGGTACGGGCGGCTTGAGT	823
Aviscosus	GCTGAAGGGACCAAGCTTGCTGGTCTCGGATGAGTGGCGAACGGGTGAGTA	109	Aviscosus	AATCCTCTGGCTTAACCTGGGCGCTGCGGTGGGTACGGGCGGCTTGAGT	658
Aurogenitalis	GCTGAAGCT-CCAGCTTGCTGGGG-TGGATGAGTGGCGAACGGGTGAGTA	348	Aurogenitalis	AATCCTCTGGCTTAACCTGGGCGCTGCGGTGGGTACGGGCGGCTTGAGT	887
	* *****			** ** *****	
Aodontolyticus16srRNA	ACACGTGAGTAACCTGCCCCCTTCTTTGGGATAACGCCGGAAACGGGTG	125	Aodontolyticus16srRNA	GCGGTAGGGGAGACTGGAATCCTGGTGTAGCGGTGGAATGCGCAGATAT	661
Mcurtisii	ACACGTGAGTAACCTGTCCTTTCTTTGGGATAACGCCGGAAACGGGCTG	338	Mcurtisii	GCGGTAGGGGTGACTGGAATTCCTGGTGTAGCGGTGGAATGCGCAGATAT	873
Aviscosus	ACACGTGAGTAACCTGCCCCCTTCTTCTGGATAACGCCGATGAAAGTGTGG	159	Aviscosus	GCGGTAGGGGAGACTGGAATCCTGGTGTAGCGGTGGAATGCGCAGATAT	708
Aurogenitalis	ACACGTGAGTAACCTGCCCCCTTCTTCTGGATAACGCCGATGAAAGTGTAG	398	Aurogenitalis	GCGGTAGGGGAGACTGGAATTCCTGGTGTAGCGGTGGAATGCGCAGATAT	937
	*****			*****	
Aodontolyticus16srRNA	CTAATACIGGATATTCAGTGTCTTCGCATGCGGGTGTGGAAAGGT--	173	Aodontolyticus16srRNA	CAGGAAGAACACCGGTGGCGAAGGCGGGTCTCTGGGCCGTTACTGACGCT	711
Mcurtisii	CTAATACIGGATATTCAGGCGTACCGCATGCTGGTGTGGAAAGGT--	386	Mcurtisii	CAGGAGGAACACCGATGGCGAAGGCGAGTCACTGGGCCGTTACTGACACT	923
Aviscosus	CTAATACGGGATATTCGGGTCTGTCGCATGACGGGCCCGGAAAGATGC	209	Aviscosus	CAGGAAGAACACCGGTGGCGAAGGCGGGTCTCTGGGCCGTTACTGACGCT	758
Aurogenitalis	CTAATACGGGATATTCGGCTGCTCGCATGCGGTGGTGTGGAAAGGT--	446	Aurogenitalis	CAGGAGGAACACCGGTGGCGAAGGCGGGTCTCTGGGCCGTTACTGACGCT	987
	*****			*****	
Aodontolyticus16srRNA	-----TTTTTCTGGTGGGGGATGGGCTCGCGGCTATCAGCTTGT	214	Aodontolyticus16srRNA	GAGGAGCGAAGCGTGGGGAGCGAACAGGATTAGATACCCCTGGTAGTCCA	761
Mcurtisii	-----TTTTTCTGGGATTGGTGGGCTCGCGGCTATCAGCTTGT	427	Mcurtisii	GAGGAGCGAAGCGTGGGGAGCGAACAGGATTAGATACCCCTGGTAGTCCA	973
Aviscosus	GCCTTTGGGTGTTTTGGTGGGGGATGGGCTCGCGGCTATCAGCTTGT	269	Aviscosus	GAGGAGCGAAGCGTGGGGAGCGAACAGGATTAGATACCCCTGGTAGTCCA	808
Aurogenitalis	-----TTTTTCTGGTGGGGATGGGCTCGCGGCTATCAGCTTGT	487	Aurogenitalis	GAGGAGCGAAGCGTGGGGAGCGAACAGGATTAGATACCCCTGGTAGTCCA	1037
	*****			*****	
Aodontolyticus16srRNA	GGTGGGGTGTGGCCATACCAAGGCTTTGACGGGTAGCCGGCTGAGAGGG	264	Aodontolyticus16srRNA	CGCTGTAACCGTTGGGCACTAGTGTGGGG---GCCACCGTGGTTCTG	808
Mcurtisii	GGTGGGGTGTGGCCATACCAAGGCTTTGACGGGTAGCCGGCTGAGAGGG	477	Mcurtisii	CGCTGTAACCGTTGGGCACTAGTGTGGGG---TGCTATCCTGTGTTCTG	1022
Aviscosus	GGTGGGGTGTGGCCATACCAAGGCGGTGACGGGTAGCCGGCTGAGAGGG	309	Aviscosus	CGCCGTAAACGTTGGGCACTAGTGTGGGGGCTTTTCCGGCTCTTCCG	858
Aurogenitalis	GGTGGGGTGTGGCCATACCAAGGCGGTGACGGGTAGCCGGCTGAGAGGG	537	Aurogenitalis	CGCCGTAAACGTTGGGCACTAGTGTGGGG---CTCTTTCCGGGTTTCCG	1086
	*****			*****	
Aodontolyticus16srRNA	TGACCGGTCACATGGGACTGAGATACGGCCAGACTCCTACGGGAGGCA	314	Aodontolyticus16srRNA	CGCCGTAGCTAACGCTTTAAGTGCCTCCCTGGGGAGTACGGCCGCAAGG	858
Mcurtisii	TGGTCGGTCCGACTGGGACTGAGATACGGCCAGACTCCTACGGGAGGCA	527	Mcurtisii	CGCCGTAGCTAACGCTTAAAGTTCCTCCCTGGGGAGTACGGTCCGCAAG	1072
Aviscosus	TGGACGGTCCGACTGGGACTGAGACACGGCCAGACTCCTACGGGAGGCA	359	Aviscosus	CGCCGTAGCTAACGCTTAAAGTGCCTCCCTGGGGAGTACGGCCGCAAGG	908
Aurogenitalis	TGGACGGCCACACTGGGACTGAGACACGGCCAGACTCCTACGGGAGGCA	587	Aurogenitalis	CGCCGTAGCTAACGCTTAAAGTGCCTCCCTGGGGAGTACGGCCGCAAGG	1136
	*****			*****	
Aodontolyticus16srRNA	GCAGTGGGGAATATTGCACAATGGGCGAAGGCTGATGCAGCGACGCCGC	364	Aodontolyticus16srRNA	CTAAACTCAAAGGAATTGACGGGGGCCGCACAAGCGGGGAGCATGCG	908
Mcurtisii	GCAGTGGGGAATATTGCACAATGGGCGAAGGTTGATGCAGCGACGCCGC	577	Mcurtisii	CTAAACTCAAAGGAATTGACGGGGGCCGCACAAGCGGGGAGCATGCG	1122
Aviscosus	GCAGTGGGGAATATTGCACAATGGGCGCARGOCTGATGCAGCGACGCCGC	409	Aviscosus	CTAAACTCAAAGGAATTGACGGGGGCCGCACAAGCGGGGAGCATGCG	958
Aurogenitalis	GCAGTGGGGAATATTGCACAATGGGCGAAGGCTGATGCAGCGACGCCGC	637	Aurogenitalis	CTAAACTCAAAGGAATTGACGGGGGCCGCACAAGCGGGGAGCATGCG	1186
	*****			*****	
Aodontolyticus16srRNA	GTGAGGGATGGAGCCCTTCGGGTTGTGAACCTCTTTCTCATGGTCAAG	414	Aodontolyticus16srRNA	GATTAATTCGATGCAACCGCAAGAACCCTTACCAGGCTTGACATGCAC	958
Mcurtisii	GTGAGGGTGTAGGCCCTTCGGGTTGTGAACCTCTTTCTCATGGTCAAG	627	Mcurtisii	GATTAATTCGATGCAACCGCAAGAACCCTTACCAGGCTTGACATGCAC	1172
Aviscosus	GTGAGGGATGGAGCCCTTCGGGTTGTAAACCTCTTTCTCATGGTCAAG	459	Aviscosus	GATTAATTCGATGCAACCGCAAGAACCCTTACCAGGCTTGACATGTC-C	1007
Aurogenitalis	GTGAGGGATGGAGCCCTTCGGGTTGTAAACCTCTTTCTCATGGTCAAG	687	Aurogenitalis	GATTAATTCGATGCAACCGCAAGAACCCTTACCAGGCTTGACATGTC-A	1235
	*****			*****	
Aodontolyticus16srRNA	CCG---C	461	Aodontolyticus16srRNA	CGGCA-CTGCAGAGA	1004
Mcurtisii	GCA---CAGTTTT-GGCTGTGTTGATGGTAGTGGGGAAAGAGCGCCGGC	673	Mcurtisii	CGATGTTCCAGAGATGGGCCAGCCTTCGG--GGTG--GTGTACAGGTG	1217
Aviscosus	GCC-TGCTCCTGTGGTGGGTTGACGGTAGCTGGATAAAGAGCGCCGGC	508	Aviscosus	GGTCGGCTCCGGAGACGGGGCTTCCTCCTTGTGGGGCCGGTTCACAGGTG	1057
Aurogenitalis	GCCATCTCTTTGTTGGGTTGACGGTAGCTGGATAAAGAGCGCCGGC	737	Aurogenitalis	CGTCTGCCTCAGAGATGGGGTTTCTCCTTGTGGGGCCGCTTTCACAGGTG	1285
	*****			*****	

Figure 92. Gene alignments for design of primer: b) *A. odontolyticus* (16s rRNA; accession number AJ234054). 90% sequence match to *A. viscosus* 16s rRNA, 91% sequence match to *A. urogenitalis*, 90% sequence match to *M. curtitii*.

Nmucosa	CAATATCGACGGTAAAGGTCAGGAAGGTTTGGAACTGTCCGCGTGAAGACAGTCTGCATGG	60	Nmucosa	TTCCAACGTCGGTACCAGCAAACCTGTCTGCAAAATTCACCTCCTAAAGAAATGTATGATT	600
Nsicca	-----CGGCAAAAGGACAGGAAGGCTTGGAAATGTCCGCGTGAAGACAGTCTGCATGG	51	Nsicca	TTCCAACGTCGGTACCAGCAAACCTGTCTGCAAAATTCACCTCCTAAAGAAATGTATGATT	591
	*****			*****	
Nmucosa	TCCGGACGGTGCAGAAAGTAGTTCTTCGCGACAATAAAGGCAATATCGTCGACAGTTTGG	120	Nmucosa	TTATCATGATTTAGGTGTGGGCGTGGGATGCACCTCCGGTTTCCCGGTTGAGACAGCCGG	660
Nsicca	TCCGGACGGTGCAGAAAGTAGTTCTTCGCGACAATAAAGGCAATATCGTCGACAGTTTGG	111	Nsicca	TTATCATGATTTAGGTGTGGGCGTGGGATGCACCTCCGGTTTCCCGGTTGAGACAGCCGG	651
	*****			*****	
					forward primer site
Nmucosa	TTGCCACGCAACAGGCATCCGAAAAACGGTCAGGACA	180	Nmucosa	TCTTTTGAGAAGCTGGCGCAGATGGCAACCGAATGAACAGGCAACCATGCTTTTCGGTTA	720
Nsicca	CTCTCCCGCAACAGGCATCCGAAAAACGGTCAGGACA	171	Nsicca	TCTTTTGAGAAGCTGGCGCAGATGGCAACCGAATGAACAGGCAACCATGCTTTTCGGTTA	711
	*****			*****	
Nmucosa	TATTCAAACATTTGCCTATGATGAAGTGAATAAAGCAGTGGCTTATCATAAAGCCAAAGC	240	Nmucosa	CGGTTTGCATTTAGCCTGCTGCAGTTGGCGCGTGTATACCATGTTGACACATGACGG	780
Nsicca	TATTCAAACATTTGCCTATGATGAAGTGAATAAAGCAGTGGCTTATCATAAAGCCAAAGC	231	Nsicca	CGGTTTGCATTTAGCCTGCTGCAGTTGGCGCGTGTATACCATGTTGACACATGACGG	771
	*****			*****	
Nmucosa	AGGTACCGTTGTGGTATTGGATGCGCAAAACCGCGCAAAATTTTGGCTTTGGTTAATAGTCC	300	Nmucosa	CGAATTGTTGCCGGTCAAGTTTGAAGAAGCAGGCGGTTGCCCCAAAGGCAACCGGTCAT	840
Nsicca	AGGTACCGTTGTGGTATTGGATGCGCAAAACCGCGCAAAATTTTGGCTTTGGTTAATAGTCC	291	Nsicca	CGAATTGTTGCCGGTCAAGTTTGAAGAAGCAGGCGGTTGCCCCAAAGGCAACCGGTCAT	831
	*****			*****	
Nmucosa	TGCCTATGATCCTAACCAACCGGSCAGTCCGATAGCGAAGCAGCCGCTAACCGTGCCTG	360	Nmucosa	TAAAGCAACGACCCGCGTGAAGTTCGGTATTGATGTTTCTGTAACCGAACCCGCGCG	900
Nsicca	TGCCTATGATCCTAACCAACCGGSCAGTCCGATAGCGAAGCAGCCGCTAACCGTGCCTG	351	Nsicca	TAAAGCTTCGACCCGCGTGAAGTTCGGTATTGATGTTTCTGTAACCGAACCCGCGCG	891
	*****			*****	
Nmucosa	TACCGATATGATCGAGCCGGTCTGCCATGAAGCCGTTTACGATTGCCAAAAGCATTGGA	420	Nmucosa	TACAGGTACAGCAGGTCCGTTAGTGGTTTCGACGTCGGCGCAAAAACCGGTACGGCGCG	960
Nsicca	TACCGATATGATCGAGCCGGTCTGCCATGAAGCCGTTTACGATTGCCAAAAGCATTGGA	411	Nsicca	TACGGGTACAGCAGGTCCGTTAGTGGTTTCGACGTCGGCGCAAAAACCGGTACGGCGCG	951
	*****			*****	
					reverse primer site
Nmucosa	TTCCGCAAAAGTCGGTGT	480	Nmucosa	TAAGTGGTTAATGGACGTTACGTCGATAACAACACGTTGCTACTTTCATCGGTTTTC	1020
Nsicca	TTCCGCAAAAGTCGGTGT	471	Nsicca	TAAGTGGTTAATGGACGTTACGTTGATAACAACACGTTGCTACTTTCATCGGTTTTC	1011
	*****			*****	
Nmucosa	TACTGTACCGGATACCCATGATATCCCACTTTGGATGTGCGCGGCAICATGCCAAAATC	540	Nmucosa	CCCTGCCAAAATCCCGCTGTGATTGTGGCGGTAACCATCGACGAACCGACTGCAAAACG	1080
Nsicca	TACCCTACCGGATACCCATGATATCCCACTTTGGATGTGCGCGGCAICATGCCAAAATC	531	Nsicca	CCCTGCCAAAATCCCGCTGTGATTGTGGCGGTAACCATCGACGAACCGACTGCAAAACG	1071
	*****			*****	
Nmucosa	TTCCAACGTCGGTACCAGCAAACCTGTCTGCAAAATTCACCTCCTAAAGAAATGTATGATT	600	Nmucosa	TTACTACGCGGTTAGTGGCAGTCCGGTCTTCAAACAAGTCATGGGCGGACGCTGAA	1140
Nsicca	TTCCAACGTCGGTACCAGCAAACCTGTCTGCAAAATTCACCTCCTAAAGAAATGTATGATT	591	Nsicca	TTACTACGCGGTTAGTGGCAGTCCGGTCTTCAAACAAGTCATGGGCGGACGCTGAA	1131
	*****			*****	
Nmucosa	TTATCATGATTTAGGTGTGGGCGTGGGATGCACCTCCGGTTTCCCGGTTGAGACAGCCGG	660	Nmucosa	CATCTTGGGCGTTTCTCCGACCAAACCTCTGACTAATGTTGCAGCCGTCAAAACACCGTC	1200
Nsicca	TTATCATGATTTAGGTGTGGGCGTGGGATGCACCTCCGGTTTCCCGGTTGAGACAGCCGG	651	Nsicca	TATCTTGGGCGTTTCCCCACCAAGCCTCTGACCAATGTTGCAGCCGTCAAAACACCGTC	1191
	*****			*****	
Nmucosa	TCTTTTGAGAAGCTGGCGCAGATGGCAACCGAATGAACAGGCAACCATGCTTTTCGGTTA	720	Nmucosa	TTAATCCGAGTATCAACGAGATATTTTATGTTGACGCAAGTTAACCCCTTTAGCTGAAAC	1260
Nsicca	TCTTTTGAGAAGCTGGCGCAGATGGCAACCGAATGAACAGGCAACCATGCTTTTCGGTTA	711	Nsicca	TTAATCCGAGTATCAACGAGATATTTTATGTTGACGCAAGTTAACCCCTTTAGCTGAAAC	1251
	*****			*****	
Nmucosa	CGGTTTGCATTTAGCCTGCTGCAGTTGGCGCGTGTATACCATGTTGACACATGACGG	780	Nmucosa	CAACATTCGCGCTCTGCTGTGTGCAAAACGACGAGGCGGTTTGTTCATTTCAGACAGCCG	1320
Nsicca	CGGTTTGCATTTAGCCTGCTGCAGTTGGCGCGTGTATACCATGTTGACACATGACGG	771	Nsicca	CAACATTCGCGCTCTGCTGTGTGCAAAACGACGAGGCGGTTTGTTCATTTCAGACAGCCG	1311
	*****			*****	
Nmucosa	CGAATTGTTGCCGGTCAAGTTTGAAGAAGCAGGCGGTTGCCCCAAAGGCAACCGGTCAT	840	Nmucosa	TCAAATTAACAAGGTGATAATTTTCGTTGCCTGTACGGGCGAATATACCGAACGCGCCGAG	1369
Nsicca	CGAATTGTTGCCGGTCAAGTTTGAAGAAGCAGGCGGTTGCCCCAAAGGCAACCGGTCAT	831	Nsicca	TCAAATTAACAAGGTGATAATTTTCGTTGCCTGTACGGGCGAATATACCGAACGCGCCGAG	1371
	*****			*****	
Nmucosa	TAAAGCAACGACCCGCGTGAAGTTCGGTATTGATGTTTCTGTAACCGAACCCGCGCG	900	Nmucosa	-----	
Nsicca	TAAAGCTTCGACCCGCGTGAAGTTCGGTATTGATGTTTCTGTAACCGAACCCGCGCG	891	Nsicca	TTATATCCC	1380
	*****			*****	

Figure 92. Gene alignments for design of primer: c) *N. mucosa* (penicillin binding protein A; accession number X59635). 93% sequence match to *N. sicca*.

Pdenticola16srRNA	-----TACAGTGGAGAGTTTGATCCTGGCT	26	Pdenticola16srRNA	TCGTGTAGCGGTGAAATGCTTAGATATGACGAAGAACCCONATTGCGAAGSCAGCCGGCG	743
Fmelaninogenica	AITTTATCACCCATCAGTTATCACAAAACATATTTTACAATGGAGAGTTTGATCCTGGCT	60	Fmelaninogenica	TCGTGTAGCGGTGAAATGCTTAGATATGACGAAGAACCCGATTGCGAAGSCAGCTGACG	778
Pintermedia16srRNA	-----AGAGTTGATCCTGGCT	17	Pintermedia16srRNA	TGGTGTAGCGGTGAAATGCTTAGATATCATGACGAACCTCCGATTGCGAAGSCAGCGTACG	797
	*****			*****	
Pdenticola16srRNA	CAGGATNAACGCTGGCTACAGGCTTAACACATGNCAGTCGAGGGGAAACGGCATTGAGTG	86	Pdenticola16srRNA	GGAGCGCAACTGACGCTGAAGCTNNAAGGTGCGGGTATCGAACAGGATTAGATACCCTGG	803
Fmelaninogenica	CAGGATGAACGCTAGCTACAGGCTTAACACATGCAAGTCGAGGGGAAACGGCATTGAGTG	120	Fmelaninogenica	GGAGCGCAACTGACGCTTAAGCTCGAAGGTGCGGGTATCGAACAGGATTAGATACCCTGG	838
Pintermedia16srRNA	CAGGATGAACGCTAGCTATAGGCTTAACACATGCAAGTCGAGGGGAAACGGCATTGAGTG	77	Pintermedia16srRNA	GGAGCTTACTGACGCTTAAGCTCGAAGGTGCGGGTATCGAACAGGATTAGATACCCTGG	797
	*****			*****	
Pdenticola16srRNA	CTTGCACTNAATGGACGTGACCGGCGCAGCGGTGAGTAACGCGTATCCAACTTCCCGT	145	Pdenticola16srRNA	TAGTCCGACAGGTAAACGATGGATGCCCGCTGCTGGTCCCTGCGCCAGCGGCCAAGCGA	863
Fmelaninogenica	CTTGCACTCTTTGACGTGACCGGCGCAGCGGTGAGTAACGCGTATCCAACTTCCCGT	180	Fmelaninogenica	TAGTCCGACAGGTAAACGATGGATGCCCGCTGTTGGTACCTGGTATCAGCGGCTAAGCGA	898
Pintermedia16srRNA	CTTGCACTTTTGGACGTGACCGGCGCAGCGGTGAGTATCGCGTATCCAACTTCCCGT	137	Pintermedia16srRNA	TAGTCCGACAGGTAAACGATGGATGCCCGCTGTTAGCGCTGGCGCTTACGGGCTAAGCGA	857
	*****			*****	
				forward primer site	
Pdenticola16srRNA	TACTGCGGGATAACCTGCCGAAAGGSCAGACTAATACCGCAT	205	Pdenticola16srRNA	AAGCGTTAAGCATCCNACCTGGGAGTACGCGCGCAACGGTGAACCTCAAAGGAATTGAC	923
Fmelaninogenica	TACTGTGGGATAACCTGCCGAAAGGSCAGACTAATACCGCATAGCTTCGATGACGGCATT	240	Fmelaninogenica	AAGCATTAAAGCATCCCACTGGGAGTACGCGCGCAACGGTGAACCTCAAAGGAATTGAC	958
Pintermedia16srRNA	CACCTGGGGATAACCCGTTGAAAGACGGCTAATACCGCATGTTGTCACATATGGCATT	197	Pintermedia16srRNA	AAGCATTAAAGCATCCCACTGGGAGTACGCGCGCAACGGTGAACCTCAAAGGAATTGAC	917
	*****			*****	
Pdenticola16srRNA	AGATTGGAAGCAAGATCCCTCGGTAACGAGGGGGATGCGTCTGATTAGCTAGTTGGCG	265	Pdenticola16srRNA	GGGGGCCGACACAAGCGGAGGAACATGTGGTTAATTGATGATACGCGAGGAACCTTAC	983
Fmelaninogenica	AGATTGGAAGTAAAGATTTATCGGTAATGGATGGGATGCGTCTGATTAGCTTGTGGCG	300	Fmelaninogenica	GGGGGCCGACACAAGCGGAGGAACATGTGGTTAATTGATGATACGCGAGGAACCTTAC	1018
Pintermedia16srRNA	TGACGTGGACCAAGATTCATCGGTTGAGGATGGGGATGCGTCTGATTAGCTTGTGGCG	257	Pintermedia16srRNA	GGGGGCCGACACAAGCGGAGGAACATGTGGTTAATTGATGATACGCGAGGAACCTTAC	977
	*****			*****	
Pdenticola16srRNA	-GGGCGAGCGCCACCAGGSCAGCATCAGTAGGGGTTCTGAGAGGAAGGTCCCCACAT	324	Pdenticola16srRNA	CCGGGCTGAATTGACAGGAGAAGGATACAGAGATGTTGAGTCCCTCGGGACTCCTGCGA	1043
Fmelaninogenica	-GGGTAACGCGCCACCAGGSCAAGCATCAGTAGGGGTTCTGAGAGGAAGGTCCCCACAT	359	Fmelaninogenica	CCGGGCTGAATTGACAGGAGAAGGATACAGAGATGTTGAGTCCCTCGGGACTCCTGCGA	1078
Pintermedia16srRNA	CCGGTAACGCGCCACCAGGSCAAGCATCAGTAGGGGTTCTGAGAGGAAGGTCCCCACAT	317	Pintermedia16srRNA	CCGGGCTGAATTGACAGGAGAAGGATACAGAGATGTTGAGTCCCTCGGGACTCCTGCGA	1037
	*****			*****	
Pdenticola16srRNA	TGGAAGTGAAGACAGGTCGAACTCCTACGAGGAGGACAGTGAAGGAATATTGGTCAATG	384	Pdenticola16srRNA	AGGTGCTGCATGTTGCTGCTCAGCTCGTCCCGTGAAGTGTGCGGCTTAAAGTCCCATACGA	1103
Fmelaninogenica	TGGAAGTGAAGACAGGTCGAACTCCTACGAGGAGGACAGTGAAGGAATATTGGTCAATG	419	Fmelaninogenica	AGGTGCTGCATGTTGCTGCTCAGCTCGTCCCGTGAAGTGTGCGGCTTAAAGTCCCATACGA	1138
Pintermedia16srRNA	TGGAAGTGAAGACAGGTCGAACTCCTACGAGGAGGACAGTGAAGGAATATTGGTCAATG	377	Pintermedia16srRNA	AGGTGCTGCATGTTGCTGCTCAGCTCGTCCCGTGAAGTGTGCGGCTTAAAGTCCCATACGA	1097
	*****			*****	
Pdenticola16srRNA	GGCGAAGCCTNAACCGCAAGTAGCGTGCAGGAT-GACGGCCCTACGGGTTGTAAGT	443	Pdenticola16srRNA	GCGCAACCCCTCTCCCCAGTTGCCATCGGGTATGCGGGCACTCCGGGGACACTGCCGC	1163
Fmelaninogenica	GACGGAAGTCTGAACCGCAAGTAGCGTGCAGGAT-GACGGCCCTACGGGTTGTAAGT	478	Fmelaninogenica	GCGCAACCCCTCTCTTCAGTTGCCATCAGGTTAAGTGGGCACTCTGGAGACACTGCCAC	1198
Pintermedia16srRNA	GACGGAAGTCTGAACCGCAAGTAGCGTGCAGGATGACGGCCCTACGGGTTGTAAGT	437	Pintermedia16srRNA	GCGCAACCCCTCTCTTCAGTTGCCATCAGGTTAAGTGGGCACTCTGGGACACTGCCAC	1157
	*****			*****	
Pdenticola16srRNA	GCITTTATGCGGGGATAAAGTGAAGNACGNNCCNNTTTCAGGATACCGCATGAATAAG	503	Pdenticola16srRNA	CGCAAGGTGCGAGGAAGGCGGGGATGACGTCAAAATCAGCACNGCCCTTACGTCGGGGCT	1223
Fmelaninogenica	GCITTTGATGCGGGATAAAGTGAAGNACGNNCCNNTTTCAGGATACCGCATGAATAAG	538	Fmelaninogenica	CGTAAGGTGCGAGGAAGGCGGGGATGACGTCAAAATCAGCACNGCCCTTACGTCGGGGCT	1258
Pintermedia16srRNA	GCITTTGTTGGGGATAAAGCGGGGTACGTTGTCGCCCTTTCGCAATTCACCTTCGAATAAG	497	Pintermedia16srRNA	CGCAAGGTGCGAGGAAGGCGGGGATGACGTCAAAATCAGCACNGCCCTTACGTCGGGGCT	1217
	*****			*****	
Pdenticola16srRNA	GACCGGCTAATTCGCTGCCAGCAGCCCGGTAATACGGAAGTCCNGGGTATCCGGAT	563	Pdenticola16srRNA	ACACACGTTTACAATGCGCGGCACAGAGTACNNGTNGCGCGAGCCGATCTAATCTT	1283
Fmelaninogenica	GACCGGCTAATTCGCTGCCAGCAGCCCGGTAATACGGAAGTCCNGGGTATCCGGAT	598	Fmelaninogenica	ACACACGTTTACAATGCGCGGCACAGAGTACNNGTNGCGCGAGCCGATCTAATCTT	1318
Pintermedia16srRNA	GACCGGCTAATTCGCTGCCAGCAGCCCGGTAATACGGAAGTCCAGCGGTTATCCGGAT	557	Pintermedia16srRNA	ACACACGTTTACAATGCGCGGCACAGAGTACNNGTNGCGCGAGCCGATCTAATCTT	1277
	*****			*****	
				reverse primer site	
Pdenticola16srRNA	TTATTGGTTTAAAGGGAGCTAGGCCGGGATTAAGTGTGTTGTAAT	623	Pdenticola16srRNA	GAAAACCGGCTCAGTTGCGACTGGGGTCTGCAACCCGACCCCAAGCTGGATTGCT	1343
Fmelaninogenica	TTATTGGTTTAAAGGGAGCTAGGCCGGGATTAAGTGTGTTGTAAT	658	Fmelaninogenica	GAAAACCGGCTCAGTTGCGACTGGGGTCTGCAACCCGACCCCAAGCTGGATTGCT	1378
Pintermedia16srRNA	TTATTGGTTTAAAGGGAGTGTAGGCCGGTCTGTTAAGCGTGTGTAARATTTAGGTGCT	617	Pintermedia16srRNA	GAAAACCGGCTCAGTTGCGACTGGGGTCTGCAACCCGACCCCAAGCTGGATTGCT	1337
	*****			*****	
Pdenticola16srRNA	AACGCTGATTTGCAGCGCATACTGGTTCCCTTGAGTACGCGCAACCGCGGGAATTCC	683	Pdenticola16srRNA	AGTAATCGCGCATCAGCCACGGCGGTTGAATAAGTTCGCGGGCTTGTACACACCGGCC	1403
Fmelaninogenica	AACGCTGATTTGCAGCGCATACTGGTTCCCTTGAGTACGCGCAACCGCGGGAATTCC	718	Fmelaninogenica	AGTAATCGCGCATCAGCCACGGCGGTTGAATAAGTTCGCGGGCTTGTACACACCGGCC	1438
Pintermedia16srRNA	AACATCTACCTTGCAGCGCAACTGGGCGACTTGAGTGCAGCGCAACCGTATCGGGAATTCA	677	Pintermedia16srRNA	AGTAATCGCGCATCAGCCACGGCGGTTGAATAAGTTCGCGGGCTTGTACACACCGGCC	1397
	*****			*****	

Figure 92. Gene alignments for design of primer: d) *P. denticola* (16s rRNA; accession number L16467). 91% sequence match to *P. melaninogenica*, 87% sequence match to *P. intermedia*.

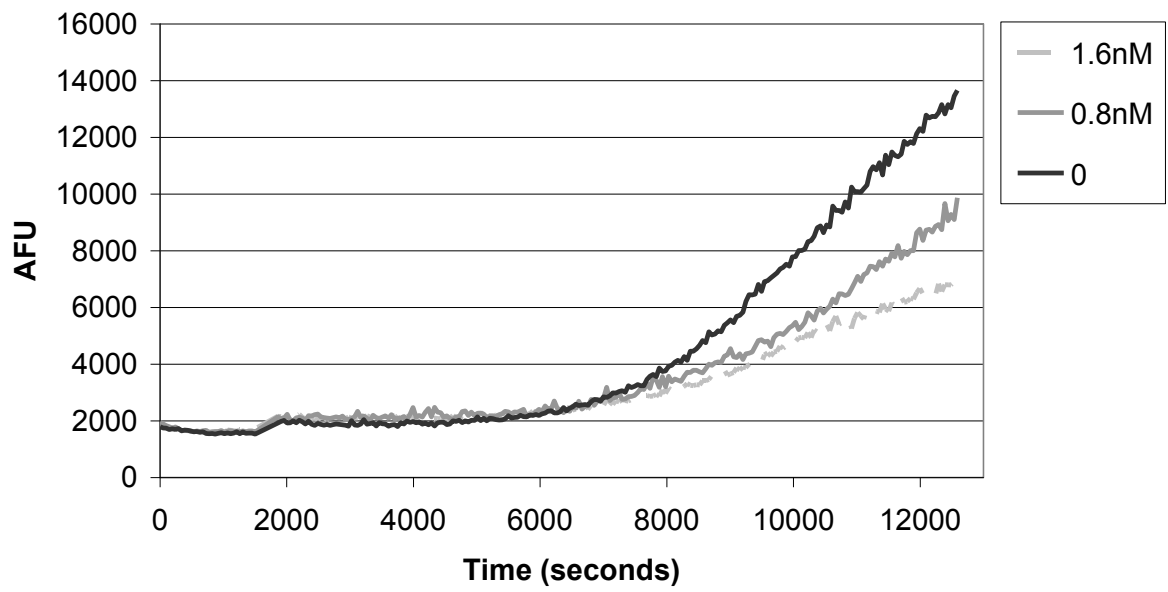
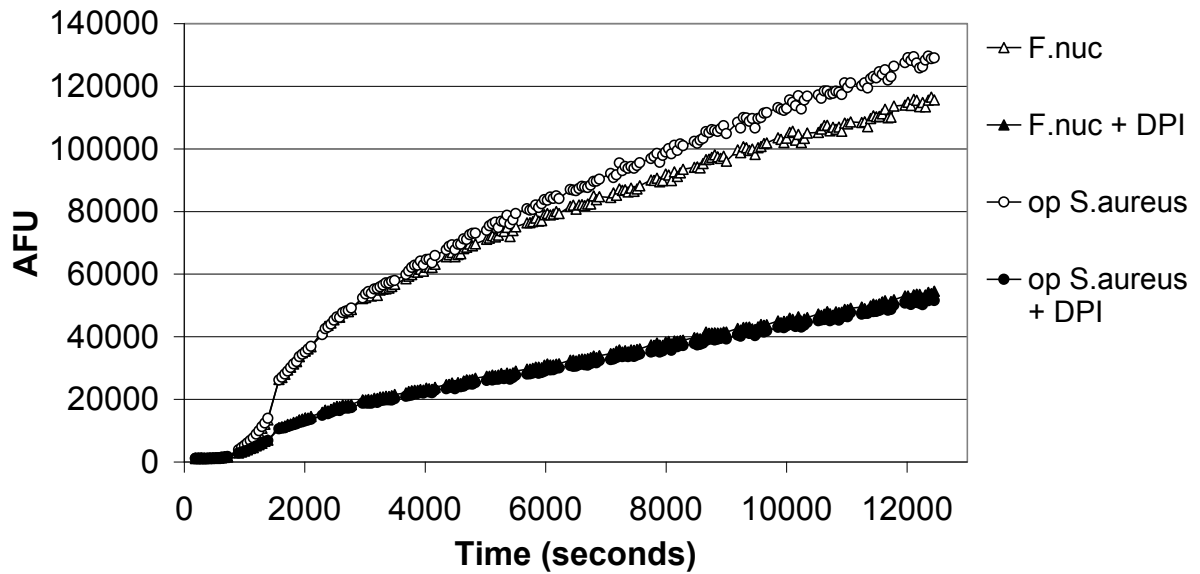


Figure 93. Effect of low PMA concentrations (0-1.6nM) on NET release measured by real-time fluorescence. Results show mean of experiment performed in triplicate.

a) Dead cell stain



b) Live cell stain

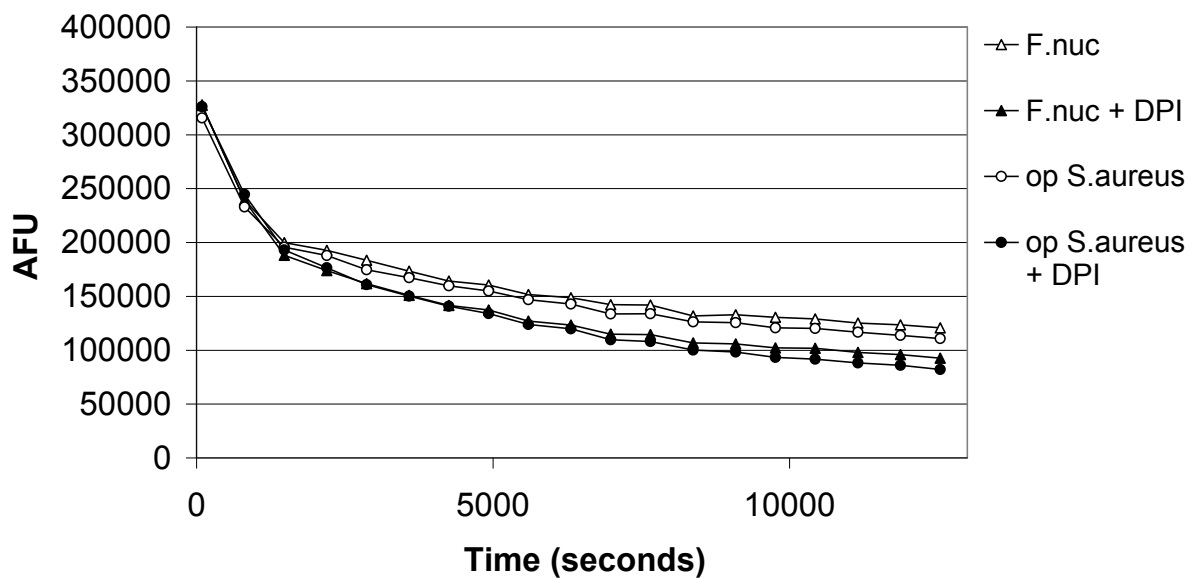


Figure 94. Time course analysis of the effect of DPI (25 μ M) on cell viability using the protease dependant MultiTox-Fluor Multiplex Cytotoxicity assay (Promega). a) dead cell stain read using filter 485/535nm, b) live cell stain read at 355/460nm. Cells stimulated using bacteria (*F. nucleatum* subsp. *polymorphum* and opsonised *S. aureus* MOI 1:150). Results show mean of experiment performed in triplicate.

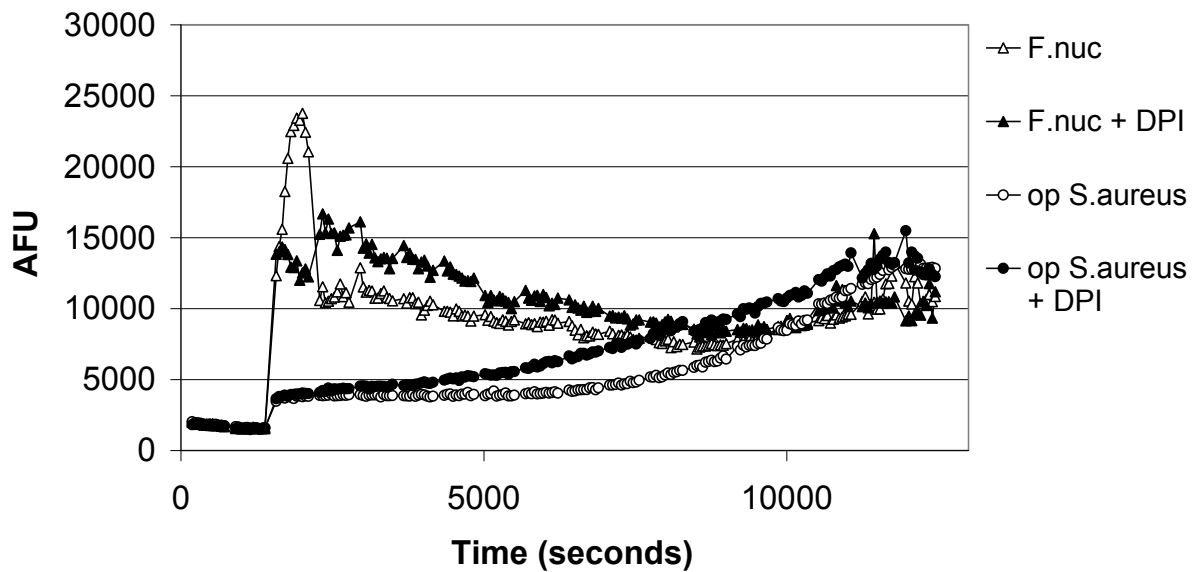


Figure 95. Effect of DPI (25 μ M) on cell viability detected by SYTOX[®] fluorescence over 3 hours incubation using bacterial stimuli (*F. nucleatum* subsp. *polymorphum* and opsonised *S. aureus* MOI 1:150). Results show mean of experiment performed in triplicate.

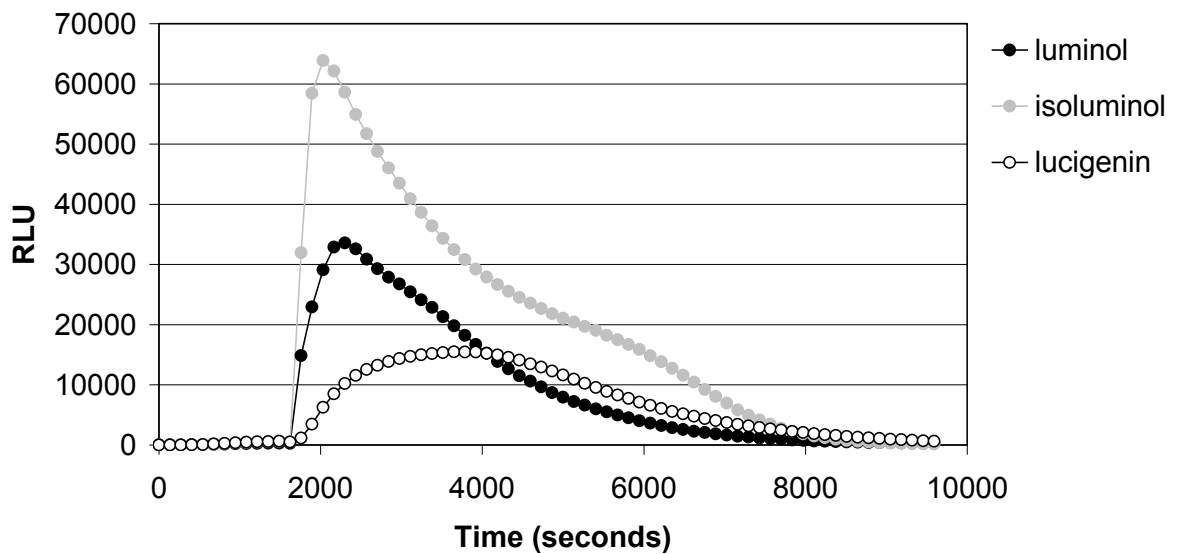


Figure 96. Kinetics of ROS production in primary neutrophils stimulated with PMA 50nM. Results show mean of experiment performed in triplicate.

a) *A. naeslundii* (fimbrial protein; accession number AF106034) → product size 999bp.

```

5581 cttcgtcgtc acctgcccga tgaccaaccg ggagaagacc accgagtgga actacaaccgt
5641 ccacgtctac cccaagaaca ccgtctccgg tgttgacaag caggtctccg acaagcaggt
5701 ctccggatcc ggtaacgaca tcacctacac gatcacgacc tccatcccga aggtcgcacta
5761 cgccggcggt gccaggatca agcgcctacga ggttgctcgac cagctcgaca agcgcacataa
5821 gaaggaccag ctgacgccgg ttgtcaagat catcggcgcc gcaggcggga atccggagat
5881 caccctggtg gatggaacgg actacaccgt catcactgct gacggggcga accacaactg
5941 ggcgacgatc cagctcaccg aggagggggcg caggaaggcc gctgaggccc gtgccaacgg
6001 caccggtgag accaaggttc aggtgactct caccgccaag ttcgactctg acgtcgatct
6061 ggagggaaac ctgtccaaca ccgctggtct cattccctcc gacagtccca acttcgactg
6121 ggacccgagc aaccccggtg cggatgtccc cggatttccc accaccccaa cgatctccaa
6181 gtacggcaag gtgaatctga ccaagaccgg taccgacaac ctcgccgaca agaccaagta
6241 caacggtgct gagttccagg tctacgagtg caccaagacc gccacggggc cactctcaa
6301 ggacgctgac gcctcgaccg ctgacaaggt agaccctctg accatcgggtg gtaagcagac
6361 cttcacgact gagggccagg gcatggtctc gatcgcgact ctgcgcgcca acgactacgt
6421 caatggtgct gagaagcagc tcaccgacga tgactactac tgctcgtcgc agaccaaggc
6481 ccctgagggg tacaccctcc aggccgaccg gatccccttc cgagtcctgg ccgctgatgc
6541 tgagaagaag atcccgactg aggtgaccgt caccgacgtc ccgaagaacg caggtttccg
6601 cctgccgctc accggtgcca acggcgctcat cttcctcacc atcgccggcg cctgctcgt
6661 ggccggtggc gcggtcgcgg cctacgcca caagcgtcgc aacgccgcca agcgtgagc

```

b) *A. viscosus* (fimbrial protein; accession number M32067) → product size 993bp.

```

541 gcctacctcg tcagcgagac gcgcaccccc gacaaggcca tcccggccga ggacttcgtc
601 gtcaccctgc ccatgaccaa cccgcaggac accgccaagt ggaactacaa gtccacgctc
661 taccccaaga acaccctctc cgggtgtggac aagcagggtg ccgacaagcc ggcccccggc
721 tccggggcgcg acatcaccta caccatcacc acctccatcc cgaagggtga ctaccccggc
781 ggtgcgcgca tcaagcgcta cgaggtcgtt gaccgcctcg acaagcgcac caagaaggaa
841 gccctgacct cggctgtcaa gatcgtcggg cagaacgagg tgaccctggc ggagaccacc
901 gactacacc tcatcactgc cgagggtaag gaccacaact gggccaccat ccagctcacc
961 gaggagggcc gccgcaaggc ctccgaggcg cgtacaacg gcaacggcga gaccaagctc
1021 caggtgacct tgaacgcca gtctgacgcc gccgtcaacc tccgaggcga cctgtccaac
1081 accgcggggc tcattcccaa cgacagcccc aacttcacct gggaccgcaa caaccccggc
1141 accaccacgg acatccccgg catccccacc acccccgtgc tctccaagta cggcaagggtg
1201 gttctcacca agaccggtac ggacgacctg gccgacaaga ccaagtacaa cggcgcccag
1261 ttccaggtct acgagtgcac caagaccgcc agcgggtgca cgtcgcgtga ctccgacccc
1321 agcaccaga ccgtcgacct gctgacctac ggtggggaga agaccttac caccgcccggc
1381 cagggcaccg tggagatcaa ctacctgccc gccaacgact acgtcaacgg tgcgaagaag
1441 gaccagctga ccgacgagga ctactactgc ctctggtgga ccaaggcccc cgagggctac
1501 aacctccagg ccgacccgct ccccttccgg gtccctggctg agaaggccga gaagaaggcc
1561 gcgaccgagq tgaccgtcac cgacatcccg aagaacgccc gttccgcct gccgctgacc
1621 gggccaacg gcgtcatctt cctgaccat gccggcgccc tgctggtggc cgggtggcgg
1681 gtggctgcct acgccaacaa gcgcgctcac gttgccaagc actgacagcc tctggcagcc

```

Figure 97. Primer specificity for a) *A. naeslundii* (target species) and b) *A. viscosus* (cross-reactive species). Red nucleotides indicate matches to forward and reverse primers.